

Paper Spray Mass Spectrometry for the Quantitation of Drugs of Abuse in Biofluids and  
Street Drug Samples

by

Scott Arthur Borden

B.Sc., Thompson Rivers University, 2014

A Dissertation Submitted in Partial Fulfillment of the  
Requirements for the Degree of

DOCTOR OF PHILOSOPHY

In the Department of Chemistry

© Scott Borden, 2023

University of Victoria

All rights reserved. This dissertation may not be reproduced in whole or in part, by  
photocopying or other means, without the permission of the author.

# Supervisory Committee

Paper Spray Mass Spectrometry for the Quantitation of Drugs of Abuse in Biofluids and Street Drug Samples

by

Scott Arthur Borden

B.Sc., Thompson Rivers University, 2014

Dr. Chris G. Gill (Department of Chemistry)

*Co-supervisor*

Dr. Alexandre G. Brolo (Department of Chemistry)

*Co-supervisor*

Dr. Erik T. Krogh (Department of Chemistry)

*Departmental Member*

Dr. Rustom Bhiladvala (Department of Mechanical Engineering)

*Outside Member*

# Abstract

## Supervisory Committee

Dr. Chris G. Gill (Department of Chemistry)

*Co-supervisor*

Dr. Alexandre G. Brolo (Department of Chemistry)

*Co-supervisor*

Dr. Erik T. Krogh (Department of Chemistry)

*Departmental Member*

Dr. Rustom Bhiladvala (Department of Mechanical Engineering)

*Outside Member*

Paper spray mass spectrometry (PS-MS) has been developed as a tool for the analysis of drugs of abuse (DoA) in street drug samples, urine, and oral fluid. PS-MS is presented as a viable alternative to the traditional gas chromatography and liquid chromatography-mass spectrometry methods. PS-MS achieves sensitive and quantitative results in as little as 1-2 minutes with little to no sample preparation. Initial research presented in this thesis illustrates how PS-MS was developed for the analysis of fentanyl and related analogs of powdered drug slurries acting as a proxy for street drug samples, as a proof of concept for real world drug checking. Analysis of DoA in these pseudo-drug samples demonstrated the potential for both quantitative and qualitative analysis of fentanyl analogs. PS-MS was then demonstrated and evaluated for its effectiveness for real world drug checking applications during a world first demonstration of PS-MS for on-site drug checking in the Downtown Eastside of Vancouver, British Columbia, a recognized epicenter of the opioid overdose crisis. During the pilot test, 113 samples were submitted for analysis and successfully quantified using PS-MS, which targeted and quantified 49 different drug targets. Of these 113 drug samples, 44% of all samples were found to contain fentanyl, with a median concentration of 3.6% (w/w). The benzodiazepine etizolam was detected in 10 samples, none of the people who submitted these 10 samples expected a benzodiazepine to be present in their sample. It was later found that other drug checking technologies in use were underreporting the presence of etizolam or other benzodiazepines present in drug samples. These results, coupled with the quantitative capabilities and low levels of detection observed during the pilot test of PS-MS for drug checking demonstrated the efficacy of PS-MS and inspired further development of the application. PS-MS was then implemented by the Vancouver Island Drug Checking Project for the routine quantitative measurement of thousands of drug samples. During the span of this routine measurement, two unidentified compounds began appearing in carfentanil-containing drug samples. High resolution accurate mass

(HRAM) mass spectrometry was used to determine the chemical composition of these two unknowns as  $C_{23}H_{29}N_3O_2$  ( $m/z$  380.2333) and  $C_{23}H_{29}N_2O_3$  ( $m/z$  381.2137). Further tandem mass spectrometry experiments were used for structural elucidation and the unknowns were putatively identified as desmethylcarfentanil amide and desmethylcarfentanil acid. LC-MS data on different drug samples containing the same compounds further supported the identification of these carfentanil structural analogs.  $\mu$ -Opioid receptor binding modeling determined that the binding poses, and binding energies of these structural analogs were nearly identical to that of carfentanil, suggesting potentially similar activities/toxicities. PS-MS was further applied to the analysis of cannabinoids in urine and oral fluid samples. Due to the inherently low ionization efficiencies and sensitivity to cannabinoids observed with PS-MS, a reactive paper spray ionization method utilizing a diazonium salt as a on-paper derivatization reagent was developed. The derivatization scheme dramatically lowered the limits of detection for tetrahydrocannabinol (THC) in oral fluid and THC metabolite in urine, to levels able to meet forensic and clinical cutoff values (low parts per billion). The quantitative results were compared to a LC-MS results from a commercial clinical laboratory, demonstrating good agreement between the two methods. The results presented herein demonstrate the applicability and dramatic benefits of PS-MS for drug checking applications, as well as for cannabinoids in oral fluid and urine. High resolution mass spectrometry is demonstrated for the structural elucidation and identification of unknown drug compounds in an ever-changing street drug supply.

# Table of Contents

<b>SUPERVISORY COMMITTEE</b> .....	<b>II</b>
<b>ABSTRACT</b> .....	<b>III</b>
<b>TABLE OF CONTENTS</b> .....	<b>V</b>
<b>LIST OF TABLES</b> .....	<b>VIII</b>
<b>LIST OF FIGURES</b> .....	<b>XI</b>
<b>LIST OF ABBREVIATIONS AND DEFINITIONS</b> .....	<b>XVI</b>
<b>ACKNOWLEDGEMENTS</b> .....	<b>XIX</b>
<b>DEDICATION</b> .....	<b>XX</b>
<b>1 INTRODUCTION</b> .....	<b>1</b>
<b>2 MASS SPECTROMETRY ANALYSIS OF DRUGS OF ABUSE: CHALLENGES AND EMERGING STRATEGIES</b> .....	<b>4</b>
2.1 PREFACE.....	4
2.2 ABSTRACT .....	4
2.3 INTRODUCTION .....	4
2.4 SAMPLE PREPARATION CONSIDERATIONS .....	6
2.4.1 Hydrolysis.....	6
2.4.2 Derivatization.....	15
2.5 GAS CHROMATOGRAPHY MASS SPECTROMETRY .....	16
2.5.1 Introduction, History .....	16
2.5.2 Ionization Techniques .....	17
2.5.3 Analyzers.....	18
2.6 LIQUID-CHROMATOGRAPHY MASS SPECTROMETRY .....	21
2.6.1 Introduction.....	21
2.6.2 Sample Preparation.....	22
2.6.3 Separation Methods .....	24
2.6.4 Detection Techniques.....	24
2.6.5 Sensitivity and Specificity of Compound Identification.....	27
2.6.6 Range of Compounds Identified .....	30
2.6.7 Quantitation .....	34
2.7 AMBIENT IONIZATION MASS SPECTROMETRY .....	35
2.7.1 Introduction.....	35
2.7.2 Liquid/Spray-Based Techniques.....	36
2.7.3 Other Solid-Substrate Electrospray Ionization Techniques .....	46
2.7.4 Plasma-Based Techniques.....	48
2.8 OTHER TECHNIQUES .....	58
2.8.1 Desorption Atmospheric Pressure Photoionization .....	59
2.8.2 Laser Ablation-Based Techniques.....	61

2.9 CONCLUSIONS AND FUTURE OUTLOOK .....	63
<b>3 RAPID AND QUANTITATIVE DETERMINATION OF FENTANYLS AND PHARMACEUTICALS FROM POWDERED DRUG SAMPLES BY PAPER SPRAY MASS SPECTROMETRY .....</b>	<b>64</b>
3.1 PREFACE.....	64
3.2 ABSTRACT .....	64
3.3 INTRODUCTION .....	64
3.4 MATERIALS AND METHODS .....	67
3.4.1 Reagents and Standards.....	67
3.4.2 Mass Spectrometry .....	67
3.4.3 Paper Spray .....	68
3.4.4 Sample Preparation.....	68
3.4.5 Method Validation.....	69
3.4.6 Data Analysis .....	69
3.5 RESULTS AND DISCUSSION .....	70
3.5.1 Matrix Effects in Paper Spray and Electrospray .....	70
3.5.2 Fentanyl Analysis in Various Matrices.....	71
3.5.3 Fentanyl Analog Method Validation Studies.....	73
3.5.4 Direct Qualitative Analysis of Pharmaceutical Samples .....	74
3.5.5 Quantitative Analysis of Pharmaceutical Samples .....	77
3.6 CONCLUSION .....	79
3.7 SUPPORTING INFORMATION .....	81
<b>4 A NEW QUANTITATIVE DRUG CHECKING TECHNOLOGY FOR HARM REDUCTION: PILOT STUDY IN VANCOUVER, CANADA USING PAPER SPRAY MASS SPECTROMETRY .....</b>	<b>89</b>
4.1 PREFACE.....	89
4.2 ABSTRACT .....	89
4.3 INTRODUCTION .....	90
4.4 METHODS.....	91
4.4.1 Location and Approvals.....	91
4.4.2 Analytical Method .....	92
4.4.3 Sample Collection .....	93
4.4.4 Sample Preparation.....	93
4.4.5 Quantitation .....	93
4.4.6 Data Reporting .....	94
4.5 RESULTS.....	94
4.5.1 Concordance of Client Expectations with PS-MS Results .....	94
4.5.2 Discordant Results and Unexpected Substances.....	95
4.5.3 Quantitative Results .....	96
4.6 DISCUSSION .....	97
4.6.1 Discordant Results and Unexpected Substances.....	97

4.6.2	Quantitative Results .....	99
4.6.3	Practical Considerations.....	99
4.7	CONCLUSION .....	99
4.8	SUPPORTING INFORMATION .....	100
4.8.1	Paper Spray Sampling Protocol .....	100
4.8.2	Target Drugs .....	100
4.8.3	Standards .....	101
4.8.4	Sample Collection .....	101
4.8.5	Tables.....	102
<b>5</b>	<b>A DIRECT MASS SPECTROMETRY METHOD FOR CANNABINOID QUANTITATION IN URINE AND ORAL FLUID UTILIZING REACTIVE PAPER SPRAY IONIZATION .....</b>	<b>120</b>
5.1	PREFACE.....	120
5.2	ABSTRACT.....	120
5.3	INTRODUCTION .....	120
5.4	EXPERIMENTAL .....	122
5.4.1	Materials and Reagents .....	122
5.4.2	Standard and Sample Preparation .....	122
5.4.3	Mass Spectrometry .....	122
5.4.4	Reactive Paper Spray Mass Spectrometry.....	122
5.4.5	Data Analysis .....	123
5.4.6	Method Validation.....	123
5.4.7	Liquid Chromatography Mass Spectrometry .....	124
5.5	RESULTS AND DISCUSSION .....	124
5.5.1	Cannabinoid Standard Analysis .....	124
5.5.2	Reactive Paper Spray Mass Spectrometry.....	125
5.5.3	Biofluid Quantitation .....	127
5.5.4	Validation and Comparison to LC-MS/MS.....	130
5.6	FUTURE WORK .....	132
5.7	CONCLUSION.....	133
5.8	SUPPORTING INFORMATION .....	134
<b>6</b>	<b>DETECTION OF CARFENTANIL ANALOGS IN STREET DRUGS BY PAPER SPRAY MASS SPECTROMETRY AND THEIR CHARACTERIZATION BY HIGH RESOLUTION MASS SPECTROMETRY.....</b>	<b>146</b>
6.1	PREFACE.....	146
6.2	ABSTRACT.....	146
6.3	INTRODUCTION .....	147
6.4	EXPERIMENTAL .....	148
6.4.1	Materials and Reagents .....	148
6.4.2	Sample Collection .....	148
6.4.3	Sample Preparation.....	149

6.4.4	Paper Spray Mass Spectrometry.....	149
6.4.5	High Resolution Mass Spectrometry .....	149
6.4.6	$\mu$ -Opioid Receptor Binding Modeling.....	150
6.5	RESULTS AND DISCUSSION .....	150
6.5.1	Carfentanil and Carfentanil Structural Analogs in Street Drug Samples....	150
6.5.2	Characterization of Carfentanil Structural Analogs.....	154
6.5.3	$\mu$ -Opioid Receptor Binding Modeling.....	159
6.6	CONCLUSION .....	161
6.7	SUPPORTING INFORMATION.....	162
<b>7</b>	<b>CONCLUSIONS AND OUTLOOK.....</b>	<b>178</b>
	<b>REFERENCES.....</b>	<b>180</b>

## List of Tables

Table 2.1 Limitations of compound detection range.....	31
Table 2.2 Desorption/ionization conditions for ambient ionization MS techniques. ....	36
Table 2.3 Plasma-based ambient techniques. ....	49
Table 3.1 Comparison of the LOD and LLOQ values for fentanyl analogs in methanol and the 0.1% (w/v) composite OTC mixture.....	73
Table 3.2 Intra-day and inter-day precision values (%CV) and accuracy (%bias) results from method validation experiments for fentanyl analogs in the 1 mg/mL composite OTC mixture. ....	74
Table 3.3 PS-MS measurement of active ingredients in pharmaceutical tablets, three diluted slurries (T1-T3) were prepared for each type of tablet (using a new tablet each time) and analyzed in triplicate. ....	79
Table 3.4 Mass spectrometer parameters used for all experiments.....	83
Table 3.5 Analyte specific instrumental parameters (first product ion listed is the quantifier ion, second listed is the qualifier ion).....	83
Table 3.6 Components in the 11 over the counter composite pill matrix. ....	84
Table 3.7 Components in the pharmaceutical over the counter cold medication tablet used for fentanyl calibrations in various matrices and matrix effects studies. ....	87
Table 3.8 Calibration models (n = 3 replicates) for the fentanyl analogs in methanol. Fentanyl-d5 (30.0 ng/g) was used as the internal standard for acryl fentanyl, furanyl fentanyl, and FIBF. Carfentanil-d5 (28.2 ng/g) was used as the internal standard for carfentanil.....	87
Table 3.9 Calibration models (n = 3 replicates) for the analysis of fentanyl in various matrices.....	87
Table 3.10 Calibration models (n = 4 replicates) for the analysis of active ingredients in pharmaceutical tablets. ....	88
Table 4.1 Paper spray mass spectrometry global parameters. ....	102
Table 4.2 Analyte dependant tandem mass spectrometry (MS/MS) ion transition parameters. MS/MS transitions optimized in the lab using direct infusion electrospray ionization. ....	103
Table 4.3 Paper spray mass spectrometry solvent dispense conditions. ....	109
Table 4.4 Mass spectrometry time-dependent voltage parameters.....	109
Table 4.5 Tandem mass spectrometry (MS/MS) method settings.....	109
Table 4.6 Mass spectrometry full scan (Q3) method settings.....	109
Table 4.7 Medicinal and non-medicinal ingredients of the over the counter (OTC) composite mixture. ....	110
Table 4.8 Calibration models for the targeted drug list based on target ion MS/MS (1 – 1,000 ng/mL, 9 levels, 6 replicates, internal standard concentration at 100 ng/mL)....	113
Table 4.9 Limits of detection (LOD), lower limits of quantitation (LLOQ), and limits of reporting (LOR) for targeted drugs. ....	115

Table 4.10 Quantitative results (w/w%) and expected substance for all samples tested. .....	117
Table 5.1 Comparison of LOD and LLOQ values derivatized and underivatized cannabinoids in biofluids and methanol.....	127
Table 5.2 Quality control data for THC-COOH in prepared fortified human urine (diluted to 70/30 urine/methanol) using reactive PS-MS/MS. Data from 6 replicates daily for 6 days.....	130
Table 5.3 Paper spray mass spectrometry analyte-independent parameters. ....	134
Table 5.4 Mass-dependent selected reaction monitoring (SRM) transition parameters of underivatized cannabinoids and isotopically labelled internal standards. The first ion listed is the quantifier ion, and the reported ion ratio is between the first and second ions listed.....	134
Table 5.5 Mass-dependent selected reaction monitoring (SRM) transition parameters of derivatized cannabinoids and isotopically labelled internal standards. The first ion listed is the quantifier ion, and the reported ion ratio is between the first and second ions listed.....	135
Table 5.6 Paper spray mass spectrometry solvent dispense conditions. ....	135
Table 5.7 Mass spectrometry time-dependent voltage parameters.....	136
Table 5.8 PS-MS calibrations for underivatized cannabinoids in methanol (n = 4, 8 levels [2,5,10,20,40,100,250,500 ng/mL], [internal standard] = 200 ng/mL) using acetonitrile with 0.1% formic acid as spray solvent. ....	136
Table 5.9 Reactive PS-MS calibrations for derivatized cannabinoids in methanol (n = 4, 8 levels [2,5,10,20,40,100,250,500 ng/mL], [internal standard] = 200 ng/mL) using acetonitrile with 0.1% formic acid as spray solvent. ....	136
Table 5.10 Cut-off values for drug testing of THC in oral fluid and THC-COOH in urine recommended by regulatory bodies. ....	137
Table 5.11 Preparation of protein-free artificial urine in deionized water, pH = 6.0 (adjusted using 1.0 M hydrochloric acid). ....	138
Table 5.12 Comparison of reactive PS-MS and LC-MS for the analysis of prepared human urine samples for THC-COOH content. PS-MS results averaged from 6 replicates, LC-MS results from single analysis. ....	138
Table 6.1. HRAM-MS full scan mass errors and formulae assignment of a carfentanil containing drug sample. ....	155
Table 6.2. HRAM-MS/MS product ion scan mass errors, formulae assignments, and relative intensities for fragments of carfentanil, NPS1, and NPS2 in a carfentanil- containing drug sample. ....	157
Table 6.3. Calculated binding energies of the carfentanil structural analogs on the $\mu$ - opioid receptor and their binding energies relative to carfentanil. ....	161
Table 6.4. Selected reaction monitoring (SRM) transition parameters of carfentanil and carfentanil-d5 on the Fortis QqQ mass spectrometer.....	162

Table 6.5. Paper spray mass spectrometry analyte-independent parameters. ....	162
Table 6.6. Paper spray mass spectrometry solvent dispense conditions. ....	162
Table 6.7. LOD and LLOQ values for carfentanil in prepared drug samples (solution B). .....	163
Table 6.8. Paper spray mass spectrometry calibration of carfentanil (n = 6, 11 levels @ [1, 2.5, 5, 10, 15, 25, 40, 75, 125, 250, 500 ng/mL], [carfentanil-d <sub>5</sub> ] = 100 ng/mL) on the Fortis QqQ mass spectrometer. ....	163
Table 6.9. Orbitrap Exploris 120 parameters.....	163
Table 6.10. Relative intensity data for the comparison of PS-MS QqQ product ion scans collected with a collision energy ramp of 5-50 V of a carfentanil analytical reference standard and a carfentanil-containing drug sample. A '-' indicates a relative intensity > 1. .....	167
Table 6.11. Peak heights of NPS1 and 2 relative to the peak height of carfentanil in the same sample.....	168
Table 6.12. Elements in use for elemental composition determination within Freestyle software. A mass tolerance of 5.00 ppm was used for prediction and fragment matching. .....	169
Table 6.13. Fragment identities, mass errors, and relative intensities of fragments from HRAM-MS/MS of NPS1 (380.2 m/z) at 50% HCD collision energy.....	170
Table 6.14. Fragment identities, mass errors, and relative intensities of fragments from HRAM-MS/MS of NPS2 (381.2 m/z) at 50% HCD collision energy.....	171

## List of Figures

Figure 2.1 Growth of mass spectrometry-based drug testing publications between 2008 and 2019. ....	5
Figure 2.2 Extraction modes in solid phase microextraction (SPME). (A) Direct immersion SPME, (B) headspace SPME, and (C) membrane protected SPME. Not to scale. ....	8
Figure 2.3 Microextraction with packed sorbent workflow. (A) Sampling, (B) washing, (C) elution solvent, and (D) injection. Not to scale. ....	9
Figure 2.4 Extraction mode in single drop microextraction (SDME). (A) Direct-immersion SDME, (B) headspace SDME, (C), three-phase SDME, (D) drop-to-drop microextraction, (E) bubble-in-drop SDME, and (F) continuous-flow microextraction. Not to scale. ....	11
Figure 2.5 Classical dispersive liquid-liquid microextraction workflow. Not to scale. ....	12
Figure 2.6 Steps of operation with hollow-fibre liquid-phase microextraction (HF-LPME). (A) Filling syringe with acceptor phase, (B) filling the HF lumen with acceptor phase, (C) bending the HF (U shape) and insertion into the aqueous sample, (D) agitation, (E) instrumental analysis. Not to scale. ....	13
Figure 2.7 Generalized instrumental schematics for (A) desorption electrospray ionization (DESI), (B) thermal-desorption electrospray ionization, (C) easy ambient sonic-spray ionization (EASI), (D) paper spray ionization (PSI), and (E) coated blade spray ionization (CBS). Not to scale. ....	37
Figure 2.8 Generalized instrumental schematics for (A) direct analysis in real time (DART), (B) atmospheric solids analysis probe (ASAP), (C) flowing atmospheric-pressure afterglow (FAPA), (D) direct sample analysis (DSA), (E) dielectric barrier discharge ionization (DBDI), (F) low-temperature plasma (LTP). Not to scale. ....	50
Figure 2.9 Generalized instrumental schematics for (A) desorption atmospheric pressure photoionization, (B) matrix-assisted laser desorption ionization (MALDI), and (C) surface-assisted laser desorption ionization (SALDI). Not to scale. ....	59
Figure 3.1 Comparison of signal suppression observed in paper spray (◆) and direct injection electrospray (●) for ca. 75 ng/g fentanyl present in samples with increasing concentrations of suspended solids from an over the counter cold medication tablet matrix in methanol (logarithmic x-axis). Signal intensities are normalized to those obtained for fentanyl present in neat methanol with no added matrix. ....	70
Figure 3.2 Calibrations of fentanyl (0.5 – 200 ng/g, n = 3) in methanol (★), in methanol with 10% (w/w) mannitol (◆), 5% (w/v) of an OTC cold medication tablet slurry in methanol (▲), and 5% (w/v) of an OTC cold medication tablet slurry in methanol with an additional 15 µg of heroin per g of methanol (●) using the signal area ratio of fentanyl (m/z 337.0 □ 188.1) to that for fentanyl-d5 internal standard (m/z 342.2 → 188.1) at 30 ng/g. ....	72

Figure 3.3 Direct qualitative analysis of a approximately 1 mg of a crushed pharmaceutical tablet deposited directly on the PS sampling strip showing <b>A)</b> an image of the crushed tablet directly on the PS cartridge, <b>B)</b> the full scan (100 – 350 m/z) mass spectrum, <b>C)</b> the product scan (50 – 175 m/z) of pseudoephedrine (15 eV collision energy), and <b>D)</b> MS/MS chromatogram of the crushed tablet samples (P1-P4) and caffeine tablets containing no pseudoephedrine as blanks (B1-B3).....	76
Figure 3.4 Calibrations (5 levels, 4 replicates) of <b>A)</b> caffeine, <b>B)</b> acetaminophen, <b>C)</b> pseudoephedrine, and <b>D)</b> chlorpheniramine with results from quantitation of the prepared diluted slurries of pharmaceutical tablets (T1-T3) interpolated on the figure..	78
Figure 3.5 Chemical structures of the drugs examined in this study. ....	81
Figure 3.6 Photographs of the experimental setup used, illustrating the custom 3D printed mount, Prosolia™ cartridge in front of the mass spectrometer inlet, and the Waters Micromass Quattro Ultima LC mass spectrometer.....	82
Figure 3.7 Representative integrated signal chronogram on MassLynx version 4.1 software for a typical PS-MS measurement. ....	82
Figure 4.1 Sampling workflow and reporting of results for samples submitted by clients. ....	93
Figure 4.2 Example of the automatically generated report printout given to HRW to relay to client.....	94
Figure 4.3 Concordance of client expectation with PS-MS results for drug identity by expected drug category (FEN = fentanyl, MAMP = methamphetamine, COC = cocaine, HER = heroin, MDMA = 3,4-methylenedioxymethamphetamine, KET = ketamine). ....	95
Figure 4.4 Calculated amounts (w/w%) of fentanyl (—), 4-ANPP (—), etizolam (—), and heroin (—) in expected opioid samples and unknown samples. A) expected opioid samples containing exclusively fentanyl and 4-ANPP, B) expected opioid samples containing heroin and/or fentanyl, and C) expected opioid samples where etizolam was detected. The upper limit of quantitation (ULOQ) was 10% w/w. ....	97
Figure 5.1 Workflow for reactive paper spray mass spectrometry measurements. <b>A)</b> 10 µL aliquot of 1.5 mM Fast Red RC in 5.0 mM ammonium acetate (aq), <b>B)</b> 10 µL aliquot of cannabinoid standard or biofluid sample with spiked internal standard <b>C)</b> two 10-µL aliquots of dichloromethane, and <b>D)</b> automated, high-throughput PS-MS analysis of derivatized cannabinoids. *Derivatization can occur either ortho or para to the hydroxyl group <sup>484</sup> .....	123
Figure 5.2 Reactive PS-MS signal intensities for A) residual, underivatized THC and B) derivatized THC, obtained for a methanolic calibration of THC (2 – 500 ng/mL) with 10 µL of derivatization solution pre-spotted on the paper substrate. Dashed lines indicate the average (n = 6) signal intensity observed for blank measurements, with the shaded bar displaying the measurement standard deviation. Logarithmic X-axis for visual clarity. ....	126

Figure 5.3 A) Reactive PS-MS signal intensities obtained for 200 ng/mL derivatized THC-COOH-d <sub>3</sub> in prepared blank human urine with two aliquots of DCM spotted on dried urine spot and with no DCM spotted and B) a boxplot of the signal intensities with and without DCM.....	128
Figure 5.4 Reactive PS-MS calibrations (n = 3 replicates) of A) derivatized THC in human oral fluid (2-250 ng/mL) and B) derivatized THC-COOH in human urine (2-500 ng/mL) .....	129
Figure 5.5 Bland-Altman relative difference plot of reactive PS-MS and LC-MS THC-COOH measurements from fortified blank human urine samples. ....	131
Figure 5.6 Reactive PS-MS signal chronograms for 250 ng/mL of derivatized THC-COOH in A) undiluted human urine using 90/9.9/0.1% acetonitrile/water/formic acid as spray solvent, B) human urine diluted with methanol (70/30 v/v%) using 90/9.9/0.1 acetonitrile/water/formic acid as spray solvent, and C) human urine diluted with methanol (70/30 v/v%) using acetonitrile with 0.1% formic acid as a spray solvent and application of two 10 µL aliquots of DCM to the dried sample spot prior to measurement. ....	139
Figure 5.7 Direct infusion electrospray ionization product ion MS/MS spectra of A) THC, B) CBD, C) derivatized THC, and D) derivatized CBD. ....	140
Figure 5.8 Reactive PS-MS signal chronograms for 200 ng/mL of derivatized THC-COOH using acetonitrile with 0.1% formic acid as spray solvent in A) artificial urine spiked with 0.14 µg/mL bovine serum albumin, and B) protein-free artificial urine.....	141
Figure 5.9 Measured THC-COOH levels from reactive paper spray measurements (n=3) for prepared urine samples (300 ng/mL) measured at various intervals using PS-MS sample strips prepared in advance with pre-deposited derivatization reagent. 300 ng/mL is represented by the solid line, with ± 20% bias represented by the dashed lines and shaded grey box. Error bars represent ± one standard deviation.....	142
Figure 5.10 Log signal area intensities of derivatized THC-COOH from reactive paper spray measurements (n=3) of prepared urine samples (300 ng/mL THC-COOH) obtained at various intervals using PS-MS sample strips prepared in advance with pre-deposited derivatization reagent. The dashed line indicates the mean signal intensity of blank measurements (n=6) with the shaded grey box representing ± one standard deviation. Error bars represent ± one standard deviation.....	143
Figure 5.11 Measured THC-COOH levels for reactive PS-MS measurements of prepared urine samples (300 ng/mL) using a 60°C oven for two 1.5-minute drying steps (after Fast Red RC spotting, and after urine spotting). The shaded grey box represents ± 20% bias. The 6 samples were prepared on 6 unique PS-MS sample plates and measured at different times.....	144
Figure 5.12 Direct infusion electrospray ionization full scan mass spectra (500-750 m/z) of A) THC-COOH glucuronide derivatized with Fast Red RC at a source fragmentation	

of 0V, and B) THC-COOH glucuronide derivatized with Fast Red RC at a source fragmentation of 100V* .....	145
Figure 6.1 A) PS-MS calibration of carfentanil (n = 6 replicates, 10 levels [1, 2.5, 5, 10, 15, 25, 40, 75, 125, 250, 500 ng/mL], [carfentanil-d <sub>5</sub> = 100 ng/mL], 1/x weighting. B) Quantified amount (w/w%) of carfentanil in the original drug sample.....	151
Figure 6.2 PS-MS QqQ full scan (50-500 m/z) of a carfentanil containing drug sample (solution A).....	152
Figure 6.3 A) PS-MS QqQ relative peak heights of NPS1 (blue) and NPS2 (red) intermediates relative to that for carfentanil (value of 1) and B) estimated w/w concentration of NPS1 and NPS2 in the original drug sample. ....	153
Figure 6.4 Direct infusion HRAM-MS full scan spectrum of a carfentanil-containing drug sample dissolved in spray solvent (90/9.9/0.1 v/v% acetonitrile/water/formic acid).....	154
Figure 6.5 HRAM-MS/MS product ion spectra of a carfentanil containing drug samples for A) m/z 395.5 (carfentanil), B) m/z 380.2 (NPS1), and C) m/z 381.2 (NPS2). All spectra are compared to the product ion spectrum of a carfentanil analytical reference standard (top panels). All spectra were collected at 20% HCD collision energy. ....	156
Figure 6.6. $\mu$ -Opioid receptor binding poses of (a) carfentanil, (b) desmethylocarfentanil amide (new psychoactive substance 1), (c) desmethylocarfentanil acid (new psychoactive substance 2), and (d) all three structures overlaid.....	160
Figure 6.7. QqQ PS-MS full scan of 10 $\mu$ L of 200 ng/mL carfentanil analytical reference standard in methanol.....	164
Figure 6.8. HRAM direct infusion electrospray full scan of 200 ng/mL carfentanil analytical reference standard in methanol.....	164
Figure 6.9. QqQ PS-MS full scan of a carfentanil-containing drug sample, no peaks present at 380.2 or 381.2 m/z. ....	165
Figure 6.10. Comparison of PS-MS QqQ product ion scans (50-400 m/z) of carfentanil analytical reference standard (top) to a carfentanil-containing drug sample (bottom): <b>A</b> ) carfentanil (m/z 395.5), <b>B</b> ) NPS1 (m/z 380.2), and <b>C</b> ) NPS2 (m/z 381.2). Collision energy ramp of 5-50 V.....	166
Figure 6.11. Chemical structures of A) fentanyl, B) carfentanil, C) carfentanil amide (NPS1), D) desmethylocarfentanil acid (NPS2), E) benzyl carfentanil, and F) acetyl carfentanil, G) methylenedioxy fentanyl. ....	169
Figure 6.12. Direct infusion HRAM-MS/MS spectrum (50-350 m/z) of NPS1 (380.2 m/z) in a drug sample, 50% HCD collision energy. ....	170
Figure 6.13. Direct infusion HRAM-MS/MS spectrum (50-350 m/z) of NPS2 in a drug sample, 50% HCD collision energy. ....	171
Figure 6.14. HRAM-MS/MS spectra of A) benzyl carfentanil, B) acetyl carfentanil, and C) 3,4-methylenedioxyfentanyl from the HighResNPS database. *	172

- Figure 6.15. HRAM-MS full scan mass spectrum (379.5 – 382 m/z) of a carfentanil-containing drug sample. Red box schematically indicates the 0.4 m/z isolation width for MS/MS. \*Interferents within the isolation window of NPS2..... 173
- Figure 6.16. Fragmentation pathways leading to the formation of the A) 246.15 m/z ion from carfentanil, B) 113.06 m/z ion from carfentanil, C) 231.15 m/z ion from desmethylcarfentanil amide, D) 98.06 m/z ion from desmethylcarfentanil amide, E) 232.13 m/z ion from desmethylcarfentanil acid, and F) 99.04 m/z ion from desmethylcarfentanil acid. Generated with Thermo Fisher Mass Frontier™ 7.0 Spectral Interpretation Software..... 174
- Figure 6.17. LC-MS/MS (Orbitrap HRAM) data from Canadian Centre for Addiction and Mental Health (Toronto) for a used drug paraphernalia sample. A) Full scan (75 – 800 m/z) mass spectrum at retention time 9.80 minutes and B) MS/MS spectrum (50 – 400 m/z) of 380.2334 m/z, retention time 9.80 minutes, 66.67 V HCD collision energy..... 175
- Figure 6.18. LC-MS/MS (Orbitrap HRAM) data from Canadian Centre for Addiction and Mental Health (Toronto) for a used drug paraphernalia sample. A) Full scan (75 – 800 m/z) mass spectrum at retention time 8.67 minutes and B) MS/MS spectrum (50 – 400 m/z) of 381.2366 m/z, retention time 8.67 minutes, 66.67 V HCD collision energy..... 176
- Figure 6.19. LC-MS (Orbitrap HRAM) chromatograms from the Canadian Centre for Addiction and Mental Health (Toronto) of a used paraphernalia sample. A) Carfentanil (m/z 395.2309 - 395.2349, 11.18 min), B) desmethylcarfentanil amide (m/z 380.2314 - 380.2352, 9.80 min), and C) desmethylcarfentanil acid (m/z 381.2154 - 381.2192, 8.67 min). ..... 177

## List of Abbreviations and Definitions

4-ANPP	4-anilino-N-phenethyl-piperidine
AC	Acetylation
AMP	Amphetamines
amu	Atomic mass unit
APCI	Atmospheric pressure chemical ionization
APPI	Atmospheric pressure photoionization
ASAP	Atmospheric pressure solids analysis probe
BDZ	Benzodiazepine
BSA	Bovine serum albumin
BUP	Buprenorphine
CBD	Cannabidiol
CBN	Cannabinol
CBS	Coated blade spray
CE	Capillary electrophoresis
CID	Collisional-induced dissociation
COC	Cocaine
COD	Codeine
Da	Dalton
DAPPI	Desorption atmospheric pressure photoionization
DART	Direct analysis in real time
DBDI	Dielectric barrier discharge ionization
DCM	Dichloromethane
DDA	Data-dependent analysis
DESI	Desorption electrospray ionization
DeSSI	Desorption sonic-spray ionization
DIA	Data-independent analysis
DI-SPME	Direct-immersion solid-phase microextraction
DLLME	dispersive liquid-liquid microextraction
DoA	Drugs of abuse
DoM	Drugs of misuse
DSA	Direct sample analysis
DUID	Driving under influence of drugs
EASI	Easy ambient sonic-spray ionization
EI	Electron ionization
ELDI	Electrospray-assisted laser desorption ionization
ESI	Electrospray ionization
FAPA	Flowing atmospheric-pressure afterglow
Fast Red RC	5-chloro-2-methoxybenzenediazonium chloride hemi (zinc chloride) salt
FEN	Fentanyl
FIBF	4-fluoro-isobutyryl fentanyl

FID	Flame ionization detector
FTIR	Fourier-transform infrared spectroscopy
FWHM	Full width at half maximum
GC	Gas chromatography
GC-MS	Gas chromatography mass spectrometry
GHB	g-hydroxybutyrate
HCD	Higher-energy C-trap dissociation
HER	Heroin
HF-LPME	hollow fiber microextraction
HRAM	High resolution accurate mass
HRDC	Harm reduction drug checking
HRMS	High resolution mass spectrometry
HRW	Harm reduction worker
HS-SPME	Headspace solid phase microextraction
IMS	Ion mobility spectrometry
IT	Ion trap
KET	Ketamine
LAESI	Laser ablation electrospray ionization
LC	Liquid chromatography
LC-MS	Liquid chromatography mass spectrometry
LDTD	Laser diode thermal desorption
LLE	Liquid-liquid extraction
LLOQ	Lower limit of quantitation
LOD	Limit of detection
LOQ	Limit of quantitation
LOR	Limit of reporting
LSD	Lysergic acid diethylamide
LTP	Low-temperature plasma
MALDI	Matrix-assisted laser desorption ionization
m-CPP	meta-chlorophenylpiperazine
MDA	3,4-methylenedioxiamphetamine
MDEA	3,4-methylenedioxy-N-ethylamphetamine
MDF	Mass defect filter
MDMA	3,4-methylenedioxyamphetamine
MRM	Multiple reaction monitoring
MS	Mass spectrometry / Mass spectrometer
MS/MS	Tandem mass spectrometry
NICI	Negative ion chemical ionization
NIST	National Institute of Standards and Technology
NKET	Norketamine
NPS	Novel psychoactive substance
OPS	Overdose prevention site
OTC	Over the counter

PCSI	Paper cone spray ionization
PICI	Positive ion chemical ionization
POC	Point-of-care
PSI	Paper spray ionization
PS-MS	Paper spray mass spectrometry
PWUD	People who use drugs
Q	Quadrupole
QqQ	Triple quadrupole
QuEChERS	Quick, easy, cheap, effective, rugged, and safe
RT	Retention time
SALDI	Surface-assisted laser desorption ionization
SAMHSA	Substance Abuse and Mental Health Services Administration
SAR	Signal area ratio
SCS	Supervised consumption site
SIM	Selected ion monitoring
SPE	Solid phase extraction
SRM	Selected reaction monitoring
SWGTOX	Scientific working group for forensic toxicology
TD	Thermal desorption
THC	tetrahydrocannabinol
THC-COOH	11-nor-9-carboxy- $\Delta^9$ -tetrahydrocannabinol
TLC	Thin layer chromatography
ToF	Time of flight
ULOQ	Upper limit of quantitation

## Acknowledgements

First and foremost, I would like to thank Chris Gill for the unwavering mentorship, support, guidance, and encouragement. Thank you for your patience, understanding, expert advice, and belief in me. Further thanks are extended to my committee members Erik Krogh, Alexandre Brolo, and Rustom Bhiladvala for their contributions and advice regarding this dissertation.

I was fortunate to work with an amazing group of people at the AERL, thank you to all of you I have worked with throughout the years. I would especially like to acknowledge Gregory Vandergrift. Thank you for training me and being an amazing colleague, and an even better friend. Much of this work was made possible by contributions from my collaborator Armin Saatchi, may you rest in peace friend, your passionate and spirited personality will never be forgotten. John-Clare Laxton, thank you for being an amazing friend, I am thankful that we were able to go through this together.

Further thanks are extended to the members of the Vancouver Island Drug Checking Project. To Dennis Hore and Bruce Wallace, thank you for facilitating collaborations that have led to amazing outputs. Jarred Aasen, Lea Gozdziński, Margo Ramsay, Ashley Lardner - it was a pleasure to work with you all.

I would further like to thank all co-authors and collaborators I have worked with throughout this degree. Jan Palaty, thank you for enabling various projects and for diligently answering my many questions. A further thank you to my Italian collaborators Achille Cappiello, Pierangela Palma, and Veronica Termopoli.

Last but not least, thank you to my family and friends. Your support has meant the world.

# Dedication

For my parents.

Thank you for being my greatest supporters.

# 1 Introduction

The analysis of drugs of abuse (DoA) presents a myriad of challenges and requires that the measurement of analytes, often at the parts per billion (ppb) level, can be accomplished with a high degree of certainty given the substantial implications when answering forensic or clinical questions. The high level of sensitivity and selectivity provided by mass spectrometry (MS) has solidified its position as the 'gold standard' analytical technique for the analysis of DoA.<sup>1</sup> Traditionally, liquid chromatography (LC) or gas chromatography (GC) is interfaced with a mass spectrometer to separate chemical compounds. The coupling of these chromatographic methods with MS yields the selectivity needed to make reliable, trustworthy decisions for legal and clinical purposes.<sup>2</sup> Unfortunately, the time required for sufficient chromatographic resolution (tens of minutes to an hour or more) and the possible need for sample preparation often leads to large sample backlogs in the laboratories operating these analyses, and often the results are not disseminated fast enough to provide timely, meaningful answers to the questions at hand.<sup>3</sup> In the last two decades, major developments in the rapidly growing field of ambient ionization techniques for mass spectrometry have presented alternatives to chromatography while maintaining the sensitivity required for the analysis of DoA.<sup>4-7</sup>

Selectivity of these methods can be limited by the lack of chromatographic separation, but nonetheless, these techniques remain viable alternatives for many assays performed in these settings, particularly for targeted applications. Ambient ionization techniques operate under ambient (open air) conditions and usually require little to no sample preparation. Paper spray mass spectrometry (PS-MS) is an ambient ionization technique that will be discussed at length in this dissertation.<sup>8,9</sup> PS-MS can overcome some of the disadvantages inherent to GC-MS and LC-MS methods for the analysis of DoA. The applications presented in this dissertation require little to no sample preparation, and forgo chromatographic separation, allowing for results to be obtained in as little as 2 minutes. Chapter 2 presents a thorough review and introduction to the operating principles, history, and future directions for the analysis of DoA by mass spectrometry. The chapter critically reviews the state of GC-MS, LC-MS, and various ambient ionization techniques (including PS-MS) and presents a wide range of the types of assays performed for DoA by mass spectrometry. Chapter 2 further offers a thorough introduction to mass spectrometry in general and can be viewed as an extension of this introduction.

On April 14th, 2016, the province of British Columbia declared the opioid overdose crisis to be a public health emergency. As a result, various harm reduction services have been implemented across the province (and in many other jurisdictions) in an attempt to mitigate the harm caused by the opioid overdose crisis. One of these services is drug checking. Drug checking is a service offered to people who use drugs (PWUD), allowing them to check the chemical composition of the substance they intend to use, facilitating evidence-based informed use.<sup>10-13</sup> It was immediately apparent in these settings that results needed to be reported back to PWUD within minutes, rather than hours. As a result, GC-MS and LC-MS are poorly suited to these environments. Various other

techniques including immunoassay test strips, Fourier-transform infrared spectroscopy (FTIR), Raman spectroscopy, and ion mobility spectroscopy have been used with some success.<sup>14-17</sup> However, these methods suffer from one or more of the following issues: lack of selectivity to differentiate between closely related compounds with wildly different toxicities, insufficient sensitivity to detect potent trace level compounds, inability to quantify the components present in drug mixtures, and/or inability to rapidly adapt to changes in the drug supply and the emergence of novel psychoactive substances (NPS).

Paper spray mass spectrometry was therefore explored and developed for drug checking applications to overcome the limitations of the drug checking techniques in use at the time. Chapter 3 describes the initial development phase of PS-MS for drug checking applications prior to our laboratory's designation as an Overdose Prevention Site (OPS) which allowed for the testing of real drug samples.<sup>18</sup> To develop PS-MS for future drug checking applications, fentanyl and a selection of fentanyl analog standards were spiked into powdered slurries, acting as proxies for real drug samples, and directly measured by PS-MS. Using these slurries, PS-MS was able to quantify picogram quantities of these fentanyls from a single milligram of a drug sample. The analysis could be completed in less than two minutes, with a relatively high degree of selectivity. Quality control and validation of the analysis revealed sufficient accuracy and precision as outlined by the Scientific Working Group for Forensic Toxicology (SWGTOX) guidelines.<sup>19</sup> Building upon the success of the analysis of fentanyls in pseudo-drug samples, PS-MS was further developed for real world drug checking application. Chapter 4 presents the world first on-site use of PS-MS for drug checking.<sup>20</sup> The instrument was relocated to the Downtown Eastside of Vancouver, British Columbia for a two-day pilot test of the instrumentation and application. Over 100 samples were submitted and successfully quantified using a panel of 49 target drugs. The developed PS-MS method successfully demonstrated sufficient sensitivity and selectivity, even for trace level compounds, and was able to return quantitative results to PWUD within 2-5 minutes. Although not presented in this dissertation, PS-MS for drug checking applications development continued and the instrument was adopted by the Vancouver Island Drug Checking Project in November 2020, where it has quantitatively analyzed over 12,000 drug samples to date.

On October 17th, 2018, the Cannabis Act was passed federally in Canada, legalizing the possession and use of cannabis and cannabis related products. As a result, the need for the chemical analysis of cannabis, as well as the analysis of biofluids for cannabis metabolites grew exponentially. Given this landscape, the efficacy of PS-MS for the measurement of cannabinoid metabolites in biofluids was investigated. Chapter 5 presents the use of PS-MS for the quantitation of tetrahydrocannabinol (THC) in oral fluid and for THC metabolite (11-Nor-9-carboxy-tetrahydrocannabinol i.e., THC-COOH) in urine.<sup>21</sup> Forensic and clinical cutoff values for these compounds are in the single to double-digit ppb range. THC and THC-COOH exhibit poor ionization efficiency in both positive and negative ion-mode for PS-MS. To achieve the required low ppb limits of quantitation required for these types of analyses, a reactive paper spray ionization approach was developed. Reactive paper spray ionization uses derivatization reagents

to chemically modify analytes of interest and increase their ionization efficiencies. The diazonium salt Fast Red RC was deposited onto the paper substrate and allowed to dry. THC and THC-COOH biofluids were then deposited onto the same paper substrate, and a derivatization reaction occurred directly on the paper. This reactive paper spray scheme gleaned dramatically improved limits of detection (LOD) and lower limits of quantitation (LLOQ) for both THC in oral fluid and THC-COOH in urine. As a result, clinical and forensic cutoff values were able to be achieved by the developed reactive PS-MS method. The developed reactive PS-MS method was validated through comparison to LC-MS results from a clinical laboratory.

The PS-MS method utilized in collaboration with the Vancouver Island Drug Checking Project is primarily used for the quantitative, targeted measurements of drugs, but also includes interlaced non-targeted scans. Chapter 6 discusses how further analysis of the non-targeted scans from ongoing measurements at the Vancouver Island Drug Checking Project, revealed the appearance of two unknown compounds that began routinely appearing in over half of the carfentanil-containing drug samples tested.<sup>22</sup> Initial tandem MS experiments revealed that these compounds may be structural analogs of carfentanil. Solutions of these drug samples were directly infused into a high-resolution mass spectrometer to determine the chemical formula of these compounds. Further tandem MS experiments were used to determine the identity of these chemical compounds as desmethylcarfentanil amide and desmethylcarfentanil acid, structural analogs of carfentanil. LC-MS data from the Centre for Addiction and Mental Health in Toronto supported the identification assignment of these compounds. As structural analogs of carfentanil, one of the most potent synthetic opioids ever developed, it was hypothesized that these compounds may exhibit similar toxicities.  $\mu$ -Opioid receptor binding modeling determined that the binding poses and binding energies of these analogs to the  $\mu$ -opioid receptor were nearly identical to that of carfentanil, but further research is needed to determine the toxicities of these compounds. Chapter 7 concludes the work presented in this thesis and offers potential avenues for future work. The contents of Chapters 2 through 6 presented in this thesis have been peer reviewed and published in academic journals.<sup>18, 20-23</sup>

## 2 Mass Spectrometry Analysis of Drugs of Abuse: Challenges and Emerging Strategies

This chapter has been adapted from Borden, S.A., Palaty, J., Termopoli, V., Famigliani, G., Cappiello, A., Gill, C.G. and Palma, P., 2020. Mass spectrometry analysis of drugs of abuse: challenges and emerging strategies. *Mass Spectrometry Reviews*, 39(5-6), pp.703-744. doi.org/10.1002/mas.21624 with permission from John Wiley & Sons Inc.

### 2.1 Preface

Corresponding author P. Palma was invited by the editor to submit a review to *Mass Spectrometry Reviews* for special issues dedicated to Professor Dominic M. Desiderio (Volume 39, Issue 5-6). S.A. Borden produced all original figures and organized references. Sections 2.2, 2.3, and 2.9 were a collaborative writing effort between all listed authors. Sections 2.4 and 2.5 were primarily drafted by P. Palma, A. Cappiello, V. Termopoli, and G. Famigliani. Section 2.6 was primarily drafted by J. Palaty. Sections 2.7 and 2.8 were primarily drafted by S.A. Borden and C.G. Gill. All authors contributed intellectually and editorially to the final manuscript.

### 2.2 Abstract

Mass spectrometry has been the 'gold standard' for drugs of abuse (DoA) analysis for many decades because of the selectivity and sensitivity it affords. Recent progress in all aspects of mass spectrometry has seen significant developments in the field of DoA analysis. Mass spectrometry is particularly well suited to address the rapidly proliferating number of very high potency, novel psychoactive substances (NPS) that are causing an alarming number of fatalities worldwide. This review surveys advancements in the areas of sample preparation, gas and liquid chromatography mass spectrometry, as well as the rapidly emerging field of ambient ionization mass spectrometry. We have predominantly targeted literature progress over the past ten years and present our outlook for the future.

### 2.3 Introduction

Mass spectrometry (MS) is the accepted 'gold standard' in the broad field of drug analysis because of its sensitivity, specificity, and flexibility. In the area of toxicology, MS-based drug testing is used in a wide variety of applications such as establishing cause of death, monitoring prescription drug levels in blood, and verifying substance identity and levels in impaired driving cases. A literature search with Web of Science for 'forensic', 'drugs', and 'mass spectrometry' from 2010 to 2019 yields the following distribution of publications presented in Figure 2.1.

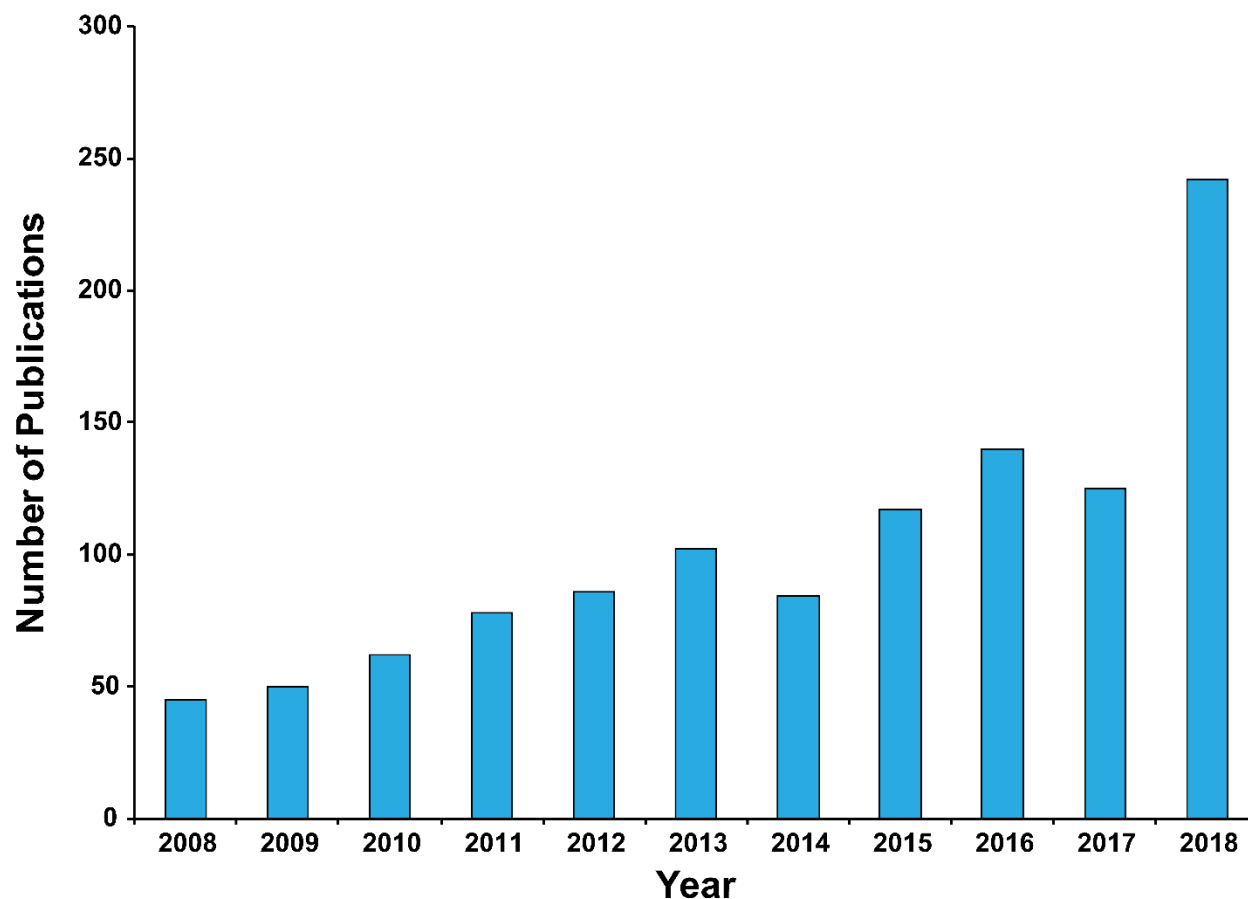


Figure 2.1 Growth of mass spectrometry-based drug testing publications between 2008 and 2019.

While assembling this review, it was immediately apparent that a complete review of all recent aspects of MS-based toxicological drug analysis would be better served by a book (or series), in order to address all facets of this complex field. To narrow the scope, we have chosen to focus upon the use of MS for the analysis of “drugs of abuse” (DoA) in terms of current practices in forensic toxicology and exploring areas of growth aimed at addressing unmet needs. We define DoA (better termed by the less stigmatizing “drugs of misuse”, or DoM) as compounds that include illicit substances (e.g., heroin) as well as those that may be used therapeutically but are also commonly misused for recreational (e.g., cannabinoids) or other (e.g., diversion of prescribed drug) purposes. These can be categorized broadly into the following areas: anti-depressants (e.g., benzodiazepines), stimulants (e.g., amphetamines, cocaine), opioids, hallucinogens and cannabinoids. We have purposely chosen to exclude alcohol, inhalants and tobacco from this list to further limit the scope for this review. Although topics addressed in this manuscript necessarily bridge all the disciplines identified above, we will predominantly focus upon the MS analysis of drugs that have important forensic relevance, which we define as providing definitive evidence for legal purposes, whether in living donors or post-mortem.

There is significant overlap between forensic drug testing applications and those from closely related fields, most notably clinical toxicology. Forensic toxicology, for example, measures drugs in the context of death or human performance (e.g., impaired driving, sports doping, workplace testing) in a wide range of sample matrices. Clinical toxicology, by contrast, deals with the impact of drugs in both acute poisoning and long-term monitoring (e.g., substance use disorders) and is largely confined to urine and blood. However, the differences between such fields dissolve with progression down the standard analytical sequence: for example, the methods used for compound identification by high-resolution MS (HRMS) in forensic, clinical, wastewater, and food residue applications are essentially indistinguishable. This review will cover sample preparation considerations, chromatographic methods such as gas and liquid chromatography separations coupled with MS, and the growing field of direct MS based methods including ambient and other ionization strategies. Each analysis strategy inevitably has specific advantages and challenges with respect to the classes of DoA, sample type and required sample preparation(s). The issue of whether qualitative or quantitative measurements are possible and/or required will also be examined.

## **2.4 Sample Preparation Considerations**

Given the diversity of sample types and analytes involved in MS-based drug measurements, we begin with a synopsis of the steps taken to prepare samples for analysis, including hydrolysis, derivatization (most common for gas chromatography, or GC) and extraction strategies. The emerging field of ambient ionization, where samples are directly measured, frequently obviates most sample derivatization and extraction steps, though several specific cases using solid phase microextraction (SPME) and other sample preparation methods will be discussed in section V.

### **2.4.1 Hydrolysis**

Sample hydrolysis to liberate free drugs from their metabolized conjugates is generally restricted to urine measurements, though this step is often omitted for 'dilute-and-shoot' liquid chromatography (LC) methods<sup>24, 25</sup>. While drug conjugates are amenable to MS analysis<sup>26-28</sup>, they show poor sensitivity and often lack commercially available standards. Hydrolysis is typically conducted with commercial glucuronidase enzyme, a product whose purity and activity has markedly increased. Historically, hydrolysis was achieved with either acid (which hydrolyzed acetylmorphine and compromised benzodiazepines) or fairly crude enzyme preparations of low activity, requiring hours to achieve even partial hydrolysis for the most resistant compounds such as codeine<sup>29</sup>. By contrast, Sitasuwan et al. reported >80% hydrolysis of codeine glucuronide with different recombinant glucuronidase products in 30 min<sup>30</sup>.

#### **2.4.1.1 Sample Extraction**

The classical extraction methods of DoA from various matrices are liquid-liquid extraction (LLE) and solid-phase extraction (SPE), and are still widely reported, despite the fact that they use large volumes of organic solvents (LLE) and are time-consuming. SPE offers

the advantage of high pre-concentration factors but requires larger sample sizes and a multistep procedure that can reduce analyte recoveries. The concept of “green chemistry”, centered on 12 principles, aims to reduce the environmental impact of synthetic chemistry <sup>31, 32</sup>. Green analytical chemistry in turn, is based on another 12 principles with the goal of combining good performance with environmental sustainability <sup>33</sup>. Microextraction techniques based on different concepts have been developed with the idea of “miniaturization” in mind and range from novel solid extracting phases to the use of very low volumes of solvents (micro to nanoliters). Novel solid-phase microextraction (SPME) techniques have been thoroughly reviewed, starting from the pioneering work of Arthur and Pawliszyn, who developed SPME in 1990 <sup>34</sup>, explaining advantages and disadvantages, application fields, and matrices of interest <sup>35</sup>. In another recent review, different microextraction techniques for the analysis of cannabinoids and their metabolites are described and discussed <sup>36</sup>, and an overview of the most common microextraction techniques applied to forensic toxicology for the determination of DoA in biological samples highlights the importance of sample preparation before introduction in the suitable instrument <sup>37</sup>. In this review, we limit our discussion to microextraction and green extraction techniques.

#### **2.4.1.2 Solid-Phase Microextraction**

SPME was first presented in 1990, and since then its use has increased steadily in various application fields <sup>34</sup>. In its most straightforward configuration, an SPME device consists of a fused silica fiber coated with an extraction phase fit on a syringe-like device (Figure 2.2).

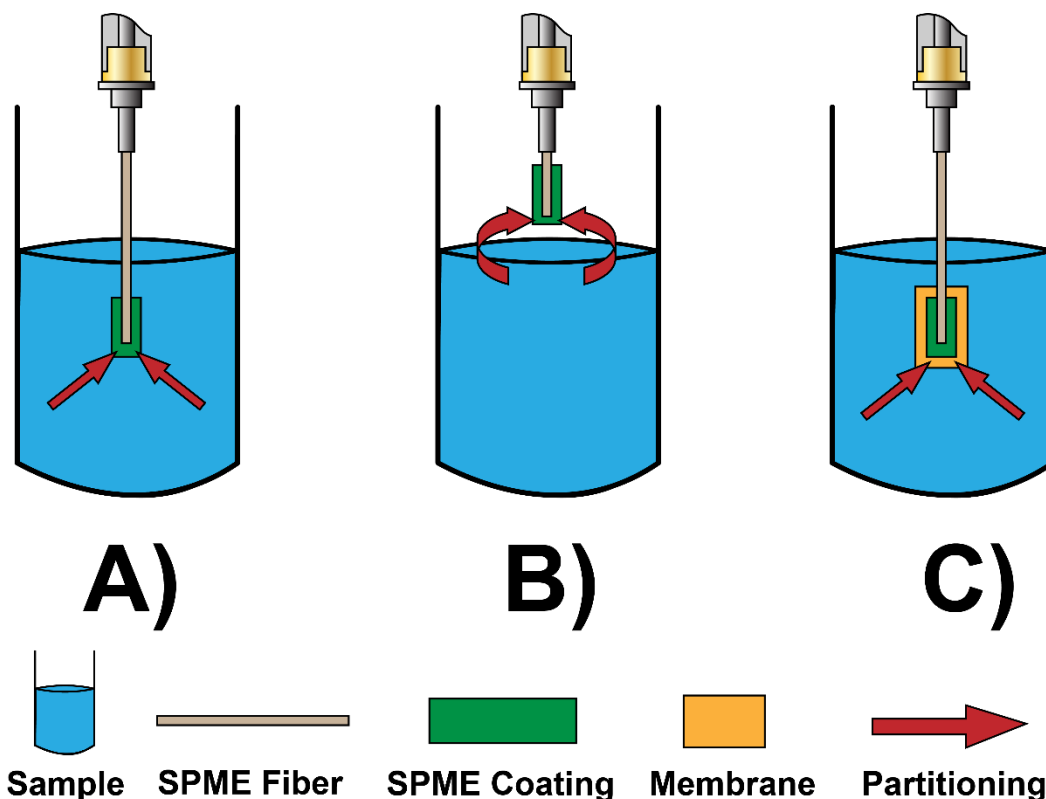


Figure 2.2 Extraction modes in solid phase microextraction (SPME). (A) Direct immersion SPME, (B) headspace SPME, and (C) membrane protected SPME. Not to scale.

The SPME fiber can be immersed directly in a liquid sample (DI-SPME) or exposed to its headspace (HS-SPME), with the extraction of the analytes based on partitioning between the two phases. Non-volatile, high-molecular weight compounds require a membrane-coated fiber for better reproducibility and accuracy. In general, DI-SPME has been used more frequently in LC-based methods, whereas HS-SPME is recommended for the extraction of more volatile and semi-volatile compounds typical in GC-MS measurements. If derivatization is needed, it can also be done directly on the fiber, prior to GC analysis.

DI-SPME-GC-MS has been used for the determination of levamisole and minor cocaine (COC) congeners in hair samples<sup>38</sup>, and amphetamines (AMPs) in oral fluid<sup>39</sup>. Various fiber coatings, extraction strategies and other variables (temperature, stirring, pH, in-tube, automation, etc.) have been presented<sup>40</sup>, demonstrating the versatility of this approach, which is still on the cutting edge, even 30 years after the original prototype was presented. A recent review examines all aspects of SPME in drug analysis and toxicology<sup>41</sup>. Among the most recent approaches, the use of a stainless-steel wire coated with acid-oxidized multi-walled carbon nanotubes has been reported for the HS-SPME of AMP-like stimulants in human urine before GC-Quadrupole (Q)MS analysis<sup>42</sup>. Particularly interesting is the use of microliter-scale tips equipped with biocompatible SPME fibers (polydimethylsiloxane-divinylbenzene; C18; C18-SCX silica) for the GC-QMS determination of amphetamines, cathinones and metabolites in human urine. Optimum derivatization was achieved with pentafluoro-propionic anhydride after extraction<sup>43</sup>.

HS-SPME was used to extract several amphetamines and tetrahydrocannabinol (THC) from DrugWipe®5 sweat screening devices. After HS sampling (10 min), the fiber was exposed for 3 min at 90 °C in another vial containing a derivatizing agent before final desorption into the GC-MS injector<sup>44</sup>. Polydimethylsiloxane coated fibers were used to extract fourteen illicit drugs belonging to the groups of phenethylamines, cathinones, a piperidine derivative, a tryptamine derivative, and synthetic cannabinoids in raw liquid, powder, and herbal samples using the direct-heating HS-SPME. Analytes were desorbed from the fiber into a GC-QMS instrument.<sup>45</sup> Other examples report the simultaneous determination of 17 compounds belonging to the classes of opioids, and AMPs<sup>46</sup>, as well as opiates in adult and pediatric hair using HS-SPME-GC-QMS.<sup>47</sup> The use of SPME in the extraction of cannabinoids has been thoroughly surveyed in a recent review article.<sup>36</sup>

#### 2.4.1.3 Microextraction with Packed Sorbent

The technique microextraction with packed sorbent (MEPS) is a miniaturization of SPE, in which the sorbent is immobilized within a special removable needle in a syringe-like device (Figure 2.3). This was first presented in 2004, and since then, MEPS use has been growing steadily<sup>48</sup>.

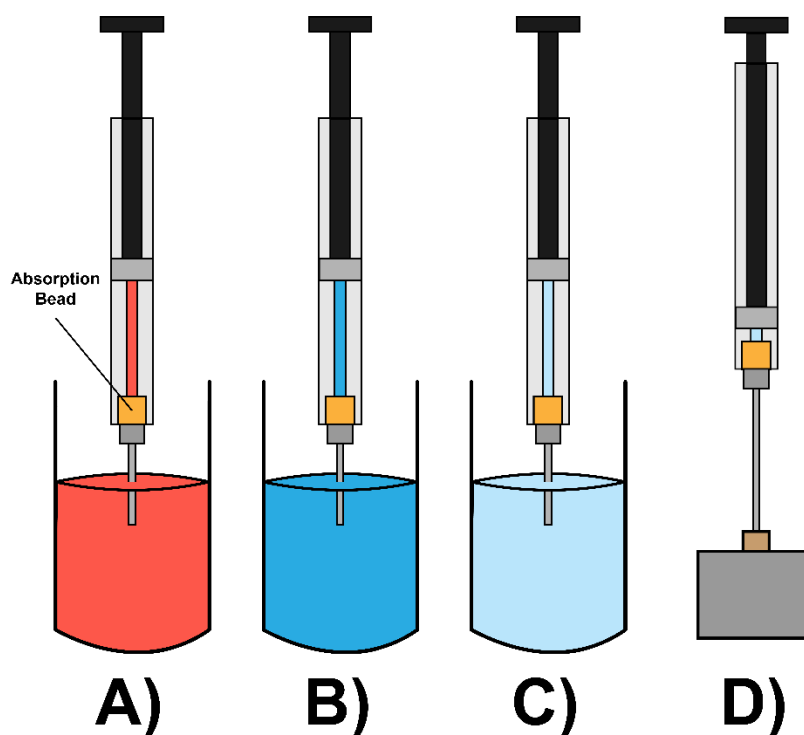


Figure 2.3 Microextraction with packed sorbent workflow. (A) Sampling, (B) washing, (C) elution solvent, and (D) injection. Not to scale.

The selection of sorbents for MEPS is the same as in conventional SPE. Sample loadings are typically between 10 and 250  $\mu\text{L}$ , and the devices can be operated either manually or automatically, as described in a comprehensive review by the inventor<sup>49</sup>. A fast method (15 min) based on MEPS-GC-QMS for the simultaneous determination of COC and its metabolites in human urine was recently reported<sup>50</sup>. Microwave-assisted derivatization

using N-methyl-N-(trimethylsilyl) trifluoroacetamide and 5% trimethylchlorosilane in 2 min has also been presented <sup>51</sup>. MEPS has been used in combination with micro pulverized extraction and aqueous acetylation for the determination of AMPs in human hair before GC-triple quadrupole (QqQ)MS analysis. The method presented is faster and more straightforward when compared with previous approaches for hair as a matrix <sup>52</sup>.

#### **2.4.1.4 Other Solid-Phase Extraction Approaches**

In solid-liquid extraction with low-temperature purification, analytes partition between a solid matrix and water-miscible organic phase at room temperature. When the temperature is lowered to -20 °C, the aqueous phase solidifies, and analytes in the supernatant organic-phase can be directly introduced into the GC-MS system. This procedure has been demonstrated with GC-QMS analysis of COC in eight post-mortem human livers <sup>53</sup>.

Disposable pipette extraction has been used as an alternative to classic SPE in the determination of COC and metabolites, nicotine and cotinine in meconium followed by GC-QMS. The solid phase is packed at the bottom of a pipette tip, and the operating protocol, though very similar to classic SPE, involves only a few microliters of solvent for analyte extraction <sup>54</sup>. Another interesting approach consists of the use of molecularly imprinted polymers for the SPE determination of AMP-like stimulants from whole blood <sup>55</sup>.

#### **2.4.1.5 Liquid-Phase Based Microextraction Techniques**

There are several extraction procedures described under the acronym of LPME, based on liquid-phase extractions with minimal amounts of solvent (e.g., microliters) to extract and pre-concentrate drug analytes from different samples. The main LPME techniques fall into three main groups: single-drop microextraction (SDME), dispersive liquid-liquid microextraction (DLLME) and hollow-fiber microextraction (HF-LPME). An exhaustive description of these techniques falls beyond the scope of this review, and only a simple introduction will be given. The principles of operation, advantages, and pitfalls are thoroughly explained in several review articles <sup>56, 57</sup>.

The basic principle of SDME utilizes a drop of organic solvent that is either immersed in an aqueous solution (direct-immersion-SDME) or suspended at the tip of a syringe (headspace extraction-SDME) <sup>58</sup> (Figure 2.4).

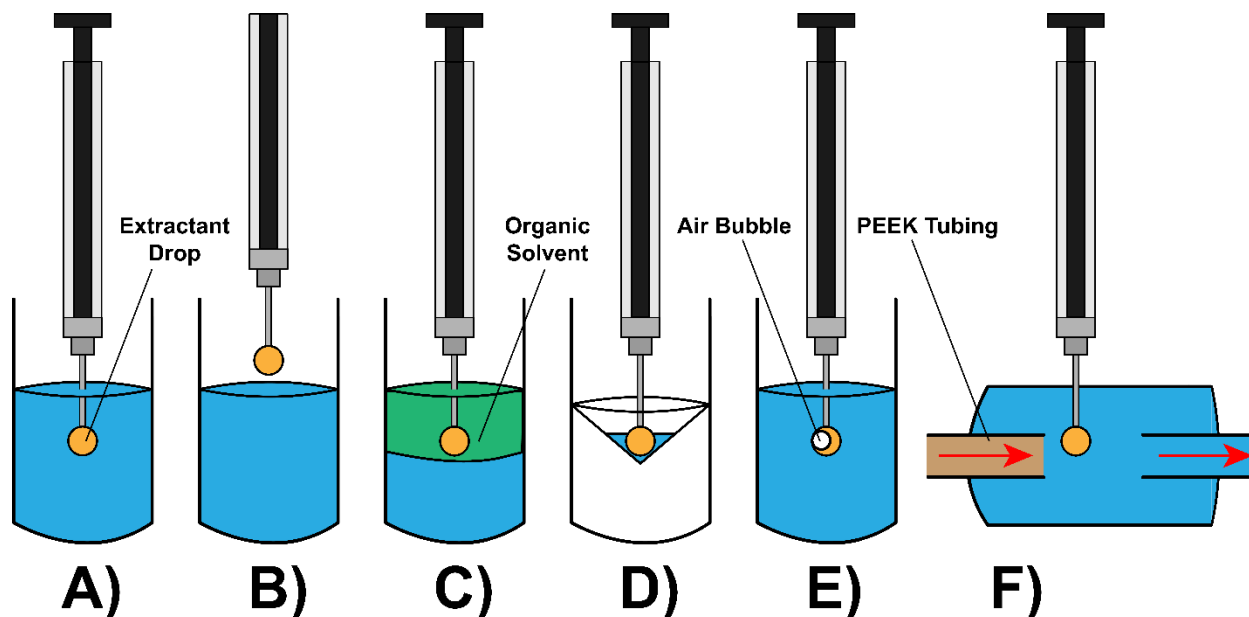


Figure 2.4 Extraction mode in single drop microextraction (SDME). (A) Direct-immersion SDME, (B) headspace SDME, (C), three-phase SDME, (D) drop-to-drop microextraction, (E) bubble-in-drop SDME, and (F) continuous-flow microextraction. Not to scale.

High enrichment factors are obtained because the volume of the acceptor phase drop is small (micro- to sub-microliters) and is done using simple equipment. In the case of headspace extraction, only volatile or semi-volatile analytes are sampled, further decreasing any interferences. Since its first introduction, several SDME modes have been presented to boost extraction efficiencies, such as three-phase mode<sup>59</sup>, bubble-in-drop<sup>60</sup>, and continuous-flow microextraction<sup>61</sup>. Recent reviews provide a comprehensive overview of SDME<sup>62, 63</sup>.

Presented in 2006, DLLME uses a ternary system comprised of an aqueous sample, a water immiscible extractive solvent, and a dispersive solvent (miscible with both water and the extractive solvent)<sup>64</sup> (Figure 2.5).

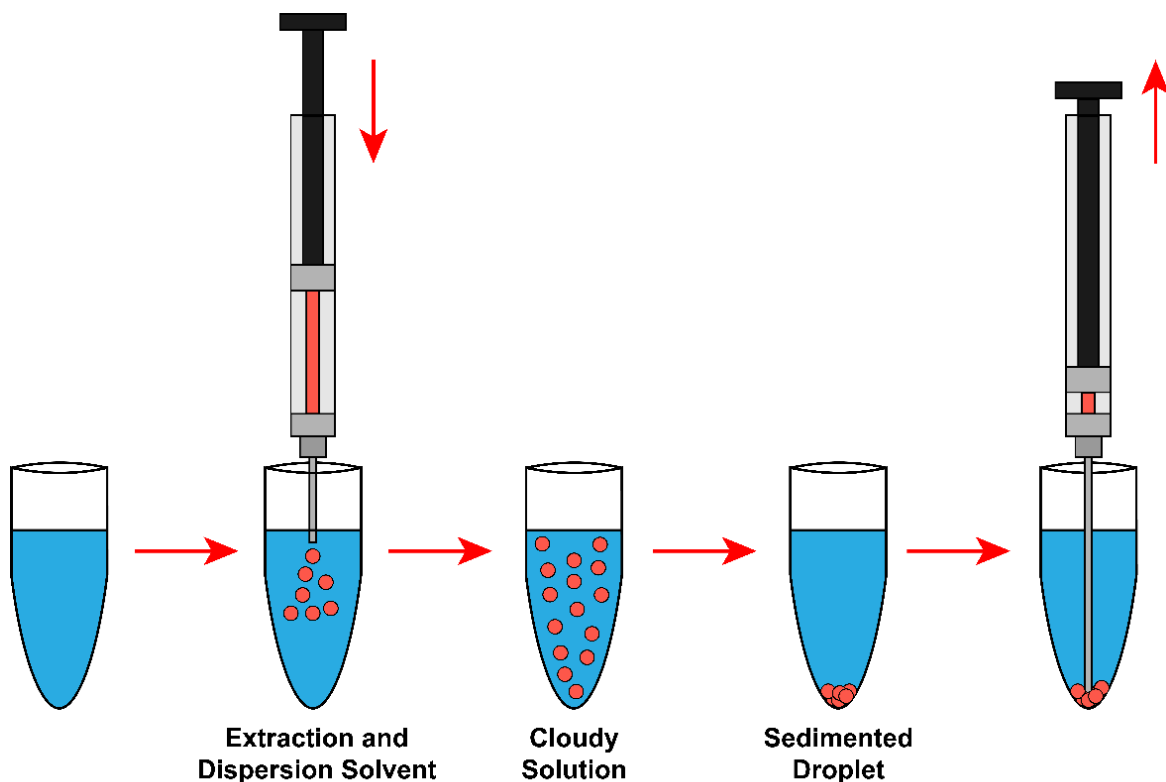


Figure 2.5 Classical dispersive liquid-liquid microextraction workflow. Not to scale.

Extractive and dispersive solvents are mixed and transferred into an aqueous sample, forming a cloudy emulsion. Rapid equilibrium and mass transfer of analytes between organic and aqueous phases is achieved. Centrifugation separates the extractive solvent containing the analytes at the bottom of the tube, which are subsequently removed with a syringe. Various strategies such as salt addition or ultrasound assistance, can be used to boost recoveries. DLLME has been widely used in DoA analysis because its simplicity, versatility, high pre-concentration factor, and extraction recoveries. DLLME has been used for the extraction of various classes of compounds of forensic interest, as reported in a recent review article <sup>65</sup>.

In the case of polar analytes, silylation is often used for derivatization, requiring anhydrous conditions to avoid silylating agent hydrolysis, since DLLME is mainly conducted in water. A combination of DLLME and injector port silylation (IPS) has been described and validated for the analysis of quinine in urine GC-MS <sup>66</sup>. A comparison of three extraction procedures, SPE, LLE, and DLLME was performed for the determination of fentanyl (FEN) in urine with GC-QMS. The results obtained for a real sample with the different techniques were in good agreement, demonstrating that the use of DLLME can be successfully utilized in forensic analysis <sup>67</sup>. The technique was also reported for the extraction of free AMP-type stimulants, fenproporex, diethylpropion, and sibutramine in urine before GC-QMS analysis. High recovery percentages (>91%) were obtained for all drugs. No derivatization was needed; the organic phase was withdrawn from the

extraction vial and injected directly in the GC-MS system <sup>68</sup>. In another study, two microextraction techniques, hollow fiber liquid-phase microextraction (HF-LPME) and ultrasound-assisted low-density solvent dispersive liquid-liquid microextraction (UA-LDS-DLLME) were applied and compared for the extraction of a variety of DoA in urine and blood samples, followed by GC-QMS analysis. UA-LDS-DLME makes use of ultrasound assistance for emulsification, avoiding the need for a dispersive solvent, making the technique even “greener”. These procedures are comparable in terms of simplicity, rapidity, and recoveries, albeit with slightly higher recoveries for UA-LDS-DLLME, spanning from 79 to >100%. LDS-DLLME is an excellent strategy to avoid possible matrix effects, and is faster than HF-LPME, but both techniques prove excellent for biological samples <sup>69, 70</sup>. Another investigation reported the use of UA-DLLME for the extraction of AMP-like drugs from whole blood before GC-QMS analysis <sup>71</sup>.

The HF-LPME technique was introduced in 1999 for the extraction of methamphetamine (MAMP) as a model compound from aqueous samples (human urine and plasma) <sup>72</sup> (Figure 2.6).

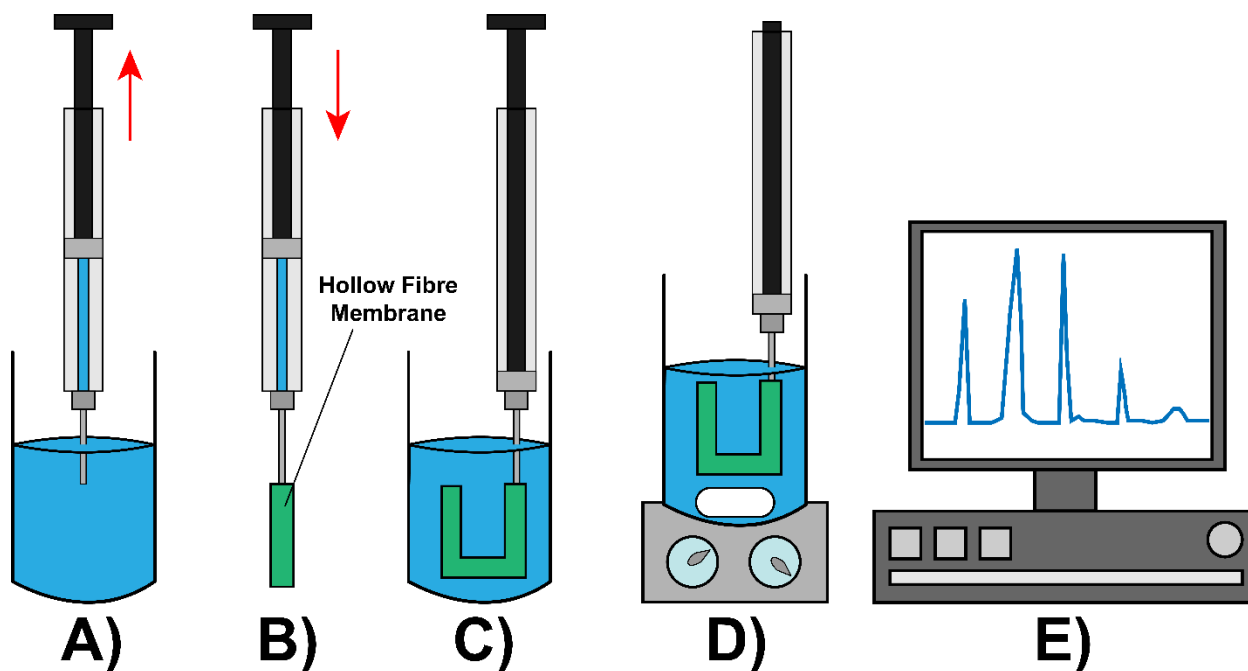


Figure 2.6 Steps of operation with hollow-fibre liquid-phase microextraction (HF-LPME). (A) Filling syringe with acceptor phase, (B) filling the HF lumen with acceptor phase, (C) bending the HF (U shape) and insertion into the aqueous sample, (D) agitation, (E) instrumental analysis. Not to scale.

In the classic mode of operation, organic solvent is trapped in the pores of a porous polypropylene hollow fiber, forming a thin layer on the walls. The internal volume of the HF is filled with a suitable acceptor phase solvent, and then the fiber is dipped into a vial containing the analytes in an aqueous sample (donor phase). The analytes are extracted from the donor to the acceptor phase via the organic solvent immobilized in the HF pores,

which has formed a supported liquid membrane. The extracted solution is then removed and analyzed. Depending on the number of phases, two-phase or three-phase HF-LPME can be distinguished: in the two-phase approach, the trapped organic solvent and acceptor phase are the same, and it is generally used for analytes immiscible with water. The three-phase approach is suitable for acidic or basic analytes with ionizable functions; the analytes in the aqueous sample are extracted via the immobilized organic solvent, and then into the aqueous acceptor phase inside the internal volume of the HF. The control of pH is key in this mode: analytes must be kept in their neutral form in the sample (donor) to dissolve into the liquid membrane, and the acceptor phase pH must be adjusted to ensure their subsequent extraction for analysis.

HF-LPME can also be conducted either in static or dynamic modes. Static mode uses vibration or stirring to speed up extraction into the acceptor volume, whereas dynamic mode, uses a syringe pump to repeatedly pull the aqueous sample in and out of the HF for more efficient extraction, requiring optimization and increased instrumental control<sup>73</sup>. Full automation has been proposed, where all steps could be performed by a commercial autosampler with dedicated software<sup>74</sup>. Various parameters can be adjusted to enhance extraction efficiency in HF-LPME, such as different fiber materials, organic solvents, pH, use of modifiers, temperature, stirring speed and time, and other variables linked to the instrumentation being used. A three-phase, static-mode approach was successfully used for the determination of amphetamines in 50 mg hair samples. After decontamination, hair samples were placed in tubes containing water with NaCl as a modifier, a three-phase HF-LPME using diethyl ether and a 0.1 M HCl solution as the acceptor phase allowed quantitative extraction of the analytes before GC-ion trap (IT)MS analysis<sup>75</sup>. An HF-LPME method based on two immiscible organic solvents, n-dodecane in the pores of the HF and acetonitrile as the acceptor phase, followed by GC-QMS detection was validated for the efficient extraction and determination of COC, ketamine (KET), and lidocaine in human urine. No additional cleanup was needed, and LODs were sufficiently low for toxicological analyses<sup>76</sup>. Another article reports the GC-QMS determination of 11 benzodiazepines (BDZs) and their main metabolites using three-phase mode HF-LPME from human urine. The analytes were derivatized using tert-butyldimethylchlorosilane, and/or trifluoroacetic anhydride<sup>77</sup>.

#### **2.4.1.6 Other Liquid-Phase Extraction Approaches**

Switchable hydrophilicity solvents (SHS) can switch between two forms: hydrophobic and immiscible in water when in air, and fully miscible in water when in an atmosphere of CO<sub>2</sub><sup>78, 79</sup>. These solvents (e.g., N,N,N'-tributylpentanamidine; N,N-dimethylcyclohexylamine) can be used in microextraction techniques<sup>79</sup>. Liquid-liquid microextraction based on switchable hydrophilicity solvent (SHS-LLME) has been validated for the GC-QMS determination of 11 DoA in the urine of a suspected KET user. The method involves small amounts of solvent ( $\leq 500 \mu\text{L}$ ) and is a "green" alternative<sup>80</sup>.

## 2.4.2 Derivatization

For GC-MS analyses, derivatization is frequently necessary to increase the thermal stability and volatility of polar, thermolabile, and low volatility compounds. It employs a myriad of chemical modifications to achieve this, including acetylation (AC), trifluoroacetylation (TFA), pentafluoropropionylation (PFP), heptafluorobutyration (HFB), trimethylsilylation (TMS) for basic compounds. Methylation (ME), extractive ME, PFP, TMS, and tert-butyldimethylsilylation (TBDMS) are typically used for acidic compounds<sup>81</sup>. As described later in the GC-MS section, negative ion chemical ionization (NICI) in GC-MS is frequently used in trace analysis for its high sensitivity. In the case of compounds without electronegative substituents, a suitable derivatization reaction is employed to add them. Perfluoroacyl and pentafluorobenzyl (PFB) derivatives are typically used, though sometimes they exhibit extensive fragmentation, leading to low molecular ion abundances. Frequently, *o*-(pentafluorobenzoyloxycarbonyl)-benzoylchloride (PBBCl) and *o*-(pentafluorobenzoyloxycarbonyl)-2,3,4,5-tetrafluorobenzoyl chloride (PBTFBCl) are used as derivatizing agents for primary and secondary amines to achieve high sensitivity in NICI-GC-MS analysis, such as for the measurement of methylphenidate<sup>82</sup> and AMPs in plasma<sup>83</sup>. In another example, 11-nor-9-carboxy- $\Delta^9$ -tetrahydrocannabinol (THC-COOH) in urine is considered a valid biomarker for cannabis use, extracting THC-COOH from the matrix via SPE before derivatization. A silylation procedure with *N,O*-bis-trimethyl-silyl-trifluoroacetamide (BSTFA) has also been validated and optimized for use with GC-IT tandem MS (MS/MS)<sup>84</sup>. THC and COC have been extracted from hair samples and analyzed with GC-QMS without derivatization. Hair samples were decontaminated with dichloromethane, enzymatically digested with Proteinase K, then extracted by LLE with pentane. The organic fraction was neutralized, evaporated, then reconstituted with hexane before injection<sup>85</sup>.

Injection port silylation has been used for  $\gamma$ -hydroxybutyrate (GHB) GC-MS measurements, where GHB is converted into di-trimethylsilyl derivatives just prior to analysis. Derivatization occurs in the GC injection port, yielding a faster reaction and avoiding derivative degradation that can occur during off-line silylation. IPS has been used to produce GHB and trans-4-hydroxycrotonic acid (used as a potential internal standard) derivatives using *N*-methyl-*N*-[tert-butyldimethylsilyl]trifluoroacetamide with tert-butyldimethylchlorosilane (99:1) to determine the concentration of endogenous GHB in urine samples, optimizing injector temperatures to achieve the highest derivatization yields. This method has been applied to toxicological analyses<sup>86</sup>.

The use of monolithic silica spin columns has been proposed for the simultaneous extraction and derivatization of AMPs in human urine. The procedure is very similar to a classic SPE extraction with cartridge pre-activation, sample loading, and washing steps, but is done in an apparatus spinning at 5000 rotations per minute (rpm). In the last step, both elution and derivatization with ethyl acetate containing 1% propyl chloroformate occur at the same time, with centrifugation rate determining derivatized analyte elution times. This method is "green", requiring small solvent volumes and no evaporation,

reducing sample loss, and is easy to perform <sup>87</sup>. An “in-vial” derivatization procedure has also been proposed for GHB methylation in urine, plasma, and whole blood that reduces reagent quantities and accommodates small sample volumes <sup>88</sup>.

Microwave heating can be exploited to speed up derivatization protocols, reducing them to a few minutes, because higher temperatures can be reached in less time. In an interesting study, three popular derivatization reactions were evaluated, demonstrating the time-saving advantages over conventional heating: acetylation for morphine (MOR) and codeine (COD), pentafluoropropionylation for 6-monoacetylmorphine (6-AM), and trimethylsilylation for THC. Detection was achieved in these studies using GC-MS, LC-MS and LC-MS/MS <sup>89</sup>. An orthogonal design was also proposed to improve the performance of microwave-assisted derivatization of AMP and MAMP followed by NICI-GC-MS using 2,3,4,5,6-pentafluorobenzoyl chloride as derivatization reagent <sup>90</sup>. In another investigation, microwave assistance was satisfactorily used for on-spot derivatization of GHB and gabapentin for their determination in dried blood spots <sup>91</sup>. The quantitative trimethylsilylation of 11 phenylalkyl amines, including AMP and 3,4-methylenedioxiamphetamine (MDA), in urine using N-methyl-N-(trimethylsilyl)-trifluoroacetamide in several solvents in the presence of suitable catalysts has also been presented, and is highly efficient using microwave heating when compared to other procedures <sup>92</sup>.

## **2.5 Gas Chromatography Mass Spectrometry**

### **2.5.1 Introduction, History**

In this section we give an overview of research utilizing GC-MS since 2010 related to the analysis of DoA in different biological matrices.

The list of illicit drugs has increased rapidly because of the emergence of new drug classes (new psychoactive drugs, NPD). In 2016, the EU (European Union) Directorate-General for Internal Policies published a review of EU drug policy revealing that, in general, cannabis is the most commonly used drug in the EU, followed by COC, MDMA, and AMPs). The use of the different drugs can vary considerably between countries; however, there is an increasing tendency for the use of NPD. Immunoassays can be used for rapid confirmatory screening tests but are not available for all compounds. In the case of positive immunoassay results, suitable analytical methods and techniques are needed to identify and quantify the increasing number of potential substances, focusing on identification, confirmation, and quantitation. When analytes are unknown, efficient GC, and/or comprehensive, two-dimensional (2D) gas chromatography (GCxGC) separations, coupled with electron ionization (EI) MS are used. This strategy provides fragment rich mass spectra and remains the reference technique of choice for the analysis of volatile, semi-volatile, low-polarity, low-molecular weight (MW), and non-LC-MS amenable DoA <sup>93, 94</sup>, despite the fact that in many cases, elaborate sample preparation and derivatization steps are required.

## 2.5.2 Ionization Techniques

The ionization technique of choice in GC-MS is EI for the majority of drugs, providing legally defensible identification and reliable qualitative and quantitative analysis at high sensitivity and selectivity. EI is a gas-phase, hard ionization technique that occurs in a high temperature and high vacuum environment. Because of this, ion-ion or ion-molecule reactions are unlikely to occur. Consequently, matrix effects are very limited or absent, compared to LC-MS. The ionization process is the result of intra-molecular reactions only and is reproducible with a wide variety instruments and conditions, not influenced by external agents that can also be present in the ion source. This results in highly reproducible mass spectra that can be compared with those present in spectral database libraries such as National Institute of Standards and Technology (NIST), MassBank, and others, for the unequivocal identification of the analyte. Those libraries can be used when confirmation is needed (targeted analyte), but also in the case of untargeted analytes.

In the case of scarce or absent molecular ion formation, and to follow metabolic pathways of new designer drugs, positive-ion chemical ionization (PCI) can be used to obtain information on the molecular weight <sup>95-97</sup>. In the analysis of AMPs in urine <sup>98</sup>, EI yields a high degree of fragmentation, with interfering low m/z ions that limit selectivity and interfere with ion intensities. These authors tested different PCI reagents (methane; methanol; acetonitrile; carbon disulfide; tetrahydrofuran; furan), obtaining the highest selectivity with furan. The metabolism of three designer drugs, mephedrone, butylone, and methylone was also followed in rat and human urine using PCI-GC-MS <sup>99</sup>. NICI with GC-MS has been reported in several studies for the determination of cannabinoids in hair <sup>100</sup> as well as BDZs and associated metabolites in whole blood <sup>101, 102</sup>, using methane as the reagent gas. NICI was also used for the determination of 50 DoA belonging to different classes in oral fluid as an alternative sample matrix <sup>103</sup>. MDMA and its unconjugated phase I metabolites, have also been analyzed with NICI-GC-MS in human urine <sup>104</sup>. The value of integrated GC-EI-MS and GC-NICI-MS in human hair to give higher sensitivity and complementary results has also been demonstrated for opiates, AMPs, MDMA, KET, and metabolites <sup>105</sup>.

An innovative interface to obtain enhanced molecular ions, while retaining library matchable typical EI spectra, has been proposed by Amirav <sup>106</sup>. It is called GC-MS with Cold EI, based on EI of vibrationally cold molecules in supersonic molecular beams. An additional advantage of this interface is that sensitivity is not influenced by the column flow rate; therefore, this can be increased up to 100 ml/min for fast screening without losing sensitivity, and the authors have demonstrated its use for the fast analysis of heroin (HER) and COC.

A unique approach to obtain soft ionization in GC-MS has also been presented by the Zenobi Group. They use a dielectric barrier discharge ionization (DBDI) source <sup>107</sup>, in which an appropriate voltage is applied to an active capillary plasma source connected to the MS inlet. A low-temperature plasma is formed within the device, yielding [M+H]<sup>+</sup> ions with almost no fragmentation or adduct formation with either air or nitrogen as plasma

gases. This source has been successfully used to measure 14 DoA in a standard mixture<sup>107</sup>. The DBDI source is further discussed later in the ambient ionization section.

### 2.5.3 Analyzers

Single-stage, low-resolution quadrupole mass analyzers are the workhorse in DoA analysis because of their simplicity, relatively low-cost, and operation in both in full-scan and in selected-ion monitoring (SIM) modes. Most GC-MS publications still utilize this type of analyzer for measurements in many different sample matrices (e.g., urine, blood, hair, nails, oral fluid, etc.), providing limits of detection (LOD) suitable for many forensic and toxicological purposes. Superior sensitivity and selectivity can also be achieved with ion trap (IT), hybrid Q-Time of Flight (Q-TOF), Orbitrap, and triple quadrupole (QqQ) analyzers operating in MS/MS mode. Their use has increased enormously in the last few years in DoA analysis as well as many other diverse areas, particularly when coupled with LC-MS and ambient ionization methods, as will be discussed later.

#### 2.5.3.1 Quadrupole

DoA can be used in criminal activities, often in combination with alcoholic drinks, for so-called drug-facilitated crimes, where the victim is involuntarily incapacitated, leaving them with no memory of the subsequent assault. A wide range of drugs have been used in drug facilitated crimes, making their identification in biological specimens and beverage/food residues challenging, especially when considering their rapid excretion and/or metabolite formation. GC-EI-QMS has been used for the simultaneous determination of 128 drug-facilitated sexual assault drugs in urine, after SPE extraction<sup>108</sup>. Quick, Easy, Cheap, Effective, Rugged and Safe (QuEChERS) extraction method followed by GC-QMS was used for the determination of eight BDZs in a milk-based alcoholic drink, a complex matrix due to the presence of proteins and fatty acids<sup>109</sup>. Other examples of the detection of BDZs and KET in common alcoholic and non-alcoholic drinks can be found in the literature<sup>110, 111</sup>.

A rapid screening, fast GC-MS method, utilizing a short column (10 m x 0.18 mm i.d., 0.18  $\mu$ m film thickness) and QMS was developed for THC-COOH, COC, opiates, buprenorphine (BUP), FEN and metabolites in urine in 6 minutes<sup>112</sup>. The same approach was used for the determination of 52 stimulants and narcotics in urine<sup>113</sup>. The same authors also describe the simultaneous determination of several fentanyl and their metabolites in urine<sup>114</sup>. Twenty-five DoA in blood and urine were simultaneously determined using a GC-QMS after flash derivatization directly in the matrix and DLLME extraction<sup>115</sup>.

Hair is a complementary matrix to urine and blood for screening DoA, and GC-QMS proved to be a valid and less expensive alternative to LC-MS/MS approaches for this matrix<sup>116</sup>. In many cases, hair is preferable to fluids because it is easier to collect and store, and provides detectable drug signatures after extended periods from the time of use. A comprehensive review of analytical methods for various classes of DoA in hair offers an overview of pre-treatment steps and analytical approaches<sup>117</sup>. An example is the identification and quantification of DoA in human hair using GC-QMS in SIM mode.

Opiates were extracted using a mixed-mode SPE from a small amount of hair samples and semi-quantitatively determined by GC-QMS<sup>118</sup>. GC-QMS was used to identify and quantify six designer synthetic cathinones in human urine<sup>119</sup>.

Sweat represents another non-invasive, simple matrix for DoA screening, and it can be collected by DrugWipe®5A, a sweat drug screening device. The device is used to rub the forehead skin, allowing the simultaneous detection of opiates, COC, AMP/MAMP, and cannabinoids. If the result is positive, a second sample is collected and analyzed using HS-SPME followed by GC-MS. This two-tiered approach allows the determination of a wide range of DoA with GC-QMS<sup>44</sup>. This HS-SPME GC-QMS strategy has been used for the determination of the same DoA in hair<sup>120</sup>.

Another matrix that is gaining attention in forensic analysis is fingernail clippings. DoA accumulate inside the nails, remaining stable for a long time. AMP-like drugs and KET can be successfully extracted from nails and determined with GC-QMS<sup>121</sup>. Teeth are another alternative tissue that can be used for drug testing, together with nails, hair, and bones, even in post-mortem specimens. Teeth are much more resistant to degradation from temperature and pressure than other tissues and can be used to detect drugs for an extended period of time in post-mortem samples. Following the same sample preparation used for hair, cannabinoid compounds were determined in teeth with GC-QMS<sup>122</sup>. AMP can be determined in oral fluid, an easily collected matrix that is also difficult to adulterate<sup>123</sup>. Cannabinoids have also been extracted from human breast milk samples using HS-SPME and quantified using GC-QMS<sup>124</sup>. The same authors also investigated LPME as extraction method for cocaine-like compounds and metabolites from human breastmilk followed by GC-QMS analysis<sup>125</sup>. An uncommon specimen for DoA testing is human placenta, which has been analyzed with GC-MS for DoA and other compounds<sup>126</sup>. In this work, human placenta from a voluntary pregnancy interruption was used, but non-invasive tissue collection in a full-term pregnancy is feasible and would be able to provide evidence of in utero exposure.

In emergency toxicology, fast semi-quantification of analyte/s is imperative to make a fast, life-saving decision regarding the most suitable treatment for the patient. A fast LLE, multi-analyte procedure was developed for the quantification of 40 DoA in urine, followed by full scan GC-QMS and one-point calibration<sup>127</sup>.

### **2.5.3.2 Ion Traps**

One of the potential limitations of ITMS is matrix interference, which can lower sensitivity when working in full scan mode. On the other hand, it offers the possibility to perform tandem MS experiments with less expensive instrumentation. GC-ITMS was used in the determination of trace levels of N,N'-dimethyltryptamine in beverages, such as Ayahuasca and Vinho da Jurema, often consumed in religious rituals in South America<sup>128</sup>. Ecstasy (MDMA) and metabolites in plasma and urine were also determined using GC-ITMS<sup>129</sup>. The simultaneous quantification of cocaine-like compounds and opioids in blood, muscle tissue, and water (as a simulation of the vitreous humor) demonstrated the advantages of GC-ITMS/MS to remove matrix interferences while preserving good

sensitivity and selectivity <sup>130</sup>. Cannabinoids were extracted from hair samples using HS-SPME and determined using GC-ITMS/MS <sup>131</sup>. The same research group reports the extraction of the same compounds from human hair samples using HF-LPME followed by GC-ITMS/MS. A factorial design was employed to optimize the operative conditions <sup>132</sup>. Several barbiturates were also determined in head hair samples with prior alkaline digestion and LPME <sup>133</sup>. PICI GC-ITMS was also used in the determination of GHB and its precursors,  $\gamma$ -butyrolactone and 1,4 butanediol in dietary supplements, utilizing isotope dilution MS <sup>134</sup>. Pregabalin has been determined in hair samples using GC-ITMS/MS coupled with ethyl chloroformate derivatization and DLLME <sup>135</sup>.

### **2.5.3.3 Time-of-Flight**

To date, a very limited number of publications report the use of TOF in the GC-MS analysis of DoA. This analyzer offers fast scanning and sufficient data points across the peak, and for this reason, it is more advantageous for fast-GC and GCxGC. An example is given by the determination of 35 BDZs in urine, preceded by SPE <sup>136</sup>. In the case of fast separations and GCxGC, high-speed TOF instruments allow the detection of narrow peaks with nominal mass resolving power.

### **2.5.3.4 Orbitraps**

In the growing world of NPS, there is a mandatory requirement for fast identification and quantification in seized materials. In most cases, neither certified standards nor scientific data are available. High-resolution mass spectrometry (HRMS) using different analyzers, such as Orbitrap (and TOF) can provide sufficient mass accuracy to resolve isobaric ions for possible identification of untargeted compounds <sup>137</sup>. The only drawbacks of such high-end systems are their higher costs and the need for highly trained personnel. In an interesting study, Frison et al. used a combined approach that included GC-QMS, Orbitrap LC-electrospray ionization (ESI), ESI-MS<sup>n</sup> ITMS, and nuclear magnetic resonance (<sup>1</sup>H and <sup>13</sup>C NMR) for the characterization of 102 seized powders. This multiple approach allowed the identification and the molecular structure characterization of a new designer drug, a KET analog called deschloroketamine <sup>138</sup>. Recently, Orbitrap technology with GC-HRMS was used to develop a high-throughput screening for 288 DoA and poisons in human blood <sup>139</sup>.

### **2.5.3.5 Triple Quadrupole**

Many procedures report the use of QqQ analyzers in the GC-MS/MS determination of DoA in various matrices because of their quantitative highly reproducible results, high sensitivity, and specificity via multiple reaction monitoring (MRM). Examples include the determination of AMP-type stimulants in blood and urine <sup>140</sup>, THC-COOH in oral fluid <sup>141</sup> and in human plasma <sup>142</sup>, KET and norketamine (NKET) in urine and plasma <sup>143</sup>, and GHB in ante-mortem and post-mortem whole blood samples <sup>144</sup>.

### **2.5.3.6 Two-Dimensional Gas Chromatography**

The development of two-dimensional gas chromatography (2D GCxGC; GCxGC) represents an outstanding step forward for GC analysis. This approach was first developed in 1991 <sup>145</sup> and has become very popular because of its vastly improved peak

capacity, especially for very complex samples, where MS identification can be impaired by matrix composition and co-eluting analytes. There are numerous advantages that 2D GCxGC offers over 1D GC, including superior increases in selectivity, sensitivity, and separation power. Two exhaustive reviews on this topic appeared in 2008<sup>146</sup> and 2016<sup>147</sup>, describing the many advantages over 1D GC, and recent advancements made in combination with different MS analyzers. Mitrevski et al. have reviewed 1D and 2D GCxGC methods in drug profiling, highlighting differences and advantages of the two approaches<sup>148</sup>.

To simply describe GCxGC, two columns, generally of different polarities, are connected in series with a transfer system called a modulator. The first column is a conventional GC column that separates the analytes based on their volatility, generating peaks typically 30-60 s wide. The modulator collects, focuses, and injects the eluting peak into the second column in a few short pulses. The second column is a short (1-2 m) microbore column that allows very fast separations, typically a few seconds. The combination of the refocusing process and orthogonal separation increases the number of peaks being resolved, boosting analyte profiling. The chromatographic peaks are very narrow and rapidly eluting, requiring fast acquisition rates.

Low-resolution TOF is by far the most popular because of its high sensitivity, fast scanning speed, and full spectrum acquisition. For example, residues of opiates, opioids, cocaine-like compounds, sedatives, and other drugs were quantitatively screened in three hair samples using GCxGC-TOF-MS. Their identification was confirmed using automated library spectra searches<sup>149</sup>. GCxGC-TOF-MS was employed for MDMA extracts<sup>150</sup>, HER and COC profiling with pixel-based chemometric processing<sup>151</sup>, and compared with GC-QMS in targeted and non-targeted analysis<sup>152</sup>.

New generation, rapid-scanning QMS can also be coupled with GCxGC. These analyzers offer a less expensive option for qualitative purposes and identification confirmation because of their fast acquisition speeds (compared with older systems), and there are indications that they can allow for quantitative analysis. Kolbrich and coworkers used a GCxGC-QMS system for the simultaneous quantification of amphetamines and metabolites in human plasma prior to derivatization<sup>153</sup>. GCxGC-QMS was also used in a validated method to extract (SPE) and quantify buprenorphine (BUP) in post-mortem blood samples<sup>154</sup>. GCxGC was successfully used for the detection of THC-COOH in human fingernail clippings and head hair with a detection limit of 10 fg/mg using a QqQMS detector<sup>155</sup>.

## **2.6 Liquid-Chromatography Mass Spectrometry**

### **2.6.1 Introduction**

In this section, we focus primarily on mass spectrometry combined with liquid chromatography for the analysis of a large number of chemically diverse DoA in biological matrices (rather than seized drugs) and discuss issues related to sample preparation, instrumental techniques of separation and identification. Our aim is to describe selected

broad-spectrum screening methods used in daily production work rather than proof-of-concept studies or methods aimed at a specific class of compounds. The area of forensic LC-MS has been reviewed extensively over the years by the Maurer group<sup>156-158</sup>.

The compatibility of an LC-MS screen with a large and rapidly evolving number of compounds is essential in forensic toxicology, as the samples encountered are typically positive for multiple drugs and metabolites<sup>159</sup>. However, “forensic” toxicology, as noted in the Introduction, also includes fields where a limited range of target compounds has been clearly defined by a regulatory agency. The reader is also referred to literature from related fields, most notably wastewater,<sup>160</sup> metabolomics,<sup>161</sup> pesticide residue analysis,<sup>162</sup> where similar challenges and techniques are encountered. The accepted rule in forensic (vs clinical) toxicology is that initial identification of a drug must be confirmed by a second orthogonal method<sup>163</sup>. As a result, most of the methods described here are confined to a qualitative screening, with the intention of subsequent confirmation being performed with a targeted quantitative assay.

### 2.6.2 Sample Preparation

As per any type of analytical step, the sample preparation method must consider the classic trio of cost, quality, and time. A busy clinical laboratory dealing with an overdosed patient may opt for an ‘dilute-and-shoot’ procedure for urine<sup>164, 165</sup> or solvent precipitation<sup>166</sup> for serum, while a forensic lab may choose a more robust and comprehensive method despite the added cost and time<sup>167</sup>. Moreover, both clinical and human performance testing are largely confined to a small number of matrices (i.e., urine, serum, blood), and even dermal absorption samples,<sup>168</sup> while a forensic lab must be prepared to process a wide range of ante-mortem and post-mortem sample types (e.g., hair, nails, gastric contents). The specificity of sample preparation may also be dictated by the range of compounds sought, so specific extraction methods are often contraindicated in broad-spectrum testing. The role of automation should also be considered: specifically, whether the gains in productivity are justified by the increased risk of contamination between samples. We will survey these methods in turn, starting with the most basic.

A simple dilution of the sample (typically urine) with solvent containing internal standards is widely used owing to its ease and speed as well as having the non-specificity needed for broad spectrum testing.<sup>169</sup> Two drawbacks of this technique are its limitation to unconjugated drugs present at relatively high concentrations, and the potential for significant sample matrix effects. However, the approach is ideal for the analysis of seized synthetic drug powders where dilution, rather than any concentration or matrix removal, is all that is needed.<sup>170</sup> Preparation of seized biological products for the identification of low-concentration drugs such as synthetic cannabinoids, by contrast, is considerably more involved.<sup>171</sup> A variant of the ‘dilute-and-shoot’ procedure is protein precipitation, where sample proteins are precipitated with an appropriate mix of solvents, retaining the target compounds in solution. This step is typically only done once, though some have found two cycles to be more effective.<sup>28</sup> Protein precipitation is amenable to a broader

range of matrices, including various forms of blood, and has a low compound specificity that is ideal for broad-spectrum screening.

LLE has been the classic technique for GC-MS sample preparation but is diminishing in use with the growing popularity of both automated liquid handlers (to which LLE is poorly suited) and LC-MS, with its acceptance of aqueous samples requiring minimal preparation. LLE is infrequently used in broad-spectrum analysis<sup>172</sup> and is seen more often in group-specific testing.<sup>173</sup> Two interesting versions of LC-MS-aimed LLE have recently appeared in the drug testing literature. The first is the use of ionic liquids, which have attractive features such as an exceptionally low ratio of extracting solvent to sample and no requirement for an evaporation step. Unfortunately, recoveries tend to be modest, matrix effects high and use to date has been restricted to non-polar drugs, such as anti-depressants<sup>174</sup> and BDZs.<sup>175</sup> There is also the problem of isolating the (heavier) extracting solvent from the sample-solvent mixture, though the use of magnetic ionic liquids has been suggested as a means of making the process compatible with lab automation.<sup>176</sup> The other recent development in LLE is the use of supramolecular solvents, where essentially quantitative recovery with negligible matrix effect has been reported for 11 illicit phenethylamines extracted from oral fluid with a mixture of alkaline hexanol and tetrahydrofuran.<sup>177</sup>

Solid phase extraction (SPE) has seen extensive use in forensic broad-spectrum applications.<sup>178-181</sup> This approach typically combines cation exchange with hydrophobic interaction: while this works well for most drugs, there may be significant blind spots for small polar or neutral species such as GHB and alcohol. Some groups<sup>182, 183</sup> have addressed this problem by targeting minor metabolites of such species (e.g., glucuronides, carnitines), which have sufficient hydrophobicity to improve both extraction and chromatographic retention, but the incorporation of these drugs into a broad-spectrum assay remains an elusive challenge. On the other hand, inefficient extraction may be desirable for compounds such as gabapentin, where even therapeutic concentrations may be far higher than those of other drugs.<sup>184</sup>

The lengthy commitment of the MS instrument to signal acquisition during a typical chromatographic separation has prompted the exploration of parallel online extraction methods such as turbulent flow chromatography (TFC), to exploit this available time increase throughput. Grant has described a multiplex TFC to process >1000 serum samples per day but pointed out that the greatest gains can only be realized with a minimal acquisition window i.e., a small portion of the LC run.<sup>185</sup> TFC has also been used with the goal of reducing manual handling rather than increasing throughput: a single-channel TFC instrument was used to analyze serum, urine and whole blood for a broad mix of compounds ranging from acetaminophen to diazepam using three extraction columns in series linked to a phenylhexyl separation column.<sup>186</sup> With plasma samples, TFC combined with protein precipitation offered a slight reduction in matrix effect and improved recovery of lipophilic species such as diazepam while protein precipitation alone provided superior recovery for polar compounds (e.g., opiates).<sup>187</sup>

### 2.6.3 Separation Methods

While chromatographic procedures for drug analysis exist in countless forms, the needs of a forensic broad-spectrum analysis veer towards the non-specific and so the choice of chromatographic conditions needs to be a compromise between the most polar analytes (e.g., benzylpiperazines, GHB, opiates) and the least (e.g., BDZs, cannabinoids). While earlier workers regularly used C18 columns having a solely partition-based mechanism of retention, the current trend is towards a stationary phase with an additional pi-pi component (e.g., biphenyl, phenylhexyl). An alternative approach to polar analytes is to target a minor (but less polar) metabolite rather than the parent compound (see above).

Separation methods need not be confined to chromatography, with much recent interest in ion mobility (with or without LC) to very rapidly provide some separation of species based on the differential migration of ions in an electric field in a manner unrelated to their molecular weight.<sup>188</sup> This is especially pertinent for compound groups prone to isobaric forms, such as cathinones<sup>189</sup> and opiates.<sup>190</sup> In the latter study, the authors found that while ion mobility did not offer clear separation gains over LC and required the use of an a priori library of collisional cross-section values to optimize separation, it provided an independent parameter for compound identification which, unlike RT or fragment ion ratios, was not affected by concentration. Isobaric compounds of similar structures present a problem better suited for chromatography rather than mass spectrometry: yet, it is uncommon for the adequacy of chromatographic separation to be evaluated extensively with a large mix of isobaric compounds having similar retention times.<sup>187</sup>

Chromatographic run times vary markedly, often exceeding 30 min.<sup>25, 191</sup> While 10-15 min is more typical, even this still translates to a fraction of the throughput achievable on a clinical immunoassay platform and highlights the chronic turnaround time problem facing forensic laboratories.<sup>192, 193</sup> For example, a forensic lab in Florida<sup>194</sup> found an average reporting time of 19 days for blood screen requests. Some efficiencies can be gained through parallel processing during sample preparation (e.g., 96-well plates, liquid handlers) but the LC separation remains a bottleneck in that lengthy periods of analysis time are devoted to the processing of a single sample: consequently, there is little opportunity to increase throughput through LC multiplexing as has been reported for single-analyte tests such as 25-OH vitamin D.<sup>195</sup>

### 2.6.4 Detection Techniques

A wide variety of MS detection techniques have evolved, each tailored to the needs of the end user. For example, laboratories with a large daily workload of workplace testing samples, minimally experienced staff, an uncompromising client expectation of a rapid turnaround time, a predominance of a handful of drugs with no requirements for non-targeted analysis will choose a QqQ system rather than an elaborate TOF with library searching. By contrast, a lab specializing in post-mortem work and needing to ensure a comprehensive search will likely prefer to use HRMS for screening with a QqQ for confirmation, though some<sup>196</sup> chose the reverse strategy. While most attention is typically focused on identification of positives, the certainty of negative results is equally important:

QqQ may enjoy some advantage here over HRMS, as its extended periods of dedicating the instrument to a specific compound make it less prone to the stochastic issues that can confound HRMS due to brief acquisition times.<sup>197</sup>

Still, there is a trend towards broad-spectrum HRMS screening methods owing to the challenges presented by NPS: specifically, their rapid proliferation and geographically heterogeneous distribution (European Drug Report 2019).<sup>198</sup> While targeted QqQ methods remain widely used, they are arguably more dependent than HRMS on the availability of reference standards which hinders their ability to definitively identify this endlessly mutating group of compounds.

Regardless of the type of MS used, the predominant LC-MS ionization interface in forensic LC applications is electrospray ionization (ESI) rather than atmospheric pressure chemical ionization (APCI). The latter is less prone to ion suppression/enhancement but at the cost of significantly lower sensitivity: this is especially important for HRMS methods where sensitivity is typically compromised in order to achieve comprehensive compound identification. APCI has been employed primarily for lipophilic neutral drugs such as cannabinoids,<sup>199</sup> BDZs,<sup>200</sup> anti-psychotics,<sup>201</sup> as well as a broad-spectrum panel.<sup>202</sup> In a non-forensic application, a combined ESI and APCI source delivered stronger signals with superior signal-to-noise than either mode alone for the analysis of nine BDZs and zolpidem in pharmaceutical products.<sup>203</sup>

Mass separation by single-QMS has effectively been replaced by either fragmentation or high-resolution methods. Fragmentation is usually performed in a collision cell and only infrequently within the source itself. The in-source fragmentation technique is limited by its inability to fragment compounds requiring a high collision energy, as well as by a strong dependence on conditions such as source design, gas pressure, and the presence of co-eluting matrix compounds, all of which tend to give poor reproducibility, requiring instrument-specific spectral libraries.<sup>204</sup> Nevertheless, one study found fewer false positive samples with added in-source fragmentation compared to LC-TOF-MS alone: this came at the cost of slightly more false negatives, though exclusively at levels near the lower reporting threshold.<sup>205</sup> In another study, the detection of drugs in post-mortem blood by UHPLC-MS with in-source fragmentation was found to be only slightly inferior (73.1% sensitivity) compared to LC-MS/MS (74.4%).<sup>206</sup> By contrast, LC-TOF-MS with in-source fragmentation accurately detected two fragment ions in only 75% of a panel of 200 sports doping drugs, compared to 100% when using LC-QTOF.<sup>207</sup>

Initial broad-spectrum quadrupole methods were based on collision cells used selected reaction monitoring (SRM),<sup>208-210</sup> with data being collected in defined intervals over the course of a chromatographic run. This approach has given way to scheduled MRM (sMRM) where each channel has its own retention time (RT) window: the duty cycle is reduced, by acquiring at any given time only those compounds within a narrow window of their expected RT and set to a fixed value to provide consistent data acquisition across all chromatographic peaks. The shorter duty cycle permits the inclusion of additional channels (e.g., qualifier ions or new compounds) or simply more data points across a

chromatographic peak. Further specificity was added by data-dependent analysis (DDA), where an initial MS<sup>211</sup> or MS/MS<sup>178, 212</sup> scan is used to trigger a product ion scan based on survey ions exceeding a given threshold: for compounds with inherently rich spectra, this can greatly enhance identification confidence but the gains are limited for compounds with inherently few fragments, such as amphetamines. While the dependent scan adds appreciably to the duty cycle, risking a sub-optimal number of data points per chromatographic peak, its acquisition frequency can be limited by a fixed number of survey signal triggers and a post-acquisition exclusion period.

The use of QqQ instruments continues to be widespread because to their modest cost, ease of implementation and the reduced complexity of interpreting MRM data, but there have been few recent advances in their data acquisition. A likely reason is that chromatographic peak width and data acquisition capability (in the form of minimum dwell time) inherently limit the number of MRMs and dependent scans achievable in a duty cycle. In addition, MRM-based QqQ methods require continual updating with the emergence of new drugs and cannot be used to perform retrospective analyses: these concerns do not apply to MS scan-triggered DDA but its ability to reliably identify new compounds is limited by unit mass resolution.

By contrast, HRMS methods play an increasingly prominent role in the broad-spectrum screening literature, in part through their provision of accurate mass for both precursor and fragment ions, which reduces the number of likely candidates for a given chromatographic peak. Early HRMS methods were based on single-stage mass scanning to identify compounds by accurate precursor ion mass and retention time only.<sup>156</sup> While some methods used in-source fragmentation to generate spectra,<sup>207, 213</sup> their modest and variable effectiveness in generating multiple fragment ions has led to them being largely replaced by collision-induced dissociation methods. These techniques include DDA, as described above, with the triggering event for the dependent scan being a precursor ion selected from the most abundant ions and/or an inclusion list of compounds of interest.

The other broad family of HRMS techniques is data-independent analysis (DIA), where the spectra derived from all precursor ions are acquired with varying degrees of precursor ion selectivity. A significant benefit of DIA over DDA is an improved rate of detection because all precursor ions (and their spectra) are detected: by contrast, DDA may fail to detect compounds if the precursor signal is below threshold, the spectrum is dominated by other species or precursor ion selection is based solely on an inclusion list. In the basic form of DIA, originally named 'MS<sup>E</sup>',<sup>214</sup> precursor ions are detected by an initial survey scan followed by fragmentation at fixed<sup>180</sup> or multiple<sup>173</sup> collision energies to create spectra for library searching. This allows for retrospective analyses for emerging drugs such as U-47700<sup>215</sup> or, interestingly, established drugs (barbiturates) previously thought to be detectable solely by negative mode ionization.<sup>216</sup> Also, provided that the LC method is suitably universal, there is no need to continually update the MS detection method: only the MS library needs to be kept current.

The specificity of DIA is enhanced in techniques such as Sequential Windowed Acquisition of All Theoretical Fragment Ion Mass Spectra (SWATH™) which, unlike MS<sup>E</sup>, fragment the precursor ions in fixed<sup>217</sup> or variable<sup>218</sup>  $m/z$  segments to narrow the lineage of each fragment ion scan. The high resolution and scan speed of HRMS are essential, making this approach unsuitable for QqQ instruments. A feature of all HRMS methods is their ability to measure isotopic ratios, or the distribution of isotopologues based on known molecular formula and prevalence of individual isotopes. An important limitation of this identification parameter is that the unavoidably lower intensities of the higher  $m/z$  ions may increase the rate of falsely rejected identifications: consequently, the use of isotopic ratios for identification is inconsistent in the HRMS screening literature. We will provide some highlights of the forensic screening MS literature since 2010 under the following three indices of performance: sensitivity and specificity of target compound identification, range of target compounds identified, and quantitation.

### 2.6.5 Sensitivity and Specificity of Compound Identification

The identification reliability required of an MS method is dependent on its role in the analytical process. A screening method places a premium on sensitivity rather than specificity and so is less bound to guidelines for definitive identification<sup>163, 219</sup> based on scoring systems for data from the LC (i.e., RT) as well as the MS (e.g., # of qualifiers and their relative intensities). As a result, the RT tolerance in screening methods for compound identification varies broadly from, for example, 0.15 min<sup>220</sup> to 1.5 min,<sup>211</sup> depending on the origin of the RT targets. In any case, the RT criterion is less essential with HRMS, as shown by Colby and coworkers who evaluated a graded series of identification workflows for 100 urine samples containing 170 drugs and metabolites analyzed by a DDA-based QTOF method.<sup>221</sup> They found that a scheme based on purely MS data (accurate mass, isotopic pattern and fragment ions) had a positive predictive value of 82% for correctly predicting structures, compared to a modestly improved 96% when RT was included, concluding that this parameter was not required to identify drugs with a reasonable level of accuracy by HRMS.

The use of a tight RT criterion typically requires that a standard be run concurrently, which becomes impractical when these are unavailable or large in number. To overcome this limitation, Sauvage and coworkers showed that QqQ DDA data could enhance identification confidence over targeted MRM results even when the latter used an RT criterion and qualifier MRMs.<sup>178, 222</sup> Specifically, lysergic acid diethylamide (LSD), atropine and clomipramine gave false positive results using an RT criterion compared to purely full scan MS data acquired at three fixed collision energies. This DDA approach was elaborated by the addition of a collision energy spread rather than fixed values, allowing for a significant decrease in the duty cycle, by groups such as Dresen and coworkers who used sMRM for 700 compounds (one channel each) to trigger a dependent scan for the two most abundant precursor ions from urine samples.<sup>212</sup> Identification of a broad range of compounds, from morphine glucuronide to THC, was based on purity against a reference library. Still, full reliance on MS data must be applied with caution, especially with incompletely resolved isobaric compounds. Sundström and coworkers found that an

MSE acquisition correctly identified all members in four sets of isobaric amphetamine-type compounds in pure solvent without the use of an RT parameter, while DDA with a pre-defined list of precursor ions was only able to distinguish compounds in two sets.<sup>223</sup>

Numerous groups have demonstrated the reliability of the non-targeted DIA approach. Rosano and coworkers used MSE to screen for over 950 compounds in blood from 300 forensic cases with a QTOF instrument.<sup>224</sup> Using identification requirements for RT ( $\pm 0.3$ min), precursor mass ( $\pm 5$  ppm) and one fragment mass ( $\pm 5$  ppm), they obtained a detection rate of 99% of 1528 compounds by QTOF compared with 80% for combined LC-MS and LC-MS/MS quadrupole methods. The large majority (73%) of the additional compounds detected by the QTOF were simply metabolites of drugs already identified, but 21% were revealed as new drugs based on isotope ratio patterns and the presence of  $\geq 2$  fragment ions. This approach was further refined by Rosano et al. as a quantitative confirmatory method using the same identification criteria as above. No discrepant results were obtained for 114 urine samples when compared against a targeted 64-compound QqQ MS/MS method.<sup>196</sup>

The effectiveness of positive mode DDA was evaluated in 50 autopsy samples against a library that included 2500 compounds (including fragment spectra at 3 collision energies) and an additional 5000 having accurate precursor mass only.<sup>225</sup> Several chemical groups were under-represented in the library owing to inadequate ESI signals, the formation of sodium adducts, signal instability or the presence of multiply-charged species. In the autopsy samples, they identified 311 compounds (based on accurate mass, library match and isotope pattern) derived from 125 drugs, compared with 178 compounds from 94 drugs determined by LC coupled to a diode array detector and GC-MS. However, low-level compounds such as THC and some BDZs, as well as compounds with a preference for negative mode ionization were either missed or detected only at higher levels.

SWATH<sup>TM</sup> has also proven to be effective in drug identification but has received limited attention in the literature to date, mainly in the form of a comparison with DDA. The prevailing view is that while DDA provides better quality spectra (on account of its greater precursor selectivity), SWATH<sup>TM</sup> gives fewer false negative results due to precursor ions not subjected to MS/MS.<sup>226</sup> This inherent balance between compound identification and range was shown for DDA (with and without precursor restrictions), SWATH<sup>TM</sup> and MS<sup>E</sup> through their ability to detect drug metabolites prepared by incubating 8 test compounds with rat liver microsomes. Of the 227 metabolites ultimately found in the mixture, 5% did not generate MS/MS data by DDA: this figure rose to 29% when the mixture was added to a blank urine matrix, illustrating the role of competitive interference from additional ions triggering MS/MS scans. Both SWATH<sup>TM</sup> and MS<sup>E</sup> scored 100% for both sample types, but the overall order was reversed when MS/MS data quality was considered: 9 of the 10 most abundant product ions in the MS/MS spectra of the 8 test compounds recorded by DDA scans of the rat liver microsomes originated from the test compounds themselves, compared to only 6 and 3 for SWATH<sup>TM</sup> and MS<sup>E</sup>, respectively.<sup>227</sup>

The merits of DDA vs DIA have been evaluated by numerous groups.<sup>218, 223, 226, 227</sup> In one example using urine samples, a list of 200 compounds was examined in a DDA experiment to select precursor ions by mass, RT and signal strength, followed by fragmentation at compound-specific collision energy for up to 3 consecutive scans.<sup>223</sup> A 5 Da precursor selection window helped capture a wider range of isotopes to enhance information in the acquired spectra. Identification was based on precursor mass ( $\pm 25$  mDa), RT ( $\pm 0.3$  min) and spectral purity ( $>80\%$ , a combination of fit and reverse fit). In the DIA arm,  $m/z$  50-700 precursor ions were fragmented at a fixed collision energy in every second scan. Compounds were identified by precursor mass (2.5 mDa), RT (0.2 min), and minimum abundances for precursor and qualifier ions. Using these criteria for the limit of identification (LOI) of drugs spiked into urine from six volunteers, DIA achieved a consistently lower LOI than DDA. The authors pointed out that the fixed collision energy value used to create spectra libraries may impair spectral quality of compounds with optimal values lying outside the usual range. Both techniques were applied to 50 authentic samples, where DIA made 266 identifications for 46 different substances; the results for DDA were 225 and 42, respectively, the lower values likely being due to inherently higher LOI and interference from co-eluting compounds.

In a study more pertinent to forensic screening, SWATH™ was compared with DDA for drug screening in blood.<sup>228</sup> The SWATH™ survey scan was set to  $m/z$  100-700 with 20 Da sections submitted to a  $m/z$  100-650 dependent scan with a collision energy ramp of  $35 \pm 15$ . Settings for DDA were similar, with selection criteria of 10 most significant ions and a half-peak width exclusion time. Identification was based on accurate mass, isotope ratio (albeit with large tolerance) and purity score against a library of 534 compounds. The authors observed a concentration dependence for fragment ions with SWATH™ but noted the phenomenon was not confined to this technique. The fragment ion spectra could also be distorted by the presence of deuterated internal standards, especially if these shared common ions with target precursors. DDA was found to deliver better quality spectra, but this difference was considered insignificant when compared with the inferior results obtained by MSE. The screening sensitivity of the two techniques was evaluated using flow injection (vs column chromatography) of mixtures of 6, 16 and 20 analytes. Both methods were similar at  $n=6$  analytes, but DDA detected only 13/16 and 15/20 analytes in the respective mixtures, even at a setting of 20 experiments. SWATH™, by contrast, identified 6/6, 15/16 and 20/20 of analytes present. The sensitivity of DDA can also be compromised by ion suppression due to co-eluting analytes and an inappropriately wide isotope exclusion window, which may result in the rejection of ions from compounds with similar masses. Pointing out the infrequent specification of the precursor window in DDA papers, intended to avoid needless triggering of dependent scans by the  $[M+H]^+$  peak, the authors commented on the risk of false negative results when a compound's precursor mass lies within the exclusion window of a dominant neighbour. While such precursors would clearly not be missed with SWATH™, the presence of multiple precursor ions may limit the usefulness of SWATH™ if paired with a DDA-acquired library typically acquired with a precursor window of 1 Da.

Two important parameters for method robustness are addressed infrequently but deserve mention. The first is spectral reproducibility: for example, an assessment of how reliably compounds in a test mixture are identified at three levels over several weeks.<sup>229</sup> The second is the number of fragments required for a library match: this may be as low as 1 or is often simply not specified at all, illustrating the risk of reliance on a simple purity score.<sup>230</sup>

### **2.6.6 Range of Compounds Identified**

Most LC-MS methods described here were intended for screening purposes only. In a forensic environment, samples screening positive would require a targeted confirmatory analysis. The compound range of this second assay is of lesser concern as the target is already suspected: the main challenge is the initial identification of candidate drugs for further evaluation. While this range of method-compatible compounds is largely defined by physicochemical properties such as lipophilicity and preference for forming cationic vs anionic precursor ions, most LC-MS papers choose instead to describe the compound range in terms of the total number of targets. The main factors dictating an LC-MS method's ability to detect drugs are listed in Table 2.1.

Table 2.1 Limitations of compound detection range.

Issue	Example	References
Adulteration	Substituted human performance sample	231, 232
Stability issues with sample collection, storage, preparation	Ethanol, cathinones	233
	Synthetic cannabinoids	234
Drug present in sample as metabolite only		88
Incompatibility with LC conditions	GHB	216
Incompatibility with source polarity	Barbiturates	
Data not acquired	Absent from inclusion list (DDA) or MRM list (QqQ); interfering substance (DDA)	235
Very low concentrations	LSD	
Unavailability of standards or reference spectra	NPS	

A method's detection range will unavoidably affect turnaround time. Recognizing this limitation of a typical LC-MS screening method in detecting the wide range of drugs encountered in a clinical setting, McMillin et al. , opted for a hybrid immunoassay-MS strategy where drug screening of specific groups was assigned to immunoassays where conventional LC-MS added significantly to reporting time while exhibiting poor detection (e.g., barbiturates, THC-COOH) or providing no added information.<sup>236</sup>

In a forensic lab, though, there is lower urgency to deliver rapid results, and a greater need to maximize the range of detectable compounds. These requirements were balanced with a DIA (MS<sup>E</sup>) method which incorporated an exceptionally broad group of 467 compounds ranging from GHB to THC-COOH glucuronide in ante- and post-mortem blood using identification by accurate mass, RT, isotope pattern and presence of qualifier ions against an in-house library.<sup>237</sup> Interestingly, this list included drugs typically analyzed in negative ionization mode, such as phenobarbital and salicylate, as their toxic levels are typically high enough to permit detection in positive mode. GHB was prone to marked matrix interference, but not at a level that would impair recognition of a true positive case. The method was shown to be robust with respect to RT, response, mass error and resolving power over six months.

A positive ionization DDA method of similar scope was used for whole blood samples extracted with butyl chloride to screen 320 compounds, quantitate 39, and search for unknowns in a 15 min chromatographic run.<sup>172</sup> The compounds ranged from the less polar opioids (e.g., codeine) to methadone and synthetic cannabinoids but did not include GHB or THC-COOH. MS/MS scans were prioritized (or excluded: e.g., internal standards, known interferences) from an inclusion list of about 450 masses followed by the two most abundant precursor ions. Compounds in the inclusion list ranged from established drugs with available reference materials to presumptive metabolites and tentatively identified NPS. Criteria for a positive screen were precursor mass  $\pm 10$  mDa and RT  $\pm 0.5$  min, with presumptive positives submitted for manual review against more rigorous standards for identification (mass  $\pm 2$  mDa, RT 2%, MS/MS consistent with contemporaneous reference standard). Storage of centroid (vs continuous) data using a relatively high signal threshold allowed individual sample files to be kept to a reasonable 30 Mb size limit. This is an important consideration for a production assay (of which this paper was an uncommon example), as any LC-MS service will struggle if required to process a large number of samples daily with continuum data file sizes of 500 Mb or more. Lastly, synthetic cannabinoids were found to be particularly prone to sample carryover, providing a cautionary note about directly reporting LC-MS results without a second confirmatory test.

The compound range issue has also been approached through the use of a publicly shared MS database to maximize the size of the reference library available for the analysis of NPS in hair.<sup>238</sup> This matrix also has the advantage of acting as a potential reservoir for novel parent drugs, an especially important feature for synthetic cannabinoids where metabolism is both extensive and uncertain. An atypical feature of the DDA method was the use of two exclusion lists (to reduce interference from endogenous substances) and no inclusion list (to avoid selection bias). A similar public library strategy for HRMS has been promoted by others.<sup>239</sup>

It is worth pointing out that most methods described as 'non-targeted' still rely on a mass spectral library of a fixed number of known compounds. Consequently, the determination of truly 'unknown unknowns' must be achieved by some other means, such as *in silico* fragmentation to predict retention time and spectra. The latter approach was illustrated

for blood samples with the supplementation of an in-house MS library with in silico fragmentation using MS<sup>E</sup>.<sup>240</sup> Compounds were first tentatively identified with a targeted approach against an in-house library of 1457 compounds by using precursor *m/z*, RT, fragment ions and isotopic pattern. Those peaks not identified were then filtered from further consideration based on RT, low response, common endogenous and exogenous (e.g., dietary) compounds, recurring masses, co-elution with a dominant target and adducts alternate to a protonated pseudo-molecular ion. This reduced the number of spectra to be reviewed by 3 orders of magnitude while retaining 73% of true positives identified by a targeted screen. The molecular formula was then determined based on accurate mass and isotope pattern and compared against several large chemical structure libraries. Lastly, the resultant candidate structures were in silico fragment-matched using a combinatorial fragmentation approach to the observed spectra. Several limitations were noted. First, the threshold intensity filter reduced the effectiveness of identification by isotopic pattern in the subsequent step, though the authors noted that this could be partially avoided by making the threshold mass-dependent, as low molecular weight compounds such as MAMP can be reliably identified by accurate mass alone. Second, a few compounds do not reliably form protonated pseudo-molecular ions. Lastly, frequently occurring but illicit compounds may be incorrectly excluded, though the authors pointed out that this would not be an issue in practice, as the sequence would have been run only after a targeted search, which should have detected these compounds. The result of the non-targeted screen applied to 44 driving under influence of drugs (DUID) samples was the discovery of 3 drugs and 14 metabolites not identified by the targeted approach. The sensitivity of the non-targeted workflow alone was shown using samples spiked with 11 novel BDZs where the LOI for 9 drugs was within an order of magnitude of that obtained by the targeted method.

In the absence of commercially available standards, investigators have used incubations of parent drug with human liver microsomes to obtain LC-MS properties of predicted metabolites of NPS such as synthetic cannabinoids<sup>241</sup> or the novel fentanyl analog, cyclopropyl-fentanyl.<sup>242</sup> An alternate approach used metabolite targets for 45 anti-depressants through dosing of parent drugs to rats and identifying metabolites in urine.<sup>243</sup> This approach not only increases sensitivity and specificity of drug detection, but also provided evidence that the subject had consumed the drug in question.

The consumption of a drug can also be inferred by searching for its metabolites with a mass defect filter (MDF).<sup>244</sup> MDF was included in the DDA study mentioned above,<sup>227</sup> where MS/MS spectra were acquired for precursor ions having *m/z*  $\pm 50$  mDa and mass defect  $\pm 40$  mDa compared to the parent drug's respective values. They found that while only 95% and 96% of drug-related material precursor ions generated MS/MS spectra when triggered by the most prominent ions and the MDF, respectively, the MS spectra quality was significantly superior to those obtained by SWATH<sup>TM</sup> and MS<sup>E</sup>.

While efforts to increase the range of detectable compounds are commendable, it is worth pointing out that a small number of drugs likely account for most of the compounds

identified. One forensic lab commented that in their experience 20 drugs were responsible for up to 80% of fatal poisonings.<sup>245</sup> Considering the turnaround time pressures mentioned earlier, each laboratory needs to determine its own point of diminishing returns with respect to the range of detected compounds. Similarly, the sample selection criteria for drug screening should be carefully considered: in a group of 576 misdemeanour and felony DUID cases, it was found that the drug testing results, even when positive, rarely added value in supporting a DUID charge.<sup>194</sup>

### 2.6.7 Quantitation

A broad-spectrum quantitative LC-MS method for forensic work is beset by issues not faced by a purely qualitative assay. These begin with the challenge of preparing calibration mixtures containing dozens of compounds at suitable levels in compatible solvents and culminate in ensuring acceptability of a potentially vast number of calibration curves and quality control results. These problems are obviously not unique to forensic LC-MS, as they also confront workers in fields such as doping control and residue analysis. However, some of these challenges can be avoided by limiting quantitation to a subset of all targets<sup>172, 246</sup>, using stored calibration curves<sup>159</sup> or simply using the method as a qualitative screen only, which appears to be the route taken most often.

A novel standard addition-type approach that has yet to see widespread use is the use of threshold accurate calibration<sup>247</sup>, where each urine sample is analyzed separately both with and without known amounts of added target compound. As a result, each sample serves as its own calibrator, which allowed the avoidance of internal standards and the acceptance of potentially marked matrix effects through the use of simple dilution rather than a more elaborate extraction.

A distinctive challenge of forensic drug testing, whether in biological matrices or seized samples, is that the very wide range of concentrations routinely encountered creates the risk of carryover in the LC-MS. The problem is magnified by the prevalence of high-concentration samples in a large analytical batch, whose size discourages inter-sample blanks or repeat analyses with diluted samples. Moreover, quantitation over several orders of magnitude may exceed the ability of the MS instrument, a problem which has been addressed by monitoring the target compound's pseudo-molecular ion and a minor isotopologue (i.e.,  $[M+H+2]^+$ ) at low and high concentrations, respectively.<sup>248</sup> This approach has been used to quantitate MAMP across a concentration range of 50-200,000 ng/mL.<sup>249</sup>

There is limited forensic toxicology literature on quantitation by DDA and DIA broad-spectrum methods. Using SWATH<sup>TM</sup> acquisition, results for 76 internal standard-matched compounds obtained by daily external multi-point calibration were compared with those from weekly external calibration, daily external one-point calibration and internal calibration (i.e., using a compound's response factor vs its internal standard).<sup>250</sup> Accuracy for three levels of QC material spanning a range from toxic to lethal blood concentration was found to be similar for all levels except the lowest. The authors concluded that external calibration in either format met the requirements for accurate quantitation while

one-point internal calibration was the best choice for rapid screening. They found no issues with selectivity but did not comment on whether the internal standards interfered with target compound spectra, especially if the two shared common fragments.

## 2.7 Ambient Ionization Mass Spectrometry

### 2.7.1 Introduction

Ambient ionization MS methods are those which operate under ambient (open air) conditions and require little to no sample preparation for the formation of ions from samples in their native environment, outside of the MS. Classical methods of ion generation require the introduction of the analyte either directly to high vacuum or contained in solution from which ions can be extracted into or generated in the gas phase. Atmospheric pressure ionization techniques that create ions from dilute sample solutions are not truly considered ambient (e.g., ESI, APCI, APPI, AP-MALDI) and will not thoroughly be discussed here. Ambient techniques tweak the desorption properties of these well-established techniques for true ambient analysis; however, these techniques often heavily rely on these processes for ionization. As such, the reader is directed to discussions of ionization mechanisms for electrospray ionization (ESI),<sup>251</sup> atmospheric pressure chemical ionization (APCI),<sup>252, 253</sup> and atmospheric pressure photoionization (APPI)<sup>254</sup> processes, as they are relevant to the discussion below.

The introduction of the ambient mass spectrometry techniques such as desorption electrospray ionization (DESI) in 2004 and direct analysis in real time (DART) in 2005 have seen significant growth in the literature and uptake from the clinical and forensic communities. Commercial systems for both sources have been developed and have seen broad use in a wide variety of applications. The success and simplicity of these approaches has spun off an ever-growing body of related ambient ionization techniques, with more than 80 techniques now described in the literature. Given that a discussion of all these techniques is infeasible, this review will focus on ambient methods that have appeared in the literature for multiple (> 5) demonstrations of drug analysis. This section presents individual sections for the ambient ionization techniques discussed, which are outlined in Table 2.2 along with desorption / ionization characteristics. Short fundamental descriptions of the technique are presented, but it is not germane to this review to describe the nuances of each of the techniques in full. The reader is directed to a number of thorough reviews of ambient ionization that have been reported in the recent literature, including reviews on: general aspects of ambient ionization,<sup>5, 255, 256</sup> plasma-based ambient techniques,<sup>257-259</sup> forensic analysis,<sup>4, 260</sup> clinical applications,<sup>6</sup> applications in high-throughput screening,<sup>7</sup> and ambient ionization from the perspective of green analytical chemistry.<sup>261</sup>

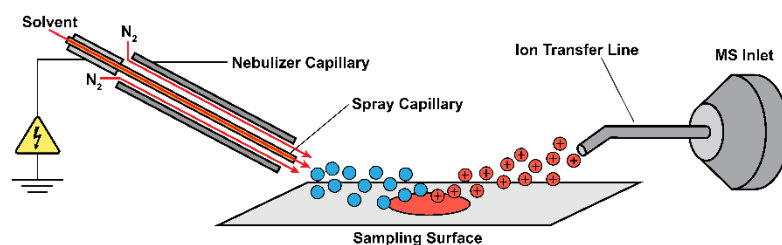
Table 2.2 Desorption/ionization conditions for ambient ionization MS techniques.

Technique	Name	Year	Desorption	Ionization
DESI	Desorption electrospray ionization	2004 <sup>262</sup>	liquid extraction	electrospray
DART	Direct analysis in real time	2005 <sup>263</sup>	plasma desorption	corona discharge
ELDI	Electrospray-assisted laser desorption/ionization	2005 <sup>264</sup>	laser ablation	electrospray
ASAP	Atmospheric solids analysis probe	2005 <sup>265</sup>	thermal desorption	corona discharge
EASI	Easy ambient sonic-spray ionization	2006 <sup>266</sup>	liquid extraction	sonic spray
FAPA	Flowing atmospheric-pressure afterglow	2006 <sup>267</sup>	plasma desorption	corona discharge
DBDI	Dielectric barrier discharge ionization	2007 <sup>268</sup>	plasma desorption	dielectric barrier discharge
DAPPI	Desorption atmospheric pressure photoionization	2007 <sup>269</sup>	plasma desorption	photoionization
LAESI	Laser ablation electrospray ionization	2007 <sup>270</sup>	laser ablation	electrospray
DSA	Direct sample analysis	2007 <sup>271</sup>	thermal desorption	corona discharge
LTP	Low-temperature plasma	2008 <sup>272</sup>	plasma desorption	dielectric barrier discharge
PSI	Paper spray ionization	2010 <sup>9</sup>	liquid extraction	electrospray
CBS	Coated blade spray	2014 <sup>273</sup>	liquid extraction	electrospray

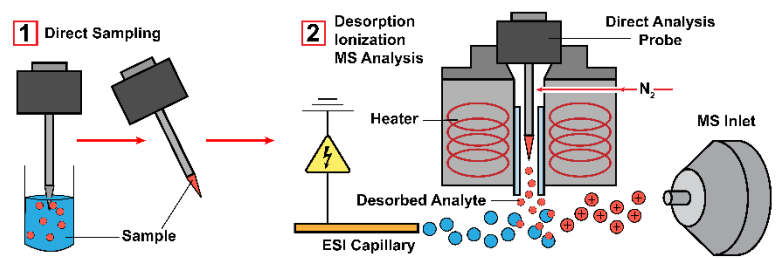
### 2.7.2 Liquid/Spray-Based Techniques

The majority of publications involving drug analysis with the liquid/spray-based techniques have utilized desorption electrospray ionization (DESI) and paper spray mass spectrometry (PS-MS), with significant literature contributions from easy ambient sonic-spray ionization (EASI) and coated blade spray (CBS), and more minor contributions from thermal-desorption electrospray ionization (TD-ESI) and solid-substrate electrospray ionization techniques. All of these techniques produce ions from evaporating aerosol droplets, in a manner similar to that observed in electrospray as described by<sup>251</sup> (note that EASI does not require applied high voltage). A generalized instrumental schematic for each of the techniques is presented in Figure 2.7, but other geometries and designs have been implemented as well.

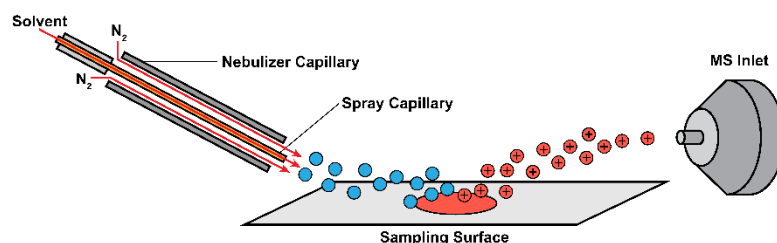
### A) Desorption Electrospray Ionization:



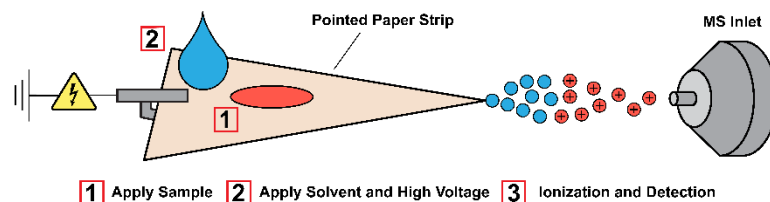
### B) Thermal Desorption-Electrospray Ionization:



### C) Easy Ambient Sonic-Spray Ionization:



### D) Paper Spray Ionization:



### E) Coated Blade Spray Ionization:

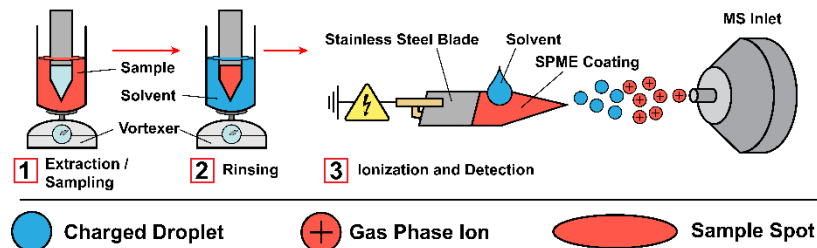


Figure 2.7 Generalized instrumental schematics for (A) desorption electrospray ionization (DESI), (B) thermal-desorption electrospray ionization, (C) easy ambient sonic-spray ionization (EASI), (D) paper spray ionization (PSI), and (E) coated blade spray ionization (CBS). Not to scale.

### 2.7.2.1 Desorption Electrospray Ionization

Desorption electrospray ionization (DESI) was the first ambient ionization technique described in the literature, paving the way for the development of a large variety of related ambient ionization techniques that appeared in the ensuing decade.<sup>262</sup> DESI is achieved by spraying solvent from an ESI probe onto a surface to be analyzed. The charged droplets desorb analytes from the surface, and the ionization of analytes occurs in an electrospray-like fashion, with evidence for both a heterogenous charge-transfer and a droplet pick-up ionization mechanism described in the literature.<sup>274</sup> Many applications of DESI involve chemical imaging of biological tissues, which is one of the unique strengths of this method; however, imaging studies in drug analysis are most often directed towards therapeutic drug monitoring and are not thoroughly discussed here.<sup>275, 276</sup> The reader is directed to two DESI reviews in the literature.<sup>277, 278</sup> The success of DESI has led to the development of commercialized ion sources.

Initially, DESI was demonstrated for a variety of rapid qualitative screening applications, including the detection of AMP, opiates, cannabinoids and BDZs from untreated, and urine extract samples.<sup>279</sup> Although Kauppila et al. reported no matrix effects in their analysis of urine, a more thorough study into matrix effects using opioids as a model compound by Suni et al. found that sensitivity was decreased by 20-160-fold for urine.<sup>280</sup> In another forensic screening application, DESI was used for the rapid determination of BDZs in alcoholic beverages without any sample pretreatment.<sup>281</sup> DESI was also demonstrated for the non-invasive qualitative detection of COC and metabolites from fingerprints, using only a small area of the fingerprint, allowing for high-throughput, replicate analysis.<sup>282</sup> DESI has been used for the qualitative analysis of illicit COC samples from 3 seizure events by Australian police, and preliminary geographical origin determination was demonstrated.<sup>283</sup> In an indirect screening method, Bianchi et al. tested a variety of sample substrates coupled to DESI for increased signal and stability in the screening of NPS in oral fluid samples in both positive and negative ionization modes.<sup>284</sup> The use of these sample substrates allowed for improved LLOQs and method validation was demonstrated, however, some isomers were unable to be differentiated. While the use of sample substrates improved sensitivity and precision in this study, the full analysis time of 15 min required was significantly slower than direct DESI screening applications.

Further development of DESI involving coupling with SPME or other extraction procedures allowed for sensitive quantitative analysis. The direct DESI-MS/MS screening and quantitative measurement of DoA on SPME fibers for the analysis of from raw urine was achieved by Kennedy et al. in good agreement with conventional immunoassay, GC-MS, and LC-MS/MS results.<sup>285</sup> Thunig et al. employed hollow fiber liquid-phase microextraction (LPME) with DESI to measure 4 DoA from urine samples.<sup>286</sup> LPME significantly reduced the matrix effects observed in direct DESI urine analysis, allowing for a LOQ for diphenhydramine of 140 ng/mL to be achieved.

Since DESI is an ambient method that lacks chromatographic separation, it must rely on MS/MS or HRAM data for selectivity, though in many cases this is not sufficient for

structural isomer differentiation. Ion mobility has been used with other ambient techniques to increase selectivity and the use of DESI coupled to an ion mobility TOF-MS has been demonstrated by Roscioli et al.<sup>287</sup> The analysis of drug tablets and creams was achieved, and though there was no differentiation of structural isomers, IMS coupling with DESI demonstrated increased selectivity and sensitivity.

Ambient sampling, portable mass spectrometers have significant potential for in situ forensic or clinical analyses, and DESI is well suited for these systems, evidenced by the first ever coupling of an ambient technique to a handheld IT-MS.<sup>288</sup> They used the handheld MS system to analyze COC on a variety of surfaces, including currency. Further applications of DESI with portable MS include the use of an IT-MS for the rapid screening of synthetic cathinones and AMP in forensic samples with low or sub ng/mL LOD values.<sup>289</sup> Their ruggedized CIT-MS has also been used to sample positive and negative controls, as well as forensic drug powders for 32 different DoA.<sup>290</sup> Structural confirmation and identity were achieved using MS/MS and automated library searching using established reference libraries. In a further development of this portable MS, a flexible source platform was developed, allowing for ambient sources (including PSI, DESI, swab touch spray, and APCI) to be rapidly interchanged to target specific applications.<sup>291</sup> Anticipating an incorporation of this system into forensic practice and routine analysis, Mulligan et al. performed comprehensive analytical validation studies using common DoA and a variety of NPS to demonstrate the throughput, selectivity, accuracy, precision, robustness and ruggedness of the portable MS system featuring interchangeable sources.<sup>292</sup> The use of portable DESI-MS systems, and especially a system featuring interchangeable sources has demonstrated strong potential for use in *in situ* forensic applications as well as high-throughput screening.

### **2.7.2.2 Thermal-Desorption Electrospray Ionization**

A major application in forensics involves the remote sampling of large and/or immovable objects (e.g., luggage, in situ analysis), presenting challenges for traditional forensic techniques. Given that drug concentrations are often high in these types of applications, eliminating sample carryover or interference can be more important than sensitivity. When sampling is done using probes, switching between sampling probes can be cumbersome with significant carry-over, otherwise significant sample preparation is required for sample introduction. In thermal desorption-electrospray ionization (TD-ESI), a removable metal probe can be used to sample immovable, remote surfaces or other solids and liquids and then be inserted into a standard ESI source (following simple modifications), with typical analysis times of 10 s.<sup>293</sup> The probe is quickly cleaned with a gas torch post analysis, eliminating sample carry-over. Heated nitrogen gas acts to desorb thermally stable analytes from the probe and transfer them to the ESI plume, where ions are subsequently generated through the interaction of the desorbed analytes with charged solvent species. Sampling, desorption, and ionization are separate events in space and time.

In the first demonstration of TD-ESI with the metal sampling probe, MDMA and codeine standards were deposited on different surfaces (e.g., business card, wooden desk at

~50ng/cm<sup>2</sup>) and sampled with a fine metal probe for their successful qualitative detection.<sup>293</sup> TD-ESI was further applied to the rapid identification of drugs in drained gastric lavage fluid and whole blood from drug overdose patients.<sup>294</sup> In this study, the entire analytical process was completed in < 30 seconds without sample pre-treatment, characterizing flunitrazepam, LSD and MDMA in drained gastric lavage fluid with reported LODs of 500, 500, and 1 ppb, respectively. Prepared whole blood samples from overdose patients were analyzed for KET, COC, AMP and NKET with reported LODs of 1-10 ppb. Stability was demonstrated through replicate drug measurements in both dilute gastric juice and whole blood. Calibrations indicated that TD-ESI may be suitable for quantitation of drugs of abuse in gastric lavage fluid and extracted whole blood.

The versatility of the TD-ESI source was highlighted in the analysis of 30 DoA directly from tablets, soft drinks and drug powders without sample preparation, as well as in drug-laced cigarettes and instant coffee, following a quick methanol extraction.<sup>295</sup> TD-ESI, in this case, was applied as a rapid (30 seconds per analysis) qualitative pre-screening tool using MS/MS data that could be directly compared with ESI-MS/MS libraries. Active ingredients in seized drug materials were detected at less than 2 mg/g of the total sample weight, and consecutive analysis of tablets using an acupuncture needle as the sampling probe did not show cross contamination or interference. Acceptable precision was demonstrated for all compounds, and LODs were determined as 1-60 ng/g in a tobacco/coffee matrix.

Detection of illicit drugs using TD-ESI/MS was further applied to a variety of food and drink matrices of forensic interest as well as stamps.<sup>296</sup> Many of these sample matrix components are either non-volatile or will thermally degrade in the source, thus minimizing matrix effects and interferences for the analytes using TD-ESI/MS. Green tea, whole fat milk, and fruit and vegetable juice were spiked with BDZs, AMPs and NPS, yielding LODs of 100 ppb with direct analysis. Similarly, direct analysis of instant coffee and matcha powders for KET, AMP, para-methoxyamphetamine (PMMA) and LSD gave LODs of 100-1000 ppb. Direct analysis of KET, MDMA, 5-MeO-AMT and LSD on postage stamps returned LODs of 1.3 pg/mm<sup>2</sup> - 6.5pg/mm<sup>2</sup>. DoA have also been found in gummy candies, a challenging matrix. A gummy bear was prepared using gelatin and grape juice spiked with BDZs and a gelatin and green tea mixture used as an outer coating such that the drugs were contained only within the gummy bear, and not on the surface. Sampling of the outer layer detected only caffeine and other green tea components, while sampling the inner part successfully detected the presence of BDZs.

TD-ESI/MS has been demonstrated in the literature as a rapid screening technique that is amenable to quantitative analysis. The source can easily be interchanged for conventional ESI and the sampling probe is removable and can be brought to the sampling site, enabling a wide range of sampling options and has been demonstrated for the direct analysis of an impressive number of matrices with minor matrix effects observed. Preliminary tests indicate TD-ESI could be used for quantitative work, though this has not been thoroughly demonstrated.

### 2.7.2.3 Easy Ambient Sonic-Spray Ionization

Easy ambient sonic-spray ionization (EASI) was originally reported as 'desorption sonic-spray ionization (DeSSI)' in 2006.<sup>266</sup> EASI operates at ambient pressures and, uniquely, uses no high voltages at the spray capillary, heating, auxiliary gases, or corona discharges. A supersonic nebulizing gas, often nitrogen, coaxial to the spray capillary, leads to the formation of aerosol droplets and the subsequent production of gaseous ions. Although the formation of ions with EASI is well supported through various applications, a detailed investigation into the underlying mechanism of ionization in sonic methods has not been reported. EASI-MS was recently reviewed by the inventors of the technique.<sup>297</sup> It should be noted that sonic-spray ionization (SSI) at atmospheric pressures was originally reported in 1994 as an ionization interface in CE-MS and LC-MS systems<sup>298</sup> and further developed as a novel ion source in 2003.<sup>299</sup> Uniquely, EASI-MS combines the ionization concept of SSI with the desorptive concept of DESI; in EASI-MS the supersonic spray is used to both desorb and ionize the analytes of interest. Given the absence of an applied high-voltage and overall simplicity of the ion source design/implementation, the technique shows potential for on-site testing for forensic applications by minimally trained personnel.

The first demonstration of EASI-MS compared its performance with DESI for the analysis of diazepam and therapeutic drugs in tablets. EASI demonstrated similar sensitivities, had mass spectra with less abundant solvent cluster ions, and enabled increased sample matrix penetration, resulting in longer lasting signals relative to DESI.<sup>266</sup> EASI-MS was successfully demonstrated in both positive and negative ionization modes, generating representative mass spectra a few seconds after exposing the drug tablet to the supersonic spray. It was noted that operating conditions (gas flows, angles etc.) greatly affect signal intensities and stability; under optimized conditions, EASI showed signal variations around 20%.

EASI-MS is a logical pairing with thin layer chromatography (TLC), which is commonly used for initial forensic screening. Developed TLC plates can be rapidly tested with EASI-MS, confirming or identifying resolved compound identities in 10 seconds/spot with increased specificity, providing more defensible results. Several publications demonstrating EASI-MS coupled with thin layer chromatography (TLC) have appeared, including the analysis of ecstasy tablets<sup>300</sup> and COC and crack COC sample measurements.<sup>301</sup> Seized ecstasy drug tablets were subjected to TLC for the separation of 5 amphetamines, KET and the common cutting agents caffeine and lidocaine.<sup>300</sup> Primarily  $[M+H]^+$  ions were observed for all of the drugs with the exception of MDEA which was also produced water and sodium adducts. These studies demonstrated detection limits in the low  $\mu\text{g}$  range. EASI-MS has been applied to the analysis of NPS such as meta-chlorophenylpiperazine (m-CPP) in seized ecstasy tablets using QMS in parallel with other techniques to provide a complete chemical profile of the tablets, since EASI-MS was unable to differentiate the ortho and para isomers from m-CPP.<sup>302</sup> The analysis of seized blotter papers suspected to contain LSD has been demonstrated using EASI-MS.<sup>303</sup> Identification of LSD in forensics is often done using the Ehrlich spot test, a

nonspecific colorimetric analysis. This lack of specificity presents a major problem as an increasing number of structurally similar NPS appear in the drug stream that could yield false negatives using the colorimetric test. Authorities identified the presence of one such NPS, 9,10-dihydro-LSD, in several of the blotters and EASI-MS analysis was applied, however, it was found that the lack of MS/MS required the use of EASI-FT-ICR in order to avoid false positives. Additionally, EASI-MS was applied to TLC plate measurements. EASI-MS and TLC-EASI-MS are presented as screening techniques where sensitivity for LSD and 9,10-dihydro-LSD was found to be comparable to LC-UV.

In an effort to further simplify EASI-MS, the self-pumping of solvents or liquid samples by utilizing the Venturi effect was demonstrated, eliminating the need for mechanical pumping, further lowering both the cost and complexity of the method.<sup>304</sup> Venturi-EASI (V-EASI) operates by inserting a thin fused silica capillary into a liquid sample, using the nebulizing gas to aspirate the sample and perform ionization. Compared to direct infusion electrospray, V-EASI gives a lower (2-3 times) absolute signal intensity but superior signal-to-noise ratios, with less ionization suppression and adduct/dimer formation.

At the current stage of development, EASI-MS and V-EASI-MS are most suited to initial qualitative screening techniques, although preliminary quantitative demonstrations have been presented. Applications of EASI-MS have primarily employed single quadrupole mass analyzers and lack structural confirmation, though can be coupled to MS<sup>n</sup> or HRMS systems. However, it is more likely that due to the simplicity of EASI, that applications will be directed towards portable MS systems for in situ analysis of drugs of abuse. Indeed, a V-EASI source coupled to a portable MS featuring canned air and disposable parts has been reported as 'one of the easiest and cheapest ways to make ions'.<sup>305</sup>

#### **2.7.2.4 Paper Spray Ionization**

Paper spray ionization mass spectrometry (PS-MS), first introduced in 2010,<sup>9</sup> is a rapid ambient ionization technique that is garnering considerable attention in the recent literature for a wide range of applications, including in forensic and clinical analysis. In PS-MS, small amounts of unprepared samples (ca. 10  $\mu$ L) are directly spotted on pointed paper strips (acting as a porous solid-substrate), which are then positioned in front of (ca. 5 mm away) the MS inlet. Solvent and high voltage (ca. 3-5 kV) are then applied: as solvent wicks to the tip of the paper it transfers analytes with it, and ionization occurs in a manner similar to that observed for electrospray/nanospray<sup>306</sup> with the notable difference that no pneumatic assistance is needed. Alternatively, solid surfaces can be swiped with the paper strips prior to measurement, as demonstrated for the qualitative MS/MS analysis of small amounts of HER and COC from surfaces.<sup>8</sup>

Paper properties (e.g., pore size, thickness, flow rate, and type) can have significant impacts on the analysis. Many different papers, including filter, glass fiber, and chromatography papers have been characterized for use in PS-MS<sup>9</sup> as well as a series of papers made from natural fibers, thin synthetic fibers, a microarray membrane, and various nanofibers,<sup>307</sup> silica coated papers,<sup>308</sup> polymers,<sup>309</sup> and molecularly imprinted polymer substrates.<sup>310</sup> A thorough investigation on the impact of paper properties on

matrix effects in the analysis of FEN and synthetic cannabinoids found that there is a trade-off between analyte recovery and ionization efficiency, and that no one paper is optimal.<sup>311</sup> Solvent choice was also shown to be more impactful on PS-MS results than paper properties. Ionization suppression and recovery in direct measurements of whole blood, plasma, and urine, have been investigated using alprazolam, benzoylecgonine (BEG), methadone, and MOR, among others; ionization suppression is generally highest in urine and lowest in blood, whereas recovery was lowest in blood and highest in urine.<sup>312</sup> Imperfections in the production of the paper points, particularly the angle and quality of the tip has been shown to significantly impact the analytical performance of PSI.<sup>313, 314</sup> Improvements in reproducibility can be achieved using commercially available paper spray cartridges, which are simpler to handle and whose tip quality is more consistent, allowing high-throughput, automated analysis. Espy et al. demonstrated the use of these PS cartridges for the quantitative analysis of AMPs, MOR, COC and  $\Delta^9$ -THC in whole blood and achieved improved sample to sample variations of 1-5% RSD with < 10  $\mu$ L of blood and inter-assay accuracies and precisions 87-117.9% and 1.3-16.5% (respectively, excluding morphine).<sup>315</sup> A bespoke PS cartridge with an integrated solid phase extraction step that improved detection limits in the analysis of plasma samples has been demonstrated.<sup>316</sup> Recently, a commercial PS system utilizing a multiplexed sampling plate containing 24 individual paper spray tips that can be coupled to an autosampler and has demonstrated its use for the detection of controlled substances in blood.<sup>317</sup>

There is a considerable need in forensic and clinical analysis for rapid screening methods to reduce sample backlogs: given the ease and speed of sampling, PS-MS is especially well suited for these applications. PS-MS has been demonstrated to rapidly screen for 4-chloroAMP in human saliva<sup>318</sup> as well as a variety of other chloro- and fluoroAMPs in saliva with improved LODs compared to AP-MALDI or ELDI.<sup>319</sup> NPS are often sold in the form of blotter papers, which can be cut into triangles and directly measured for DoA by PS-MS.<sup>320</sup> PS-MS has also been applied to the identification of a variety of synthetic cannabinoids and cathinones and other drugs (41 total) from 42 different powder or plant materials, and notably an e-cigarette liquid found to contain AB-CHMINACA and PB-22 using high resolution accurate mass (HRAM) MS and MS/MS with an analysis time of < 2 min; this technique allows for both targeted and non-targeted analysis.<sup>321</sup> PS with HR-MS/MS was further developed as a targeted semi-quantitative MS/MS drug screening methodology for over 130 drugs and drug metabolites in the positive ion mode as well as for a set of barbiturates and structural analogs in the negative ion mode, demonstrating potential for acidic drug analysis.<sup>322</sup> The authors report good qualitative agreement with LC-MS/MS and a true positive rate of 92% and true negative rate of over 98% when applied to post-mortem blood samples. While HRMS systems (such as Q-TOF and Q-Orbitrap methods) offer higher selectivity by combining exact mass with MS/MS, they require more frequent calibrations and are expensive, making them inaccessible to many forensic laboratories. The use of QqQ-MS systems for PS offers a cheaper, more robust, and thus more accessible alternative. PS-QqQ-MS has been used for rapid, direct, and quantitative drug and metabolite screening at low ng/mL levels in post-mortem blood samples.<sup>323</sup> In a direct comparison of PS-HR-MS/MS and LC-HR-MS/MS for

comprehensive urine drug testing using 103 authentic human urine samples, it was found that the direct PS method offered comparable screening power to the LC method, which included urine precipitation, conjugate cleavage, and liquid extraction.<sup>324</sup> A thorough review of PS-MS for the analysis of different bio-fluids has also been reported.<sup>325</sup>

Aside from the direct analysis of bio-fluids, PS-MS has been used for several other interesting forensic applications. Costa et al. demonstrate the analysis of DoA from fingerprint samples while retaining ridge detail by using a silver nitrate solution.<sup>326</sup> Paper spray lacks a chromatographic separation, and frequently employs MS/MS or HRAM for additional selectivity, though these couplings are often still unable to differentiate structural isomers. A coupling of PS-MS and surface-enhanced Raman spectroscopy (SERS), using paper SERS substrates which can be inkjet printed, demonstrates the increased selectivity and confirmation gained from the use of SERS through the differentiation of the isomers MOR and hydromorphone.<sup>327</sup> Selectivity can also be enhanced by utilizing ion mobility spectrometry. A coupling of PS to high-field asymmetric waveform ion mobility demonstrated the separation of morphine, hydromorphone, and norcodeine, which cannot be differentiated using MS/MS alone.<sup>328</sup> Another logical pairing to increase selectivity in PS application is TLC, since PS-MS can be achieved directly from TLC papers used for drug analysis.<sup>329</sup> Santos et al. used TLC papers with Dragendorff reagent (revealing agent) to positively identify COC, lidocaine, and levamisole in ten street crack samples.<sup>330</sup> PS-MS was then applied to revealed spots for quantification, and the authors reported no significant difference between PS-MS and GC-FID results. Recently, PS-MS has been presented as a promising analytical tool for drug checking, with the potential to prevent accidental overdoses.<sup>331</sup>

Among the ambient methods, PS-MS is among the most applicable for quantitative analysis because of the ease of internal standard introduction (either pre-spotted onto the paper prior to sample introduction or mixed into the sample). Quantitative analysis with PS-MS has been investigated for therapeutic drugs in dried blood spots,<sup>332</sup> the determination of eight AMPs in whole blood, with reported detection limits between 15 and 50 ng/mL,<sup>333</sup> the semi-quantitative measurement of FEN and norfentanyl in methanol, urine, and an analgesic slurry,<sup>314</sup> and quantitative analysis of COC and several opiates in prepared dried blood spots, with reported LOQs of 0.5 – 16 ng/mL and a linear range that encompasses the entire therapeutic range.<sup>334</sup> Quantitative analysis of substance use disorder patient urine samples for high-throughput analysis of FEN analogs and other NPS in urine was achieved using HRMS and MS/MS with commercial PS cartridges.<sup>335</sup>

The robustness and simplicity of PS-MS makes it especially well suited for in situ applications with miniature or portable mass spectrometers. A review of PS for portable mass spectrometry has recently been published.<sup>336</sup> Notable demonstrations of PS coupled to miniature MS systems include the analysis of synthetic cannabinoids using an IT,<sup>337</sup> and a FLIR® cylindrical IT-MS with automated MS/MS library searching.<sup>290</sup> The FLIR® system analyzed 25 positive controls, 4 negative controls, and 3 authentic powdered drug samples. For the positive control samples, 68 of 69 MS/MS spectra

collected produce relative average match probabilities high enough for “true positive” identification, no negative control samples resulted in false positives, and all of the powdered drug evidence samples were correctly identified using the automated, commercially available “Wiley Registry of Tandem Mass Spectral Data, MSforID” library. These results indicate that field-portable MS systems can be used in situ for drug analysis and the automated library searching feature eliminates the need for user interpretation of spectra and can allow for use by non-technical operators.

PS-MS has been demonstrated for a wide range of forensic and clinical applications, and given the rapidity, simplicity, low-cost of implementation, and demonstrated use with portable MS systems, it has the potential to reduce crime and clinical lab backlogs, and be implemented in roadside testing, point-of-care, or other in situ applications.

#### **2.7.2.5 Coated Blade Spray**

The lack of sample preparation for many ambient methods makes them attractive, but there are instances where sample preparation should not be overlooked, as it can greatly reduce ion suppression, matrix effects, and improve limits of detection. Coated blade spray (CBS) shares many characteristics observed in PSI but incorporates an extraction and pre-concentration sample preparation step by using a SPME coated, pointed stainless steel blade. This has the potential to greatly improve analytical performance and can be tailored to the analysis of specific matrices or analytes. A review of SPME materials and applications has been reported recently.<sup>338</sup>

CBS was first demonstrated by Pawliszyn et al. in 2014,<sup>273</sup> and reports that an entire analysis (analyte extraction, rinsing, desorption/ionization, peak integration, and quantitation) can be completed in less than 3 min with LOQs in the low pg/mL range, considerably lower than many of the other ambient techniques. CBS can be considered a solid-substrate ESI technique, using a thin stainless-steel blade as the substrate.<sup>273, 339</sup> Prior to sampling, the blade is ‘preconditioned’ by vortex agitation in a solution of methanol/water. Sampling/extraction occurs by immersing the preconditioned blade in a vial containing the sample matrix or by spotting a small volume of biofluid directly onto the SPME coated blade. This is followed by a quick (ca. 10 sec) rinse in water with vortex agitation, shown to be critical for reducing ionization suppression. A small volume (< 20  $\mu$ L) of desorption solvent (typically organic) is directly applied to the coated blade and high voltage (ca. 3.5 kV) applied to generate gas phase ions.

Similar to other solid-substrate ESI based methods, CBS signal intensity and duration are affected by the desorption solvent choice and volume, the wetting time, and the voltage applied, as well as by the amount of analyte extracted from the matrix by the SPME coating.<sup>273</sup> Analyte extraction from the sample solution or bio-fluid droplet is governed by the kinetics of analyte partitioning, though short, pre-equilibrium extractions are often used (e.g., 10 sec). The SPME coating (extraction phase) can either be a polymer or polymeric particles attached to the substrate (steel blade) using a chemical binder. The first demonstration of CBS used the biocompatible polymer C18-polyacrylonitrile (C18-PAN) for the effective extraction of hydrophobic small molecule drugs including COC and

diazepam from plasma and urine samples<sup>273</sup> with low pg/mL LOQs. Additionally, a variety of AMPs, opioids, and COC were quantified in phosphate-buffered saline with similar LOQs.

A desirable feature of CBS is the robustness and reproducibility of the sampling devices and technique. Other solid-substrate ESI methods (e.g., PS-MS, wooden tip ESI, etc.) use porous nonconductive substrates with poorly defined tips, leading to the generation of multiple ESI events at the tip, reducing the efficiency of ion transfer into the MS. Stainless-steel blades can be reliably machined to produce sharp, well defined tips, which increase the ionization efficiency.<sup>339</sup> In a continuation of complex sample analysis with CBS, diazepam and COC were quantitatively analyzed in phosphate buffered saline and methadone and oxycodone in urine, and the use of a 10  $\mu$ L sample directly applied to the coated blade (with various coatings) was investigated.<sup>340</sup>

A validated (with respect to linearity, precision, accuracy and LOQ) quantitative analysis of drugs (including AMPs, COC, opioids and BDZs) using CBS for biofluid spots (10  $\mu$ L – plasma and whole blood) has been presented in the literature as a new approach for sensitive rapid screening.<sup>341</sup> The method required 7 min total analysis time, offering a balance between improved analytical performance from sample preparation and high-throughput analysis. The sample preparation step allows for low LOQ values; LOQs were < 10 ng/mL in blood spots and < 5 ng/mL in plasma spots. Stability studies showed that most compounds were stable on the coating even at room temperature for up to seven days, with longer stability noted at lower temperatures. In an extension of this quantitative work, a high-throughput methodology was developed in which 96 CBS extractions were performed simultaneously on spiked urine and plasma samples allowing the total analysis time to be reduced to 55 s per sample, while maintaining excellent analytical performance and low limits of quantification (LOQ) for a variety of illicit and commonly abused drugs.<sup>342</sup>

A recent review of CBS is presented in the literature.<sup>339</sup> While the technique is slightly more complicated than PS or other related methods, CBS presents a balance between sample preparation and rapid analysis. The analytical performance achieved with CBS is superior to the other solid-substrate techniques in many cases due to the extraction of samples – concentrating analytes while leaving behind matrix species, including enzymes, which can convert or degrade analytes, making it especially well suited for the analysis of bio-fluids. The ability to interface the technique with 96 well-plates and robotics can bring the analysis time down to 55 s per sample. The inventors of the technique speculate that future applications may improve selectivity by using smart coating materials, on-coating derivatization, determination of total drug concentration in urine through enzymatic hydrolysis prior to extraction, as well as improvements in automation allowing for total analysis times of 10-15 s.<sup>339</sup>

### 2.7.3 Other Solid-Substrate Electrospray Ionization Techniques

Throughout the development of ambient mass spectrometry, many applications involving ESI from noncapillary solid substrates such as leaves and other plant material, bone, toothpicks, bamboo, fabrics, sponges, pipette-tips, medical swabs, metal needles, copper

wires, nanostructured tungsten oxide, among others, have been developed; an overview of solid-substrate ESI has been presented by Hu et al.<sup>343</sup> These substrates simplify sampling loading and avoid clogging issues prevalent in classical ESI methods. PS-MS and CBS-MS are also considered solid-substrate ESI techniques but have been discussed in separate sections due to the wealth of literature on these methods. Of the solid-substrate ESI techniques, several applications for the analysis of drugs of abuse have been shown, including the use of wooden tips,<sup>344-347</sup> bamboo pen nibs,<sup>348</sup> C18 pipette-tips,<sup>349</sup> and medical swabs.<sup>350, 351</sup> The technique is remarkably simple, the analyst need only apply sample, solvent, and high voltage to the substrate and position the substrate in front of the MS inlet to induce electrospray-like ionization.

Wooden tips have been used in several examples for DoA analysis. Benefits of the technique include its simplicity, low cost and ease of coupling with nano-ESI ion sources. Liquid samples are loaded by pipetting them onto the tip of a device or dipping the tip into solution, and solid samples can be scraped from crevasses, corners, and small openings, a unique advantage for forensic applications. The hydrophilic and porous properties of the wooden tips increase the duration of the signal. A sharper tip generates a much higher quality signal, and thus wooden tips are often sharpened prior to analysis. The first demonstration of the technique for drugs of abuse analysis analyzed KET collected 'from a tiny crack on a concrete floor'.<sup>344</sup> The tip was first pre-wetted to allow the powder to adhere, then 5  $\mu$ L of solvent was applied to facilitate the spray, and data was collected over 20 s. The technique was further applied to the pre-screening analysis of KET and NKET in urine and oral fluid samples with minimal sample preparation (dilution with methanol).<sup>346</sup> So, Ng et al. found that diluted urine and oral fluid aliquots of 2  $\mu$ L were sufficient for the quantitative MS/MS detection of KET and NKET with LODs of 20 ng/mL and 50 ng/mL in oral fluid and urine, respectively. In another application using wooden tip-ESI, 144 herbal dietary supplements were tested for 33 common adulterating drugs, detecting mainly BDZs.<sup>345</sup> The development of a sampling system incorporating a moving stage with 20 wooden tips attached in this study allowed for high-throughput analysis (ca. 15 seconds per sample). The presented method is a qualitative pre-screening method as no internal standard was used. The quantitative capabilities of wooden tip-ESI was explored by analyzing a variety of common DoA in urine and oral fluid in a continuation of So, Ng et al.'s previous work with KET and NKET.<sup>347</sup> Most analytes demonstrated acceptable detection limits that meet internationally established cutoff values, but THC and THC-COOH performed very poorly in these analyses. Overall, wooden tips as a solid substrate have been demonstrated for the quantitative analyses of many drugs of abuse in a variety of different matrices, require very small sample loadings, exhibit no carryover, and are extremely simple and economical to use.

In another solid-substrate ESI application, commercial C18 pipette-tips (conventional pipette tips with a C18 resin acting as an extraction phase) were used to purify and enrich KET and NKET in urine to generate much lower detection limits (0.3 and 0.8 ng/mL, respectively) than observed previously in wooden tip-ESI.<sup>349</sup> The method also gave superior analytical performance based on several other measures including linearity,

precision and accuracy. One drawback is the necessary sample preparation step that required 2-3 minutes for a total analysis time of ca. 5 minutes per sample.

Medical swabs are ubiquitously used to non-invasively sample biological fluids for a variety of clinical tests and in forensic toxicology. Given that they are already approved for medical use, they represent an opportunity to use as a solid substrate for MS analysis in a wide range of forensic and clinical applications. Pirro et al. demonstrated their proof-of-concept use for qualitative DoA detection in oral fluid, analyzing 14 common DoA, with the intended application of point-of-care drug testing or in situ forensic applications.<sup>351</sup> Using a LIT-MS, MS<sup>2</sup> and MS<sup>3</sup> experiments were performed in a total analysis time of 4 min (following a 15 min drying step after sampling) to provide acceptable detection limits and identification, except for BUP and THC, presumably due to poor ionization characteristics. Quantitative analysis or in vivo sampling was not achieved in this study, and sample volumes could only be estimated (ca. 40  $\mu$ L). However, medical swabs have been developed for volumetric sampling and demonstrate potential for quantitative sampling. Morato et al. have demonstrated the use of volumetric absorptive microsampling swabs as substrates for the quantitative analysis of 30 common DoA using 10  $\mu$ L samples of oral fluid, optimal for forensic or toxicological applications given that small volumes are often all that can be collected.<sup>350</sup> The authors made considerable effort to fully validate the MS/MS method, which yields results within 2 minutes (following a 15 min drying step) with satisfactory analytical performance. LODs for the compounds ranged from 0.08 – 4.86 ng/mL except for AMP, MAMP, and mephedrone, and no carryover effects were observed. For quantitative in vivo sampling, an internal standard mixture must be spotted onto the swab following sampling, resulting in a slight overall reduction in analytical performance. The quantitative performance is still acceptable given that only three drugs (6-AM, AMP, and MAMP) gave LOD values above cutoff values established by DRUID.

Medical swabs for the analysis of drugs of abuse in oral fluid are a promising choice given their already established and extensive use in the medical field as non-invasive sampling devices. The swabs are cheap, can volumetrically sample small amounts (10  $\mu$ L), and have been validated for quantitative analysis. The method requires no sample preparation (except for a drying step), and the promising applications presented thus far indicate the potential for this technique to be used in roadside drug testing, point-of-care, or other forensic and clinical in situ applications.

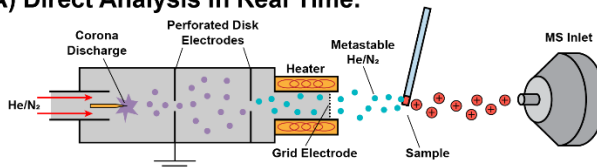
#### **2.7.4 Plasma-Based Techniques**

Plasma based ambient ionization techniques operate via similar principles as APCI, in that energetic/reactive species generated by some form of plasma are subsequently used to ionize analytes. Table 2.3 summarizes a variety of these approaches. Figure 2.8 illustrates generalized schematics for plasma-based ambient ionization techniques. The reader is directed to two recent reviews on plasma-based ambient ionization mass spectrometry techniques.<sup>258, 259</sup>

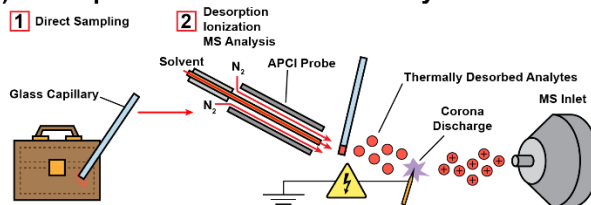
Table 2.3 Plasma-based ambient techniques.

<b>Technique</b>	<b>Sampling Principles</b>	<b>Plasma</b>
Direct analysis in real time (DART)	Metastable neutrals (e.g., N <sub>2</sub> , He) are generated in a confined plasma and passed over a sample outside of the source with heat for desorption / ionization.	Corona or glow discharge
Atmospheric solids analysis probe (ASAP)	A probe is used to introduce sample into a heated desolvation gas stream (from an APCI or ESI probe), thermally desorbed analytes are ionized by a corona discharge.	Corona discharge
Flowing atmospheric-pressure afterglow (FAPA)	The plasma discharge is physically and electrically isolated from the sample. The sample is introduced into the flowing afterglow and analytes are desorbed / ionized.	Corona or glow discharge
Direct sample analysis (DSA)	A probe is used as a solids sampling device, or liquids samples are deposited onto a mesh. A corona discharge is generated by an APCI source with N <sub>2</sub> and the produced reagent ions are directed to the probe or mesh to facilitate desorption / ionization.	Corona discharge
Dielectric barrier discharge ionization (DBDI)	A plasma is generated within the source and passed over a sample for desorption / ionization.	Dielectric barrier discharge
Low temperature (LTP)	An alternating current electric field generates a low temperature plasma that extends from the source and directly interacts with the sample to effect desorption / ionization.	Dielectric barrier discharge

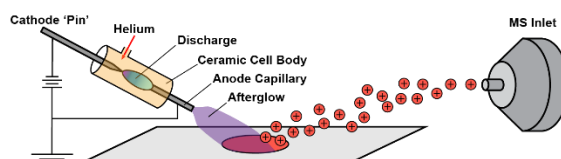
### A) Direct Analysis in Real Time:



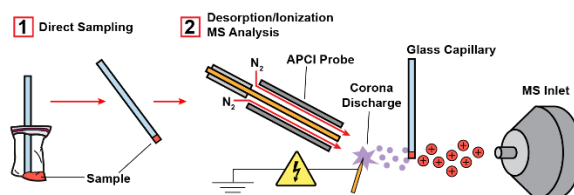
### B) Atmospheric Pressure Solids Analysis Probe:



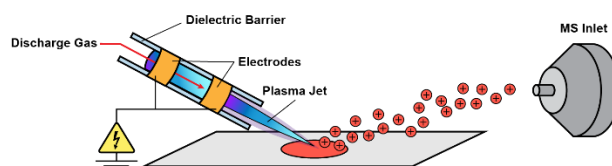
### C) Flowing Atmospheric-Pressure Afterglow:



### D) Direct Sample Analysis



### E) Dielectric Barrier Discharge Ionization:



### F) Low Temperature Plasma Ionization:

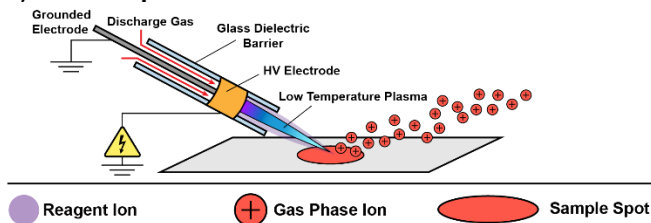


Figure 2.8 Generalized instrumental schematics for (A) direct analysis in real time (DART), (B) atmospheric solids analysis probe (ASAP), (C) flowing atmospheric-pressure afterglow (FAPA), (D) direct sample analysis (DSA), (E) dielectric barrier discharge ionization (DBDI), (F) low-temperature plasma (LTP). Not to scale.

### 2.7.4.1 Direct Analysis in Real Time

Since its introduction in 2005,<sup>263</sup> direct analysis in real time (DART) has become an established technique for rapid mass spectral analysis in a wide range of forensic and clinical sampling applications. It can analyze solid, liquid, and gas samples; a critical review of the technique is presented by Gross<sup>352</sup> as well as a review discussing forensic and security applications.<sup>353</sup> If the technique were to be named from its desorption/ionization characteristics, then perhaps a name like thermal desorption penning ionization-induced atmospheric pressure chemical ionization may have been chosen. The ionization mechanism has been investigated for both positive ion<sup>354</sup> and negative ion modes.<sup>355</sup> In DART, metastable neutrals (e.g., He, N<sub>2</sub>) generated in a confined plasma source are used to effect analyte ionization by directing them onto a surface to be measured. In comparison to other ambient methods, DART particularly excels at the analysis of surfaces.<sup>356</sup> In the initial demonstration of DART, it was applied to the analysis of DoA on business cards, pharmaceutical tablets, concrete, cocktail glasses, plastics, leaves, currency, airline boarding passes and human skin, among many others, and was able to detect GHB spiked into gin (at 10 ppm) within seconds, a compound that is particularly challenging to analyze with LC-MS.<sup>263</sup> Coupling of DART to a QqQ MS was used to investigate the direct quantification of drugs in biological matrices.<sup>357</sup> The authors investigated matrix effects from plasma samples and found them to be analyte specific. Reproducibility, sensitivity, linearity, bias, matrix effects, and a direct comparison to LC-MS/MS found the technique to be generally adequate for bioanalytical or forensic applications, though noted limitations include poor selectivity in some cases, and 'harder' ionization that fragments more labile compounds, such as glucuronides, within the source. DART has been demonstrated for a number of forensic and clinical screening applications, including: the analysis of synthetic cannabinoids from commercial herbal products,<sup>358-361</sup> the direct detection of THC from hair samples,<sup>362</sup> the rapid (0.5 min) screening of NPS with confirmation by LC-MS,<sup>363</sup> detection of synthetic cathinones and metabolites in urine with SPME-DART coupling,<sup>364</sup> as well as the untargeted analysis of DoA in hair,<sup>365</sup> among others. In 2009, a validation of the DART source coupled to an accurate mass TOF-MS for use in forensic screening of DoA was achieved, allowing the Virginia Department of Forensic Science to incorporate DART for the qualitative screening of solid forms of DoA.<sup>366</sup>

Though DART is primarily used as a screening or qualitative analysis technique, a few quantitative applications have been demonstrated. The quantification of DoA in biological matrices was achieved in both in vivo and in vitro applications, demonstrating comparable results to LC-MS/MS and potential as an effective tool for high-throughput, real time bioanalysis.<sup>357</sup> A coupling of DART to SPME devices made from PEEK mesh was demonstrated for DoA quantitation in oral fluid and urine with satisfactory LOQs (ca. 0.5 ng/mL), linearity, and accuracy over the evaluated range (0.5 – 200 ng/mL).<sup>367</sup>

DART, like other ambient techniques, has reduced selectivity when compared to chromatographic methods. To address this, Musah et al. utilized in-source CID and HRMS for a variety of NPS,<sup>368</sup> as did Lesiak et al. who demonstrated differentiation of

closely related isobaric synthetic cathinones.<sup>369</sup> Advanced statistical treatments of data generated from high resolution DART measurements have been used to identify heroin sources,<sup>370</sup> and identify NPS from neutral loss spectra.<sup>371</sup>

Portable MS applications with DART are particularly attractive given the simplicity of the source and its commercial availability. DART with portable MS has been demonstrated for the identification of powdered drug samples, tablets, and herbal samples<sup>372</sup> as well as for DoA in biofluids by coupling SPME to a portable single quadrupole system.<sup>373</sup> In summary, DART based methods can rapidly desorb and ionize analytes, particularly from solids or solid surfaces, providing real-time information regarding DoA, and the technique has been commercialized for portable applications.

#### **2.7.4.2 Atmospheric Pressure Solids Analysis Probe**

The Atmospheric Pressure Solids Analysis Probe (ASAP) allows for the direct analysis of liquid or solid samples in seconds and can be accomplished using any commercial instrument with an ESI or APCI source by creating a port to insert the sample probe into the heated desolvation gas stream. The technique, first described in 2005, uses the heated nitrogen desolvation gas from an ESI or APCI source to thermally desorb analytes from a sampling probe, with subsequent ionization of the vapour occurring via the APCI corona discharge.<sup>265</sup> The probe used to introduce sample must be free of volatile components that may interfere with analysis, and glass melting point capillary tubes are most often employed as sampling probes. The MS/MS detection of COC from several U.S. 1-dollar bills has been demonstrated by directly introducing them into the heated desolvation gas stream. The range of compounds amenable ASAP is limited to compounds with some polar character, that can be thermally desorbed and do not thermally degrade, as well as those that can be ionized by APCI. Although the ASAP method has not been extensively demonstrated for the analysis of DoA, there are a few select applications of note.

Jagerdeo et al. demonstrated the direct, rapid analysis of black tar HER and impurities (including codeine, morphine, noscapine, papaverine and 6-AM), crack COC, alprazolam from urine, as well as a rodenticide which has increasingly been reported to be detected in seized drug samples as an adulterant.<sup>374</sup> A capillary tube was rubbed on solid samples or submerged into liquid samples and allowed to dry, then transferred to the source into the path of the hot nitrogen gas supplied by an APCI probe. The ASAP source, in this case, was coupled to a linear ion trap MS system to facilitate full scan, MS<sup>n</sup>, and rapid polarity switching. Quantitative work was not thoroughly investigated, though a calibration of alprazolam in urine was demonstrated to suggest quantitation could be achieved. ASAP-MS/MS has been used for the direct analysis of raw urine samples for the qualitative trace detection of AMPs.<sup>375</sup> The LOD for the compounds was determined to be 0.002 to 0.4 ng/mL with acceptable precision. No sample carryover or matrix suppression effects were observed.

ASAP coupled with HRMS (LTQ-Orbitrap) has also been used for the direct analysis of black tar HER (and impurities) and "Spice" packets containing 10 different synthetic

cannabinoids and a synthetic cathinone in positive APCI mode, comparing it to laser diode thermal desorption (LDTD).<sup>376</sup> The signal for the analysis of black tar HER using ASAP lasted for more than 8 minutes, which allowed for a full scan and six MS/MS experiments to be completed. Optimization allowed the total MS analysis time to be reduced to < 1 min.

Given that ASAP can be easily interfaced with any commercial mass spectrometer, often requires no sample preparation, uses disposable, inexpensive glass capillaries for sampling that eliminate carryover, exhibits lessened matrix effects due to APCI ionization, can sustain a signal for minutes, and allows for rapid analysis and high throughput, it is a very attractive candidate in rapid, routine analysis of forensic samples for both targeted and non-targeted analysis, provided that the analytes are amenable to the method.

#### **2.7.4.3 Flowing Atmospheric-Pressure Afterglow**

Flowing atmospheric-pressure afterglow (FAPA) is a plasma-based source traditionally used for elemental analysis. It has appeared in the literature in recent years for the analysis of organic compounds at atmospheric pressure with soft ionization. In FAPA, analytes are directly desorbed and ionized from a sample of any phase (solid, liquid, gas) with minimal sample preparation; desorption is presumably due to the temperature of the helium gas (> 200°C) and the presence of excited species. The exact ionization mechanism is unclear but occurs either directly by Penning ionization or through interaction with reagent ions such as protonated water clusters.<sup>377</sup> FAPA was originally termed helium atmospheric-pressure glow discharge and was first reported in a paper that thoroughly outlines the design and behaviour of the ionization source.<sup>267</sup> In an improved geometry over the original pin-to-plate design, a pin-to-capillary geometry significantly reduced background noise and improved analytical performance in both positive and negative ionization modes. It has been used for the detection of MAMP in tap water, with a demonstrated LOD of 0.7 ng/mL, and applied to untreated urine analysis with minimal sensitivity losses.<sup>377</sup> This new FAPA design allowed its sensitive and quantitative use for DoA detection, with less matrix effects than other plasma-based sources. It has been used for rapid direct analysis of methcathinone from crude reaction mixtures without sample preparation<sup>378</sup> with an estimated LOD of 10 ng. FAPA is not very effective at analyzing compounds > 400 Da. The analysis of the designer drugs JWH-122, 4BMC, pentedrone, 3,4-DNNC and ethcathinone has been demonstrated using two FAPA sampling methods (methanolic aerosol from nebuliser or heated crucible for thermal desorption).<sup>379</sup> The variety of forms in which these NPSs are distributed, including being deposited on various sorbents or biomasses and as trace components amongst other adulterants and additives can cause challenges with traditional methods. FAPA-MS is a direct technique that appears capable of performing direct analyses in the already extensive and increasing number of NPS sample matrices. The method demonstrates sensitivity that is comparable to direct inlet probe EI analysis since ca. 5 ng of material can be detected. The methanolic aerosol method was investigated for quantitative use with 10 µL injections of an ethcathinone solution, demonstrating acceptable quantitative

or semi-quantitative performance, though notably not as sensitive as some of the other plasma-based techniques.

FAPA has been interfaced with an electrochemical flow cell to identify electrochemically produced drug metabolites, especially important to the field of predictive toxicology for the analysis of NPS whose metabolic pathways are unknown or poorly understood.<sup>380</sup> The authors report much higher LODs than previously established by other demonstrations of FAPA (e.g., 2.5 µg/mL MAMP) but note that the goal was to demonstrate the utility of the coupling of the electrochemical cell to a FAPA source for use in predictive toxicology and presented the first coupling of a flowing liquid system to FAPA. The 'halo-shaped' FAPA or h-FAPA improves the reproducibility of sample introduction.<sup>381</sup> It uses concentric tubular electrodes to form a halo-shaped discharge, and allows sample introduction (solution, vapour, or aerosol) through an inner capillary, improving the interaction between sample and plasma to enhance both desorption and ionization, while retaining surface sampling capabilities. Proof of concept DoA testing demonstrated superior sensitivity and precision over earlier FAPA designs for COC and metabolites.

FAPA is a direct, rapid method of analysis with potential for use in a wide range of forensic applications given that no or minimal sample preparation is needed, and can analyze solid, liquid, or gaseous samples. New source geometries have significantly improved its analytical performance. The technique is not nearly as well represented in the literature as other plasma-based sources like DART and DBDI, and though some quantitative measurements have been demonstrated for drugs, there is still work to be done to establish FAPA as a viable source for forensic and clinical applications for DoA.

#### **2.7.4.4 Direct Sample Analysis**

Direct sample analysis (DSA) is an ambient technique that has been commercialized by PerkinElmer, originally termed surface desorption atmospheric pressure chemical ionization in 2007. The technique combines the features of DESI and APCI; a corona discharge is generated by an APCI source with nitrogen gas and the produced primary ions (protonated water clusters) are directed to a liquid or solid sample absorbed onto a surface (or powder) to desorb and ionize analytes of interest.<sup>271</sup> A high-throughput sample introduction system interfaced with the DSA-MS can transport up to 24 samples per second with a duty cycle as low as 10 ms per sample. In this initial demonstration, pharmaceutical tablets and powders were directly analyzed in 1 minute. Much lower gas pressures (6.89 kPa) are used in the DSA source than used in a typical DESI source (~2 MPa), suggesting a more facile coupling to miniature mass spectrometers, obviating the need for compressed gas tanks.

A commercial DSA-TOF-MS system has been demonstrated for the rapid analysis of 369 DoA from seized pills, vials, powders, and urine samples.<sup>382</sup> Analyte identity is confirmed using the exact monoisotopic masses of precursor and fragment ions and isotope ratios to identify analytes through comparison with a system database containing all US Schedule 1-5 drugs. Sample introduction is achieved using disposable mesh for liquid

samples (5  $\mu\text{L}$ ) or glass capillaries for solid samples with minimal or no sample preparation. The source can easily be switched for a traditional LC source in minutes, if desired. The DSA-TOF-MS system was applied to the analysis of an emerging class of variable phenethylamines known as 'NBOMes' (which have similar properties to LSD and are variants of the 2C-X series) from blotter papers.<sup>383</sup> The analysis time for designer drugs on blotter papers was successfully reduced to ca. 15 s using the direct DSA-TOF-MS method, though it should be noted that quantitation of NBOMes was not accomplished, and the constitutional isomers 25T4-NBOMe and 25T7-NBOMe could not be differentiated. McGonigal et al. have also demonstrated the use of the AxION DSA-TOF-MS system for the detection of 26 synthetic phenethylamine street drugs (representing all commercially available compounds at the time) including some of the NBOMes previously mentioned as well as several 2C-X analogs of mescaline.<sup>384</sup> Methodologies for the rapid screening of opioids in seized street drug samples has also been developed.<sup>385</sup> A qualitative method for the determination of 18 compounds (opiates, FEN analogs, and synthetic opioids) with in-source CID was used for structural confirmation. Matrix interferences were found to be minimal, even when samples were prepared as 90% adulterants, maintaining good detection levels and mass accuracy for all analytes. In this study, 81 seized drug samples were analyzed both by traditional GC-MS and by DSA-TOF-MS, the results agreed in 80 of 81 cases. In an interesting case, a sample suspected to contain HER was analyzed by GC-MS and no controlled substance was identified, but DSA-TOF-MS with in-source CID was able to qualitatively identify furanyl FEN from its characteristic fragments and the precursor ion mass.

The PerkinElmer AxION DSA-TOF-MS system represents yet another alternative that can be used to rapidly screen forensic liquid and solid samples. Methods for DoA with this technique have largely been qualitative and focus on high resolution accurate mass combined with in-source CID for identification of compounds. DSA-TOF-MS has been successfully demonstrated for the identification of true unknowns and NPS where no reference standards or libraries exist.

#### **2.7.4.5 Dielectric Barrier Discharge Ionization**

The dielectric barrier discharge ionization (DBDI) source (a glow discharge device) is comprised of a copper sheet electrode and a discharge electrode, with an insulating glass slide in between that acts as both a dielectric barrier and sample plate (Na, Zhao et al. 2007). The DBDI source has been employed for several applications involving the direct and rapid solvent-free analysis of DoA, discussed further in a 2015 review, which also discusses a variety of different source geometries.<sup>386</sup> Advantages of DBDI include a mild discharge (soft ionization), small size, stable operation at atmospheric pressure, low power consumption, simplicity, and non-thermal characteristics, making it especially well suited to portable or miniature mass spectrometers. Kumano et al. utilized a low-pressure DBDI source to develop a prototype portable LIT-MS capable of discontinuous sample gas introduction and a vacuum headspace technique.<sup>387</sup> This prototype system was found to be sensitive enough for the qualitative MS/MS detection of 0.1 ppm MAMP, 1 ppm AMP, 1 ppm MDMA, and 10 ppm COC in an aqueous  $\text{K}_2\text{CO}_3$  sample headspace, with

the assumed sensitivity differences due to proton affinity and vapour pressures. The portability and size of the DBDI-MS limits the sensitivity that can be achieved, though the source was found to be > 50 times more sensitive than an APCI source on the same MS. Another example of a low-pressure DBDI source being coupled to a miniature MS was used to analyze drugs (caffeine, COC and MOR) and explosives using air as a carrier gas to further simplify the method.<sup>388</sup> All analytes produced  $[M+H]^+$  ions. Habib et al. demonstrated the trace level analysis of AMPs in water and urine samples with LODs in the pg/mL range.<sup>389</sup> Validation studies indicate that the method is a viable alternative to routine analytical work done by conventional GC-MS or LC-MS methods for rapid detection of amine-based drug compounds in urine for doping tests or in forensic laboratories.

Synthetic cannabinoids are a class of NPS that are often contained within botanical matrices, hampering their analysis with traditional methods without extensive sample preparation and routine screening tests often do not incorporate these types of compounds. DBDI-MS offers a direct and rapid analysis strategy for these compounds present in herbal matrices, and the use of a sample heater to assist in sample introduction has greatly increased the analytical performance of DBDI for these compounds allowing the technique to partially replace GC-MS methods for fast screening.<sup>390</sup>

In one of the most sensitive direct couplings of SPME with MS reported in the literature at the time, Mirabelli et al. reported a SPME-DBDI-MS methodology capable of sub pg/mL DoA detection limits that employs a thermal desorption of SPME fibers followed by DBDI ionization.<sup>391</sup> At the time of the publication, all direct couplings of ambient MS ionization techniques to SPME relied on the simultaneous desorption/ionization of analytes directly from the SPME device, apart from solvent desorption techniques which limit the enrichment potential of SPME. Even when a relatively short, 5 min extraction time was used, LOD of 0.3 pg/mL were achieved for diazepam and COC. Quality control experiments demonstrated that no carryover effect was observed over the entire concentration range analyzed. The remarkable sensitivity and precision demonstrated in this SPME-DBDI coupling with thermal desorption opens the possibility for forensic and clinical applications requiring very low-level analysis. For example, this coupling was used to rapidly screen drugs in beverages (vodka, wine, and cola) and biological fluids (urine and blood plasma) using ultrasound as an agitation method to affect the rapid extraction of analytes using thin film microextraction from matrix, and thermal desorption to introduce gas phase analytes to the DBDI source.<sup>392</sup> The authors note that the biocompatibility of the thin film microextraction devices used in the study may have future applications in non-invasive oral fluid or sweat sampling with rapid, trace-level analysis.

A simplified, cost-effective DBDI source was constructed and applied to the analysis of a variety of drugs including pharmaceutical compounds (AMP and scopolamine), synthetic cannabinoids, psychostimulants, methoxyphenidine and COC.<sup>393</sup> The qualitative analysis of the drug standards was demonstrated using 20  $\mu$ L samples, as well as the direct analysis of pharmaceutical tablets, and 5F-APINACA from 'Funky Buddha' leaves

(marshmallow plant). The entire DBDI circuitry can be purchased as a preassembled module from internet vendors for ca. 20 euros.

The DBDI source appears to hold significant promise as an inexpensive ambient ionization strategy for DoA measurements. Its small size, amenability for portable instrument applications and low cost should see future developments as the technique matures.

#### **2.7.4.6 Low Temperature Plasma**

Similar to the DBDI source, the low temperature plasma (LTP) source, first demonstrated in 2008, uses an alternating current electric field to induce a dielectric barrier discharge for solvent-free, low temperature desorption and ionization of compounds in the solid, liquid or gas phase with a specially designed electrode configuration.<sup>272</sup> The difference from DBDI is that the counter electrode is incorporated within the source, yielding a more direct platform for surface sampling.<sup>272</sup> The technique was initially demonstrated for a wide variety of DoA applications with little to no sample preparation, including: the direct analysis of COC on human skin, antihistamines from pharmaceutical drug tablets, caffeine and other compounds from urine, as well as the direct analysis of aqueous solutions, with reported LODs as low as 1 ppb. Although the relatively poor spatial resolution it affords does not lend itself well to high resolution chemical imaging, the tolerance to the sample position and angles used in the desorption setup are promising for the analysis of large surface areas such as the rapid screening of luggage for DoA. The LTP shares many characteristics with other plasma-based ambient desorption ionization sources with a few notable differences: the probe design allows for plasma species to be extracted from the discharging area by the discharge gas flow and electric field. A low temperature 'torch' (ca. 30°C) extends from the glass tube of the source that directly interacts with a sample or surface. Mass spectra exhibit similar but gentler ionization than ESI. The use of air as a discharge gas further increases source simplicity and its applicability for portable MS systems.

The use of LTP-MS for the direct analysis of DoA in biological matrices was demonstrated for 14 drugs from the opiate, stimulant, euphoriant, and sedative drug classes which were qualitatively analyzed in urine, saliva, and hair extracts, with quantitative measurement demonstrated using BEG in urine.<sup>394</sup> Detection limits in urine can be improved by dilution, which greatly reduces matrix effects. Although thermal assistance is not required for desorption/ionization of most compounds with the LTP, detection limits can be improved with assistive sample heating.

The LTP source has also been applied to the direct, quantitative analysis of 11 DoA in saliva including phenethylamines, synthetic cannabinoids, synthetic cathinones, piperazines, and KETs.<sup>395</sup> The higher molecular weight compounds (e.g., synthetic cannabinoids) performed poorly without thermal assistance and thus a sample temperature of 200°C was required for sensitive analysis of all compounds, and LODs for the compounds in the study ranged from 3.0 to 15.2 ng/mL, comparable to immunoassays, but with lower sensitivity than LC-MS/MS methods. Arrays of multiple

LTP probes (1, 7, and 19 probes) have been demonstrated to increase the sampling area and reduce LODs for select DoA applications.<sup>396</sup> The authors demonstrated the online chemical derivatization of mephedrone, MDMA, and methylone using trifluoroacetic anhydride increased selectivity, though it was noted that sensitivity decreased in these specific examples. The increased surface area of the arrays makes them ideal candidates for the rapid screening of larger surfaces such as suitcases as well as for integration with portable mass spectrometers.

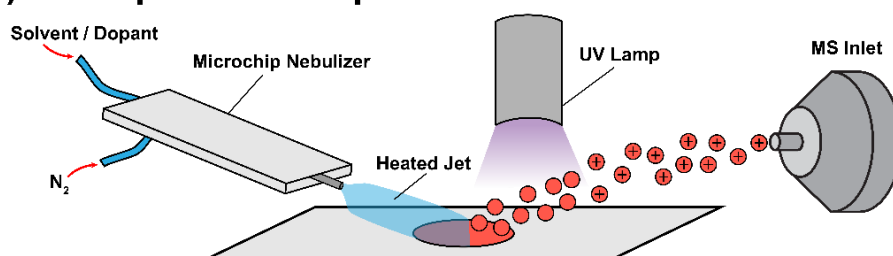
Integration of LTP probes into portable mass spectrometer systems is a logical pairing given the absence of solvent and other waste products, the low power requirements, low cost, small size, and low gas flows used. Wiley, Shelly, and Cooks have demonstrated the use of a handheld LTP probe for “point-and-shoot” analysis that weighs ca. 0.9 kg.<sup>397</sup> This source was able to sustain a plasma continuously for two hours using a small 7.4 V Li-polymer battery and a small helium or air cylinder, and was able to detect 1 µg of MAMP from a human finger two hours after its deposition using MS/MS. Despite the smaller size, lower power requirements and gas flows, analytical performance was not degraded using the handheld LTP source compared to a conventional, large-scale source.

LTP-MS has been demonstrated for both qualitative and quantitative measurements of DoA from a variety of classes. At the current stage of development LTP ionization shows the most promise for applications involving surface sampling, rapid screening, semi-quantitative screening, and most notably for integration with portable MS systems, given its small size and cost, that it operates without solvent, generates little waste, and has low power and gas flow requirements.

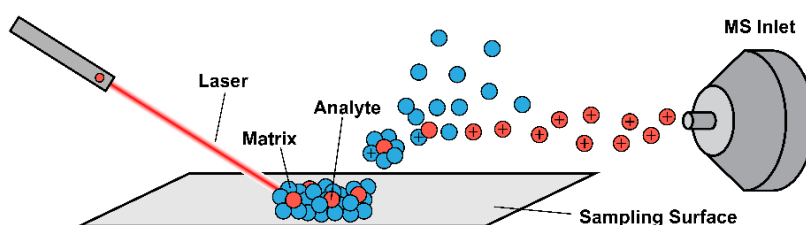
## **2.8 Other Techniques**

For completeness, this section presents the ambient ionization technique desorption atmospheric pressure photoionization (DAPPI), as well as two laser-based methods, matrix-assisted laser desorption ionization (MALDI) and surface-assisted laser desorption ionization (SALDI). The general instrumental schematics for these methods are illustrated in Figure 2.9.

### A) Desorption Atmospheric Pressure Photoionization:



### B) Matrix Assisted Laser Desorption Ionization:



### C) Surface Assisted Laser Desorption Ionization:

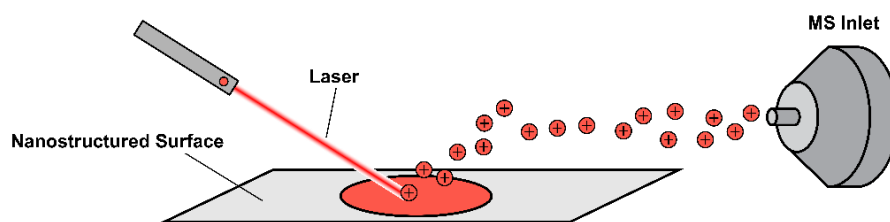


Figure 2.9 Generalized instrumental schematics for (A) desorption atmospheric pressure photoionization, (B) matrix-assisted laser desorption ionization (MALDI), and (C) surface-assisted laser desorption ionization (SALDI). Not to scale.

#### 2.8.1 Desorption Atmospheric Pressure Photoionization

Desorption atmospheric pressure photoionization (DAPPI) utilizes a heated nebulizer microchip to direct a jet of hot, vaporized solvent towards a sample on a surface for thermal desorption; desorbed analytes are directly ionized using a photoionization lamp, or indirectly via gas phase interactions with dopant (solvent) molecules.<sup>269</sup> In the first demonstration of the technique, MDMA was used as a test compound, reporting a LOD of 56 fmol using an ion trap MS. A comparison between DESI and DAPPI demonstrated the superior analytical performance of DAPPI for less to nonpolar polar compounds. In addition to dried sample spots on sample plates, DAPPI has been demonstrated for the direct qualitative analysis of drug tablets. It is noted that no significant signals were observed using pure methanol as solvent, and that the presence of a dopant solvent

(toluene or acetone) was required for efficient ionization of target analytes. Toluene forms both molecular ions (via charge exchange) and protonated molecular ions (via proton transfer) while acetone only forms protonated molecular ions. This phenomenon has been exploited for specific DoA applications, discussed below.

DAPPI was demonstrated for the qualitative analysis of DoA in tablets, blotter paper, plant resin and bloom using an ion trap MS (Kauppila, Arvola et al. 2008). MDMA and AMP were identified in confiscated ecstasy tablets and the DAPPI spectra produced were similar to those shown in previous measurements of these tablets with DESI. Similarly, phenazepam and BUP were directly detected from tablets via MS/MS, and DAPPI analysis of blotter papers qualitatively confirmed the presence of LSD and bromobenzodifuranylisopropylamine (bromo-dragonFLY, ABDF). DAPPI was further applied to the analysis of cannabis products (marijuana and hashish), generating strong THC or cannabidiol (CBD) signals, although the isomers could not be differentiated without MS2 characterization.

Confiscated powdered drug samples have also been qualitatively analyzed using DAPPI by dissolving them in solvent and spotting them on sample plates, which were dried before measurements (low ng amounts of drug deposited).<sup>398</sup> The confiscated powders were shown to contain AMP, MDMA, MAMP, HER, and COC by DAPPI and DESI, confirmed by GC/MS. For two samples confirmed to contain MAMP, DAPPI-MS using toluene dopant gave positive results for 1 sample, whereas with acetone both were positive, highlighting the importance of DAPPI dopant solvent choice. Though sensitivity can be lower in select applications using toluene, a distinct advantage of using toluene is that the production of molecular ions allows for matching of produced MS/MS spectra to extensive electron ionization mass spectral libraries.

Highlighting the versatility of the DAPPI source for a wide variety of matrices, the technique was further applied to the direct analysis of DoA in herbal products and designer drugs in tablets and powders with a quadrupole ion trap MS.<sup>399</sup> Dried *Psilocybe* mushrooms contained psilocin and psilocybin, as confirmed with GC/MS, however psilocybin could not be detected using DAPPI, which was likely due to poor thermal desorption or thermal degradation of the compound. Opium bricks were directly analyzed, and qualitative detection of several opiates was achieved. Qualitative analysis of Spice samples demonstrated detection of several synthetic cannabinoids and NPS. Seized drug tablets were analyzed using DAPPI-MS/MS for qualitative detection of 3-fluoroMAMP, m-CPP, AMP and BDZs. A white drug powder was sampled using double sided tape with the excess powder shaken off, and directly analyzed with DAPPI for the detection of MDPV and methylene.

In a direct comparison, DAPPI was shown to be more tolerant to matrix effects from urine than its predecessor DESI, with observed decreases in sensitivity for the direct analysis of benzodiazepines and opioids of ~2-15 fold for DAPPI and ~20-160 fold for DESI; the two were shown to have comparable sensitivities in neat solvent.<sup>280</sup> However, DAPPI-MS

for the analysis of DoA from urine exhibits poorer analytical performance than established LC-MS and GC-MS methodologies.

The product ion spectra of the protonated molecular ions of the isomers THC and CBD are remarkably similar, presenting a selectivity challenge to many of the other ambient ionization techniques. Kauppila et al. showed that the direct analysis of cannabis samples with DAPPI-MS/MS allows for the differentiation of THC and CBD through the use of toluene as a solvent, which produces molecular ions (rather than acetone which produces protonated molecular ions) with clearly differentiable product ion spectra.<sup>400</sup> Protonated molecular ions of THC and CBD generate nearly identical product ion spectra that cannot be differentiated by other ambient methods that produce  $[M+H]^+$  ions. DAPPI-MS may be a valuable tool in reducing forensic laboratory backlog since seized cannabis samples could be quickly analyzed, and only those cannabis samples containing very small amounts of THC would require lengthier GC-MS or GC-FID analysis.

Recently, in another ambient photoionization approach, a direct coupling of SPME and capillary APPI (cAPPI) with a confined ionization region yielding sub-ppt detection for a wide range of polar and nonpolar compounds has been reported.<sup>401</sup> The authors use the novel cAPPI source to directly interface SPME to MS for the analysis of MDMA, KET, lidocaine and FEN, among other compounds, and use the more conventional GC-cAPPI-MS to evaluate the performance of the cAPPI source. The average LOD determined for the DoA in aqueous solution in this study was 30 pg/mL, representing a significant improvement over other APPI based methods, primarily due to the pre-concentration of the analyte using a 2-minute extraction of the sample with a SPME fiber.

DAPPI has been shown to be a sensitive, effective tool for both screening and quantitative analyses of drugs of abuse. One of the unique features of DAPPI (and cAPPI) compared to other ambient ionization techniques is that using the proper solvent, molecular ions can be generated which may assist in the differentiation of isomers with tandem mass spectrometry, notably in the case of THC and CBD above, wherein the two cannot be differentiated using techniques that generate protonated molecular ions. DAPPI can also be used for the analysis of nonpolar compounds, a distinct advantage over many of the other ambient ionization techniques, extending the range of analytes amenable to analysis and making DAPPI a more universal ion source.

## 2.8.2 Laser Ablation-Based Techniques

Although not considered ambient ionization mass spectrometry strategies, because laser desorption-based techniques are relatively simple and allow direct analysis, we have chosen to include a short section on these methods and their use for drug testing. The two main laser desorption strategies that have emerged in the literature as promising drug measurement strategies are matrix assisted laser desorption ionization (MALDI) and matrix-free laser desorption ionization variants best described as surface assisted laser desorption ionization (SALDI) methods. Both of these methods have been described elsewhere.<sup>402, 403</sup>

In MALDI methods, typically a high ratio of matrix to sample is deposited on a sample plate, or directly on a sample surface, which is then introduced to the high vacuum of the MS. The matrix is a compound containing a chromophore(s) that absorbs strongly at the wavelength of the desorption laser. During the desorption step, the matrix acts to assist in both the desorption and ionization of analytes. The related method, SALDI specifically engineered surfaces such as graphenes, silica or nanostructures are used as a substrate platform to affect laser desorption ionization, obviating the need for an added matrix. Both techniques are soft ionization strategies, producing intact (or protonated) molecular ions, and are relatively simple to use.

### **2.8.2.1 Matrix-Assisted Laser Desorption Ionization**

In the recent MALDI-MS literature related to drug testing, there has been significant emphasis exploiting the method to provide spatially resolved measurements. The micron sized focal point of the desorption laser can be positioned (or moved) over different sample regions, providing profiling or imaging of analyte concentrations, ideal for detecting or imaging drugs in hair or fingerprints, useful for forensic, clinical and enforcement purposes. As MALDI-MS hair analysis examples, Vogliardi et.al. validated a fast screening method for COC in hair,<sup>404</sup> and there are numerous examples of the use of spatially resolved measurements along the length of the hair shaft to determine time of use. Other examples for the analysis of hair using MALDI-MS include the detection of COC,<sup>405, 406</sup> MAMP,<sup>407, 408</sup> KET,<sup>409</sup> zolpidem,<sup>410</sup> and synthetic cannabinoid isomers.<sup>411</sup> In a recent publication, Flinders and co-workers presented optimized sample preparation and instrumental parameters for DoA by MALDI-MS/MS imaging.<sup>412</sup>

The analysis of drugs in fingerprints is another area where MALDI-MS is seeing development. Examples include the detection of a variety of drugs present in developed, cyanoacrylate lifted latent fingerprints,<sup>413</sup> the mapping of illicit drugs in fingermarks<sup>414</sup> and real crime scene fingerprints.<sup>415</sup> These applications are predominantly forensic in nature and illustrate the potential usefulness of this direct analytical strategy.

### **2.8.2.2 Surface-Assisted Laser Desorption Ionization**

The obvious advantage of SALDI based methods is the elimination of the requirement of matrix addition prior to measurement. A variety of different surfaces have been employed as sampling substrates. Silicon based materials are common, and in early work, the Kraj group demonstrated the detection of MDMA synthesis impurities by spotting small samples on porous silicon sample plates, followed by laser desorption.<sup>416</sup> SALDI with porous silicon has been used to detect illicit drugs in saliva,<sup>417</sup> in fingerprint sweat,<sup>418</sup> and an interesting application to monitor methadone compliance by testing saliva, urine or plasma.<sup>419</sup> Nanostructured materials have been seeing increasing use for SALDI drug detection, including silicon nanopillar arrays,<sup>420</sup> nanoporous silicon microparticles,<sup>421</sup> mesoporous germanium,<sup>422</sup> and recently Ag nanoparticles/ZnO nanorods.<sup>423</sup>

## 2.9 Conclusions And Future Outlook

With the rapid growth of NPS, it is likely that HRMS instruments will become increasingly prevalent as forensic screening tools for both GC and LC modes of separation, as well as for direct, ambient ionization analysis strategies. While much attention has been dedicated to the analytical performance of these methods, their modest rate of production has gone largely unmentioned, and so it is unsurprising that forensic toxicology turnaround times are lengthy to the point where the outcome of a legal case may be compromised. To fully realize the potential of HRMS in forensic toxicology, significant reductions in both instrumental analysis and operator review times will need to be made with, ideally, the latter being eliminated entirely. Looking forward, we boldly suggest the following goal for chromatographic methods: fully automated screening and semi-quantitation of 100 blood samples daily for GHB, THC, LSD, secobarbital, an isobaric pair of compounds such as crotonyl- and cyclopropyl- fentanyl, and a previously unreported synthetic cannabinoid. When such an assay is in widespread production use, the full potential of chromatography-based MS for forensic toxicology testing may be considered to be within reach.

Turnaround time and accurate mass, by contrast, are less of an issue with ambient ionization methods, as they are intended primarily for rapid screening in the field (ideally) or in the laboratory. As with the chromatographic methods, the challenge of ambient ionization will be their implementation for routine production by minimally trained staff, as well as the immediate translation of MS data into an easily understood format. Just as the MS itself has evolved from a complex room-sized instrument with limited applications into a compact box suitable for answering a myriad of analytical questions, we expect no less of an evolution with its means of sample introduction. The future is very promising for the continued evolution of mass spectrometry-based strategies for the analysis of DoA. Over the next decade, the rapid proliferation of refined analytical systems and strategies occurring now will undoubtedly yield powerful solutions to the complex analytical challenges posed in forensic as well as clinical applications.

### **3 Rapid and Quantitative Determination of Fentanyl and Pharmaceuticals from Powdered Drug Samples by Paper Spray Mass Spectrometry**

This chapter has been adapted from Borden, S.A., Saatchi, A., Krogh, E.T. and Gill, C.G., 2020. Rapid and quantitative determination of fentanyl and pharmaceuticals from powdered drug samples by paper spray mass spectrometry. *Analytical Science Advances*, 1(2), pp.97-108. doi.org/10.1002/ansa.202000083

This article was published as open access, and therefore:

This work is licensed under the Creative Commons Attribution-NonCommercial-NoDerivatives 4.0 International License. To view a copy of this license, visit <http://creativecommons.org/licenses/by-nc-nd/4.0/> or send a letter to Creative Commons, PO Box 1866, Mountain View, CA 94042, USA.

#### **3.1 Preface**

S.A. Borden designed all experiments and generated all data with assistance from A. Saatchi. This project was supervised by C.G. Gill. S.A. Borden and C.G. Gill drafted the manuscript together with intellectual and editorial contributions from all authors.

#### **3.2 Abstract**

Paper spray mass spectrometry is presented as a direct, quantitative tool for the measurement of pharmaceutical drugs and a variety of fentanyl analogs in solid samples and powder slurries with the ultimate goal of providing meaningful harm reduction drug checking. Method development and validation was carried out for fentanyl analog slurries as a proxy for street drug samples. Lower limits of quantitation were determined to be 3.6 – 7.4 ng/g for fentanyl analogs in the pharmaceutical slurry matrix. Using 1 mg of solid sample, the method can quantify picogram quantities of these drugs, well below required thresholds for even the most potent fentanyl analogs. Quality control samples were prepared and used to assess method validity according to the Scientific Working Group for Forensic Toxicology (SWGTOX) guidelines. Performance metrics for both precision and accuracy were found to be within SWGTOX recommended guidelines. Additionally, pharmaceutical tablets were used to demonstrate the applicability of the developed paper spray methodology for the direct qualitative and quantitative analysis of active ingredients in pharmaceutical powders deposited directly onto the paper spray substrate. A proposed workflow for rapid solid drug sample measurements is presented with potential applications for point-of-use street drug measurements and other solid sample matrices.

#### **3.3 Introduction**

Global trends demonstrate high opioid prescription rates, rising non-medical opioid use, and the emergence of highly potent synthetic opioids that are diversifying global opioid markets.<sup>424</sup> The Global Burden of Diseases, Injuries, and Risk Factors Study estimated

that in 2017 over 100,000 people died from an opioid overdose.<sup>425</sup> In the United States, the Center for Disease Control and Prevention reported 49,608 opioid-related overdose deaths in 2017, and of these, 29,406 (59.3%) involved synthetic opioids such as fentanyl or related analogs (termed 'fentalogs').<sup>426</sup> The rate of drug overdose deaths involving synthetic opioids (methadone excluded) in the US increased on average by 8% per year from 1999 to 2013 with average increases of 71% per year from 2013 to 2017. This trend has been observed in Canada as well, with similar increases in drug overdose deaths from synthetic opioids observed.<sup>427</sup> In British Columbia alone, fentanyl or its analogs were detected in ca. 87% and 83% of all illicit drug toxicity deaths in 2018 and 2019, respectively.<sup>427</sup> Governments around the world have grappled with the opioid crisis in a variety of different ways. In Canada, Western European nations, and a growing number of countries, harm reduction approaches to deal with the crisis (rather than punitive approaches) are being explored.

In Canada, public health policy towards harm reduction for substance use is multi-faceted. It is aimed at mitigating the negative social, physical, and economic consequences of the ongoing opioid crisis; the approach includes needle exchange programs, opioid substitution replacement therapy (e.g., methadone or buprenorphine), naloxone distribution, and, notably, supervised consumption sites (SCS) and overdose prevention sites (OPS).<sup>428</sup> The first dedicated drug checking program to be used as a strategy for harm reduction was introduced in 1992 in the Netherlands, when the government commissioned the Drug Information and Monitoring System to monitor the recreational drug market: HRDC has subsequently spread to many other European countries.<sup>429</sup> The success of harm reduction services has led to the establishment of SCS/OPS across Australia, Western Europe, Canada, and at select locations in the United States. At these sites, people who use drugs (PWUD) have access to many of these programs. These sites can serve as a primary contact with health professionals and medical support staff. One service offered by SCS/OPS that has been successfully able to mitigate overdose events is harm reduction drug checking (HRDC).<sup>430</sup> HRDC services allow PWUD to have their recreational drugs checked for chemical composition and receive personalized evidenced-based information regarding associated risks. This allows PWUD to make informed decisions about their drug use, with the ultimate goal of behavioural modification leading to the reduction of societal, physical, and economic harm. Indeed, research has shown that HRDC does lead to behaviour modification (i.e., reduced consumption, discarding substances).<sup>430</sup> In order to effect harm reduction, chemical analysis must be achieved prior to use. Drug analysis methodologies used in forensic and clinical laboratory settings for confirmatory testing, such as gas chromatography and liquid chromatography mass spectrometry, often require extensive sample preparation with costly and lengthy analysis times using benchtop laboratory instruments. Consequently, these techniques are not well suited for on-site HRDC, where providing rapid results at the point-of-care/use can positively impact the behavior and health outcomes of PWUD.

To affect true harm reduction through informed drug use, HRDC technologies should: provide rapid results that are sensitive enough to detect trace levels of highly toxic

substances (e.g., fentanyl analogs such as carfentanil) with high specificity, be field-deployable for use at a SCS/OPS, be adaptable to address changes in the drug supply, and provide quantitative, easily interpretable results in a cost-effective manner. It is our contention, and intent to demonstrate, that paper spray mass spectrometry meets all these criteria and addresses shortcomings of existing HRDC technologies.

Currently, popular point-of-care HRDC methods include colorimetric tests, immunoassays, Fourier-transform infrared spectroscopy (FTIR), and Raman spectroscopy. Colorimetric tests have been employed for decades to provide rapid, on-site drug screening, but they are non-quantitative, not very specific and unable to distinguish trace or multiple drug components. Immunoassay drug test strips are low cost, portable and provide rapid results, with the added benefit of high sensitivity and increased selectivity, although they still are unable to differentiate closely related compounds (e.g., fentanyl vs. carfentanil) with significantly different toxicities. Spectroscopic methods are easily operated in point-of-care settings with portable instruments. These systems have modest power requirements, are relatively low cost, and have rapid analysis times. An assessment of FTIR spectroscopy and immunoassay test strips for the analysis of fentanyl in real street drug samples found that of 173 samples that tested positive for fentanyl (using quantitative nuclear magnetic resonance), 30 (17.3%) failed to detect fentanyl using FTIR spectroscopy and 4 (2.3%) did not detect fentanyl using immunoassay test strips.<sup>431</sup> FTIR was able to quantify drug and excipient content, but required concentrations  $\geq 10\%$  w/w, and even the immunoassay test strips required fentanyl concentrations  $\geq 5\%$  w/w for reliable detection. Given that lethal dosages of fentanyl have been documented to be as low as 250  $\mu\text{g}$  (0.25% in a typical 100 mg street dose), the point-of-care techniques listed above lack the necessary sensitivity and/or selectivity required for fentanyl and related synthetic opioids. Substantially lower fatal dosages for carfentanil and other synthetic opioids have been reported,<sup>432</sup> further emphasizing the need for more sensitive quantitative methods.

Paper spray mass spectrometry (PS-MS), first demonstrated in 2010, is an ambient ionization mass spectrometry technique introduced and subsequently developed by Cooks and Ouyang.<sup>9</sup> Of the innumerable ambient ionization techniques developed over the last 15 years, beginning with the introduction of desorption electrospray ionization and direct analysis in real time in 2004 and 2005, respectively,<sup>262, 263</sup> paper spray has attracted considerable interest due to the simplicity, quantitative capabilities, and low cost of implementation. In a typical PS-MS measurement, a small amount (ca.  $\leq 10 \mu\text{L}$ ) of sample (e.g., whole blood, raw urine, etc.) is directly deposited onto a triangular piece of filter paper and dried. Small amounts of solvent and a high voltage (ca. 3-6 kV) are applied. Analytes dissolved by the solvent are subsequently wicked to the tip of the paper, whereupon they are ionized in a process similar to electrospray for mass spectrometry. The technique has been thoroughly reviewed by a number of groups,<sup>331, 433, 434</sup> and in-depth fundamental PS-MS studies regarding matrix effects,<sup>312</sup> paper properties,<sup>311</sup> and the ionization mechanism<sup>306</sup> have also been presented. PS-MS coupling to miniature or portable MS has also been demonstrated and recently reviewed.<sup>336</sup>

Demonstrations of the analysis of drugs of abuse (DoA) using PS-MS in blood,<sup>315</sup> plasma,<sup>316, 435</sup> urine,<sup>335</sup> and oral fluid<sup>318, 319</sup> have been published. The measurement of DoA in biofluids assists in clinical and forensic applications, though does little to help with harm reduction via behaviour modification, since information is only available post-exposure. For drug checking purposes, selective and sensitive measurements of harmful components in drug samples are required prior to, or at the time of use. PS-MS has previously been applied to the qualitative analysis of solid drugs samples including the semi-quantitative detection of fentanyl and norfentanyl standards spiked into an analgesic slurry,<sup>314</sup> the detection of cocaine from simulated samples (following centrifugation and filtration),<sup>436</sup> and the forensic qualitative screening of drugs of abuse from various solid matrices using a variant of PS-MS called paper cone spray ionization (PCSI).<sup>437, 438</sup> However, the quantitative analysis of DoA directly from solid samples with little to no sample preparation using PS-MS is notably absent from the published literature. In this paper, we present fundamental studies and method validation of PS-MS using a series of fentanyl analogs mixed with pharmaceutical drug sample matrices, as well as rapid qualitative screening, and quantitation of active ingredients in pharmaceutical tablet slurries to demonstrate feasibility for future drug checking applications.

### 3.4 Materials and Methods

#### 3.4.1 Reagents and Standards

Legally exempt, certified reference standards (fentanyl, carfentanil oxalate, acryl fentanyl, 4-fluoro-isobutyryl fentanyl (FIBF), furanyl fentanyl, heroin, acetaminophen, chlorpheniramine maleate, and pseudoephedrine) and isotopically labeled internal standards (fentanyl-*d*<sub>5</sub>, carfentanil-*d*<sub>5</sub> oxalate, acetaminophen-*d*<sub>4</sub>, chlorpheniramine-*d*<sub>6</sub> maleate, and pseudoephedrine-*d*<sub>3</sub> HCl) were purchased from Cerilliant Corporation (Round Rock, TX, USA). Caffeine and caffeine-*d*<sub>3</sub> were purchased from Sigma-Aldrich (St. Louis, MO, USA). The structures of all drugs used in this study are given in the supplementary information (Figure 3.5). HPLC grade methanol was obtained from VWR International (Mississauga, ON, CAN). ACS grade formic acid was acquired from GFS Chemicals (Columbus, OH, USA). Deionized (DI) water was prepared using a water purification system (18.4 MΩ·cm Facility Scale Reverse Osmosis/Ion Exchange Water Purification System, Applied Membranes Inc., Vista, CA, USA). All standards were prepared gravimetrically, with w/w concentrations represented as ng of analyte per g of total mass.

#### 3.4.2 Mass Spectrometry

A triple quadrupole mass spectrometer (Micromass Quattro Ultima LC, Waters-Micromass, Altrincham, UK) was used for all analyses. The atmospheric pressure ionization inlet on this instrument was a second-generation Z-Spray™ geometry design (Waters-Micromass). Nitrogen gas (UHP grade, Praxair, Nanaimo, BC, CAN) was used as cone gas at 50 L/hr to reduce any build-up of sample material on the inlet cone. Argon collision gas (UHP grade, Praxair, Nanaimo, BC, CAN) was maintained at a pressure of ca. 3.1 mTorr for all MS/MS experiments. MS/MS scan methods were developed using

directly infused methanolic standards with positive electrospray ionization (ESI) (capillary voltage = +4.0 kV). This is standard practice for PS-MS given that the ionization mechanisms of paper spray ionization (PSI) and ESI are similar (18). Instrumental parameters, consistent across all methods, are outlined in Table 3.4, and analyte specific parameters from multiple reaction monitoring (MRM) experiments for the selection of two product ions for each precursor ion are outlined in Table 3.5.

### 3.4.3 Paper Spray

All PS-MS measurements used commercially available PS-MS sampling cartridges (Prosolia Inc., Indianapolis, IN, USA). In all cases, 10  $\mu$ L of an internal standard (or internal standard mixture) was deposited on the paper strip and allowed to air dry at ambient temperatures (ca. 15 minutes) before the application of 10  $\mu$ L of sample, which was also dried prior to analysis. A syringe pump (Fusion 100, Chemyx Inc., Stafford, VA, USA) equipped with a 10-mL gastight syringe (Hamilton Corporation, Reno, NV, USA) was used to deliver spray solvent composed of 90/10/0.1 (%v/v) methanol/DI water/formic acid to the cartridges (Prosolia Inc., Indianapolis, IN, USA) with red PEEK tubing (o.d. 1/16", i.d. 0.005") and a 8-cm length of 22 gauge stainless steel hypodermic stock (Vita Needle Co., Needham, MA, USA). Spray solvent was delivered in two stages to increase the speed of analysis: (1) 60  $\mu$ L was delivered at a rate of 100  $\mu$ L/min (36 sec) to pre-wet the paper strip, (2) 30  $\mu$ L/min was delivered for the remainder of the measurement (ca. 1 min) to maintain ion production. PS-MS cartridges were manually mounted in a custom-made PS-MS holder (Prosolia), mounted on a three-axis translation stage. A custom mounting bracket was made in-house using a stereolithographic 3-D printer (Form 2, Formlabs Inc., New Castle, DE, USA) to interface the PS-MS holder with the MS and enable reproducible alignment of the PS cartridge in front of the MS cone inlet. High voltage, supplied by the electrospray ionization (ESI) source of the MS, was applied to the cartridge using a simple metal spring clip. The PS-MS cartridge was positioned such that the paper tip was ca. 5 mm away from the MS inlet cone. Images of the custom PS-MS interface and sampling cartridge are given in Figure 3.6.

### 3.4.4 Sample Preparation

A variety of over the counter (OTC) pharmaceuticals, drugs, and supplements were purchased from local pharmacies to be used as surrogate solid drug samples. The complete list of products used, including active and inactive ingredients, are shown in Table 3.6 and Table 3.7. Tablets were ground to a fine powder using a ceramic mortar and pestle, which was cleaned with DI water and methanol washes, then air dried between samples to prevent any carry over. Because of the requirement for exemption under Section 56 of the Controlled Drugs and Substances Act in Canadian Federal Law,<sup>439</sup> OTC medications were used in several experiments as surrogates for illicit street drug sample powder matrix. For surrogate drug measurements (Table 3.1) and method validation studies (Table 3.2), a combination of 11 different OTC pharmaceutical tablets (Table 3.6) were ground together, creating a mixed powdered composite sample containing a wide variety of common excipients and surrogates for active ingredients

typically found in street drugs.<sup>440</sup> Fentanyl analogs were spiked directly into the OTC tablet powder slurries. Other experiments (Figure 3.1 and Figure 3.2) utilized a single OTC pharmaceutical cold medication tablet (Table 3.7) as the matrix with concentrations of  $10^{-5}$  to 5% (w/v) in methanol. For the analysis of pharmaceutical drugs in OTC tablets (Figure 3.3, Figure 3.4 and Table 3.3), a 1 mg of powdered tablet per mL (0.1 %w/v) slurry was prepared in methanol using a vortex mixer (Thermo Fisher Scientific, Waltham, MA, USA) for ca. 15 seconds. The resulting slurry was diluted 100-fold in methanol such that active ingredient concentrations were within the linear dynamic ranges of the target drug calibrations and the powdered tablet matrix concentration was 0.001 %w/v.

### 3.4.5 Method Validation

Method validation studies were carried out in accordance with the Scientific Working Group for Forensic Toxicology (SWGTOX) 2013 guidelines.<sup>441</sup> Within-run and between-run precision (%CV) values, and accuracy (%bias) were determined for the analysis of fentanyl analogs in the 11-component composite OTC pill powder matrix at a concentration of 0.1% (w/v) in methanol by analyzing 5 replicates of low, medium, and high quality control (QC) standards over 5 consecutive days. In accordance with the SWGTOX guidelines: the low QC concentration was approximately 3 times the value of the lowest calibration standard, the high QC concentration was approximately 80% of the highest calibration standard, and the concentration of the medium QC was approximately the midpoint of the low and high QC samples. The %bias, within-run %CV, and between-run %CV were calculated for each QC concentration.

The reported within-run %CV value is the highest value observed across 5 days. The limit of detection (LOD) was defined as the concentration value that returned a signal to noise ratio (S/N) > 3 and was determined from the lowest calibration standard used that provided a S/N value over 3. The lower limit of quantitation (LLOQ) was defined in the same manner, but with a S/N threshold value of 10. The noise was defined as the average signal area for matrix matched blanks ( $n \geq 5$ ), and the signal was the average signal area of the quantifier ion channel ( $n \geq 3$ ).

### 3.4.6 Data Analysis

In PS-MS, signals are similar to flow injection methods, appearing as analytes elute from the paper and are ionized by the applied high voltage. An example PS-MS integrated chronogram is shown in Figure 3.7. Integrated peak areas of MRM signal chronograms were recorded using the mass spectrometer's operating software (MassLynx Ver 4.1, Waters-Micromass) without any smoothing and were used for all measurements. Calibration curves were generated using the ratio of the analyte quantifier ion signal peak area to the internal standard (internal standard pairings are given in Table 3.5 quantifier ion signal peak area (termed the signal area ratio, or SAR). For all measurements, signals were collected for approximately 1 minute. Data collection was manually terminated by removing the high voltage connection from the MS system, thus ending ion production. All measurements were conducted in at least triplicate, and uncertainties/error bars are given as the standard deviation between the measurements.

## 3.5 Results and Discussion

### 3.5.1 Matrix Effects in Paper Spray and Electrospray

In order to make accurate quantitative measurements of active ingredients in actual street drug formulations, an appropriate dilution scheme and calibration model are required to mitigate any matrix effects and ensure that measurements are made within the linear dynamic range of the model. A common strategy for the reduction or elimination of matrix effects is 'dilute-and-shoot' ESI.<sup>442</sup> To assess whether dilute-and-shoot ESI might be an effective, alternate strategy for the measurement of drugs in powdered street drug formulations, and whether this translates to PS-MS, fentanyl (ca. 75 ng/g) was spiked into methanolic slurries containing varying concentrations of a single ground pharmaceutical tablet (see Table 3.7) spanning 5 orders of magnitude of suspended solids. Figure 3.1 illustrates the signal response for fentanyl (not internal standard corrected) as the concentration of the suspended solids increases from  $10^{-5}$  to 1% (w/v) in the sample (x-axis is a logarithmic scale) for both ESI and PSI.

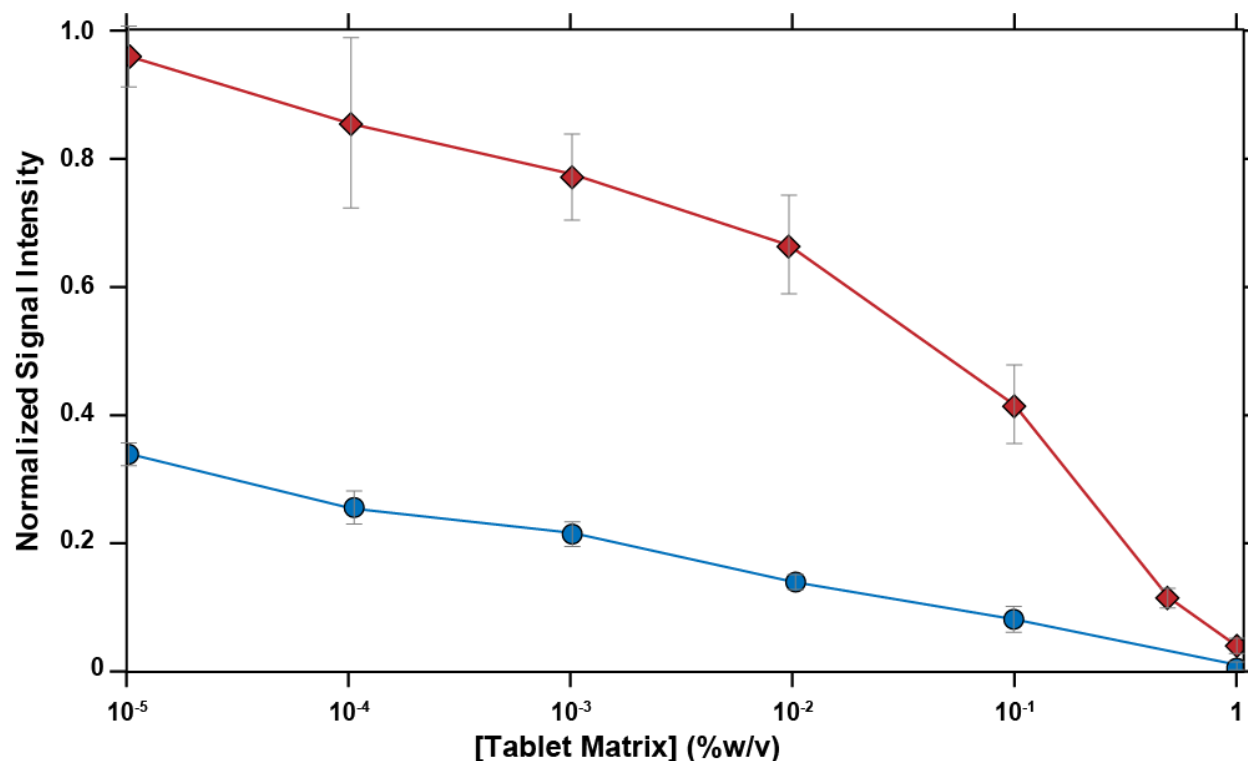


Figure 3.1 Comparison of signal suppression observed in paper spray (♦) and direct injection electrospray (●) for ca. 75 ng/g fentanyl present in samples with increasing concentrations of suspended solids from an over the counter cold medication tablet matrix in methanol (logarithmic x-axis). Signal intensities are normalized to those obtained for fentanyl present in neat methanol with no added matrix.

The signal acquired from measurements of fentanyl in pure methanol with no added solid matrix was normalized to a value of 1 (not plotted due to logarithmic scale) and subsequent measurements with added cold medication tablet matrix are represented as

a normalized signal intensity relative to the signal area obtained for fentanyl in the neat methanol measurements for both ESI and PSI. The signal areas were not corrected using an internal standard in order to assess overall signal losses from any matrix effects. We note that error bars for PS-MS measurements are inherently high when they are not internal standard corrected because of the differences between the individual paper strips used. At a concentration of 0.001% (w/v) suspended solid matrix, the total signal for fentanyl using ESI is reduced to ca. 34% of its value in neat methanol, while the PS-MS signal is relatively unaffected (ca. 97% relative intensity). Even up to concentrations of 0.1% (w/v), the PS-MS signal is still ca. 41% of the total signal area relative to measurements made in neat methanol. From this data, it is clear that PS-MS measurements of fentanyl are significantly less prone to signal suppression from the solid matrix components from a powdered pharmaceutical tablet than observed with ESI. Furthermore, ESI has been shown to have significant sample to sample carryover effects, even following extensive sample preparation and chromatographic separation,<sup>443</sup> a major problem when making measurements across significantly different concentrations, such as those encountered during the measurement of illicit drugs. Conversely, PS-MS uses a new paper substrate for each measurement, eliminating sample-to-sample carryover. This assertion has been supported in the literature.<sup>315, 443</sup> Therefore, PS-MS appears to offer superior analytical performance characteristics for the direct measurement of illicit drugs in solid samples for drug checking when compared to 'dilute-and-shoot' ESI-MS.

### 3.5.2 Fentanyl Analysis in Various Matrices

Gravimetrically prepared analytical reference standards in methanol were used to generate calibration curves for fentanyl, acryl fentanyl, 4-fluoroisobutyryl fentanyl (FIBF), furanyl fentanyl, and carfentanil. Calibration data for these synthetic opioids in methanol are listed in Table 3.8. To assess the tolerance to matrix effects of the synthetic opioids examined in this study, multipoint calibration standards of fentanyl (ranging from ca. 0.5 – 200 ng analyte per g of total solution) were constructed in four different sample matrices and analyzed in triplicate. Figure 3.2 shows calibrations carried out in a variety of matrices including: methanol, methanol in the presence of mannitol, a methanolic slurry of OTC cold medication tablet matrix with and without added heroin. Error bars are omitted for visual clarity (average %RSD = 12.8); data for the calibration models including precision are included in Table 3.9.

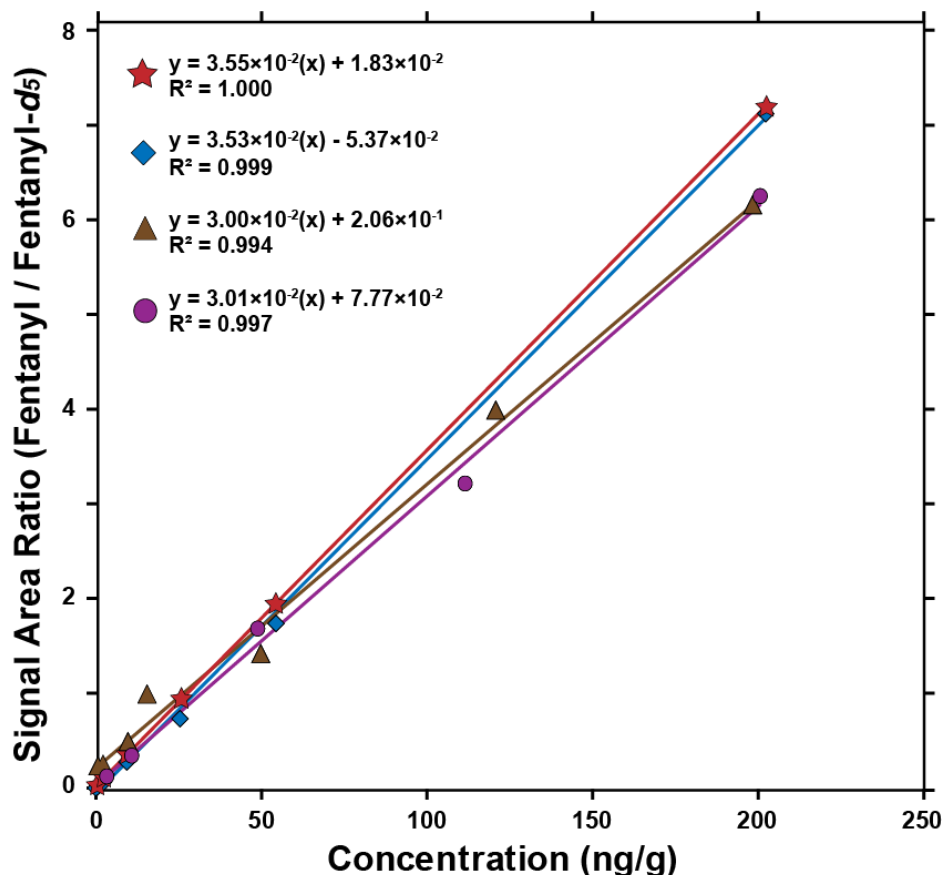


Figure 3.2 Calibrations of fentanyl (0.5 – 200 ng/g, n = 3) in methanol (★), in methanol with 10% (w/w) mannitol (◆), 5% (w/v) of an OTC cold medication tablet slurry in methanol (▲), and 5% (w/v) of an OTC cold medication tablet slurry in methanol with an additional 15  $\mu$ g of heroin per g of methanol (●) using the signal area ratio of fentanyl (m/z 337.0  $\square$  188.1) to that for fentanyl-d5 internal standard (m/z 342.2  $\rightarrow$  188.1) at 30 ng/g.

We have previously observed that mannitol, a commonly used street drug cutting agent,<sup>440</sup> demonstrated signal ionization enhancements for fentanyl and analogs in PS-MS measurements, resulting in different calibration slopes.<sup>335</sup> This was not observed in these studies, evidenced by the nearly identical calibration slopes for fentanyl in pure methanol, versus fentanyl in methanol with 10% (w/w) mannitol. This may be a MS source dependent phenomenon, as the previous study employed a capillary inlet<sup>335</sup> instead of the Z-Spray™ inlet geometry used here. However, as Figure 3.2 illustrates, even a very high solids loading of the OTC cold medication matrix (see Table 3.7 for composition) of 5% (w/v) in methanol lead to only a modest 15% reduction in the calibration sensitivity for fentanyl. This is remarkable considering the matrix loading is in considerable excess to that which would be used for proposed powdered drug sample measurements (0.001 – 0.1% w/v). The 5% (w/v) ground OTC tablet powder slurry contained many active and inactive ingredients (Table 3.7) that are often found in street drug formulations (e.g., caffeine, sugars)<sup>440</sup> as well as surrogates for drugs of abuse (e.g., pseudoephedrine). Consequently, it was used as a proxy to evaluate the potential for developing a

quantitative method for HRDC. While the expected variability in street drug formulations presents inherent challenges in creating matrix matched standards, we are encouraged by the low matrix effects observed here. Drug quantitation via the standard additions method could also be a reasonable strategy, but the additional sample preparation steps and increased analysis time is not well suited to drug checking applications, where rapid results are key for intervention before drug use. Preliminary PS-MS results suggest that internal standard use mitigates the majority of observed matrix effects even with high matrix loadings. In lieu of preparing calibrations in actual street drugs (Section 56 exemptions as required by the Canadian government were not in place at the time of this study), and with the goal of future drug checking trials in mind, calibration standards were prepared as methanolic slurries containing 0.1% (w/v) of a composite pharmaceutical powder matrix made by combining 11 different OTC medications (Table 3.6).

### 3.5.3 Fentanyl Analog Method Validation Studies

In order to demonstrate the feasibility of PS-MS for harm reduction drug checking, calibrations of the fentanyl analogs (ca. 0.5 – 250 ng/g, 7 levels, 3 replicates) were prepared in methanolic slurries containing 0.1% (w/v) of the composite OTC matrix. The calibrations demonstrated excellent linearity, with  $R^2$  values ranging from 0.995 to 0.999. These calibration standards were used to determine the LODs and LLOQs for five fentanyl analogs. These values are shown in Table 3.1 and are compared to the values obtained for methanolic standards.

Table 3.1 Comparison of the LOD and LLOQ values for fentanyl analogs in methanol and the 0.1% (w/v) composite OTC mixture.

Compound	Methanol				0.1% (w/v) Composite OTC Mixture			
	[Standard] (ng/g)	S/N	LOD (ng/g)	LLOQ (ng/g)	[Standard] (ng/g)	S/N	LOD (ng/g)	LLOQ (ng/g)
Fentanyl	2.16	7.74	0.84	2.8	2.71	4.62	1.8	5.9
Acryl fentanyl	2.52	11.2	0.67	2.3	2.25	6.21	1.1	3.6
Furanyl fentanyl	2.44	10.4	0.70	2.4	2.62	5.31	1.5	4.9
FIBF	2.52	10.2	0.74	2.5	2.46	3.33	2.2	7.4
Carfentanil	1.89	4.10	1.4	4.6	2.71	4.76	1.7	5.7

LLOQ values ranging from 3.6 – 7.4 ng/g were obtained in the composite OTC matrix, which are comparable, though slightly higher, than the LLOQ values of 2.3 – 4.6 ng/g in neat methanol. Similarly, LOD values ranged from 0.67 - 1.4 ng/g in methanol and from 1.1 – 2.2 ng/g in the composite OTC matrix slurry. The LOD value for fentanyl is similar to one previously published by our group for fentanyl in an analgesic slurry, obtained with a Z-Spray™ source inlet, but in this early work, significantly different, home-made PS-MS sample strips were used.<sup>314</sup> Given that all measurements were conducted using 10  $\mu$ L sample loadings, absolute LOD values for the fentanyl analogs in methanol were calculated to be 5.3 – 11 picograms, and 8.6 – 18 picograms in the 0.1% (w/v) composite OTC matrix. Similarly, LLOQ absolute values were found to be 18 – 36 picograms in methanol, and 29 – 59 picograms in the composite OTC mixture. Assuming a typical 100 mg street drug dosage, the LLOQ values determined for the fentanyl analogs in the composite OTC matrix would correspond to having the ability to quantitate the equivalent

of 2.9 – 5.9 µg in 100 mg of street drug powder from a 1 mg sample. Although it is difficult to determine an exact lethal dosage for fentanyl, especially given differing tolerances to opioids, 2 mg is the generally stated lethal dosage.<sup>444</sup> Even at a lower estimate of 250 µg, we are nearly two orders of magnitude more sensitive than the lethal dose. Therefore, the sensitivity of the method is more than sufficient for quantitative drug testing, even for trace components such as the synthetic opioids investigated here.

Although PS-MS is quite sensitive for fentanyl analog measurements, perhaps a more important consideration is to ensure that the method can make precise and accurate measurements across the entire calibration range. To evaluate this, validation studies were carried out according to the SWGTOX 2013 guidelines (32). Briefly, 3 levels of QC samples (low, medium, high) containing fentanyl and analogs were prepared in methanol with 1 mg of the composite OTC slurry per mL of methanol. The QC samples were analyzed daily (n = 5 replicates) over a period of 5 consecutive days. Table 3.2 presents the within-run and between-run precision (%CV), as well as the accuracy (%bias) values obtained.

Table 3.2 Intra-day and inter-day precision values (%CV) and accuracy (%bias) results from method validation experiments for fentanyl analogs in the 1 mg/mL composite OTC mixture.

Compound	Low (ca. 13 ng/g)			Medium (ca. 65 ng/g)			High (ca. 198 ng/g)		
	Within-Run Precision (%CV)	Between-Run Precision (%CV)	Accuracy (%Bias)	Within-Run Precision (%CV)	Between-Run Precision (%CV)	Accuracy (%Bias)	Within-Run Precision (%CV)	Between-Run Precision (%CV)	Accuracy (%Bias)
Fentanyl	11.9	11.7	5.64	13.4	14.2	15.2	10.1	12.1	19.4
Acryl fentanyl	12.5	11.5	11.8	12.2	13.5	10.6	8.62	10.7	12.0
Furanyl fentanyl	12.1	8.40	20.0	12.3	12.2	25.3	12.8	8.3	9.51
FIBF	12.0	10.5	16.8	14.4	12.9	18.6	8.62	6.3	4.11
Carfentanil	13.8	10.7	10.7	13.6	11.9	12.2	8.44	8.3	10.8

Table 3.2 summarizes the results and indicates that the method meets SWGTOX guidelines of precision ( $\%CV \leq 20$ ) and accuracy ( $\%bias \leq \pm 20$ ) for all compounds at all 3 QC levels in the composite OTC matrix, with the single exception of a slightly higher, 25.3% bias obtained for furanyl fentanyl in the medium QC sample.

### 3.5.4 Direct Qualitative Analysis of Pharmaceutical Samples

Both illicit street drug and pharmaceutical formulations typically contain several active ingredients as well as non-active ingredients or excipients. Additionally, active ingredient levels can vary significantly in street drugs. For example, methamphetamine may commonly constitute the majority of a street drug sample sold as methamphetamine, while other components like carfentanil may only be present at trace amounts (i.e., ~1%) in street drugs and still be pharmacologically active, or even lethal.<sup>445</sup> This wide variation in the concentration of active components is also observed in pharmaceutical formulations, and those analyzed in these studies had active ingredients that ranged from ca. 1 – 80% (w/w). Furthermore, many pharmaceutical drugs are structurally similar to illicit substances, for example pseudoephedrine is commonly found in OTC

decongestants or cold medications and is structurally very similar to methamphetamine (Figure 3.5).

The qualitative analysis of solid drug samples has many applications in forensics, notably for rapid screening of unknown substances and non-targeted analysis. PS-MS has been used for the qualitative and semi-quantitative detection of cocaine in simulated samples, though the samples were subjected to centrifugation and filtration prior to measurement and not measured as powdered slurries.<sup>436</sup> Additionally, PSI coupled with ion mobility spectrometry has been demonstrated for the detection of cocaine residues from neat standards applied to various surfaces.<sup>446</sup> Direct solids analysis of pharmaceutical powders and other solid samples has been reported by a variant of PS-MS, called Paper Cone Spray Ionization Mass Spectrometry (PCSI-MS) which uses a 3-dimensional paper cone as a sampling and ionization platform.<sup>438</sup> This methodology has since further been developed and applied to on-site forensic and environmental sample screening including drug tablets, crystal based drugs, and synthetic marijuana.<sup>437</sup> While PCSI-MS has been reported for direct powder analysis, the technique has not yet been commercialized or been used for quantitative analysis.

Presented herein is a demonstration of the qualitative measurement of pharmaceutical tablet powders using PS-MS, achieved by placing dry powder samples directly onto the PSI substrate (Figure 3.3A). A ca. 1 mg sample of a ground pharmaceutical tablet (see Table 3.7) was deposited directly onto the sampling zone of a PS-MS strip. As the applied spray solvent (90/10/0.1 methanol/water/formic acid) wicks towards the tip of the paper, analytes are mobilized from the solid powder in a quasi on-paper extraction and transferred to the paper tip, where they were subsequently ionized.

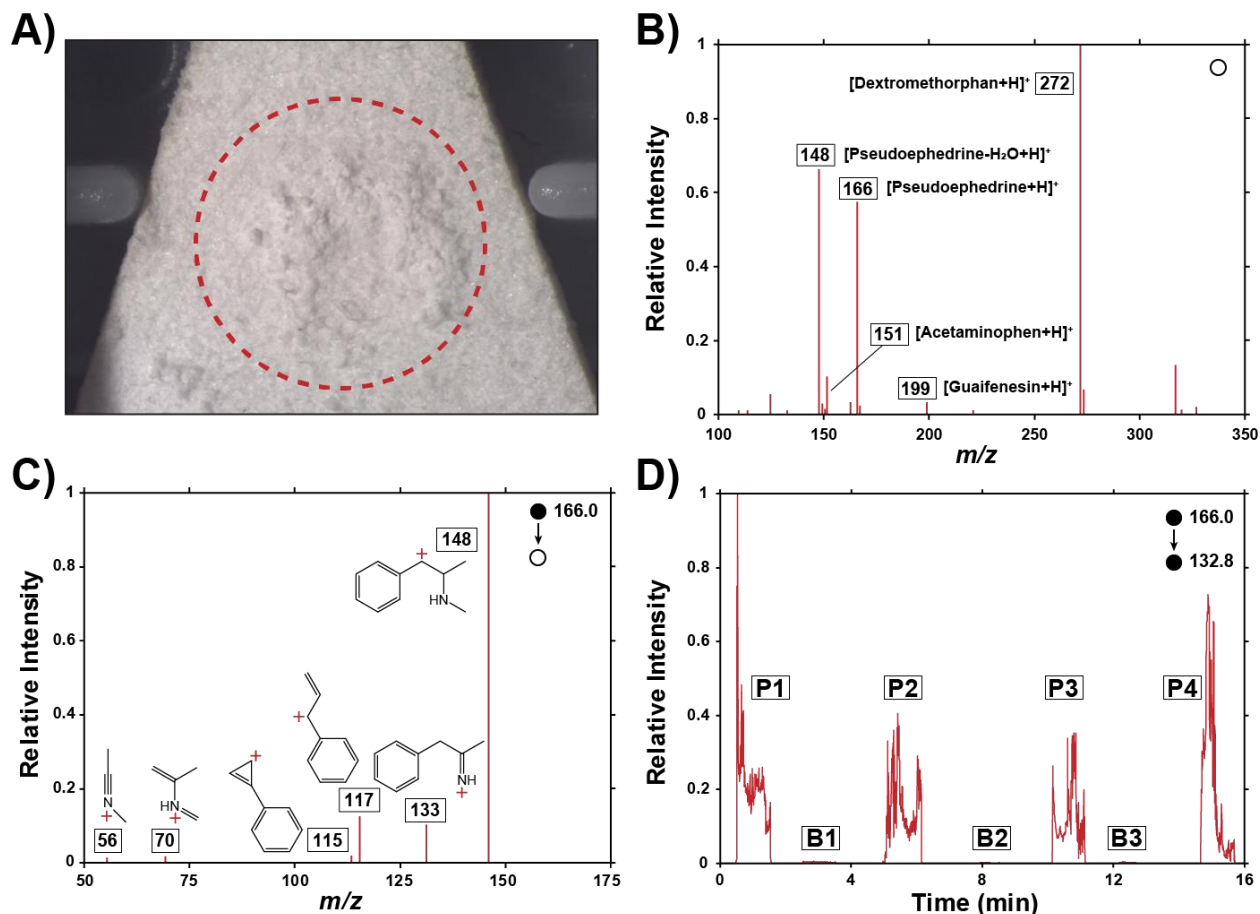


Figure 3.3 Direct qualitative analysis of a approximately 1 mg of a crushed pharmaceutical tablet deposited directly on the PS sampling strip showing **A)** an image of the crushed tablet directly on the PS cartridge, **B)** the full scan (100 – 350  $m/z$ ) mass spectrum, **C)** the product scan (50 – 175  $m/z$ ) of pseudoephedrine (15 eV collision energy), and **D)** MS/MS chromatogram of the crushed tablet samples (P1-P4) and caffeine tablets containing no pseudoephedrine as blanks (B1-B3).

The full scan mass spectrum obtained is given in Figure 3.3B, with ion signals at 272, 199, 166, and 151  $m/z$ , corresponding to the protonated molecular peaks of dextromethorphan, guaifenesin, pseudoephedrine, and acetaminophen, respectively. Additionally, an ion at  $m/z$  148 originated from in-source collision induced dissociation of pseudoephedrine, leading to the formation of an  $[M-H_2O+H]^+$  ion, confirmed by a product ion scan of pseudoephedrine (Figure 3.3C). Water loss is often considered to be a non-diagnostic transition; more diagnostic fragment ions were observed in the product ion spectrum at  $m/z$  133, 117, 115, 70, and 56, though at lower intensities. Therefore, the  $m/z$  133 product ion was used for MS/MS measurements of pseudoephedrine. Figure 3.3D illustrates the sequential MS/MS ion chronograms obtained for the measurement of powder samples from 4 individual pharmaceutical tablets (P1-P4), illustrating rapid, qualitative pseudoephedrine detection. Powder samples from commercial caffeine tablets (not containing pseudoephedrine) were measured as blanks (B1-B3) between each sample, illustrating negligible sample-to-sample carry over.

### 3.5.5 Quantitative Analysis of Pharmaceutical Samples

While there are examples of PS-MS for the quantitative analysis of drugs of abuse in various biofluids and complex samples,<sup>315, 333, 334</sup> the direct quantitation of components in solid illicit drug samples by PS-MS has not been well demonstrated in the literature. A notable exception was presented by Romão et al. who quantified cocaine using a Dragendorff reagent and thin layer chromatography followed by PS-MS, as opposed to a more direct analysis scheme.<sup>330</sup>

In order to demonstrate the feasibility of making quantitative measurements from tablets or powdered illicit street drugs samples using PS-MS, the medicinal ingredients present in a variety of OTC pharmaceutical tablets were quantified. For these studies, two calibration models were prepared: one for components typically present at high concentrations in the pharmaceutical tablets (i.e., caffeine and acetaminophen), as well as for compounds typically present at lower concentrations (i.e., pseudoephedrine and chlorpheniramine). This ensured that both high concentration and trace components present in the same sample could be accurately quantified within the linear dynamic range of the calibration models. A similar protocol could be enacted for illicit drug checking measurements.

For quantitative measurements, ca. 1 mg of the sample was used to produce a methanolic slurry, which was then further diluted 100-fold in methanol to yield analyte concentrations within the linear dynamic range of the calibration models. This simple workflow ensures only negligible sample is used. In drug checking, this is especially important, since PWUD are reluctant to provide significant amounts of their substances for testing. Theoretically, even smaller samples could be used, but smaller sample masses can limit the precision and accuracy of quantitation.

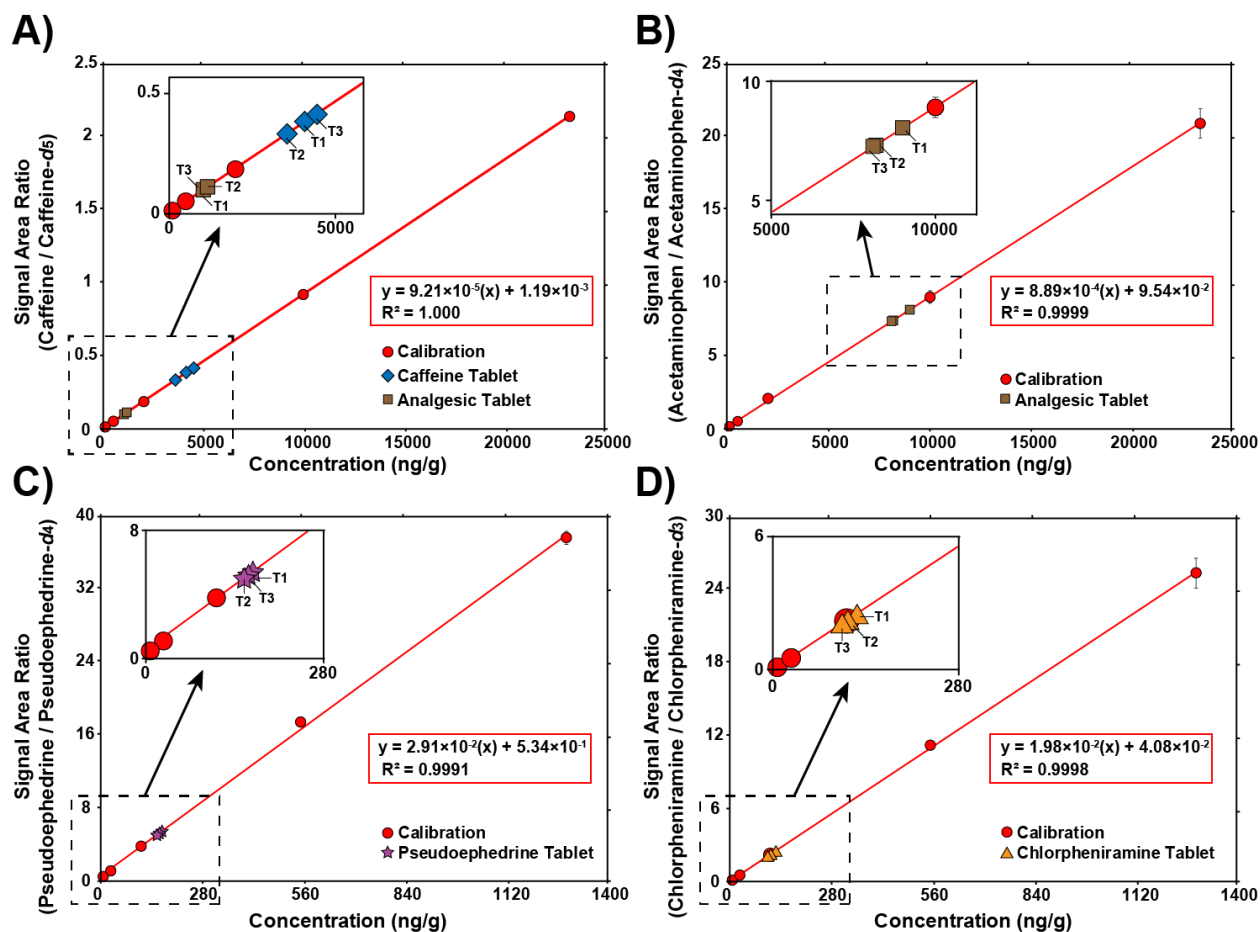


Figure 3.4 Calibrations (5 levels, 4 replicates) of **A)** caffeine, **B)** acetaminophen, **C)** pseudoephedrine, and **D)** chlorpheniramine with results from quantitation of the prepared diluted slurries of pharmaceutical tablets (T1-T3) interpolated on the figure.

Figure 3.4 illustrates the calibrations of caffeine, acetaminophen, pseudoephedrine, and chlorpheniramine in methanolic standards using characteristic MS/MS quantifier transitions and isotopically labeled internal standards (Table 3.5). Detail on the calibration models is outlined in Table 3.10. The calibrations demonstrated excellent linearity in all cases ( $R^2 > 0.9991$ ). The calibrations were used to calculate the amount of analyte in commercial pharmaceutical tablets using the experimentally determined signal area ratio, the equation of the line for the calibration, and the dilution factor. The calculated values of the concentration of analytes in the tablets (T1-T3) are overlaid on the calibrations in Figure 3.4 to demonstrate that the dilution scheme allows for the results to fall within the linear dynamic range of the calibration models. From the determination of analyte concentration by PS-MS in T1-T3, the amount (mg) of each of the active ingredients in the original tablets were determined and compared to the value reported by the manufacturer. Recognizing that these are commercial products, and not standard reference materials, a percent difference was calculated using the formula (mean calculated amount – amount specified by manufacturer) / amount specified by

manufacturer  $\times 100\%$ . Table 3.3 gives the results from the quantitative analysis of several different pharmaceutical tablets.

Table 3.3 PS-MS measurement of active ingredients in pharmaceutical tablets, three diluted slurries (T1-T3) were prepared for each type of tablet (using a new tablet each time) and analyzed in triplicate.

Tablet	Medicinal Ingredients	Amount* (mg)	Measured Amount* (mg)	%CV	%Difference
Analgesic Tablet T1	Acetaminophen	500	594	3.50	18.8
	Caffeine	65	78.0	8.47	18.4
Analgesic Tablet T2	Acetaminophen	500	534	2.14	6.74
	Caffeine	65	67.6	10.1	3.98
Analgesic Tablet T3	Acetaminophen	500	526	1.44	5.26
	Caffeine	65	76.1	16.1	17.1
Chlorpheniramine Tablet T1	Chlorpheniramine maleate	2.8	2.56	5.68	-8.98
Chlorpheniramine Tablet T2	Chlorpheniramine maleate	2.8	2.42	2.80	-14.1
Chlorpheniramine Tablet T3	Chlorpheniramine maleate	2.8	2.41	2.53	-14.5
Pseudoephedrine Tablet T1	Pseudoephedrine HCl	49	51.6	2.37	5.03
Pseudoephedrine Tablet T2	Pseudoephedrine HCl	49	47.4	2.49	-3.62
Pseudoephedrine Tablet T3	Pseudoephedrine HCl	49	50.1	8.07	1.95
Caffeine Tablet T1	Caffeine	200	200.	4.93	-0.173
Caffeine Tablet T2	Caffeine	200	179	2.24	-10.4
Caffeine Tablet T3	Caffeine	200	221	12.1	10.3

\*Amount refers to the mass of the free base (not salt) in the original pill

In these studies, three individual tablets from the same lot were prepared for measurement, and each tablet slurry obtained (T1-T3) was analyzed in triplicate. Percent difference values ranged from -14.5 to 18.8%, and precision values from triplicate measurements ranged from 2.24 to 16.1% (CV). The reported performance metrics for all samples were within the SWGTOX guidelines.<sup>441</sup> The successful quantitative analysis of these pharmaceutical tablets by PS-MS was achieved and demonstrates the potential for using this strategy to provide quantitative analysis results for illicit drug powders and tablets.

### 3.6 Conclusion

In summary, we have demonstrated the use of paper spray mass spectrometry as a quantitative method for the measurement of fentanyl and a variety of analogs in slurry samples prepared using solid pharmaceutical powders as proxies for illicit street drugs. We demonstrate excellent sensitivity for fentanyl compounds in the low ng/g range corresponding to detection limits of 8.6 – 18 picograms on-paper in a 0.1% (w/v) pharmaceutical powder matrix. Importantly, this makes the method sensitive enough to quantitatively detect even the most potent fentanyl analogs well below their lethal limits.

Method validation studies demonstrated precision and accuracy performance metrics within the SWGTOX guidelines. The technique presents several advantages including: (1) drastically reducing or eliminating powdered sample preparation, (2) allowing for precise and accurate quantitative results for active ingredients present in powdered drug samples within minutes, (3) eliminating lengthy chromatographic separations, and (4) negligible use of solvents or other chemicals. Additionally, we have demonstrated direct qualitative and quantitative analysis of the active ingredients in pharmaceutical tablet powders using paper spray mass spectrometry, with performance metrics also within SWGTOX guidelines. The direct qualitative analysis of solid powders is amenable to future applications in rapid *in situ* screening applications with portable mass spectrometers, where samples could be rapidly screened by law enforcement personnel *in situ* and subjected to further confirmatory lab-based testing if/when necessary. Given the results from method validation studies and the performance metrics presented, as well as the wealth of recent literature presented for quantitative analysis of various substances with PS-MS, confirmatory testing using PS-MS for legally defensible results seems to be an imminent possibility. The techniques presented here for the analysis of pharmaceutical tablets are immediately transferable to the quantitative analysis of real illicit street drug samples for harm reduction drug checking. Furthermore, we believe that the technique may have applications for the direct analysis of other solid samples including soils, food, biological material, and other residues.

### 3.7 Supporting Information

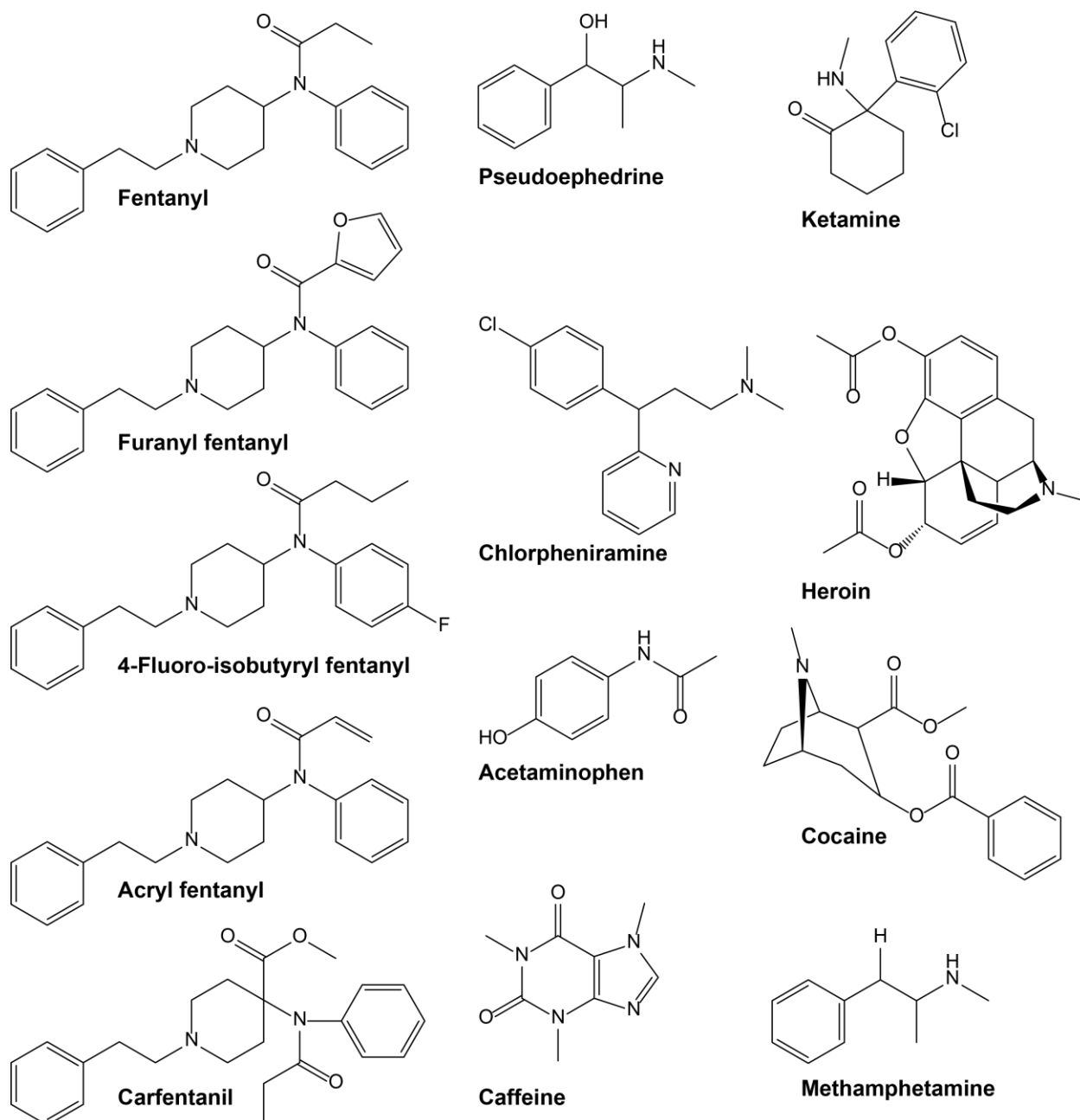


Figure 3.5 Chemical structures of the drugs examined in this study.

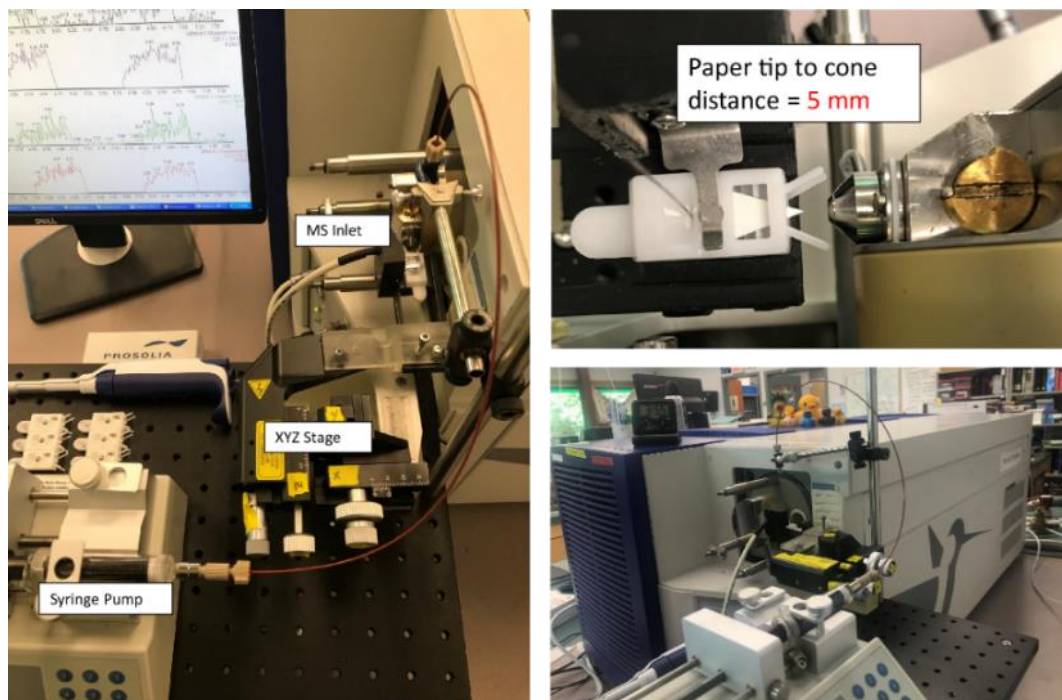


Figure 3.6 Photographs of the experimental setup used, illustrating the custom 3D printed mount, Prosolia™ cartridge in front of the mass spectrometer inlet, and the Waters Micromass Quattro Ultima LC mass spectrometer.

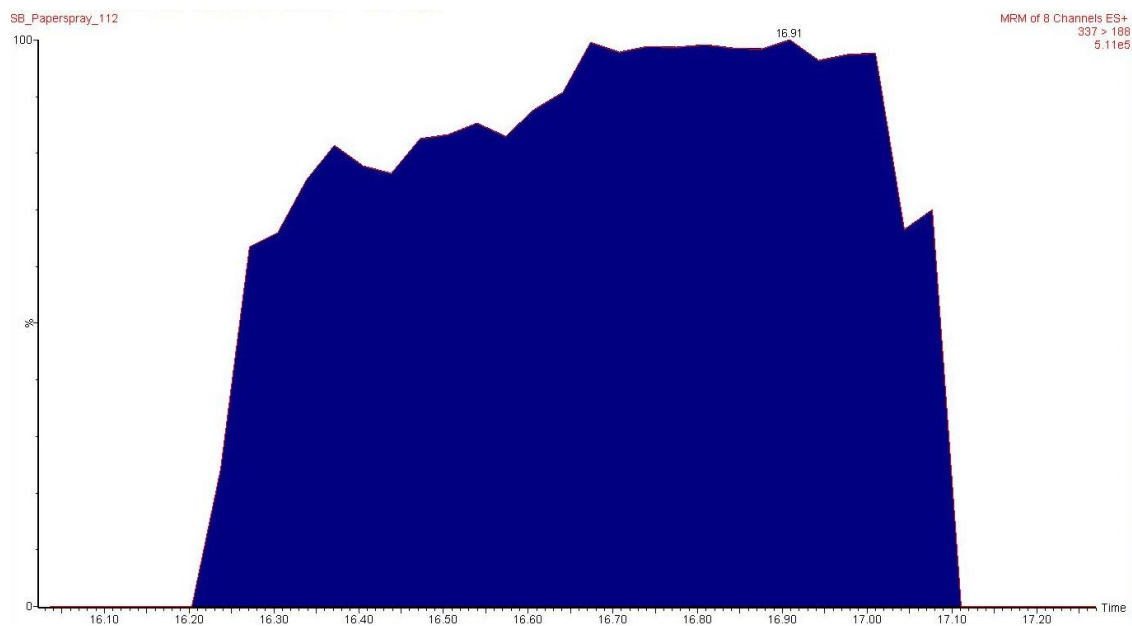


Figure 3.7 Representative integrated signal chronogram on MassLynx version 4.1 software for a typical PS-MS measurement.

Table 3.4 Mass spectrometer parameters used for all experiments.

Ion Source Parameters:	
ESI/PSI Voltage	+4.0 kV
Extractor Voltage	4 V
RF Lens Voltage	0.4 V
Cone Gas Flow	50 L / hr
Mass Analyzer Parameters:	
LM Resolution 1	12
HM Resolution 1	12
Ion Energy 1	1
Entrance	-5
Exit	1
LM Resolution 2	12
HM Resolution 2	12
Ion Energy 2	1
Multiplier	650
Collision Cell Pirani Pressure	3.1 mTorr

Table 3.5 Analyte specific instrumental parameters (first product ion listed is the quantifier ion, second listed is the qualifier ion).

Compound	Internal Standard	[Internal Standard] (ng/g)	Precursor ion	Product ions	Cone (V)	Collision Energy (eV)
Fentanyl	Fentanyl- <i>d</i> <sub>5</sub>	29.95	337.0	188.1	40	25
			337.0	104.9	40	40
Fentanyl- <i>d</i> <sub>5</sub>	-	-	342.2	188.1	35	25
			342.2	104.9	35	40
Carfentanil	Carfentanil- <i>d</i> <sub>5</sub>	28.20	395.2	335.2	25	18
			395.2	112.9	25	30
Carfentanil- <i>d</i> <sub>5</sub>	-	-	400.3	340.3	25	18
			400.3	112.9	25	30
Acrylfentanyl	Fentanyl- <i>d</i> <sub>5</sub>	29.95	335.3	188.1	35	25
			335.3	104.9	35	40
4-Fluoro-isobutyryl fentanyl (FIBF)	Fentanyl- <i>d</i> <sub>5</sub>	29.95	369.3	188.1	35	25
			369.3	104.9	35	40
Furanylfentanyl	Fentanyl- <i>d</i> <sub>5</sub>	29.95	375.3	188.1	35	25
			375.3	104.9	35	40
Acetaminophen	Acetaminophen- <i>d</i> <sub>4</sub>	1326	152.0	92.8	25	25
			152.0	109.8	25	17
Acetaminophen- <i>d</i> <sub>4</sub>	-	-	156.0	96.8	25	25
			156.0	113.8	25	18
Pseudoephedrine	Pseudoephedrine- <i>d</i> <sub>3</sub>	57.64	166.0	132.8	20	20
			166.0	147.9	20	13
Pseudoephedrine- <i>d</i> <sub>3</sub>	-	-	169.0	135.8	22	22
			169.0	150.8	22	13
Chlorpheniramine	Chlorpheniramine- <i>d</i> <sub>6</sub>	57.50	275.1	167.0	25	40
			275.1	229.9	25	23
Chlorpheniramine- <i>d</i> <sub>6</sub>	-	-	281.0	166.8	24	40
			281.0	230.0	24	20
Caffeine	Caffeine- <i>d</i> <sub>3</sub>	1147	195.0	109.9	35	25
			195.0	138.0	35	30
Caffeine- <i>d</i> <sub>3</sub>	-	-	198.0	109.9	35	25
			198.0	138.0	35	30

Table 3.6 Components in the 11 over the counter composite pill matrix.

Pill Type	Medicinal Ingredients	Amount (mg)	Non-Medicinal Ingredients
Sleep Aid	Melatonin	10	Cellulose Dicalcium Phosphate Water-Soluble Cellulose Vegetable Stearic Acid Vegetable Magnesium Stearate Modified cellulose gum Sodium Copper Chlorophyllin Silica Hydroxypropyl Cellulose
Antacid	Calcium carbonate	1000	$\alpha$ -Corn Starch Mineral Oil Natural Peppermint Flavour Sodium hexametaphosphate Sucrose Talc
NSAID	Naproxen sodium	220	Indigo Carmine Hypromellose Magnesium Stearate Microcrystalline Cellulose PEG Povidone Titanium Dioxide Talc
Analgesic	Acetaminophen Caffeine	500 65	Carnauba Wax Cellulose Corn Starch Allura Red AC Sunset Yellow FCF Hypromellose Iron Oxide Black PEG Polysorbate 80 Povidone Sodium Starch Glycolate Stearic Acid Sucralose Titanium Dioxide
NSAID	Ibuprofen	600	Carnauba Wax Colloidal Silicon Dioxide Corn Starch

			Croscarmellose Sodium Hypromellose Microcrystalline Cellulose Pharmaceutical Ink Polydextrose PEG Pregelatinized Starch Sodium Lauryl Sulfate Stearic Acid Titanium Dioxide
Analgesic	Acetaminophen	650	Carnauba Wax Colloidal Silicon Dioxide Croscarmellose Sodium Hypromellose Magnesium Stearate Maltodextrin Microcrystalline Cellulose PEG Polysorbate 80 Povidone Pregelatinized Starch Stearic Acid Titanium Dioxide
Cold Medication	Acetaminophen Phenylephrine HCl Chlorpheniramine maleate	500 5 2	Carnauba Wax Cellulose Citric Acid Corn Starch D&C Yellow no. 10 Aluminum Lake FD&C Blue no. 1 Aluminum Lake FD&C Yellow no. 6 Aluminum Lake Hypromellose Iron Oxide Black Magnesium Stearate Microcrystalline Cellulose Polydextrose PEG Propylene Glycol Sodium Starch Glycolate Titanium Dioxide Triacetin
Allergy	Loratadine	10	Corn Starch Magnesium Stearate

			Lactose Monohydrate
Allergy	Diphenhydramine HCl	25	Candelilla Wax Colloidal Silicon Dioxide Crospovidone Hypromellose Microcrystalline Cellulose PEG Povidone Pregelatinized Starch Starch Stearic Acid Titanium Dioxide Talc
Cold Medication	Acetaminophen Pseudoephedrine HCl Diphenhydramine HCl	500 30 25	Candelilla Wax Cellulose Corn Starch Croscarmellose Sodium Crospovidone FD&C Blue no. 1 Aluminum Lake Hypromellose PEG Polysorbate 80 Povidone Silica Stearic Acid Titanium Dioxide Zinc Stearate
Caffeine Tablet	Caffeine	200	Colloidal Silicon Dioxide Dicalcium Phosphate Dihydrate Magnesium Stearate Microcrystalline Cellulose

Table 3.7 Components in the pharmaceutical over the counter cold medication tablet used for fentanyl calibrations in various matrices and matrix effects studies.

Name	Medicinal Ingredients	Amount (mg)	Non-Medicinal Ingredients
Cold Medication	Dextromethorphan HBr Pseudoephedrine HCl Guaifenesin Acetaminophen	15 30 100 500	Candelilla wax Cellulose Corn starch Crospovidone D&C yellow no. 10 aluminum lake FD&C yellow no. 6 aluminum lake Hypromellose Polyethylene glycol Polysorbate 80 Povidone Silica Stearic acid Titanium dioxide Zinc stearate

Table 3.8 Calibration models (n = 3 replicates) for the fentanyl analogs in methanol. Fentanyl-d5 (30.0 ng/g) was used as the internal standard for acryl fentanyl, furanyl fentanyl, and FIBF. Carfentanil-d5 (28.2 ng/g) was used as the internal standard for carfentanil.

Acryl fentanyl			Furanyl fentanyl			FIBF			Carfentanil		
[Standard] (ng/g)	Signal Area Ratio	%RSD	[Standard] (ng/g)	Signal Area Ratio	%RSD	[Standard] (ng/g)	Signal Area Ratio	%RSD	[Standard] (ng/g)	Signal Area Ratio	%RSD
2.31	0.328	19.8	0.516	0.0347	10.4	0.511	0.0273	8.81	2.22	0.110	11.9
8.95	1.18	6.82	2.62	0.113	26.5	2.44	0.0950	7.68	9.12	0.409	9.71
30.9	1.87	7.42	9.41	0.399	5.41	9.18	0.355	2.16	22.1	0.892	6.63
119.0	4.05	7.22	26.9	1.08	22.2	17.9	0.693	7.87	48.8	1.949	9.22
187.6	6.67	2.66	50.7	2.00	9.99	52.1	1.94	6.01	195.7	6.868	11.7
			122.4	4.71	3.63	122.4	4.59	11.6			
			184.5	6.70	6.71	188.1	6.92	6.89			
Slope	y-intercept	R <sup>2</sup>	Slope	y-intercept	R <sup>2</sup>	Slope	y-intercept	R <sup>2</sup>	Slope	y-intercept	R <sup>2</sup>
3.14×10 <sup>-2</sup>	0.630	0.984	3.66×10 <sup>-2</sup>	0.706	0.999	3.69×10 <sup>-2</sup>	0.0197	0.9999	3.46×10 <sup>-2</sup>	0.119	0.9991

Table 3.9 Calibration models (n = 3 replicates) for the analysis of fentanyl in various matrices.

Methanol			10% Mannitol			5% (w/v) Tablet Matrix			5% (w/v) Tablet Matrix with 15 µg/g heroin		
[Fentanyl] (ng/g)	SAR	%RSD	[Fentanyl] (ng/g)	SAR	%RSD	[Fentanyl] (ng/g)	SAR	%RSD	[Fentanyl] (ng/g)	SAR	%RSD
2.34	0.0536	13.9	0.485	0.0173	17.8	2.12	0.227	8.09	2.55	0.148	22.7
9.34	0.340	8.44	2.34	0.0693	5.70	9.73	0.463	16.4	10.2	0.363	20.4
25.3	0.959	8.21	9.34	0.279	14.3	15.5	0.964	33.1	48.3	1.694	11.4
54.4	2.02	10.2	25.4	0.734	7.40	49.8	1.394	19.5	111	3.210	8.10
202	7.87	12.6	54.3	1.70	10.6	121	3.964	5.98	201	6.209	19.5
			202	7.07	3.10	198	6.133	6.12			
Slope	y-intercept	R <sup>2</sup>	Slope	y-intercept	R <sup>2</sup>	Slope	y-intercept	R <sup>2</sup>	Slope	y-intercept	R <sup>2</sup>
3.55×10 <sup>-2</sup>	1.83×10 <sup>-2</sup>	1.000	3.53×10 <sup>-2</sup>	-5.37×10 <sup>-1</sup>	0.999	3.00×10 <sup>-2</sup>	2.06×10 <sup>-1</sup>	0.994	3.01×10 <sup>-2</sup>	7.77×10 <sup>-2</sup>	0.997

Table 3.10 Calibration models (n = 4 replicates) for the analysis of active ingredients in pharmaceutical tablets.

Acetaminophen			Caffeine			Chlorpheniramine			Pseudoephedrine		
[Acetaminophen- <i>d</i> <sub>4</sub> ] = 1326 ng/g			[Caffeine- <i>d</i> <sub>5</sub> ] = 1147 ng/g			[Chlorpheniramine- <i>d</i> <sub>4</sub> ] = 57.50 ng/g			[Pseudoephedrine- <i>d</i> <sub>3</sub> ] = 57.64 ng/g		
[Standard] (ng/g)	Signal Area Ratio	%RSD	[Standard] (ng/g)	Signal Area Ratio	%RSD	[Standard] (ng/g)	Signal Area Ratio	%RSD	[Standard] (ng/g)	Signal Area Ratio	%RSD
112.9	0.135	5.81	112.1	0.0132	8.66	6.213	0.117	12.7	6.204	0.473	6.86
513.6	0.485	5.73	511.3	0.0507	4.88	28.31	0.530	7.50	28.27	1.11	6.19
2021	2.04	7.03	2012	0.182	15.3	111.4	2.21	6.22	111.3	3.81	10.7
10010	8.97	4.83	9930	0.916	5.47	549.9	11.2	4.28	549.1	17.3	3.01
23310	20.8	4.85	23120	2.13	1.24	1280	25.2	4.84	1278	37.4	1.87
Slope	y-intercept	R <sup>2</sup>	Slope	y-intercept	R <sup>2</sup>	Slope	y-intercept	R <sup>2</sup>	Slope	y-intercept	R <sup>2</sup>
8.89×10 <sup>-4</sup>	9.54×10 <sup>-2</sup>	0.9999	9.21×10 <sup>-5</sup>	1.19×10 <sup>-3</sup>	0.99999	1.98×10 <sup>-2</sup>	4.08×10 <sup>-2</sup>	0.9998	2.91×10 <sup>-2</sup>	5.34×10 <sup>-1</sup>	0.9991

## 4 A New Quantitative Drug Checking Technology for Harm Reduction: Pilot Study in Vancouver, Canada using Paper Spray Mass Spectrometry

This chapter has been adapted from Borden, S.A., Saatchi, A., Vandergrift, G.W., Palaty, J., Lysyshyn, M. and Gill, C.G., 2022. A new quantitative drug checking technology for harm reduction: Pilot study in Vancouver, Canada using paper spray mass spectrometry. *Drug and Alcohol Review*, 41(2), pp.410-418. doi.org/10.1111/dar.13370 with permission from John Wiley & Sons Inc.

### 4.1 Preface

This chapter presents the results from a two-day pilot study of PS-MS for drug checking applications in Vancouver, BC, Canada. Authors S.A. Borden, A. Saatchi., G.W. Vandergrift, and C.G. Gill were on location during this two-day period (August 15-16, 2019). While on site, A. Saatchi prepared the drug samples for analysis, G.W. Vandergrift acted as recordkeeper, S.A. Borden operated the instrument and prepared the data. This project was supervised by C.G. Gill. In preparation for the site visit, S.A. Borden and A. Saatchi conducted all experiments, collected all data, and prepared all calibrations. Methodology and design of experiment was done by S.A. Borden and C.G. Gill with major contributions from A. Saatchi and J. Palaty. S.A. Borden drafted the manuscript with C.G. Gill, with intellectual and editorial contributions from all authors. The PS-MS pilot study presented here was further developed for use as a drug checking technique at the Vancouver Island Drug Checking Project in Victoria, Canada.

### 4.2 Abstract

**Introduction.** Drug checking services for harm reduction and overdose prevention have been implemented in many jurisdictions as a public health intervention in response to the opioid overdose crisis. This study demonstrates the first on-site use of paper spray mass spectrometry for quantitative drug checking to address the limitations of current on-site drug checking technologies. **Methods.** Paper spray mass spectrometry was used to provide on-site drug checking services at a supervised consumption site in the Downtown Eastside of Vancouver, British Columbia, Canada during a 2-day pilot test in August 2019. The method included the targeted quantitative measurement of 49 drugs and an untargeted full scan to assist in identifying unknown/unexpected components **Results.** During the pilot, 113 samples were submitted for analysis, with 88 (78%) containing the client expected substance. Fentanyl was detected in 45 of 59 expected fentanyl samples, and in 50 (44%) samples overall at a median concentration of 3.6% (w/w%). The synthetic precursor of fentanyl, 4-anilino-N-phenethyl-piperidine (4-ANPP), was found in 74.0% of all fentanyl samples at a median concentration of 2.2%, suggesting widespread poor manufacturing practices. Etizolam was detected in 10 submitted samples anticipated to be fentanyl at a median concentration of 2.5%. No clients submitting these samples expected etizolam or a benzodiazepine in their sample. In three instances, it was co-

measured with fentanyl, and in seven cases it was detected alone. **Discussion and Conclusions.** The quantitative capabilities and low detection limits demonstrated by paper spray mass spectrometry offer distinct benefits over existing on-site drug checking methods and harm reduction services.

### 4.3 Introduction

Opioid overdoses have led to an unprecedented number of overdose deaths worldwide, particularly in recent years. According to the United Nations, there were 46 802 fatal opioid overdoses in the USA in 2018, with 67% attributed to fentanyls (includes fentanyl and related analogs, e.g., carfentanil, acetyl fentanyl and so on). Similarly, in Canada, opioid overdose deaths increased 50% from 2016 to 2018 with 4398 deaths in 2018, 80% of which involved fentanyls.<sup>447</sup> The ongoing COVID-19 pandemic has further exacerbated the opioid crisis,<sup>448</sup> leading to the highest number of fatal illicit drug overdoses ever recorded per annum in British Columbia, Canada: 1724 in 2020 compared to 984 in 2019.<sup>449</sup>

Government responses have sought alternatives to the traditional methods of prohibition and legal enforcement.<sup>10, 450, 451</sup> Drug checking is one approach that has gained considerable interest and demonstrated efficacy.<sup>430</sup> It allows people who use drugs (PWUD) to submit samples for chemical analysis and receive evidence-based information about the substance they intend to use. These services have demonstrated that providing drug test results can positively impact PWUD behaviour, including dose reduction/discard.<sup>13</sup> Drug checking technologies must be able to provide rapid results from small amounts (e.g., <10 mg) of sample to encourage participation in drug checking services. They should be selective enough to differentiate closely related substances with different toxicities (e.g., fentanyl and acetyl fentanyl), sensitive enough to detect trace levels of highly toxic substances (e.g., carfentanil), deployable for use in situ, highly adaptable to measure changes in the drug supply, operationally simple for a variety of end-users and, importantly, provide quantitative information.

Current on-site drug checking methods include colourimetric tests,<sup>452, 453</sup> ion mobility spectroscopy, liquid chromatography-mass spectrometry, gas chromatography-mass spectrometry, immunoassay test strips, Fourier-transform infrared spectroscopy (FTIR) and Raman spectroscopy.<sup>16</sup> However, these methods may suffer from one or more of the following issues: insufficient sensitivity for trace compound levels, poor differentiation of closely related compounds, inability to provide timely results and/or may not be able to quickly adapt to changes in the illicit drug supply.<sup>16, 454</sup> A technique that is currently untested in this space but is proving capable of addressing these challenges is paper spray mass spectrometry (PS-MS).<sup>18, 331</sup>

Paper spray is an ambient ionization technique for mass spectrometry first demonstrated in 2010.<sup>9</sup> In a typical measurement, a small amount ( $\leq 10 \mu\text{L}$ ) of sample is applied to a triangular piece of filter paper, and small amounts of solvent are applied. As the solvent wicks to the tip, it passes through the dried sample and mobilises analytes to the tip. A high voltage is applied to the paper, causing ionization akin to electrospray.<sup>306</sup> PS-MS has previously been used for the quantitative detection of drugs of abuse in blood,<sup>315, 333</sup>

urine,<sup>324, 335</sup> saliva,<sup>318</sup> slurries<sup>314</sup> and simulated drug samples,<sup>436</sup> but has never been implemented in drug checking. Our group published a perspectives article investigating the potential of PS-MS for drug checking<sup>331</sup> and has recently used fentanyl analog slurries and pharmaceutical tablets as a proxy for drug checking measurements with PS-MS.<sup>18</sup>

The presented study took place at a federally sanctioned supervised consumption site (SCS), the Powell Street Getaway, located in the Downtown Eastside of Vancouver, British Columbia, Canada, a recognised epicentre of the opioid overdose crisis.<sup>455</sup> The implementation of drug checking services in Vancouver has revealed the consistent detection of fentanyl in the drug supply in recent years.<sup>13, 17</sup> In addition to the routine detection of fentanyl in the Vancouver street drug supply, the direct synthetic precursor, 4-anilino-N-phenethyl-piperidine (4-ANPP) has been detected<sup>456</sup> and found in kilogram amounts in clandestine criminal laboratory drug raids in Vancouver.<sup>457</sup> Although 4-ANPP is reported to be a metabolite of fentanyl and related analogs,<sup>458, 459</sup> the presence of 4-ANPP in street drug samples indicates poor synthetic processes and/or lack of purification.<sup>460, 461</sup> Another worrying trend in the Vancouver street drug supply that began in 2019 is the detection of etizolam in opioid drug samples.<sup>456</sup> Etizolam is a thienodiazepine sedative that structurally resembles benzodiazepines and acts as an agonist for the GABA receptor.<sup>462</sup> Etizolam threatens the efficacy of naloxone distribution programs that have been effectively used to reverse and prevent fatal opioid overdose events because it does not act on the  $\mu$ -opioid receptor.<sup>463</sup> The rapidly changing drug supply and introduction of novel psychoactive substances (NPS) in many areas, especially in Vancouver,<sup>461, 464</sup> has proven to be challenging for established on-site drug checking methods (most often FTIR or immunoassay test strips) because of their lack of sensitivity and/or selectivity,<sup>16</sup> and their ability to adapt quickly and economically to these changes. While synthetic cannabinoids and designer cathinones have historically been the most popular, novel synthetic opioids have recently overshadowed these compound classes.<sup>465</sup> The introduction of synthetic opioids has introduced another challenge to current drug checking methods: many of these compounds are physiologically relevant and/or toxic at extremely low concentrations,<sup>466</sup> necessitating lower detection limits, the likes of which FTIR and Raman spectroscopy are unable to attain,<sup>16</sup> yet are achievable using PS-MS. This study presents the results from a 2-day pilot study of PS-MS for drug checking services offered at an SCS in the Downtown Eastside, Vancouver, British Columbia, Canada in August of 2019.

## 4.4 Methods

### 4.4.1 Location and Approvals

The study was conducted on 15–16 August 2019 at the Powell Street Getaway Resource Centre in the Downtown Eastside of Vancouver, BC, Canada. The Powell Street Getaway has functioned as a community resource centre since 1993 and was designated as a federally sanctioned SCS in 2017. Federal exemptions under Section 56C of the Controlled Drug and Substances Act<sup>439</sup> allow it to legally provide services such as supervised drug consumption and checking. An amendment to this exemption was approved by Health Canada that allowed the presented study to be conducted on-site as part of their Drug Checking Technology Challenge. The goals of the Drug Checking

Technology Challenge were aimed at demonstrating technologies that could provide rapid, sensitive, and quantitative detection of a wide range of drugs. Our role in this study was to pilot the use of PS-MS on-site and to provide quantitative drug test results for actual street drugs, demonstrating the efficacy of the technology. This SCS has a well-staffed harm reduction team, including medical professionals, made available to assist this study and counsel PWUD regarding drug test results. SCS clients were offered an opportunity to have their drugs checked as part of the pilot test, and all interactions with PWUD were performed by the on-site harm reduction team. Personal data regarding the PWUD and their reactions to the test results could not be collected under our exemption amendment. Client expectations for submitted drug samples were verbally relayed to the PS-MS analyst by the harm reduction workers (HRW). After testing, the HRW rapidly relayed information back to the waiting PWUD about expected and unexpected drug components, and about the relative potency of the sample based on the quantitative results.

#### **4.4.2 Analytical Method**

All analyses were performed by PS-MS using a TSQ Fortis triple quadrupole mass spectrometer and a VeriSpray paper spray ion source (Thermo Fisher Scientific, San Jose, CA, USA). Specific details regarding PS-MS method development and operation are given in the Supporting Information (Table 4.1-4.6). Samples were collected, prepared, analysed and reported according to the workflow in

Figure 4.1. This was completed in approximately 5 min, consisting of approximately 1.5 min for sample collection and recording, approximately 2 min for sample preparation and approximately 1.5 min instrument analysis time (0.7 min solvent deposition, 0.8 min analysis and reporting). An example report provided to the HRW to relay to the client is given in

Figure 4.2.

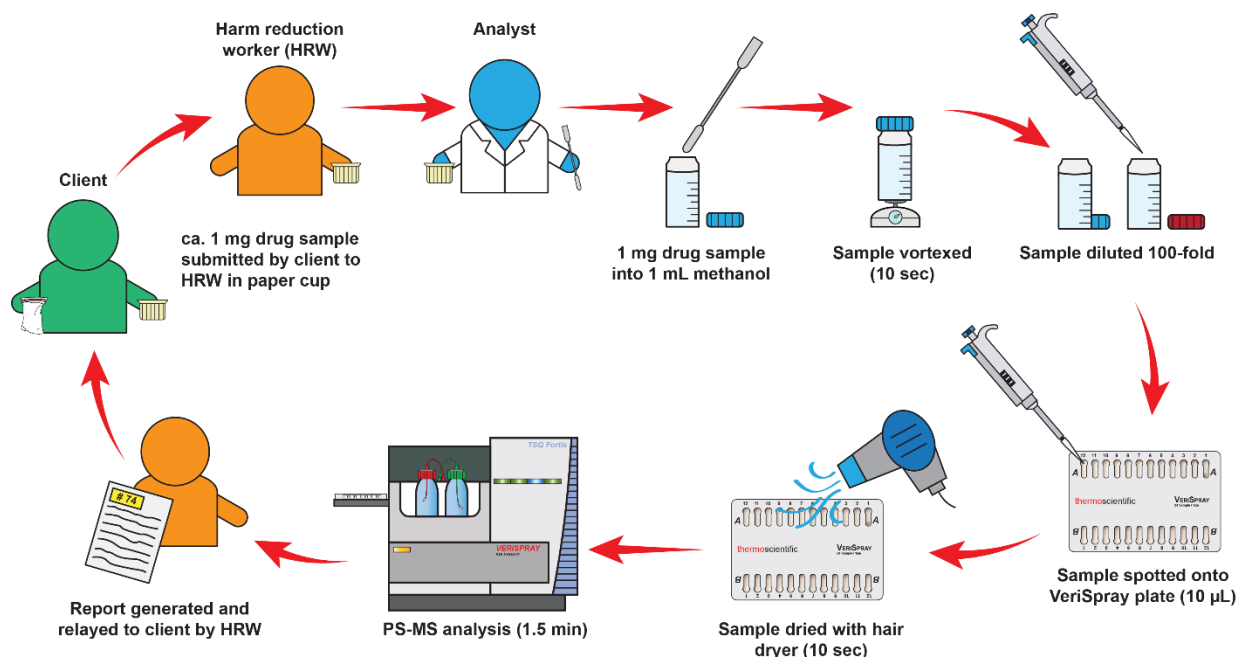


Figure 4.1 Sampling workflow and reporting of results for samples submitted by clients.

#### 4.4.3 Sample Collection

PWUD provided HRWs with a small amount (approximately 1 mg) of their drug and verbally provided their expectation of what the substance was. Specific details regarding sample collection and destruction are available in the Supporting Information. All PWUD participants were given a 5-dollar gift certificate for a local coffee shop to acknowledge and promote their participation in the study.

#### 4.4.4 Sample Preparation

Approximately 1 mg of drug sample was added to 1.00 mL of methanol in a 2-mL glass vial by the PS-MS analyst and vortexed for approximately 5 s. Visual estimates (instead of weighing samples) were utilised to reduce workflow complexity and shorten testing times. In advance of the study, visual estimates were evaluated using an analytical balance and a surrogate powder, with an estimated uncertainty of  $\pm 0.2$  mg, limiting the quantitation accuracy to  $\pm 20\%$ . Accuracy could easily be improved with an analytical balance. 100-fold dilution of this drug solution into 1.00 mL of methanol was carried out to create the 'working sample' and to lower analyte concentrations into the calibration range. A 10- $\mu$ L aliquot of the working sample was spotted onto the VeriSpray PS-MS sample plate, dried for approximately 5 s using a conventional hair dryer and immediately analysed by PS-MS.

#### 4.4.5 Quantitation

Calibration models (1 – 1,000 ng/mL; Table 4.8) for all 49 target compounds were achieved in the laboratory prior to deployment to the SCS location. The 1–1000 ng/mL correlates to mass concentrations of 0.01–10% w/w in the submitted solid drug sample.

To quantify mass concentration (w/w%) of targeted compounds in prepared drug samples, 10  $\mu$ L of an isotopically labelled internal standard cocktail (100 ng/mL each) was pre-deposited onto the PS-MS sample strips, and 10  $\mu$ L of the prepared drug sample was spotted onto the paper strip on-site. The ratio of analyte signal to internal standard signal was used for direct quantitation. The upper limit of quantitation (ULOQ) correlated to 10% w/w in the original drug sample, measurements above this were reported as >10% w/w.

#### 4.4.6 Data Reporting

Drug test reports were automatically generated (printed within 10 s) following PS-MS analysis using TraceFinder software (version 4.1 SP5, Thermo Fisher Scientific). Reports were given to the HRW, who relayed information directly to clients. Data reporting was simplified to only provide three pieces of information: the detected substance(s), percentage composition in the original sample and a short substance description. A limit of reporting was used to eliminate reporting of compounds below their lower limits of quantification or relevancy. Table 4.9 provides the limits of detection, lower limits of quantification and limits of reporting for all target compounds.

<b>Date and Time:</b>	8/15/2019 13:57	
<b>Batch:</b>	P2_A6	
<b>Sample ID #</b>	<b>24b</b>	
<b>*** Results are not guaranteed***</b>		
<b>Compound Name</b>	<b>Estimated %</b>	<b>Information</b>
Etizolam	<b>1.29</b>	Benzodiazepine (much stronger than Valium)
Fentanyl	<b>0.65</b>	Very strong opioid

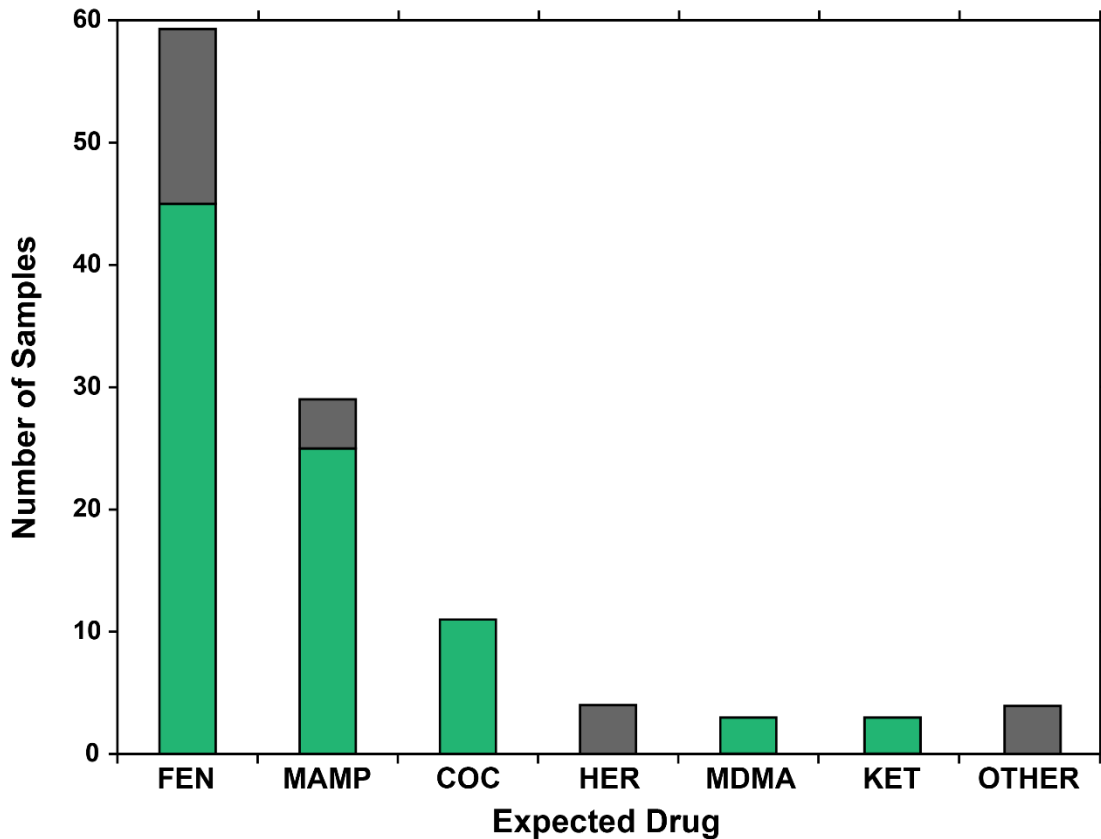
Figure 4.2 Example of the automatically generated report printout given to HRW to relay to client.

## 4.5 Results

### 4.5.1 Concordance of Client Expectations with PS-MS Results

During the 2-day pilot test, 186 PWUD visited the Powell Street Getaway SCS and 113 samples were submitted for drug checking by PS-MS, representing a 61% client uptake. Figure 4.3 shows expected drugs by sample class, as well as how concordance between client expectation and PS-MS results varied by substance. For the 111 samples where clients provided an expectation, 85 samples (77%) matched expectations, although often present with other unexpected substances. Conversely, in 26 of the 111 samples (23%), the expected substance was not detected. Fifty-nine clients (53%) expected their substance to contain fentanyl, and PS-MS detected fentanyl in 45 (76%) of these samples. Clients expected methamphetamine in 29 samples, and PS-MS detected methamphetamine in 25 (86%) of these. One hundred percent concordance between

client expectations and PS-MS results was attained for the 11 expected cocaine samples, the three expected ketamine samples and the three expected MDMA samples. Conversely, 0% concordance was observed for the four expected heroin samples. The 'other' category included an expected amphetamine sample (found to contain methamphetamine), an expected benzodiazepine (no substance detected), a sample found as a discarded drug bag on the ground (fentanyl detected) and one case where the expectation was not recorded (fentanyl detected). Fentanyl was only detected in substances that were expected to be either fentanyl or heroin (and in two cases where no expectation was given).



<span style="color: green;">■</span> Positive	45	25	11	0	3	3	0	= 87
<span style="color: grey;">■</span> Negative	14	4	0	4	0	0	4	= 26
<span style="color: green;">■</span> <span style="color: grey;">■</span> Total	59	29	11	4	3	3	4	= 113

Figure 4.3 Concordance of client expectation with PS-MS results for drug identity by expected drug category (FEN = fentanyl, MAMP = methamphetamine, COC = cocaine, HER = heroin, MDMA = 3,4-methylenedioxymethamphetamine, KET = ketamine).

#### 4.5.2 Discordant Results and Unexpected Substances

While 78% of tested samples contained the expected substance, many tests revealed the presence of unexpected adulterants or contaminants. The most adulterated/contaminated class of drugs was the opioids; only 5 (8.5%) of the 59 expected

fentanyl samples did not contain any other substances in the targeted list. The most found unexpected substance in opioid samples was 4-aminophenyl-1-phenethylpiperidine (4-ANPP). 4-ANPP was exclusively detected in samples containing fentanyl, and in the 50 samples found to contain fentanyl, 37 (74%) also contained 4-ANPP, indicating the poor quality of the Vancouver drug supply.<sup>464</sup>

The second most detected substance in expected fentanyl samples was etizolam. Etizolam was detected in 10 samples (9% of all samples and 17% of expected opioid samples). PS-MS analysis revealed that in three cases, etizolam was detected alongside fentanyl, and in the other seven cases it was the only target compound detected. Heroin was detected alongside fentanyl in three expected fentanyl samples. In the four expected heroin samples, no heroin was detected and instead, fentanyl was detected in three of these samples.

In the 29 expected methamphetamine samples, three contained MDMA only and two contained cocaine only. No discordance or unexpected substances were found in the expected cocaine, MDMA or ketamine samples tested.

### 4.5.3 Quantitative Results

Figure 4.4 illustrates quantitative results from 57 of 65 samples expected to be fentanyl, heroin or samples where no expected substance was provided. The remaining eight samples in this category were not found to contain fentanyl, 4-ANPP, etizolam or heroin. Figure 4.4A shows the 36 samples containing both fentanyl and 4-ANPP. Fentanyl was measured above the ULOQ (10% w/w) in seven of these samples, and 4-ANPP was above the ULOQ in five samples. In general, 4-ANPP concentrations were lower or roughly equal to the concentration of fentanyl measured in this sample set. Fentanyl concentrations in this sample set ranged from 0.4% to above ULOQ (median concentration 3.3%) and 4-ANPP concentrations ranged from 0.3% to above ULOQ (median concentration 2.2%). Figure 4.4B shows samples from this category where fentanyl was detected alone or alongside heroin. Heroin was measured above the ULOQ in three of the four cases, and at 7.1% in the fourth case. All heroin samples contained fentanyl. Fentanyl was measured above the ULOQ in five of the 11 samples in this category. Figure 4.4C shows samples from this category where etizolam was detected. Etizolam concentrations (n = 10) ranged from 0.68% to 8.27% (median 2.5% w/w). In three of these samples, fentanyl co-occurred at concentrations of 0.6%, 2.2% and 3.0%, with one sample also containing 4-ANPP at 1.5%. Quantitative results for all 113 samples are given in Table 4.10.

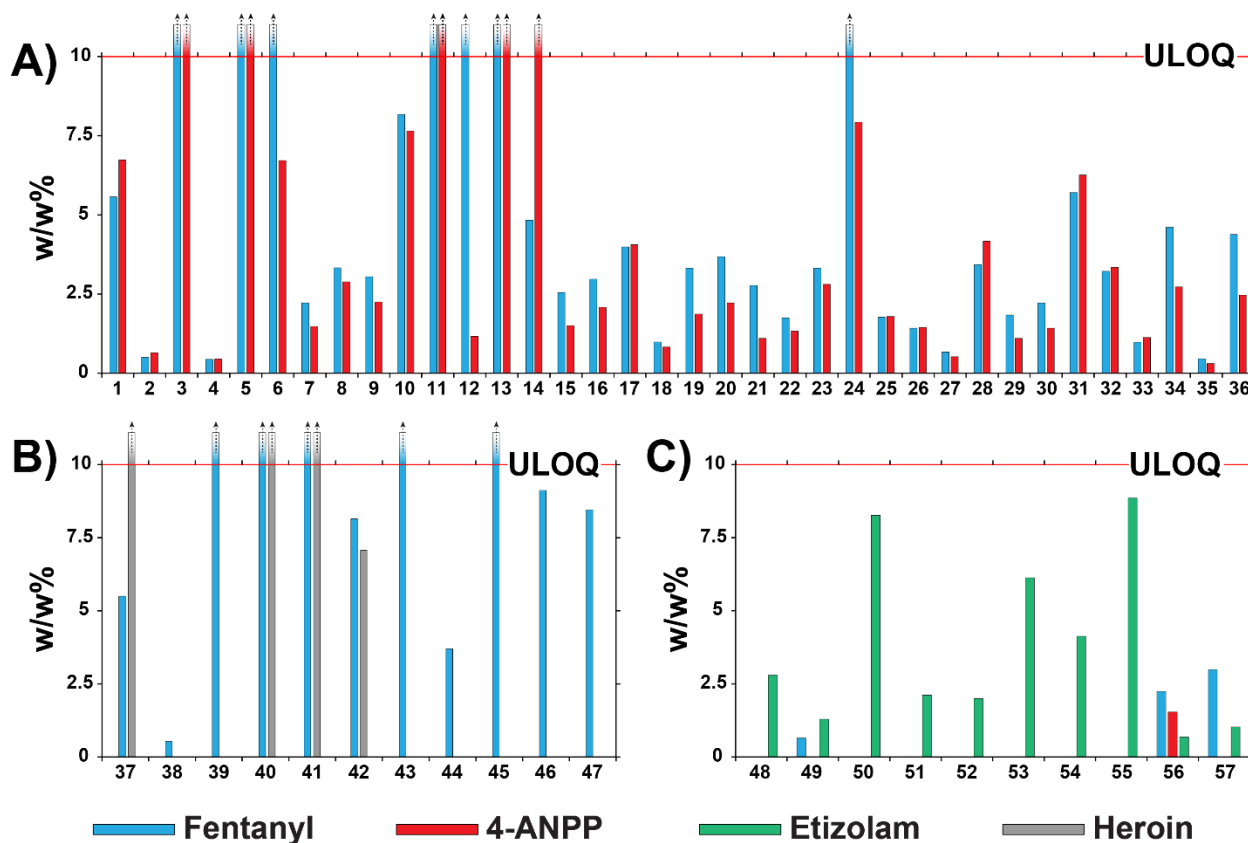


Figure 4.4 Calculated amounts (w/w%) of fentanyl (—), 4-ANPP (—), etizolam (—), and heroin (—) in expected opioid samples and unknown samples. A) expected opioid samples containing exclusively fentanyl and 4-ANPP, B) expected opioid samples containing heroin and/or fentanyl, and C) expected opioid samples where etizolam was detected. The upper limit of quantitation (ULOQ) was 10% w/w.

## 4.6 Discussion

### 4.6.1 Discordant Results and Unexpected Substances

In most cases, PWUD are aware of the substance they intend to use, evidenced by concordance rates in this study (78%) and in similar studies.<sup>17, 467</sup> While confirmation of an expected substance is beneficial information, alerting clients to substances in their drugs that they are not aware of, and quantifying unexpectedly potent or 'pure' samples offers more benefit and potential to affect behaviour modification. For example, detecting etizolam in opioid samples can allow HRWs to inform clients that naloxone may not be completely effective in reversing an overdose. In addition, an opioid sample may be assumed to be fentanyl, but the detection of a significantly more potent trace adulterant such as carfentanil (not detected at the time of this study) would substantially alter the messaging supplied to clients by HRWs. Anecdotally, the HRWs and PWUD expressed satisfaction with the rapidity of the testing and the quality of the test results. Furthermore, several samples (especially those with detected etizolam) were returned to the PS-MS

test room by the PWUD via the HRWs for destruction, suggesting positive behaviour modifications.

One of the most effective ways that community health organisations have been able to mitigate the severity of opioid overdoses is through naloxone distribution; a systematic review found that community access to naloxone distribution programs has significantly reduced fatal opioid overdoses.<sup>463</sup> Naloxone binds to the  $\mu$ -opioid receptor with a strong affinity and blocks the effects of opioids on the central or peripheral nervous system.<sup>468</sup> Naloxone is only effective when administered for opioid overdoses, and the detection of etizolam in 9% of all samples and 16% of expected opioid samples is therefore of potential concern and salient to harm reduction messaging. Furthermore, benzodiazepine immunoassay test strips cannot differentiate between benzodiazepine analogs, and the low levels of etizolam detected by PS-MS (median concentration 2.5%) would likely be missed by FTIR analysis.

The emergence of potent NPS that are often present at levels below the limits of detection of currently used on-site drug checking technologies necessitates the use of techniques that are both sensitive and selective. For example, fentanyl was quantified at <1% in four samples; these levels likely would not be detected by FTIR or Raman spectroscopy. While immunoassay test strips are sensitive, and can detect trace levels of fentanyl, they lack the selectivity to differentiate between related compounds with extremely different toxicities, provide only qualitative 'yes/no' identification, and can only detect a single analyte class at a time.

Furthermore, as NPS enter the drug supply in the future, technologies must be able to adapt and detect them. This would require development of new immunoassays for novel drug classes, or the constant updating of spectroscopic libraries in the case of FTIR and Raman spectroscopy, limited by the availability of reference standards. PS-MS, however, is capable of rapidly adapting to the introduction of NPS without reference standards, or updated libraries, through non-targeted scan functions, high-resolution accurate mass and/or structural characterisation with tandem mass spectrometry. The PS-MS method utilised in this study included an interlaced full scan to allow for the potential identification of unknowns. Mass spectrometry has a long history of using scan functions or data-independent analysis for the identification of NPS.<sup>23</sup> Palaty et al. demonstrated the use of precursor ion scans with high-resolution mass spectrometry for clinical urine samples to detect an unknown fentanyl analog(s) that had entered the Vancouver street drug supply: cyclopropylfentanyl/crotonylfentanyl.<sup>469</sup> The non-targeted methods employed in other areas of mass spectrometry are applicable to and easily implemented in PS-MS methods given sufficient hardware (e.g., high-resolution mass spectrometer). Given the rapidly changing illicit drug market and introduction of NPS on a regular basis, the adaptability of drug checking technologies must be considered, and the ability of a technique to detect increasingly potent NPS is critical to the effectiveness of drug checking technologies. The sensitivity, selectivity and/or adaptability issues faced by established drug checking

technologies highlights some of the unique strengths that PS-MS offers to drug checking services since it is both highly sensitive and selective.

#### **4.6.2 Quantitative Results**

One of the greatest strengths for PS-MS as a drug checking technique, is the ease with which quantitative results can be obtained. Given the varying concentrations of substances found in illicit drugs, valuable harm reduction messaging can be gleaned from quantifying active components. An HRW may change their messaging and be more able to provide meaningful harm reduction advice depending on whether the sample is 0.1%, 1% or 10% fentanyl (or greater). Data from quantitative PS-MS results in this study provided HRWs with valuable information and changed the information they would have relayed to the client in several instances. In the 10 instances where etizolam was detected, clients were informed that naloxone may not be able to reverse an overdose and that they should avoid using alone and contact emergency services in the event of an overdose. Clients were also alerted that their drugs may be much stronger than expected when high levels of fentanyl were measured with PS-MS.

Sample preparation steps and the calibration models used in this pilot study were specifically designed for the detection and quantitation of lower-level components from 0.01% to 10% w/w. This decision was made to detect and quantify the very low-level components (e.g., carfentanil) that may be incredibly dangerous at trace levels (<1%) and are not able to be identified/detected by other on-site testing methods. By simply adjusting the dilution factors and/or calibration range, the range of the PS-MS calibration model may be tailored on a compound-specific basis if desired (e.g., from 0.1% to 100%).

#### **4.6.3 Practical Considerations**

We have presented a summary of the feasibility of PS-MS for on-site drug checking in this manuscript. It is important to consider that at the time of the study there were legal, ethical, and temporal restrictions that did not allow for the collection of demographic data, collection and dissemination of the client response or any behaviour modification made based upon the information they received from the HRW (aside from anecdotal information from the HRWs), or detailed information on the client experience with the technology. Since the time of the study, we have worked to overcome these restrictions and improve upon some of the limitations including quantitation to 100%. We have presented many of the unique strengths of PS-MS for drug checking above. Implementation of PS-MS for drug checking beyond this first demonstration should consider the up-front cost of the equipment (a few \$100 000 USD, depending upon the desired instrument configuration), the expertise required in developing the methodology and maintaining the instrumental performance, and the on-site power/electrical requirements.

### **4.7 Conclusion**

The work presented demonstrates the first use of PS-MS for on-site, quantitative drug checking at an SCS. This pilot study was conducted over 2 days in August 2019 in the

Downtown Eastside of Vancouver, British Columbia, Canada, during which time 113 samples were submitted for analysis. Many existing drug checking technologies currently in use (on-site or otherwise) have limitations with regards to selectivity, sensitivity, adaptability and/or lengthy analysis times. PS-MS allows for rapid, selective, sensitive, and highly adaptable methods for quantitative drug checking. All existing drug checking technologies use small amounts of sample (e.g., 1 mg), and some are even non-destructive, suggesting that there is opportunity for many of these techniques to be used in tandem with PS-MS to develop extremely comprehensive drug testing. Future drug checking services using PS-MS will implement automated, non-targeted scan functions to potentially identify new drugs not in the targeted list. PS-MS is adaptable to portable mass spectrometer systems, for in situ, street level or roadside analysis. The need for drug checking technologies and services is likely to increase in the future as governments consider policy shifts such as drug decriminalisation. PS-MS has demonstrated utility in the arsenal of drug checking technologies that could be used to help prevent overdoses, and mitigate the social, economic, and personal harms that have been amplified in the wake of the ongoing opioid overdose crisis.

## **4.8 Supporting Information**

### **4.8.1 Paper Spray Sampling Protocol**

Paper spray mass spectrometry (PS-MS) sample cartridges were pre-spotted (10  $\mu$ L) in the laboratory with an internal standard cocktail (100 ng/mL) prior to deployment to the supervised consumption site (SCS) to allow for direct quantitation. The PS-MS analysis included both targeted and untargeted scans in a 0.8-minute method. Targeted scans were accomplished using tandem mass spectrometry (MS/MS) to greatly increase the selectivity of the method. From time 0.1 – 0.55 minutes, the PS-MS measurement targeted compounds and their associated internal standards by MS/MS. From time 0.6 – 0.8 minutes, the MS performed a non-targeted full scan analysis (m/z 150 – 500) to aid in identifying drugs present in the sample not in the target drug list. Immediately following the analysis, a report was generated containing information on the detected compound(s), including their % composition and a short description to aid in harm reduction. Information from the report was immediately relayed to the client by the harm reduction worker (HRW). Unknown signals (distinguishable from background signals) in the full scan data were investigated by subjecting the sample to further analysis via product scans. Through spectral comparisons of these product scans to online databases, unknown drugs not being targeted could theoretically be tentatively identified and structurally characterised. Although this data was not used for the presented pilot tests, it will be applied to future studies and datasets.

### **4.8.2 Target Drugs**

A total of 49 drugs were targeted for quantitation. Target drugs that were quantified for this study were chosen based upon publicly available illicit drugs tested in Vancouver by the federal Drug Analysis Services Laboratories (Burnaby, Canada) and anonymous test

results from urine samples collected from patients with substance use disorder (courtesy of LifeLabs Medical Laboratories, Burnaby, Canada).

### **4.8.3 Standards**

All analytical reference standards were purchased from Cerilliant Corporation (Round Rock, USA). A working multi-component methanolic drug standard cocktail was prepared from 49 analytical reference standards. The internal standard cocktail, prepared similarly, contained 43 isotopically labelled components at a concentration of 100 ng/mL. A solid sample matrix powder was created from a mixture of 11 different over the counter pharmaceuticals (Table 4.7) ground together with a mortar and pestle to simulate the wide variety of excipients that might be encountered in street drugs (e.g., sugars, caffeine, etc.). The matrix also contained active ingredients that are structurally analogous to drugs of abuse (e.g., pseudoephedrine). The working multi-component methanolic solution was used to prepare standards in methanol with the composite over the counter pharmaceutical powder matrix at a matrix loading of 1 mg/mL. The calibration models for all compounds are outlined in Table 4.8.

### **4.8.4 Sample Collection**

All samples were collected on site, in a separate room designated as a SCS, by trained HRWs familiar with the clientele. Clients were instructed to submit a small amount (ca. 1 mg) of their drug sample in a 1 oz paper portion cup; a visual aid of 1 mg of the over-the-counter surrogate powder in the paper portion cup was provided to help the client estimate the required sample size. During collection, the client's expectations of the composition of their substance was recorded by the HRW. Clients typically used colloquial language to describe their expectations of their substance. For example, methamphetamine samples were often referred to as "side" or "crystal"; samples designated as such were classified as methamphetamine samples. Similarly, fentanyl or heroin samples were referred to as "down". When a client referred to a sample as "down" the HRW clarified whether the client was referring to heroin or fentanyl. Any left-over sample was immediately returned to the client by the consulting HRW, or immediately destroyed in a Deterra drug deactivation and disposal pouch (Verde Technologies, Minnetonka, USA). Used PS-MS sample strips were disposed in the sharps waste disposal of the SCS. Records of all drug samples tested and destroyed were created, witnessed and written records maintained at the site. People who use drugs (PWUD) participants were given a \$5 gift certificate for a local coffee shop to acknowledge and promote their participation in the study. This SCS also provides a full spectrum of free services, including meals, access to clean washrooms and showers, as well as providing a sense of community, which engages a large level of PWUD, not only those using the SCS services. The honorarium probably increased service participation at some level, but anecdotal comments from the harm reduction team and PWUD suggested they were grateful for the improved results obtained using the PS-MS as a drug testing option.

#### 4.8.5 Tables

Table 4.1 Paper spray mass spectrometry global parameters.

<b>Parameter</b>	<b>Value</b>
Ionization polarity	Positive
Default charge state	1
Ion-transfer tube (°C)	300
Sweep gas	Off
Spray voltage (V)	4000

Table 4.2 Analyte dependant tandem mass spectrometry (MS/MS) ion transition parameters. MS/MS transitions optimized in the lab using direct infusion electrospray ionization.

Compound	Transition	Precursor (m/z)	Product (m/z)	Collision Energy (eV)	Lens (V)	Source Frag. (V)
4-ANPP	Target	281.2	105.1	31	75	7
	Confirming 1	281.2	103.1	46		
	Confirming 2	281.2	134.1	24		
4-ANPP- <i>d</i> <sub>5</sub>	Target	286.2	105.1	31	78	7
	Confirming 1	286.2	103.1	46		
	Confirming 2	286.2	134.2	25		
4-Fluorobutyryl fentanyl	Target	369.2	188.2	24	77	36
	Confirming 1	369.2	105.1	38		
	Confirming 2	369.2	150.1	32		
4-Fluorofentanyl- <i>d</i> <sub>3</sub>	Target	358.2	188.1	24	97	15
	Confirming 1	358.2	105.1	38		
	Confirming 2	358.2	103.1	55		
Acetyl fentanyl	Target	323.2	188.2	23	90	15
	Confirming 1	323.2	105.1	36		
	Confirming 2	323.2	103.1	52		
Acetyl fentanyl- <sup>13</sup> C <sub>6</sub>	Target	329.2	188.1	23	94	15
	Confirming 1	329.2	105.1	36		
	Confirming 2	329.2	103.1	52		
Acryl fentanyl	Target	335.2	188.1	22	93	15
	Confirming 1	335.2	105.1	36		
	Confirming 2	335.2	103.1	52		
Acryl fentanyl- <i>d</i> <sub>5</sub>	Target	340.2	188.1	23	92	13
	Confirming 1	340.2	105.1	36		
	Confirming 2	340.2	103.1	53		
Alprazolam	Target	309.1	281.1	26	109	23
	Confirming 1	309.1	205.0	41		
	Confirming 2	309.1	274.1	25		
Alprazolam- <i>d</i> <sub>5</sub>	Target	314.1	286.1	26	110	33
	Confirming 1	314.1	210.1	42		
	Confirming 2	314.1	279.2	26		
Amphetamine	Target	136.1	91.1	17	62	0
	Confirming 1	136.1	65.1	36		
	Confirming 2	136.1	51.1	53		
Amphetamine- <i>d</i> <sub>11</sub>	Target	147.2	98.1	18	69	0
	Confirming 1	147.2	70.1	38		
	Confirming 2	147.2	54.1	54		
Buprenorphine	Target	468.3	414.2	34	78	70
	Confirming 1	468.3	396.2	38		
	Confirming 2	468.3	55.1	53		
Buprenorphine- <i>d</i> <sub>4</sub>	Target	472.3	400.2	40	94	62
	Confirming 1	472.3	415.3	35		
	Confirming 2	472.3	59.1	48		

Compound	Transition	Precursor ( <i>m/z</i> )	Product ( <i>m/z</i> )	Collision Energy (eV)	Lens (V)	Source Frag. (V)
Butyryl fentanyl	Target	351.2	188.2	23	94	13
	Confirming 1	351.2	105.1	37		
	Confirming 2	351.2	230.2	23		
Butyryl fentanyl- <i>d</i> <sub>5</sub>	Target	356.3	188.1	24	95	15
	Confirming 1	356.3	105.1	39		
	Confirming 2	356.3	235.2	24		
Carfentanil	Target	395.2	335.2	18	96	10
	Confirming 1	395.2	113.1	30		
	Confirming 2	395.2	363.2	13		
Carfentanil- <i>d</i> <sub>5</sub>	Target	400.3	340.2	18	101	15
	Confirming 1	400.3	113.1	31		
	Confirming 2	400.3	368.2	13		
Cocaine	Target	304.1	182.1	19	83	10
	Confirming 1	304.1	82.1	29		
	Confirming 2	304.1	77.1	50		
Cocaine- <i>d</i> <sub>3</sub>	Target	307.2	185.1	20	82	11
	Confirming 1	307.2	85.1	30		
	Confirming 2	307.2	77.1	49		
Codeine	Target	300.2	215.1	25	102	26
	Confirming 1	300.2	165.1	41		
	Confirming 2	300.2	225.1	27		
Codeine- <i>d</i> <sub>3</sub>	Target	303.2	215.2	25	105	26
	Confirming 1	303.2	165.1	42		
	Confirming 2	303.2	225.1	27		
Cyclopropyl fentanyl	Target	349.2	188.1	24	83	28
	Confirming 1	349.2	105.1	38		
	Confirming 2	349.2	132.1	33		
Diazepam	Target	285.1	193.1	31	109	21
	Confirming 1	285.1	154.1	27		
	Confirming 2	285.1	222.1	26		
Diazepam- <i>d</i> <sub>5</sub>	Target	290.1	198.1	32	102	29
	Confirming 1	290.1	154.1	27		
	Confirming 2	290.1	227.2	28		
Dihydrocodeine	Target	302.2	199.1	33	76	46
	Confirming 1	302.2	201.1	29		
	Confirming 2	302.2	171.1	42		
Dihydrocodeine- <i>d</i> <sub>6</sub>	Target	308.2	202.1	34	78	46
	Confirming 1	308.2	204.1	30		
	Confirming 2	308.2	174.1	43		
Dimethylmethcathinone	Target	192.1	159.1	21	63	8
	Confirming 1	192.1	144.1	31		
	Confirming 2	192.1	115.1	50		
Ethylpentylone	Target	250.2	202.1	19	90	11
	Confirming 1	250.2	189.1	24		
	Confirming 2	250.2	205.1	14		
Ethylpentylone- <i>d</i> <sub>5</sub>	Target	255.2	207.2	19	77	11

Compound	Transition	Precursor ( <i>m/z</i> )	Product ( <i>m/z</i> )	Collision Energy (eV)	Lens (V)	Source Frag. (V)
	Confirming 1	255.2	194.1	25		
	Confirming 2	255.2	205.1	15		
Etizolam	Target	343.1	314.0	25	111	23
	Confirming 1	343.1	289.0	24		
	Confirming 2	343.1	274.0	41		
Etizolam- <i>d</i> <sub>3</sub>	Target	346.1	317.0	26	69	52
	Confirming 1	346.1	292.1	24		
	Confirming 2	346.1	313.1	23		
Fentanyl	Target	337.2	188.1	23	92	13
	Confirming 1	337.2	105.1	36		
	Confirming 2	337.2	103.1	51		
Fentanyl- <i>d</i> <sub>5</sub>	Target	342.3	188.1	23	91	15
	Confirming 1	342.3	105.1	37		
	Confirming 2	342.3	103.1	53		
FIBF	Target	369.2	188.1	25	83	33
	Confirming 1	369.2	105.1	38		
	Confirming 2	369.2	248.2	24		
Flunitrazepam	Target	314.1	268.1	25	105	21
	Confirming 1	314.1	239.1	34		
	Confirming 2	314.1	183.1	54		
Flunitrazepam- <i>d</i> <sub>7</sub>	Target	321.2	275.1	26	118	33
	Confirming 1	321.2	246.1	36		
	Confirming 2	321.2	245.2	36		
Furanyl fentanyl	Target	375.2	188.1	22	97	16
	Confirming 1	375.2	105.1	39		
	Confirming 2	375.2	103.1	54		
Furanyl fentanyl- <i>d</i> <sub>5</sub>	Target	380.2	188.1	23	96	11
	Confirming 1	380.2	105.1	39		
	Confirming 2	380.2	103.1	54		
Heroin	Target	370.2	268.1	28	116	29
	Confirming 1	370.2	328.2	26		
	Confirming 2	370.2	211.1	30		
Heroin- <i>d</i> <sub>9</sub>	Target	379.2	272.1	29	117	26
	Confirming 1	379.2	212.1	31		
	Confirming 2	379.2	335.1	27		
Hydrocodone	Target	300.2	171.1	39	81	42
	Confirming 1	300.2	213.1	30		
	Confirming 2	300.2	241.1	27		
Hydrocodone- <i>d</i> <sub>3</sub>	Target	303.2	171.1	39	78	46
	Confirming 1	303.2	241.0	27		
	Confirming 2	303.2	213.0	31		
Hydromorphone	Target	286.1	157.1	41	108	31
	Confirming 1	286.1	227.0	27		
	Confirming 2	286.1	199.0	30		
Hydromorphone- <i>d</i> <sub>3</sub>	Target	289.1	178.0	26	103	31
	Confirming 1	289.1	185.0	30		
	Confirming 2	289.1	157.1	42		

Compound	Transition	Precursor ( <i>m/z</i> )	Product ( <i>m/z</i> )	Collision Energy (eV)	Lens (V)	Source Frag. (V)
Hydroxythiofentanyl	Target	359.2	192.1	22	97	15
	Confirming 1	359.2	146.1	23		
	Confirming 2	359.2	285.2	20		
Isobutyrylfentanyl	Target	351.2	188.1	23	98	15
	Confirming 1	351.2	105.1	38		
	Confirming 2	351.2	103.1	55		
Ketamine	Target	238.1	125.0	29	102	21
	Confirming 1	238.1	207.1	15		
	Confirming 2	238.1	179.0	17		
Ketamine- <i>d</i> <sub>4</sub>	Target	242.1	129.1	28	77	10
	Confirming 1	242.1	211.1	15		
	Confirming 2	242.1	183.1	18		
MDA	Target	180.1	105.1	22	67	0
	Confirming 1	180.1	133.1	18		
	Confirming 2	180.1	77.1	38		
MDA- <i>d</i> <sub>5</sub>	Target	185.1	110.2	23	72	5
	Confirming 1	185.1	138.1	19		
	Confirming 2	185.1	137.1	20		
MDEA	Target	208.1	163.1	13	67	5
	Confirming 1	208.1	105.1	25		
	Confirming 2	208.1	135.1	22		
MDEA- <i>d</i> <sub>5</sub>	Target	213.2	163.1	14	63	18
	Confirming 1	213.2	105.1	26		
	Confirming 2	213.2	135.1	22		
MDMA	Target	194.1	163.1	13	63	0
	Confirming 1	194.1	105.1	24		
	Confirming 2	194.1	133.1	20		
MDMA- <i>d</i> <sub>5</sub>	Target	199.1	165.1	13	59	16
	Confirming 1	199.1	107.1	25		
	Confirming 2	199.1	135.1	21		
Meperidine	Target	248.2	220.2	21	92	18
	Confirming 1	248.2	174.1	21		
	Confirming 2	248.2	131.1	31		
Meperidine- <i>d</i> <sub>4</sub>	Target	252.2	224.2	22	94	16
	Confirming 1	252.2	178.2	21		
	Confirming 2	252.2	135.1	32		
Methadone	Target	310.2	265.2	15	68	0
	Confirming 1	310.2	105.0	27		
	Confirming 2	310.2	223.1	21		
Methadone- <i>d</i> <sub>9</sub>	Target	319.3	268.2	16	73	7
	Confirming 1	319.3	105.1	28		
	Confirming 2	319.3	226.2	22		
Methamphetamine	Target	150.1	91.1	20	66	0
	Confirming 1	150.1	119.1	11		
	Confirming 2	150.1	65.1	40		
Methamphetamine- <i>d</i> <sub>11</sub>	Target	161.2	97.1	19	68	10

Compound	Transition	Precursor ( <i>m/z</i> )	Product ( <i>m/z</i> )	Collision Energy (eV)	Lens (V)	Source Frag. (V)
		Confirming 1	161.2	127.2	12	
	Confirming 2	161.2	69.1	41		
Methoxy acetylfentanyl	Target	353.2	188.1	22	77	33
	Confirming 1	353.2	105.1	36		
	Confirming 2	353.2	103.1	51		
Methylfentanyl	Target	351.2	91.1	38	95	18
	Confirming 1	351.2	202.1	23		
	Confirming 2	351.2	119.1	27		
Morphine	Target	286.1	152.1	54	109	26
	Confirming 1	286.1	201.1	26		
	Confirming 2	286.1	181.0	36		
Morphine- <i>d</i> <sub>6</sub>	Target	292.2	152.1	55	106	26
	Confirming 1	292.2	181.1	37		
	Confirming 2	292.2	201.1	26		
MT-45	Target	349.2	181.1	23	93	13
	Confirming 1	349.2	169.2	19		
	Confirming 2	349.2	166.1	35		
Ocfentanil	Target	371.2	188.1	22	94	15
	Confirming 1	371.2	105.1	39		
	Confirming 2	371.2	103.1	53		
Oxazepam	Target	287.0	241.0	23	101	13
	Confirming 1	287.0	199.0	11		
	Confirming 2	287.0	243.0	6		
Oxazepam- <i>d</i> <sub>5</sub>	Target	292.1	246.1	23	96	13
	Confirming 1	292.1	109.1	36		
	Confirming 2	292.1	163.1	39		
Oxycodone	Target	316.2	256.1	26	105	18
	Confirming 1	316.2	212.1	42		
	Confirming 2	316.2	187.0	27		
Oxycodone- <i>d</i> <sub>6</sub>	Target	322.2	262.2	26	80	31
	Confirming 1	322.2	218.1	43		
	Confirming 2	322.2	190.1	27		
Oxymorphone	Target	302.1	198.1	44	100	16
	Confirming 1	302.1	242.1	27		
	Confirming 2	302.1	181.1	55		
Oxymorphone- <i>d</i> <sub>3</sub>	Target	305.2	230.1	30	102	18
	Confirming 1	305.2	201.1	45		
	Confirming 2	305.2	245.1	27		
Phencyclidine	Target	244.2	86.1	13	55	11
	Confirming 1	244.2	91.1	30		
	Confirming 2	244.2	159.2	14		
Phencyclidine- <i>d</i> <sub>5</sub>	Target	249.2	86.1	13	57	0
	Confirming 1	249.2	164.2	15		
	Confirming 2	249.2	96.1	32		
Remifentanil	Target	377.2	317.2	16	77	25
	Confirming 1	377.2	345.2	13		

Compound	Transition	Precursor ( <i>m/z</i> )	Product ( <i>m/z</i> )	Collision Energy (eV)	Lens (V)	Source Frag. (V)
	Confirming 2	377.2	285.2	19		
Sufentanil	Target	387.2	238.2	19	90	7
	Confirming 1	387.2	111.1	36		
	Confirming 2	387.2	355.1	19		
Sufentanil- <i>d</i> <sub>5</sub>	Target	392.2	238.2	20	93	0
	Confirming 1	392.2	111.0	36		
	Confirming 2	392.2	360.2	20		
Temazepam	Target	301.1	255.1	22	95	18
	Confirming 1	301.1	177.0	39		
	Confirming 2	301.1	193.1	35		
Temazepam- <i>d</i> <sub>5</sub>	Target	306.1	260.1	22	100	18
	Confirming 1	306.1	198.1	35		
	Confirming 2	306.1	177.0	39		
Tramadol	Target	264.2	58.1	18	69	7
	Confirming 1	264.2	180.0	15		
	Confirming 2	264.2	91.1	51		
U-47700	Target	329.1	284.0	17	80	8
	Confirming 1	329.1	173.0	31		
	Confirming 2	329.1	145.0	49		
U-47700- <i>d</i> <sub>3</sub>	Target	332.1	287.1	17	82	0
	Confirming 1	332.1	176.0	32		
	Confirming 2	332.1	148.0	51		
Valeryl fentanyl	Target	365.3	188.1	24	96	15
	Confirming 1	365.3	105.1	38		
	Confirming 2	365.3	281.2	20		
Valeryl fentanyl- <i>d</i> <sub>5</sub>	Target	370.3	188.1	24	97	13
	Confirming 1	370.3	105.1	40		
	Confirming 2	370.3	286.2	21		
Zolpidem	Target	308.1	235.2	37	102	21
	Confirming 1	308.1	263.1	26		
	Confirming 2	308.1	219.1	53		
Zolpidem- <i>d</i> <sub>7</sub>	Target	315.2	242.2	36	103	23
	Confirming 1	315.2	270.1	26		
	Confirming 2	315.2	223.1	53		

Table 4.3 Paper spray mass spectrometry solvent dispense conditions.

Rewet Solvent Dispense (10 $\mu$ L)	
Aliquot #	Delay (s)
1	1
2	1
3	10
Spray Solvent Dispense (10 $\mu$ L)	
Aliquot #	Delay (s)
1	1
2	1
3	1
4	2
5	2
6	2
7	3
8	3
9	3
10	10

Table 4.4 Mass spectrometry time-dependent voltage parameters.

Time (min)	Spray Voltage (V)
0	0
0.1	4000
0.4	0
0.56	4000
0.76	0

Table 4.5 Tandem mass spectrometry (MS/MS) method settings.

Parameter	Value
Duration (min)	0 - 0.55
Dwell Time (ms)	2.743
Q1 Resolution (FWHM)	0.7
Q3 Resolution (FWHM)	1.2
CID Gas (mTorr)	2
# of Scans Per Compound	41.9

Table 4.6 Mass spectrometry full scan (Q3) method settings.

Parameter	Value
Duration (min)	0.6-0.8
Scan Range ( $m/z$ )	150-500
Scan Rate (Da/sec)	500
Dwell Time (ms)	700
Q3 Resolution (FWHM)	0.7
Source Fragmentation (V)	5
CID Gas (mTorr)	2
# of Scans Per $m/z$	17.1

Table 4.7 Medicinal and non-medicinal ingredients of the over the counter (OTC) composite mixture.

Medication Class	Medicinal Ingredients	Amount (mg)	Non-Medicinal Ingredient
Melatonin	Melatonin	10	Cellulose Dicalcium phosphate Water-soluble cellulose Vegetable stearic acid Vegetable magnesium stearate Modified cellulose gum Sodium copper chlorophyllin Silica Hydroxypropyl cellulose
Antacid	Calcium Carbonate	1000	Alpha-corn starch Mineral oil Natural peppermint flavour Sodium hexametaphosphate Sucrose Talc
NSAID	Naproxen Sodium	220	Indigo carmine Hypromellose Magnesium stearate Microcrystalline cellulose PEG Povidone Titanium dioxide Talc
Analgesic	Acetaminophen Caffeine	500 65	Carnauba wax Cellulose Corn starch Allura red AC Sunset yellow FCF Hypromellose Iron oxide black PEG Polysorbate 80 Povidone Sodium starch glycolate Stearic acid Sucralose Titanium dioxide
NSAID	Ibuprofen	600	Carnauba wax Colloidal silicon dioxide Corn starch

			Croscarmellose sodium Hypromellose Microcrystalline cellulose Pharmaceutical ink Polydextrose PEG Pregelatinized starch Sodium Lauryl sulfate Stearic acid Titanium dioxide
Analgesic	Acetaminophen	650	Carnauba wax Colloidal silicon dioxide Croscarmellose sodium Hypromellose Magnesium stearate Maltodextrin Microcrystalline cellulose PEG Polysorbate 80 Povidone Pregelatinized starch Stearic acid Titanium dioxide
Analgesic / Cold Medication	Acetaminophen Phenylephrine HCl Chlorpheniramine Maleate	500 5 2	Carnauba wax Cellulose Citric acid Corn starch D&C yellow no. 10 aluminum lake FD&C blue no. 1 aluminum lake FD&C yellow no. 6 aluminum lake Hypromellose Iron oxide black Magnesium stearate Microcrystalline cellulose Polydextrose PEG Propylene glycol Sodium starch glycolate Titanium dioxide Triacetin
Allergy	Loratadine	10	Corn starch

			Magnesium stearate Lactose monohydrate
Allergy	Diphenhydramine HCl	25	Candelilla wax Colloidal silicon dioxide Crospovidone Hypromellose Microcrystalline cellulose PEG Povidone Pregelatinized starch Starch Stearic acid Titanium dioxide Talc
Analgesic / Cold Medication	Acetaminophen	500	Candelilla wax
	Pseudoephedrine HCl	30	Cellulose
	Diphenhydramine HCl	25	Corn starch Croscarmellose sodium Crospovidone FD&C blue no. 1 aluminum lake Hypromellose PEG Polysorbate 80 Povidone Silica Stearic acid Titanium dioxide Zinc stearate
Caffeine Tablet	Caffeine	200	Colloidal silicon dioxide Dicalcium phosphate dihydrate Magnesium stearate Microcrystalline cellulose

Table 4.8 Calibration models for the targeted drug list based on target ion MS/MS (1 – 1,000 ng/mL, 9 levels, 6 replicates, internal standard concentration at 100 ng/mL).

Compound	Internal Standard	y-int	slope	R <sup>2</sup>	Calibration Range (ng/mL)
4-ANPP	4-ANPP- <i>d</i> <sub>5</sub>	1.012×10 <sup>-2</sup>	1.011×10 <sup>-2</sup>	0.9959	1 – 1,000
4-Fluorobutyrylfentanyl	4-Fluorofentanyl- <i>d</i> <sub>3</sub>	2.136×10 <sup>-2</sup>	2.332×10 <sup>-2</sup>	0.9931	1 – 1,000
4-Fluoroisobutyrylfentanyl	Fentanyl- <i>d</i> <sub>5</sub>	2.162×10 <sup>-2</sup>	1.860×10 <sup>-2</sup>	0.9937	1 – 1,000
β-Hydroxythiofentanyl	Fentanyl- <i>d</i> <sub>5</sub>	1.037×10 <sup>-3</sup>	1.876×10 <sup>-3</sup>	0.9896	1 – 1,000
Acetylfentanyl	Acetyl fentanyl- <sup>13</sup> C <sub>6</sub>	2.066×10 <sup>-3</sup>	5.488×10 <sup>-3</sup>	0.9943	1 – 1,000
Acrylfentanyl	Acryl fentanyl- <i>d</i> <sub>5</sub>	- 2.705×10 <sup>-3</sup>	1.274×10 <sup>-2</sup>	0.9949	1 – 1,000
Alprazolam	Temazepam- <i>d</i> <sub>5</sub>	1.924×10 <sup>-2</sup>	7.080×10 <sup>-3</sup>	0.9737	10 – 1,000
Amphetamine	Amphetamine- <i>d</i> <sub>11</sub>	7.034×10 <sup>-2</sup>	1.261×10 <sup>-2</sup>	0.9871	1 – 1,000
Buprenorphine	Buprenorphine- <i>d</i> <sub>4</sub>	- 1.247×10 <sup>-2</sup>	1.044×10 <sup>-2</sup>	0.9514	25 – 1,000
Butyrylfentanyl	Fentanyl- <i>d</i> <sub>5</sub>	- 4.081×10 <sup>-3</sup>	2.528×10 <sup>-2</sup>	0.9969	1 – 1,000
Carfentanil	Carfentanil- <i>d</i> <sub>5</sub>	3.784×10 <sup>-3</sup>	1.112×10 <sup>-2</sup>	0.9973	1 – 1,000
Cocaine	Cocaine- <i>d</i> <sub>3</sub>	- 2.780×10 <sup>-3</sup>	1.189×10 <sup>-2</sup>	0.9954	1 – 1,000
Codeine	Codeine- <i>d</i> <sub>3</sub>	3.559×10 <sup>-2</sup>	8.075×10 <sup>-3</sup>	0.9445	1 – 1,000
Cyclopropylfentanyl	Furanyl fentanyl- <i>d</i> <sub>5</sub>	- 4.138×10 <sup>-3</sup>	1.343×10 <sup>-2</sup>	0.9925	1 – 1,000
Diazepam	Diazepam- <i>d</i> <sub>5</sub>	4.009×10 <sup>-2</sup>	9.119×10 <sup>-3</sup>	0.9928	1 – 1,000
Dihydrocodeine	Dihydrocodeine- <i>d</i> <sub>6</sub>	3.723×10 <sup>-2</sup>	1.061×10 <sup>-2</sup>	0.9864	10 – 1,000
Dimethylmethcathinone	Fentanyl- <i>d</i> <sub>5</sub>	- 1.191×10 <sup>-2</sup>	3.738×10 <sup>-3</sup>	0.9820	1 – 1,000
Ethylpentylone	Ethylpentylone- <i>d</i> <sub>5</sub>	1.514×10 <sup>-2</sup>	1.192×10 <sup>-2</sup>	0.9930	1 – 1,000
Etizolam	Zolpidem- <i>d</i> <sub>7</sub>	1.330×10 <sup>-3</sup>	1.408×10 <sup>-3</sup>	0.9691	1 – 1,000
Fentanyl	Fentanyl- <i>d</i> <sub>5</sub>	- 2.002×10 <sup>-2</sup>	1.234×10 <sup>-2</sup>	0.9969	1 – 1,000
Flunitrazepam	Temazepam- <i>d</i> <sub>5</sub>	2.669×10 <sup>-2</sup>	3.361×10 <sup>-3</sup>	0.9793	10 – 1,000
Furanylfentanyl	Furanyl fentanyl- <i>d</i> <sub>5</sub>	- 2.721×10 <sup>-3</sup>	1.264×10 <sup>-2</sup>	0.9958	1 – 1,000
Heroin	Heroin- <i>d</i> <sub>9</sub>	1.242×10 <sup>-1</sup>	1.272×10 <sup>-2</sup>	0.9853	10 – 1,000
Hydrocodone	Hydrocodone- <i>d</i> <sub>3</sub>	1.499×10 <sup>-1</sup>	6.655×10 <sup>-3</sup>	0.9728	25 – 1,000
Hydromorphone	Hydromorphone- <i>d</i> <sub>3</sub>	4.239×10 <sup>-2</sup>	1.188×10 <sup>-2</sup>	0.9332	1 – 1,000
Isobutyrylfentanyl	Fentanyl- <i>d</i> <sub>5</sub>	- 4.081×10 <sup>-2</sup>	2.528×10 <sup>-2</sup>	0.9969	1 – 1,000
Ketamine	Ketamine- <i>d</i> <sub>4</sub>	7.222×10 <sup>-3</sup>	1.708×10 <sup>-2</sup>	0.9932	1 – 1,000
MDA	MDEA- <i>d</i> <sub>5</sub>	1.550×10 <sup>-2</sup>	5.124×10 <sup>-4</sup>	0.9490	10 – 1,000
MDEA	MDEA- <i>d</i> <sub>5</sub>	- 1.776×10 <sup>-3</sup>	9.370×10 <sup>-3</sup>	0.9912	1 – 1,000
MDMA	MDMA- <i>d</i> <sub>5</sub>	5.510×10 <sup>-3</sup>	7.638×10 <sup>-3</sup>	0.9920	1 – 1,000
Meperidine	Meperidine- <i>d</i> <sub>4</sub>	6.573×10 <sup>-3</sup>	1.200×10 <sup>-2</sup>	0.9949	1 – 1,000
Methadone	Methadone- <i>d</i> <sub>9</sub>	- 1.937×10 <sup>-2</sup>	8.738×10 <sup>-3</sup>	0.9959	1 – 1,000
Methamphetamine	Methamphetamine- <i>d</i> <sub>11</sub>	5.263×10 <sup>-1</sup>	1.265×10 <sup>-2</sup>	0.9811	50 – 1,000
Methoxyacetylfentanyl	Fentanyl- <i>d</i> <sub>5</sub>	6.354×10 <sup>-4</sup>	9.780×10 <sup>-3</sup>	0.9958	1 – 1,000
Methylfentanyl	Fentanyl- <i>d</i> <sub>5</sub>	1.499×10 <sup>-2</sup>	8.103×10 <sup>-3</sup>	0.9920	1 – 1,000
Morphine	Heroin- <i>d</i> <sub>9</sub>	2.772×10 <sup>-1</sup>	7.578×10 <sup>-3</sup>	0.9579	25 – 1,000
MT-45	Fentanyl- <i>d</i> <sub>5</sub>	8.374×10 <sup>-3</sup>	8.449×10 <sup>-3</sup>	0.9907	1 – 1,000
Ocfentanil	Fentanyl- <i>d</i> <sub>5</sub>	1.098×10 <sup>-1</sup>	1.020×10 <sup>-2</sup>	0.9943	1 – 1,000
Oxazepam	Oxazepam- <i>d</i> <sub>5</sub>	3.406×10 <sup>-2</sup>	9.568×10 <sup>-3</sup>	0.9801	1 – 1,000
Oxycodone	Oxycodone- <i>d</i> <sub>9</sub>	4.274×10 <sup>-2</sup>	9.332×10 <sup>-3</sup>	0.9463	25 – 1,000

Oxymorphone	Oxymorphone- <i>d</i> <sub>3</sub>	6.890×10 <sup>-2</sup>	8.645×10 <sup>-3</sup>	0.9538	10 – 1,000
Phencyclidine	Phencyclidine- <i>d</i> <sub>5</sub>	9.481×10 <sup>-4</sup>	1.457×10 <sup>-2</sup>	0.9964	1 – 1,000
Remifentanil	Fentanyl- <i>d</i> <sub>5</sub>	1.477×10 <sup>-3</sup>	3.926×10 <sup>-3</sup>	0.9947	1 – 1,000
Sufentanil	Sufentanil- <i>d</i> <sub>5</sub>	4.559×10 <sup>-3</sup>	1.697×10 <sup>-2</sup>	0.9968	1 – 1,000
Temazepam	Temazepam- <i>d</i> <sub>5</sub>	4.107×10 <sup>-2</sup>	9.057×10 <sup>-3</sup>	0.9903	1 – 1,000
Tramadol	Fentanyl- <i>d</i> <sub>5</sub>	1.408×10 <sup>-3</sup>	2.673×10 <sup>-3</sup>	0.9907	1 – 1,000
U-47700	Fentanyl- <i>d</i> <sub>5</sub>	1.497×10 <sup>-4</sup>	8.232×10 <sup>-3</sup>	0.9951	1 – 1,000
Valerylentanyl	Fentanyl- <i>d</i> <sub>5</sub>	- 1.145×10 <sup>-3</sup>	1.184×10 <sup>-2</sup>	0.9950	1 – 1,000
Zolpidem	Zolpidem- <i>d</i> <sub>7</sub>	- 1.233×10 <sup>-3</sup>	1.646×10 <sup>-2</sup>	0.9951	1 – 1,000

Table 4.9 Limits of detection (LOD), lower limits of quantitation (LLOQ), and limits of reporting (LOR) for targeted drugs.

Compound	Limit of Detection (w/w%)	Lower Limit of Quantitation (w/w%)	Limit of Reporting (w/w%)
4-ANPP	0.015	0.047	0.25
4-Fluorobutyryl fentanyl	0.0039	0.012	0.25
Acetyl fentanyl	0.0077	0.023	0.25
Acryl fentanyl	0.0035	0.011	0.25
Alprazolam	0.11	0.33	0.05
Amphetamine	0.069	0.21	4
Buprenorphine	0.25	0.75	0.25
Butyryl Fentanyl	0.0060	0.018	0.25
Carfentanil	0.0089	0.027	0.025
Cocaine	0.0084	0.026	4
Codeine	0.097	0.29	0.5
Cyclopropyl fentanyl	0.0085	0.026	0.25
Diazepam	0.059	0.18	0.5
Dihydrocodeine	0.048	0.15	0.5
Dimethylmethcathinone	0.0089	0.027	4
Ethylpentylone	0.023	0.067	4
Etizolam	0.032	0.097	0.5
Fentanyl	0.0085	0.026	0.25
FIBF	0.0058	0.018	0.25
Flunitrazepam	0.14	0.44	0.05
Furanyl fentanyl	0.0050	0.015	0.75
Heroin	0.20	0.62	2.5
Hydrocodone	0.41	1.2	0.5
Hydromorphone	0.083	0.25	0.5
Hydroxythiofentanyl	0.011	0.034	0.25
Isobutyrylfentanyl	0.0060	0.018	0.25
Ketamine	0.011	0.033	0.5
MDA	0.30	0.92	4
MDEA	0.0040	0.012	4
MDMA	0.020	0.062	4
Meperidine	0.0096	0.029	0.5
Methadone	0.012	0.038	0.5
Methamphetamine	0.48	1.5	4
Methoxyacetylfentanyl	0.0052	0.016	0.25
Methylfentanyl	0.012	0.035	0.25
Morphine	0.34	1.0	4
MT-45	0.018	0.053	0.5
Ocfentanil	0.029	0.088	0.25
Oxazepam	0.074	0.23	0.5
Oxycodone	0.22	0.66	0.5
Oxymorphone	0.22	0.68	0.5

Phenylcyclidine	0.012	0.35	0.5
Remifentanil	0.014	0.041	0.025
Sufentanil	0.011	0.035	0.25
Temazepam	0.062	0.19	0.5
Tramadol	0.013	0.039	0.5
U-47700	0.0096	0.029	0.5
Valeryl fentanyl	0.0051	0.015	0.25
Zolpidem	0.0055	0.017	0.05

Table 4.10 Quantitative results (w/w%) and expected substance for all samples tested.

Expected Substance	Fentanyl (w/w%)	4-ANPP (w/w%)	Etizolam (w/w%)	Heroin (w/w%)	Methamphetamine (w/w%)	MDMA (w/w%)	Cocaine (w/w%)	Ketamine (w/w%)
Amphetamine					> 10			
Benzodiazepine								
Cocaine							> 10	
Cocaine							> 10	
Cocaine							> 10	
Cocaine							> 10	
Cocaine							> 10	
Cocaine							> 10	
Cocaine							> 10	
Cocaine							> 10	
Cocaine							> 10	
Cocaine							> 10	
Cocaine							> 10	
Fentanyl								
Fentanyl	5.6	6.7						
Fentanyl			2.8					
Fentanyl	0.50	0.65						
Fentanyl	> 10	> 10						
Fentanyl	5.5			> 10				
Fentanyl	0.44	0.45						
Fentanyl								
Fentanyl	> 10	> 10						
Fentanyl								
Fentanyl	> 10	6.72						
Fentanyl	0.53							
Fentanyl	2.2	1.5						
Fentanyl	3.3	2.9						
Fentanyl	3.1	2.3						
Fentanyl	0.65		1.3					
Fentanyl			8.3					
Fentanyl	8.2	7.7						
Fentanyl	> 10							
Fentanyl	> 10	> 10						
Fentanyl	> 10	1.2						
Fentanyl	> 10	> 10						
Fentanyl	4.8	> 10						
Fentanyl	2.6	1.5						
Fentanyl	3.0	2.1						





## 5 A Direct Mass Spectrometry Method for Cannabinoid Quantitation in Urine and Oral Fluid Utilizing Reactive Paper Spray Ionization

This chapter has been adapted from: Borden, S.A., Saatchi, A., Palaty, J. and Gill, C.G., 2022. A direct mass spectrometry method for cannabinoid quantitation in urine and oral fluid utilizing reactive paper spray ionization. *Analyst*, 147(13), pp.3109-3117. doi.org/10.1039/D2AN00743F with permission from The Royal Society of Chemistry.

### 5.1 Preface

S.A. Borden designed all experiments and generated all data with assistance from A. Saatchi. This project was supervised by C.G. Gill. All figures were produced by S.A. Borden. S.A. Borden drafted the manuscript with C.G. Gill, with intellectual and editorial contributions from all authors.

### 5.2 Abstract

A direct mass spectrometry method utilizing reactive paper spray ionization was developed for sensitive cannabinoid quantitation in biofluid matrices. The ca. 2-minute sample measurements used on-paper derivatization to significantly increase paper spray mass spectrometry (PS-MS) positive ion mode sensitivity while minimizing sample preparation steps. Calibrations demonstrate high linearity, with  $R^2 > 0.99$  for (-)-trans- $\Delta^9$ -tetrahydrocannabinol (THC) in oral fluid and 11-nor-9-carboxy- $\Delta^9$ -tetrahydrocannabinol (THC-COOH) in urine. The limit of detection and lower limit of quantitation were 0.78 and 10 ng/mL for THC in oral fluid and 1.3 and 10 ng/mL for THC-COOH in urine, respectively. THC-COOH levels measured by reactive PS-MS in seven spiked human urine samples showed bias of -9.4 to 5.9%, and percent difference values of -16.8 to 9.8% in comparison with a reference LC-MS method. Based upon the method simplicity, validation experiments, sensitivity, and rapidity, we conclude that reactive PS-MS has potential applications for rapid cannabinoid drug testing in urine and oral fluid.

### 5.3 Introduction

Drug testing for cannabis use is most often done by analyzing for THC in oral fluid or blood, and although at least eighteen acidic metabolites have been identified in urine, the analysis of the primary metabolite, 11-nor-9-carboxy- $\Delta^9$ -tetrahydrocannabinol (THC-COOH), and/or its glucuronide conjugate is the established protocol for drug testing in urine samples<sup>470, 471</sup>. The global drug testing market was valued at USD 8.1 billion in 2020, and cannabis/marijuana testing accounts for the largest revenue share of 25.9%<sup>471</sup>; this market is expected to grow as legalization/decriminalization spreads. Urine analysis is the most popular method of drug testing, with 40.8% of global revenue from the drug testing market generated from urine samples<sup>471</sup>. Oral fluid is an attractive testing sample because it can be non-invasively collected by non-medical personnel under direct observation, with minimal risk of adulteration or substitution<sup>472</sup>. However, THC

concentrations in oral fluid decrease fairly rapidly and can lead to false negatives if not sampled in an appropriate time frame (hours), and requires lower quantitation limits than analysis of THC-COOH in urine<sup>473</sup>. In 1988 the Federal Department of Health and Human Services (DHHS) issued mandatory testing guidelines for federal drug testing programs<sup>474</sup>. The guidelines stipulate that all positive results from initial screens must be confirmed by an alternative technique, and that urine would be the testing specimen of choice, though these have recently been updated to include oral fluid. These guidelines are mandatory for US federally regulated laboratories and have also been adopted by many private employers for workplace drug testing. An initial screening test that provides a positive result is always followed by a more stringent confirmatory test<sup>474</sup>. The DHHS 2017 guidelines stipulate that an initial screening test may be an immunoassay or another technology such as spectrometry, and that the confirmatory drug test must use mass spectrometric identification, though there is no explicit requirement for chromatographic separation. Still, chromatographic MS methods are considered the gold standard in forensic drug testing due in part to high sensitivity and selectivity<sup>475</sup>. Unfortunately for many confirmatory tests, extensive sample preparation steps and lengthy measurement times (typically 10-20 min<sup>476</sup>) are required for adequate analysis. Consequently, many laboratories have extensive sample backlogs of months or longer<sup>3</sup>. A potential alternative MS method with negligible sample preparation, rapid analysis (e.g., 1-2 min) and adequate sensitivity and selectivity, is paper spray mass spectrometry (PS-MS).

Paper spray is an ambient ionization, direct mass spectrometry technique first reported in 2010<sup>9</sup>. A triangular piece of filter paper is used as a sampling substrate for small amounts ( $\leq 10 \mu\text{L}$ ) of sample. For a PS-MS measurement, spray solvent and high voltage are applied to the paper to mobilize and ionize analytes from the dried sample spot in a mechanism similar to electrospray<sup>306</sup>. The PS-MS analysis of illicit drugs has been reported in the literature<sup>20, 315, 334, 477</sup>. Unfortunately, detection limits for direct THC or THC-COOH analysis with PS-MS tend to be high due to the poor ionization efficiency of cannabinoids. Some groups have increased sensitivity for cannabinoids with PS-MS, but at the cost of including undesirable reagents and/or additional sample preparation steps<sup>315, 478, 479</sup>. A less complex approach to increase sensitivity for cannabinoid measurements by PS-MS in biofluid samples could be the use of 'on-paper' derivatization (reactive paper spray mass spectrometry). In reactive PS-MS, small volumes (e.g.,  $10 \mu\text{L}$ ) of reagents and samples are deposited on paper spray substrates to achieve favourable chemical reactions or study reaction conditions<sup>480-482</sup>. The evaporative preconcentration of reagents on the paper substrate can even facilitate faster reactions than observed in bulk solution-phase reactions<sup>480</sup>. The coupling of reactive paper spray with mass spectrometry allows for the direct, quantitative analysis of analytes without additional sample handling. For this study, we employed an azo-coupling based derivatization reagent previously reported as a solution phase sample preparation procedure for LC-MS based cannabinoid measurements in breath and serum samples<sup>483, 484</sup>. Presented is a rapid, validated, high throughput analytical approach for the direct mass spectrometry quantitation of cannabinoids in urine and oral fluid sample matrices.

## 5.4 Experimental

### 5.4.1 Materials and Reagents

Analytical reference standards (-)-trans- $\Delta^9$ -tetrahydrocannabinol (THC), 11-nor-9-carboxy- $\Delta^9$ -tetrahydrocannabinol (THC-COOH), cannabidiol (CBD), cannabinol (CBN) and their associated isotopically labeled standards (THC- $d_3$ , THC-COOH- $d_3$ , CBD- $d_3$ , and CBN- $d_3$ ) were obtained from Cayman Chemical (Ann Arbor, MI, USA). ACS grade 5-chloro-2-methoxybenzenediazonium chloride hemi (zinc chloride) salt (Fast Red RC) was acquired from Sigma Aldrich (St. Louis, MI, USA). OmniPur grade bovine serum albumin (BSA) was purchased from Millipore Sigma (Burlington, MA, USA). Optima HPLC grade acetonitrile, methanol, water, and formic acid, and ACS grade ammonium acetate was obtained from Fisher Scientific (Ottawa, ON, Canada). Deionized (DI) water was prepared using a water purification system (18.4 M $\Omega$ -cm Facility Scale Reverse Osmosis/Ion Exchange Water Purification System; Applied Membranes Inc, Vista, CA, USA). VeriSpray™ sample plates for PS-MS measurements were obtained from Thermo Fisher Scientific (San Jose, CA, USA). Blank human urine and oral fluid was provided by a healthy, anonymous volunteer.

### 5.4.2 Standard and Sample Preparation

Standards were prepared volumetrically in methanol from analytical reference standards. All calibration curves used triplicate measurements with 7-8 levels (2, 5, 10, 20, 40, 100, 250 and 500 ng/mL). Biofluid standards and samples (urine and oral fluid) were spiked with analyte and internal standards and subsequently diluted with methanol to a 70/30 biofluid/methanol v/v% ratio.

### 5.4.3 Mass Spectrometry

All analyses were done by PS-MS/MS in positive-ion mode using a TSQ Fortis™ triple quadrupole tandem mass spectrometer and a VeriSpray™ paper spray ion source (Thermo Fisher Scientific, San Jose, CA, USA). The PS-MS system employed utilizes sample plates containing 24 individual sample strips, and a robotic system that accommodates 10 plates, allowing for the multiplexed, high-throughput automated (unattended) PS-MS measurement of 240 samples at a time. Direct infusion electrospray ionization was used to optimize MS/MS parameters during method development. Argon was used as collision gas at a pressure of 2.0 mTorr. Sheath, auxiliary, and sweep gas were set to zero for all measurements. Additional PS-MS parameters are given in the supplementary information (Table 5.3-6.7).

### 5.4.4 Reactive Paper Spray Mass Spectrometry

Cannabinoids were derivatized directly on the PS sample strips with pre-deposited Fast Red RC derivatization reagent. The schematic workflow for reactive PS-MS experiments is outlined in Figure 5.1.

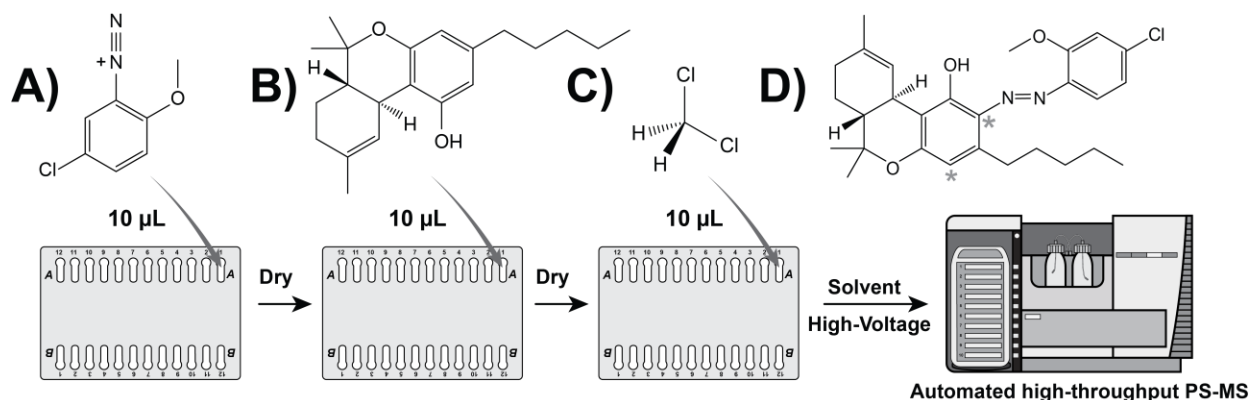


Figure 5.1 Workflow for reactive paper spray mass spectrometry measurements. **A)** 10  $\mu\text{L}$  aliquot of 1.5 mM Fast Red RC in 5.0 mM ammonium acetate (aq), **B)** 10  $\mu\text{L}$  aliquot of cannabinoid standard or biofluid sample with spiked internal standard **C)** two 10- $\mu\text{L}$  aliquots of dichloromethane, and **D)** automated, high-throughput PS-MS analysis of derivatized cannabinoids. \*Derivatization can occur either ortho or para to the hydroxyl group <sup>484</sup>.

For each measurement, 10  $\mu\text{L}$  of the Fast Red RC solution (1.5 mM in aqueous 5.0 mM ammonium acetate) was deposited onto a PS-MS strip and air dried (ca. 20 min), followed by 10  $\mu\text{L}$  of sample (containing internal standard) and another drying step. For urine and oral fluid samples, two 10  $\mu\text{L}$  aliquots of dichloromethane were spotted on top of the deposited samples before measurement. We note that the dichloromethane evaporates rapidly and was not visibly present when the samples were measured. Acetonitrile with 0.1% formic acid was used as the PS-MS spray solvent (0.88 min solvent dispense, Table 5.6) and +4.0 kV was applied to the paper for reactive PS-MS/MS analysis over a 1.2 min instrumental scan method.

#### 5.4.5 Data Analysis

Integrated signal areas of PS-MS/MS signal chronograms were recorded (TraceFinder Clinical 4.1 SP5 software, Thermo Fisher Scientific, San Jose, CA, USA) without smoothing (example signal chronograms are given in Figure 5.6). Calibration curves were produced using the ratio of the quantifier ion analyte signal area to the corresponding quantifier ion internal standard signal area (MS/MS transitions are given in Table 5.4 and Table 5.5). Ion ratios were determined as the quantifier ion analyte signal area to first quantifier ion analyte signal area ratio. Signals were collected for 1.2 minutes for all measurements, with minimum triplicate measurements for all standards and samples. Uncertainties are given as the standard deviation of replicate measurements.

#### 5.4.6 Method Validation

The Scientific Working Group for Forensic Toxicology (SWGTOX) 2013 guidelines served as the basis for method validation experiments. Accuracy (% bias), within-run precision (% CV) and between-run precision (% CV) were determined for THC-COOH in human urine by analyzing 6 replicates of low (15 ng/mL), medium (205 ng/mL), and high (400 ng/mL) quality control (QC) samples across 6 runs <sup>19</sup>. The within-run % CV is reported as

the highest value observed across the 6 runs. The limit of detection (LOD) was calculated as 3.3 times the standard deviation of the lowest calibrator divided by the slope of the calibration curve. The lower limit of quantitation (LLOQ) was defined as the lowest calibrator that meets the stringent acceptance criteria: intra-assay % CV < 15, % bias within  $\pm 20\%$ , ion ratio within  $\pm 20\%$ , and a S/N > 4.

#### 5.4.7 Liquid Chromatography Mass Spectrometry

To further validate the method, blank human urine samples were fortified with THC-COOH and THC-COOH- $d_3$  in the laboratory and were sent to an accredited clinical testing facility (LifeLabs, Burnaby, BC, Canada) for confirmatory measurements. For LC-MS analysis, urine samples were prepared by hydrolysis for 30 minutes at 50°C with recombinant glucuronidase (BG Turbo, Kura Biotech, Rancho Dominguez, CA, USA) followed by solid phase extraction on mixed-mode HP-SCX 5 mg/1 mL C18 cartridges (Tecan, Männedorf, Switzerland). Measurements for cannabinoids were performed using reverse-phase chromatography on a 50 mm  $\times$  2.1 mm biphenyl column (Phenomenex, Torrance, CA, USA) followed by negative ionization mode LC-MS/MS acquisition on two MRM channels (quantifier and qualifier) and a 6-point calibration curve. These urine samples were analyzed by reactive PS-MS on the same day as the LC-MS analysis to minimize potential differences due to sample degradation.

### 5.5 Results and Discussion

#### 5.5.1 Cannabinoid Standard Analysis

Cannabinoid analyses face several analytical challenges, one of which is the low ionization efficiency observed with 'soft' ionization techniques (e.g., electrospray, paper spray) <sup>485</sup>. To illustrate this, PS-MS calibration curves obtained for methanolic THC and THC-COOH standards (2-500 ng/mL) demonstrate poor analytical performance, including inferior LOD, LLOQ and precision metrics (Table 5.8). Poor performance was observed for both THC and THC-COOH with a LLOQ of 250 ng/mL for both compounds. Inferior calibration correlation was also observed, with  $R^2=0.902$  for THC and 0.971 with THC-COOH. Because of their poor analytical performance, there are few examples of cannabinoid analysis in the PS-MS literature. Some groups have managed to make improvements by taking additional steps. Espy et al. showed that the use of methanol with 25 mM of sulfuric acid as spray solvent could increase THC sensitivity in blood by 50-fold <sup>315</sup>. However, sulfuric acid however is well known for its potential to cause severe corrosion of the instrumentation inlet and hardware and is therefore not a desirable solution for THC analysis <sup>486</sup>. Silver-impregnated paper has been used for THC and CBD analysis in edible oils, but at high concentrations (e.g., 200 ng/mL), and it is unclear whether this technique could be applied to biofluid matrices <sup>479</sup>. Others used sesame oil to successfully preconcentrate analytes from larger sample volumes (50  $\mu$ L) prior to analysis <sup>478</sup>. However, the technique involved manual cutting of paper strips after preconcentration/extraction and could not be successfully automated for THC-COOH measurements. As an alternative, we investigated and present the use of a simple reactive PS-MS method with suitable analytical performance and sensitivity for

quantitative and high-throughput cannabinoid measurements in urine and oral fluid sample matrices.

### 5.5.2 Reactive Paper Spray Mass Spectrometry

The poor analytical sensitivity and precision observed for direct, underivatized THC and THC-COOH measurement by PS-MS (Table 5.8) are insufficient for even screening tests (Table 5.10). To address this, we explored on-paper derivatization (reactive PS-MS) using an azo-coupling derivatization reagent (Fast Red RC). The conversion to an azo compound improves cannabinoid ionization through the introduction of a strongly basic functional group. With this reagent, derivatization occurs at electron-rich sites in electrophilic aromatic substitution reactions. For cannabinoids, reaction at the ortho- and para- positions of the phenol are favoured (Figure 5.1). and both regioisomers are produced <sup>484</sup>. The Fast Red RC derivatization of cannabinoids has been previously reported for solution phase derivatization followed by LC-MS analysis for cannabinoids in breath and serum samples <sup>483, 484</sup>, but to the best of our knowledge, it has not been reported as an on-paper reaction strategy, or for cannabinoid measurements in urine or oral fluid samples. Some benefits of utilizing reactive PS-MS are that the reaction occurs very rapidly, with small sample and reagent volumes (10  $\mu$ L), at ambient temperatures and pressures, and directly on the sampling strip. This minimizes sample handling/transfers, simplifying the measurement, and eliminates sample-to-sample carry over interferences.

In the absence of available derivatized cannabinoid reference standards, it is difficult to accurately evaluate the overall on-paper derivatization reaction efficiency. The absence of a concentration-dependent increase in underivatized THC signal across a calibration series using methanolic standards for reactive PS-MS with Fast Red RC derivatization reagent suggests that the reaction is virtually complete (Figure 5.2A). The derivatization occurs in minutes under ambient conditions during the drying step after a sample is spotted on the paper substrate containing the dried reagent. In contrast, the signal for derivatized THC observed in Figure 5.2B steadily increases with amount of THC deposited. Even at 5 ng/mL, the derivatized signal ( $4.0 \times 10^4$ ) is easily distinguished from blank measurements and is outside of the blank signal intensity  $\pm 10$  standard deviations ( $1.7 \pm 1.6 \times 10^4$ ). The calibration curve obtained with the data presented in Figure 5.2B exhibits excellent correlation ( $R^2 = 0.997$ ) and a LLOQ of 10 ng/mL (Table 5.9).

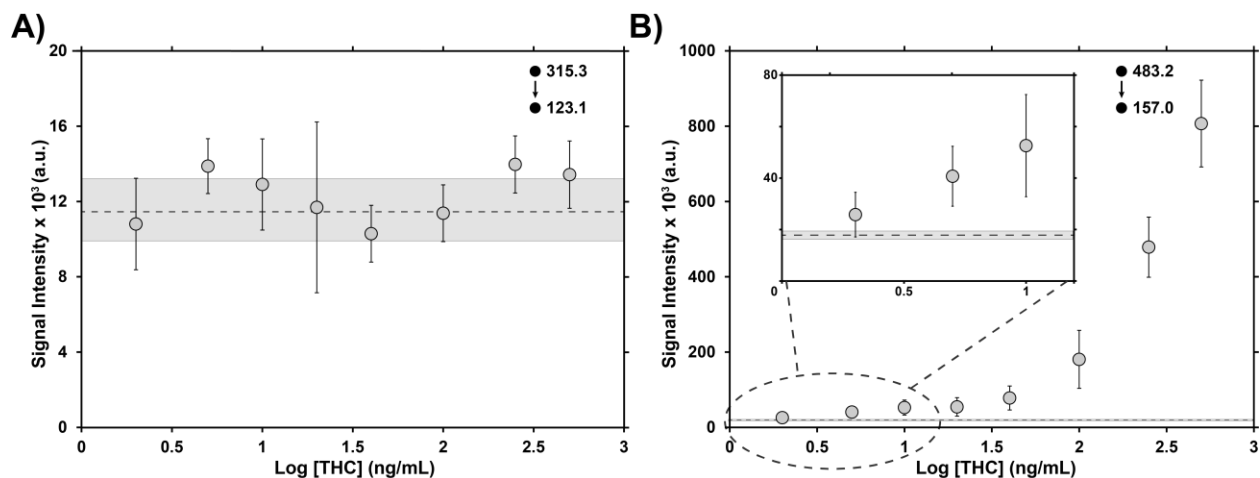


Figure 5.2 Reactive PS-MS signal intensities for A) residual, underivatized THC and B) derivatized THC, obtained for a methanolic calibration of THC (2 – 500 ng/mL) with 10  $\mu$ L of derivatization solution pre-spotted on the paper substrate. Dashed lines indicate the average ( $n = 6$ ) signal intensity observed for blank measurements, with the shaded bar displaying the measurement standard deviation. Logarithmic X-axis for visual clarity.

Data from the calibrations of THC and THC-COOH with and without derivatization were used to estimate LOD and LLOQ values (Table 5.1). Relatively high LODs for THC and THC-COOH were observed in methanol without derivatization, with underivatized LLOQ values of 250 ng/mL for both compounds. Significant analytical improvements were observed using the presented reactive PS-MS strategy; the LOD for derivatized THC and THC-COOH in methanol was significantly reduced (Table 5.1) and an LLOQ of 10 ng/mL was achieved for both analytes. This study focused on THC and THC-COOH analysis, but the reactive PS-MS method yields similar performance gains for other cannabinoids, including cannabidiol (CBD), and cannabinol (CBN), evidenced by their methanolic calibrations ( $R^2 = 0.990$  and  $0.999$ , respectively) and 10 ng/mL LLOQ values (Table 5.9). The derivatization chemistry is likely applicable to other cannabinoids since they share similar structures, with either ortho- and/or para- positions exposed on the phenolic ring. As a next step, the presented reactive PS-MS derivatization methodology was evaluated for the direct analysis of cannabinoids in urine and oral fluid sample matrices.

Table 5.1 Comparison of LOD and LLOQ values derivatized and underivatized cannabinoids in biofluids and methanol.

Analyte	Sample Matrix	LOD <sup>a</sup> (ng/mL)	LLOQ <sup>b</sup> (ng/mL)
Derivatized			
THC	Oral Fluid	0.78	10
THC-COOH	Urine	1.3	10
THC	Methanol	1.6	10
THC-COOH	Methanol	1.4	10
Underivatized			
THC	Methanol	25.2	250
THC-COOH	Methanol	47.4	250

<sup>a</sup> LOD defined as  $3.3 \times$  standard deviation of lowest calibrator / slope

<sup>b</sup> LLOQ defined as the lowest calibrator that meets the acceptance criteria: intra-assay %CV < 15, bias within  $\pm 20\%$ , ion ratio within  $\pm 20\%$ , and S/N > 4

### 5.5.3 Biofluid Quantitation

Within the context of drug testing, THC-COOH analysis in urine, and THC analysis in oral fluid are two of the most commonly ordered tests <sup>471</sup>. Although there are no universal regulations governing drug testing strategies, global standard practices typically include an initial screening test (usually immunoassay) followed by a more stringent confirmatory test (mass spectrometric detection, most often with chromatographic separation). However, reporting cut-offs vary across jurisdictions, as shown in Table 5.10. For example, the Substance Abuse and Mental Health Services Administration (SAMHSA) in the United States guidelines for mandatory workplace drug testing of federally regulated employees uses a urine THC-COOH screening cut-off of 50 ng/mL with a confirmatory cut-off of 15 ng/mL <sup>474</sup>. For THC in oral fluid, a 4 ng/mL cut-off is recommended for screening with 2 ng/mL for confirmation. Generally, cut-off values in Canada, Europe and Australia are higher than those recommended by SAMHSA (Table 5.10). It was with these levels in mind that reactive PS-MS/MS was evaluated for biofluid screening and/or confirmatory drug testing applications.

As a next step, reactive PS-MS was evaluated for the direct analyses of cannabinoids in urine and oral fluid samples. When directly analyzing these biofluids, we used a PS-MS spray solvent of 90/9.9/0.1% acetonitrile/water/formic acid (v/v%) in initial tests but observed abnormally high spray PS-MS currents ( $> 5 \mu\text{A}$ ), leading to erratic signal chromatograms from spray instability (Figure 5.6A). Some sensitivity improvement was achieved through a slight dilution of the biofluid samples with methanol (70/30 biofluid/methanol v/v%) and the use of 90/10/0.1 acetonitrile/water/formic acid as the spray solvent (Figure 5.6B). Ultimately, slight dilution paired with using acetonitrile with 0.1% formic acid (no water) as a spray solvent corrected this problem, achieving stable signals with spray current values of ca.  $0.2 \mu\text{A}$ .

Reactive PS-MS analysis of THC-COOH in urine samples initially yielded abnormally low signal levels, even after dilution and spray solvent adjustment achieved stable sprays. We hypothesized that this was due to cannabinoids associating with a component in the urine matrix<sup>487</sup>, rather than ionization suppression, since our previous PS-MS urine analysis of other drugs and metabolites with the same dilution scheme demonstrated no such issues<sup>488</sup>. A simple acetonitrile protein precipitation for urine samples produced higher intensity signals, but the sample dilution required for this step (1:4) significantly reduced analytical sensitivity, and this additional solution phase sample preparation step added additional sample handling/transfer steps. To evaluate the potential influence of matrix protein levels on THC-COOH analysis, 0.14  $\mu\text{g/mL}$  bovine serum albumin (BSA) was added to protein-free artificial urine samples (Table 5.11) spiked with THC-COOH. Negligible signals for THC-COOH were observed for these BSA spiked samples (Figure 5.8A), further suggesting that urine protein content could be contributing to the inferior analytical performance. To avoid sample dilution and additional preparation/sample transfer steps, an alternative was required. We found that the simple addition of 2 aliquots of 10- $\mu\text{L}$  of dichloromethane (DCM) on top of the dried sample spot yielded significant increases in the derivatized THC-COOH signals (Figure 5.6C), without any additional steps such as protein precipitation. Figure 5.3A illustrates the raw signal intensities for 200 ng/mL of derivatized THC-COOH- $d_3$  obtained from calibrations with and without the use of the simple DCM spotting. Figure 5.3B shows the corresponding boxplot. On average signal intensities were increased 7.8-fold. It should be noted that all PS-MS measurements use area ratios of the analyte to internal standard signals and the observed signal area variability, typical of all PS-MS measurements, does not hinder quantitation.

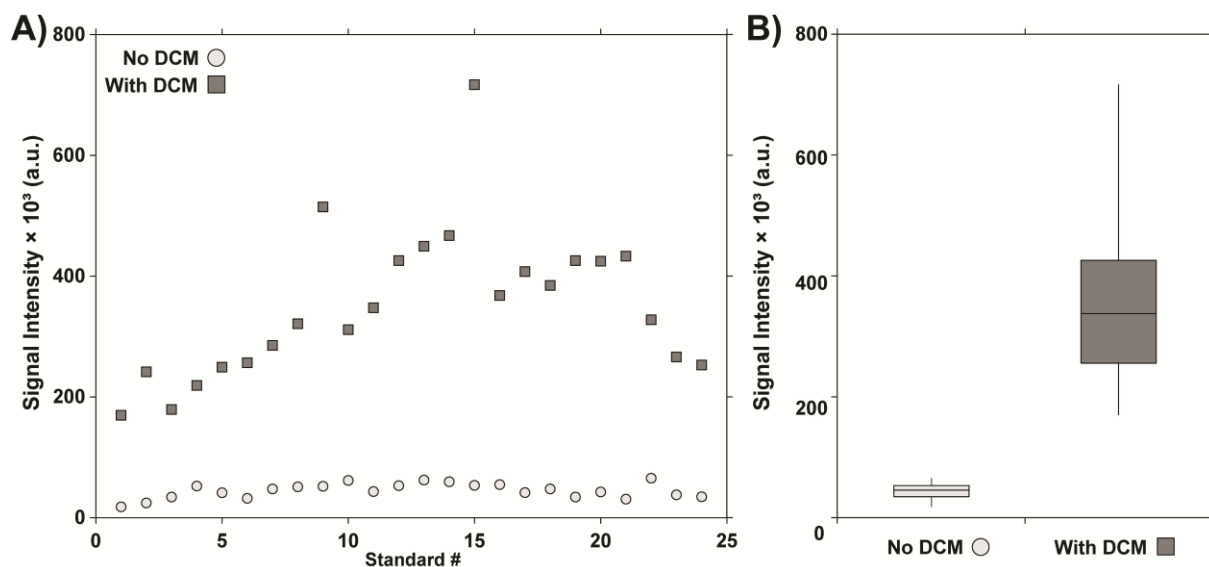


Figure 5.3 A) Reactive PS-MS signal intensities obtained for 200 ng/mL derivatized THC-COOH- $d_3$  in prepared blank human urine with two aliquots of DCM spotted on dried urine spot and with no DCM spotted and B) a boxplot of the signal intensities with and without DCM.

While the mechanism of the observed signal increase with the DCM addition is unclear, we hypothesize that the sensitivity increase is due to either disrupted protein binding<sup>489</sup> and/or an increased solubility of THC-COOH in the DCM, mobilizing it out of the matrix components. In any case, this method also avoids additional sample preparation or solution phase handling/transfer steps, especially important for the analysis of THC-COOH in urine, since large amounts can be lost during storage, handling, or pipetting<sup>490</sup>.

The minor dilution of biofluids, absence of water in the spray solvent, and use of DCM on dried biofluid sample spots improved robustness and sensitivity, such that LOD and LLOQ values obtained were similar to those observed for methanolic standards (Table 5.1). Reactive PS-MS calibrations for THC in oral fluid and THC-COOH in urine utilizing this approach generated  $R^2$  values of 0.996 and 0.998, respectively, across 3+ orders of magnitude (Figure 5.4).

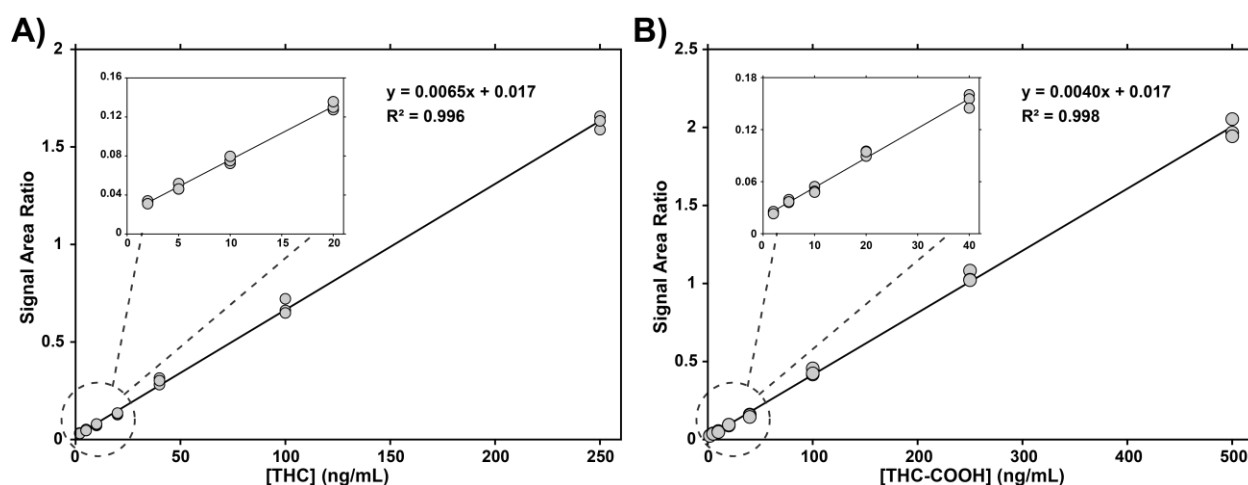


Figure 5.4 Reactive PS-MS calibrations ( $n = 3$  replicates) of A) derivatized THC in human oral fluid (2-250 ng/mL) and B) derivatized THC-COOH in human urine (2-500 ng/mL)

Using these calibrations, an LLOQ of 10 ng/mL was achieved for both THC in oral fluid and THC-COOH in urine with LODs of 0.78 and 1.3 ng/mL, respectively. Therefore, the reactive PS-MS method meets confirmatory cut-off requirements for urine analysis but may not be adequate for oral fluid, depending on the guidelines used (Table 5.10). While the presented reactive PS-MS/MS method can identify THC in oral fluid with a low LOD, it is important to note that it is not currently able to differentiate THC from CBD since the MS/MS mass spectra of these two compounds are nearly identical, even when derivatized (Figure 5.7). In a very recent publication, the rapid differentiation of cannabinoid isobar sets (including THC/CBD) was demonstrated using ion mobility for (high concentration) cannabis products<sup>491</sup>. Coupled with reactive PS-MS, this could provide a route to further improving direct mass spectrometry THC measurements in biofluids. Routine cannabinoid drug testing of biofluids in a clinical setting requires reliable, high-throughput analytical strategies. The automated system utilized for this work was purposely designed to address this need, allowing for the unattended measurement of up to 240 samples per

batch. The plates are designed with 96-well plate dimensions and can easily be interfaced with liquid handling systems for simplified clinical automation.

In order to decouple the reagent deposition step from the analytical procedure for further workflow simplification, we evaluated the stability of 'pre-spotted' derivatization reagent on the PS-MS paper strips. The reagent was spotted on PS-MS strips and allowed to dry at ambient temperatures in air. Urine samples spiked with THC-COOH were then spotted on these prepared strips at periodic intervals (then analyzed) over the next 24 hours. Figure 5.9 demonstrates that the measured amount of THC-COOH remains stable and demonstrates acceptable bias over 24 hours. Furthermore, raw signal intensities are also maintained, indicating no loss in sensitivity (Figure 5.10). It was found that rapid drying of PS-MS sample strips at 60°C in an oven (1.5 mins) during both the reagent and urine deposition steps did not significantly affect analytical results (Figure 5.11). This illustrates that PS-MS strips could be prepared in advance of measurements, and sample drying times can be accelerated, further increasing the speed of analysis.

#### 5.5.4 Validation and Comparison to LC-MS/MS

To assess whether reactive PS-MS/MS could be a candidate method for drug testing applications, validation experiments were done according to the Scientific Working Group for Forensic Toxicology (SWGTOX) 2013 Guidelines for standard practices for method validation in forensic toxicology<sup>19</sup>. Validation experiments were done for THC-COOH measurements in urine. The bias and precision of the method was evaluated by preparing three quality control (QC) standards prepared in pooled fortified blank human urine at three concentration levels: low (15 ng/mL), medium (205 ng/mL), and high (400 ng/mL). QC data was obtained for 6 replicate analyses daily over 6 days and is summarized in Table 5.2.

Table 5.2 Quality control data for THC-COOH in prepared fortified human urine (diluted to 70/30 urine/methanol) using reactive PS-MS/MS. Data from 6 replicates daily for 6 days.

Urine QC level	Concentration (ng/mL)	%Bias	Within-run precision (%CV) <sup>a</sup>	Between-run precision (%CV)
Low	15	-6.2	14.7	11.0
Medium	205	12.2	6.1	5.4
High	400	-5.9	8.4	5.7

<sup>a</sup> The reported within-run precision (%CV) is the highest %CV value observed from the 6 runs.

The SWGTOX guidelines stipulate that acceptable within-run and between-run precision is < 20 %CV and that the maximum acceptable bias is  $\pm 20\%$  at each concentration. All QC levels passed these criteria. Data from the low QC which was prepared at the confirmatory testing cut-off of 15 ng/mL showed an average bias of -6.15%, within-run %CV of 14.7, and a between-run %CV of 11.0, indicating acceptable performance even at the confirmatory testing cut-off. Similar performance metrics were observed for the medium and high QC samples.

To further evaluate reactive PS-MS/MS suitability for urine drug testing, results were directly compared to LC-MS/MS results from a clinical testing facility (Table 5.12). A pool of blank urine was spiked with varying concentrations of THC-COOH (15, 25, 50, 50, 50, 125 and 300 ng/mL) and internal standard (200 ng/mL), then analyzed by reactive PS-MS, as well as being sent to a clinical testing facility for parallel LC-MS analysis. Samples were analyzed by both PS-MS and LC-MS at the same time, one day after being prepared. A Bland-Altman relative difference plot was used to assess the performance of the reactive PS-MS method (Figure 5.5). The measured value from validated LC-MS measurement at the clinical testing facility was considered the true value for these comparisons. Relative difference measurements were within  $\pm 1.96$  standard deviations (95% confidence interval) of the mean for 44 of 46 (95.6%) reactive PS-MS measurements. The mean relative difference between reactive PS-MS and LC-MS measurements was 2.29%, indicating a slight positive bias on reactive PS-MS measurements. A notable negative bias was observed for PS-MS for the 300 ng/mL urine sample. All PS-MS measurements at the cut-off value (15 ng/mL) were within  $\pm 20\%$  of the LC-MS measurement.

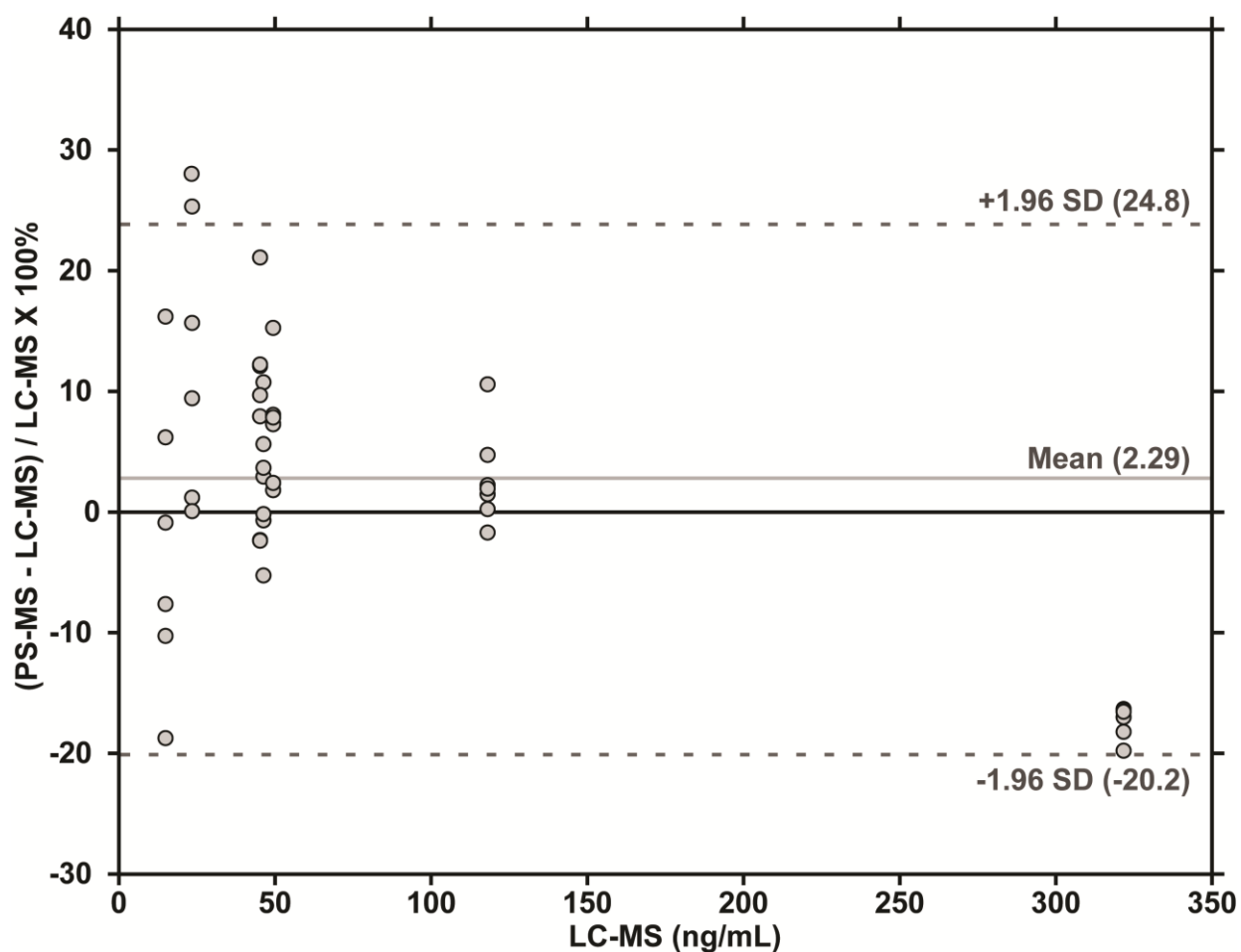


Figure 5.5 Bland-Altman relative difference plot of reactive PS-MS and LC-MS THC-COOH measurements from fortified blank human urine samples.

PS-MS results for each sample were averaged for 6-7 replicates, and the %CV ranged from 2.59% - 12.8%. The quantifier to qualifier ion ratio was used as an additional metric for validation. The target ion ratio was determined to be 0.661 from the calibration of derivatized THC-COOH in urine, and a standard  $\pm 20\%$  was used for an acceptable ion ratio range of 0.529-0.793. All reactive PS-MS results fell within this ion ratio range (Table 5.12) suggesting that potential interferences could be effectively screened for via ion ratios. PS-MS analysis demonstrated acceptable accuracy, with bias values ranging from -9.40 to 8.73%. LC-MS analysis returned similar bias values ranging from -9.62 to 7.22%. The difference between the methods ranged from -16.8 to 14.6%. The quality control data paired with the comparison to validated LC-MS results demonstrates that reactive PS-MS/MS can be used for accurate and precise quantitation of THC-COOH in urine. As was also observed during our experiments, the robust nature of PS-MS allows for reduced instrument downtime for cleaning, comparing well with the work of others, who demonstrated that PS-MS maintains sensitivity, accuracy, and precision over 240 consecutive blood samples without cleaning or downtime, and a simple wipe of the ion MS inlet allowed for another 240 consecutive samples<sup>492</sup>. PS-MS maintains this instrument cleanliness because of the small sample volumes tested, and because many matrix components are retained by the paper substrate<sup>312</sup>. Further benefits of the reactive PS-MS method compared to LC-MS demonstrated by this study include the ease of full automation, higher throughput, less liquid sample handling/transfers and preparation, and a reduced overall analytical complexity.

## 5.6 Future Work

Although the presented method shows significantly improved analytical performance for the measurement of THC and THC-COOH by PS-MS, two challenges will be addressed in future studies. Firstly, the method currently does not account for any THC-COOH bound as a glucuronide in urine, and therefore could underestimate the amount of THC-COOH present. Most often, hydrolysis by recombinant glucuronidase is used to prepare samples for LC-MS, cleaving the glucuronide, and the total amount of THC-COOH (bound and unbound) is then measured. Although reactive PS-MS could be applied to these prepared samples to measure total THC-COOH levels, the additional sample preparation steps add time, costs, and complexity, at odds with the goal of developing a rapid, lower cost method with minimal sample preparation. An alternative approach that has shown promise without the need for additional preparation steps is the use of in-source glucuronide fragmentation<sup>493</sup>. Preliminary results from our group indicate that the THC-COOH glucuronide can be effectively fragmented in-source, even after the glucuronide conjugate has been derivatized (Figure 5.12). When the MS has the source fragmentation voltage set to zero, the derivatized THC-COOH glucuronide remains intact (Figure 5.12A). By increasing the source fragmentation to 100 V, a neutral loss of 176 Da is observed for the  $[M+H]^+$ ,  $[M+Na]^+$ , and  $[M+2Na-H]^+$  ions (Figure 5.12B), indicative of glucuronide cleavage. As a screening tool, PS-MS offers potential advantages over widely used immunoassay methods, which are either lateral flow point-of-care (POC) devices or lab-based assays run on a clinical chemistry analyzer. PS-MS offers at least

semi-quantitative results (unlike POC) and, in theory, does not require the aliquoting and refrigerated shipping of fluid samples to a clinical lab, as the sample may be applied directly to the PS-MS sample strips at the collection site.

The techniques outlined above offer the potential for a rapid and robust urine drug testing method requiring minimal sample preparation that can quantify total THC-COOH levels in urine sample matrices. However, isobar differentiation between THC and CBD still needs to be addressed to avoid potential interferences. Coupling the use of ion mobility strategies may also allow for the direct resolution of cannabinoid isobars<sup>491</sup>. While the derivatization employed in this reactive PS-MS method does not produce differentiable MS/MS spectra for THC and CBD (Figure 5.7) and interference is observed, other derivatization agents may also have the potential to solve this issue. Both THC and CBD have phenolic OH groups at C1 which is a good target for derivatization. The additional phenolic OH at C3 on CBD may allow for a di-derivatization strategy. For example, the use of dabsyl chloride in LC-MS/MS has been shown to both increase ionization efficiency and to produce di-derivatized CBD which can be easily differentiated from the mono-derivatized THC even prior to MS/MS<sup>494</sup>. Other groups have shown that forming metal ion adducts can be used to differentiate between THC and CBD by MS/MS, a strategy that could be used on derivatized products<sup>479</sup>.

## 5.7 Conclusion

Reactive PS-MS using an azo-coupling derivatization on paper sample strips demonstrates promising potential for the high sensitivity, quantitative analysis of THC in oral fluid and THC-COOH in urine. The presented method requires minimal sample preparation, small sample volumes (10  $\mu$ L), generates quantitative results in 2 minutes, and can be easily multiplexed to meet high throughput clinical needs. The method was validated for precision and accuracy according to SWGTOX guidelines. Precision, accuracy, sensitivity, and comparison with LC-MS studies all indicated that the presented reactive PS-MS method could be used for both screening and confirmatory analysis of THC-COOH in urine and has potential utility for screening THC in oral fluid as well. We envision that this reactive PS-MS methodology in a clinical or forensic setting could be applied as a confirmatory test to process high-level samples far above the cut-off value, with lower-concentration samples being confirmed by more conventional chromatographic methods. Although the method has shown acceptable analytical performance at or near cut-off levels, chromatographic methods may remain more legally defensible at this time. However, reactive PS-MS has the potential to drastically reduce laboratory backlogs, since the majority of positive samples are far above the cut-off values and may not require chromatography for defensible results. This research illustrates the advantages of the use of on paper derivatization reagents for improving the PS-MS analysis of analytes exhibiting poor ionization efficiency and presents a potential alternative for biofluid cannabinoid drug testing in clinical laboratories.

## 5.8 Supporting Information

Table 5.3 Paper spray mass spectrometry analyte-independent parameters.

Parameter	Value
Ionization polarity	Positive
Spray voltage (V)	4000
Q1 FWHM resolution	0.7
Q3 FWHM resolution	1.2
Dwell time (ms)	26.3
Cycle time (sec)	1
Data points per peak	60
Argon CID gas pressure (mTorr)	2
Sweep gas (Arb)	0
Ion transfer tube (°C)	300

Table 5.4 Mass-dependent selected reaction monitoring (SRM) transition parameters of underivatized cannabinoids and isotopically labelled internal standards. The first ion listed is the quantifier ion, and the reported ion ratio is between the first and second ions listed.

Compound	Precursor Ion ( <i>m/z</i> )	Product Ion ( <i>m/z</i> )	Tube Lens (V)	Collision Energy (eV)	Source Fragmentation (V)
THC	315.3	123.1	107	32.30	10.0
	315.3	193.1	107	22.99	10.0
THC- <i>d</i> <sub>3</sub>	318.3	123.1	107	32.67	10.0
THC-COOH	345.2	299.2	128	19.90	33.0
	345.2	304.1	128	8.96	33.0
THC-COOH- <i>d</i> <sub>3</sub>	348.2	302.2	126	20.04	33.0
CBD	315.2	193.1	154	22.06	27.8
	315.2	283.2	154	5.29	27.8
CBD- <i>d</i> <sub>9</sub>	324.3	123.1	148	33.14	34.3
CBN	311.2	55.1	125	19.24	0
	311.2	87.2	125	11.70	0
CBN- <i>d</i> <sub>3</sub>	314.3	195.1	159	26.61	47.3

Table 5.5 Mass-dependent selected reaction monitoring (SRM) transition parameters of derivatized cannabinoids and isotopically labelled internal standards. The first ion listed is the quantifier ion, and the reported ion ratio is between the first and second ions listed.

Compound (Derivatized)	Precursor Ion (m/z)	Product Ion (m/z)	Tube Lens (V)	Collision Energy (eV)	Source Fragmentation (V)
THC	483.3	157.0	115	37.10	23.0
	483.3	361.2	115	25.18	23.0
THC- <i>d</i> <sub>3</sub>	486.3	157.2	115	37.39	23.0
THC-COOH	513.3	338.1	153	23.74	42.4
	513.3	310.2	153	27.37	42.4
THC-COOH- <i>d</i> <sub>3</sub>	516.3	341.2	153	24.21	42.4
CBD	483.2	157.1	121	35.40	20.2
	483.2	298.1	121	27.49	20.2
CBD- <i>d</i> <sub>9</sub>	492.3	157.1	121	36.76	20.2
CBN	479.2	222.2	130	52.43	24.0
	479.2	236.1	130	53.86	24.0
CBN- <i>d</i> <sub>3</sub>	482.3	325.1	130	20.70	24.0

Table 5.6 Paper spray mass spectrometry solvent dispense conditions.

Rewet Solvent Dispense (10 µL)	
Aliquot #	Delay (s)
1	1
2	1
Spray Solvent Dispense (10 µL)	
Aliquot #	Delay (s)
1	1
2	1
3	1
4	1
5	3
6	3
7	5
8	5
9	5
10	5
11	5
12	7
13	7
14	7

Table 5.7 Mass spectrometry time-dependent voltage parameters.

Time (min)	Spray Voltage (V)
0	0
0.1	4000
1.1	0

Table 5.8 PS-MS calibrations for underivatized cannabinoids in methanol (n = 4, 8 levels [2,5,10,20,40,100,250,500 ng/mL], [internal standard] = 200 ng/mL) using acetonitrile with 0.1% formic acid as spray solvent.

Analyte	Internal standard	Slope ( $\times 10^2$ )	y-intercept	R <sup>2</sup>	LOD <sup>a</sup> (ng/mL)	LLOQ <sup>b</sup> (ng/mL)
THC	THC- <i>d</i> <sub>3</sub>	0.268	0.070	0.902	25.2	250
THC-COOH	THC-COOH- <i>d</i> <sub>3</sub>	0.560	0.305	0.971	47.4	250

<sup>a</sup> LOD defined as  $3.3 \times$  standard deviation of lowest calibrator / slope

<sup>b</sup> LLOQ defined as the lowest calibrator that meets the acceptance criteria: intra-assay %CV < 15, %bias within  $\pm 20\%$ , ion ratio within  $\pm 20\%$ , and S/N > 4

Table 5.9 Reactive PS-MS calibrations for derivatized cannabinoids in methanol (n = 4, 8 levels [2,5,10,20,40,100,250,500 ng/mL], [internal standard] = 200 ng/mL) using acetonitrile with 0.1% formic acid as spray solvent.

Analyte	Internal standard	Slope ( $\times 10^2$ )	y-intercept	R <sup>2</sup>	LOD <sup>a</sup> (ng/mL)	LLOQ <sup>b</sup> (ng/mL)
THC	THC- <i>d</i> <sub>3</sub>	1.06	0.118	0.997	1.6	10
THC-COOH	THC-COOH- <i>d</i> <sub>3</sub>	0.84	0.0322	0.994	1.4	10
CBD	CBD- <i>d</i> <sub>9</sub>	2.01	0.00785	0.990	1.6	10
CBN	CBN- <i>d</i> <sub>3</sub>	1.27	0.0129	0.999	0.89	10

<sup>a</sup> LOD defined as  $3.3 \times$  standard deviation of lowest calibrator / slope

<sup>b</sup> LLOQ defined as the lowest calibrator that meets the acceptance criteria: intra-assay %CV < 15, %bias within  $\pm 20\%$ , ion ratio within  $\pm 20\%$ , and S/N > 4.

Table 5.10 Cut-off values for drug testing of THC in oral fluid and THC-COOH in urine recommended by regulatory bodies.

Analyte	Matrix	Screening (ng/mL)	Confirmatory (ng/mL)	Source
THC-COOH	Urine	50	15	Cann-Amm Occupational testing services
THC-COOH	Urine	50	15	US Department of Transportation
THC-COOH	Urine	50	15	Substance Abuse and Mental Health Services Administration (SAMHSA)
THC-COOH	Urine	50	15	European Workplace Drug Testing Society
THC-COOH	Urine	50	25	The Australian Standard (AS/NZ 4308:2008)
THC	Oral fluid	4	2	Cann-Amm Occupational testing services
THC	Oral fluid	25	-	Canadian Society of Forensic Sciences – Drugs and Driving Committee
THC	Oral fluid	4	2	Substance Abuse and Mental Health Services Administration (SAMSHA)
THC	Oral fluid	10	2	European Workplace Drug Testing Society
THC	Oral fluid	15	5	The Australian Standard (AS/NZ 4760:2019)

Table 5.11 Preparation of protein-free artificial urine in deionized water, pH = 6.0 (adjusted using 1.0 M hydrochloric acid).

Chemical	Concentration (mM)
Urea	170
Sodium chloride	90
Ammonium chloride	25
Sodium bicarbonate	25
Sodium sulfate	10
Potassium dihydrogen phosphate	7.0
Calcium chloride	2.5
Magnesium sulfate	2.0
Citric acid	2.0
Lactic acid	1.1

Table 5.12 Comparison of reactive PS-MS and LC-MS for the analysis of prepared human urine samples for THC-COOH content. PS-MS results averaged from 6 replicates, LC-MS results from single analysis.

[THC-COOH] (ng/mL)	PS-MS Average (ng/mL)	%CV	Avg. PS-MS Ion Ratio <sup>a</sup>	LC-MS Result (ng/mL)	PS-MS %Bias	LC-MS %Bias	%Difference
15	14.5	12.8	0.65	15.0	-2.8	-0.26	-2.6
25	25.8	9.5	0.70	23.4	3.3	-6.4	9.8
50	47.4	5.0	0.65	46.3	-5.2	-7.4	2.4
50	49.0	7.8	0.66	45.2	-2.1	-9.6	8.0
50	53.0	4.1	0.64	49.4	5.9	-1.2	6.9
125	121.3	3.9	0.58	118.0	-3.0	-5.6	2.8
300	271.8	2.6	0.53	321.7	-9.4	7.2	-16.8

<sup>a</sup> Target ion ratio =  $0.661 \pm 20\%$  (0.529 – 0.793)

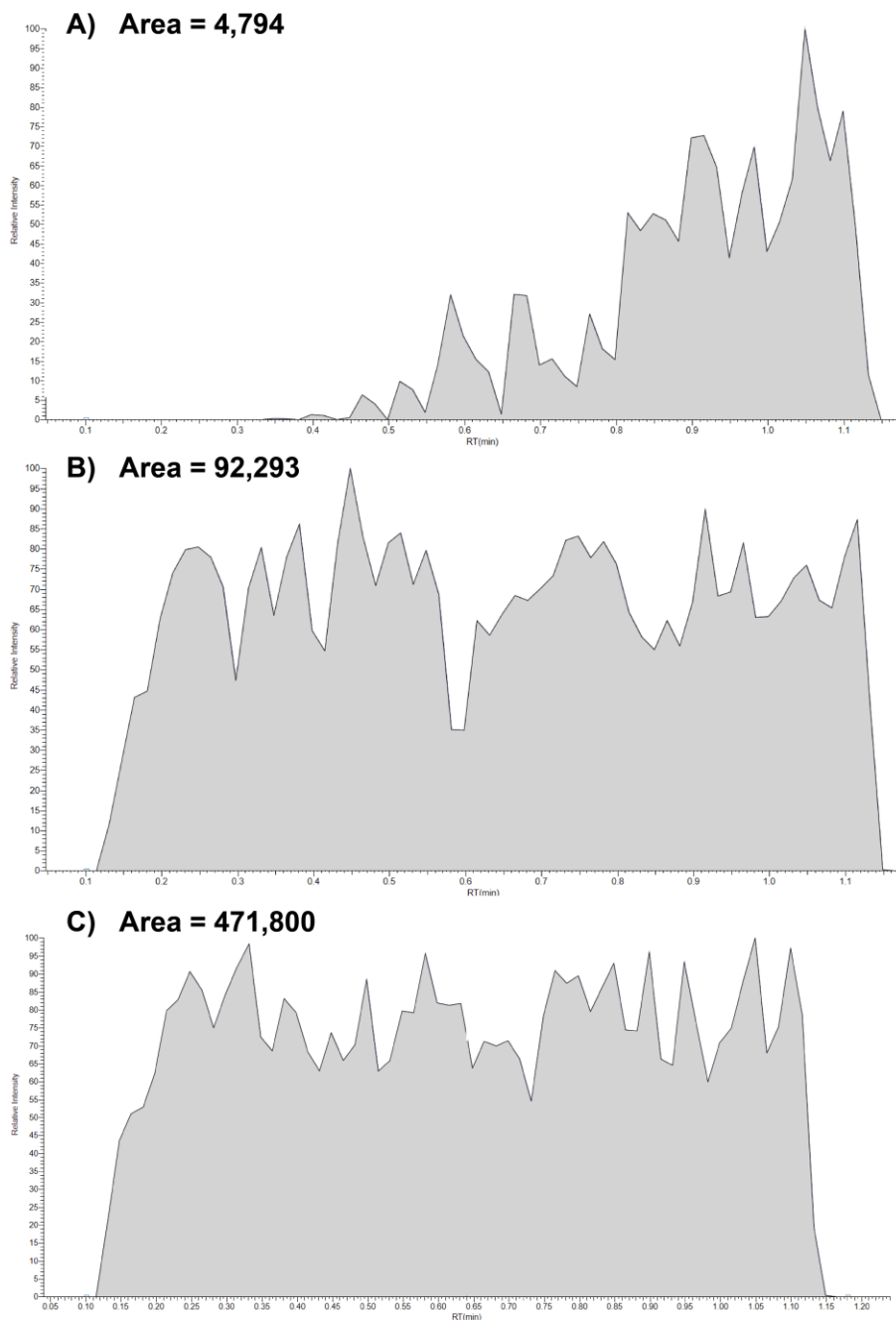


Figure 5.6 Reactive PS-MS signal chronograms for 250 ng/mL of derivatized THC-COOH in A) undiluted human urine using 90/9.9/0.1% acetonitrile/water/formic acid as spray solvent, B) human urine diluted with methanol (70/30 v/v%) using 90/9.9/0.1 acetonitrile/water/formic acid as spray solvent, and C) human urine diluted with methanol (70/30 v/v%) using acetonitrile with 0.1% formic acid as a spray solvent and application of two 10  $\mu$ L aliquots of DCM to the dried sample spot prior to measurement.

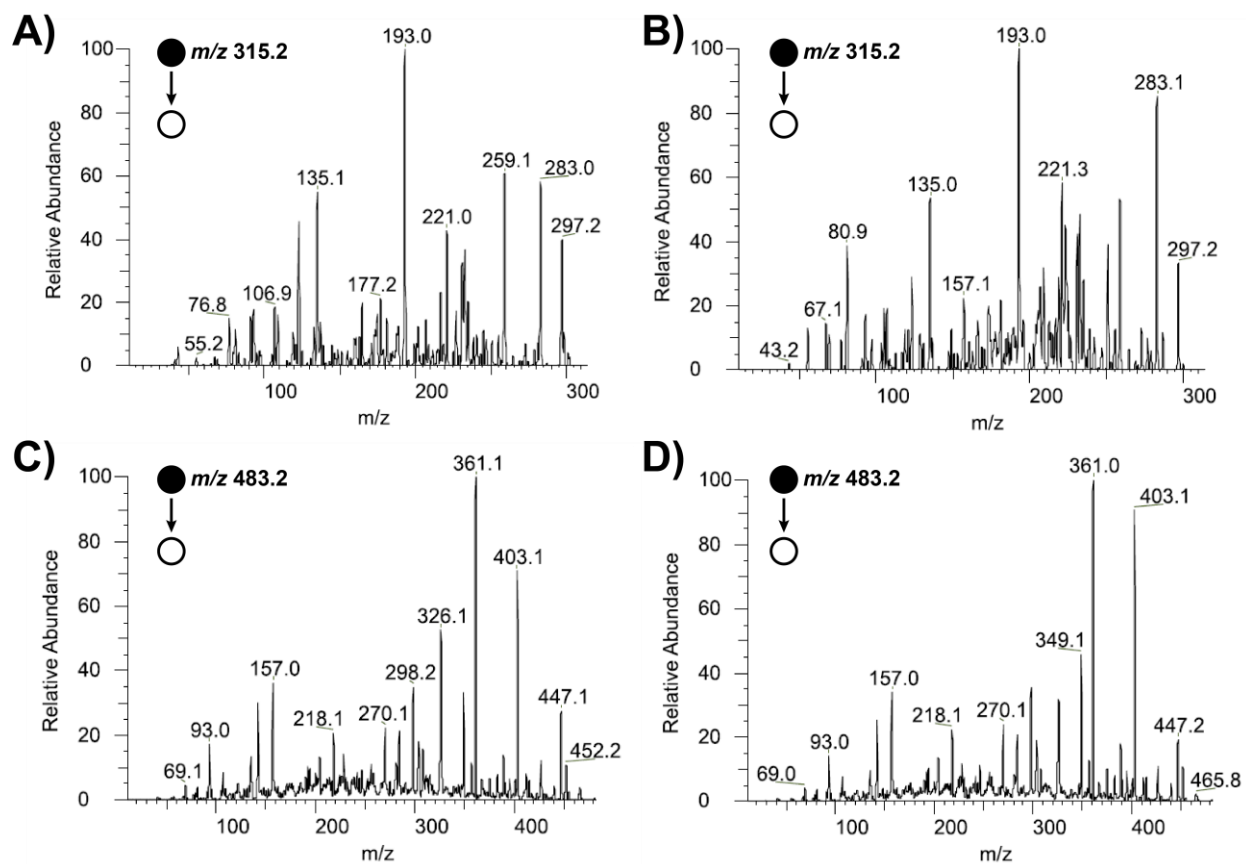


Figure 5.7 Direct infusion electrospray ionization product ion MS/MS spectra of A) THC, B) CBD, C) derivatized THC, and D) derivatized CBD.

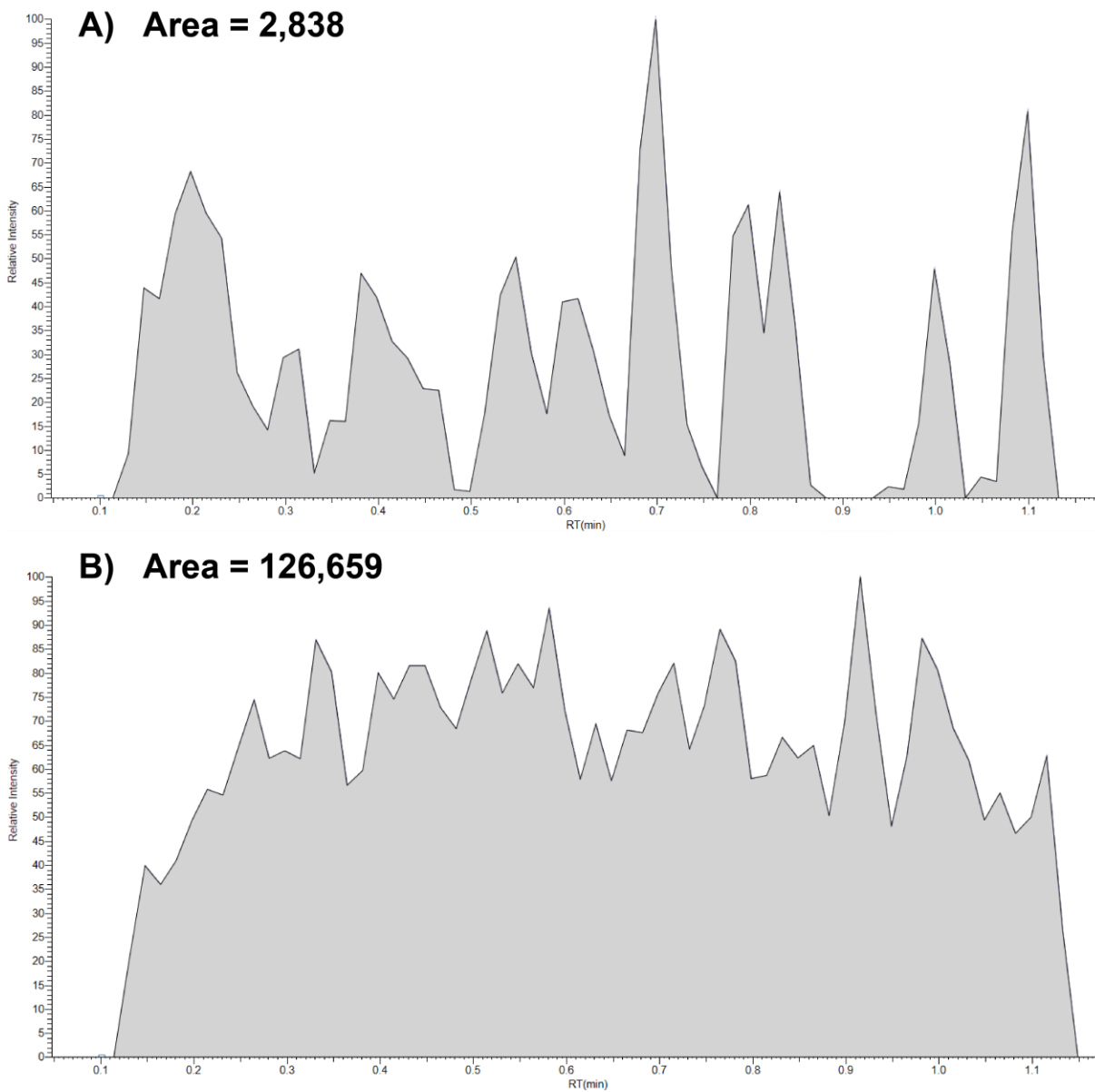


Figure 5.8 Reactive PS-MS signal chronograms for 200 ng/mL of derivatized THC-COOH using acetonitrile with 0.1% formic acid as spray solvent in A) artificial urine spiked with 0.14  $\mu\text{g/mL}$  bovine serum albumin, and B) protein-free artificial urine.

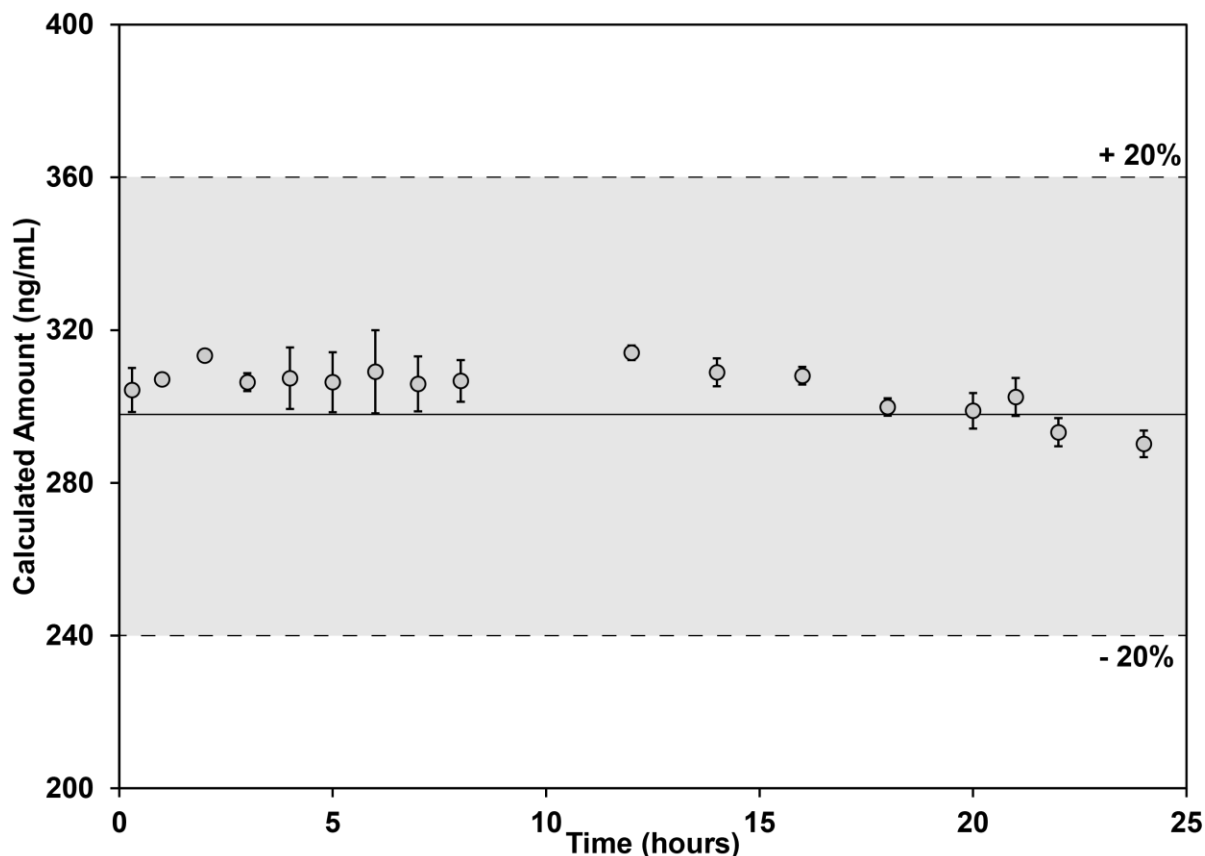


Figure 5.9 Measured THC-COOH levels from reactive paper spray measurements ( $n=3$ ) for prepared urine samples (300 ng/mL) measured at various intervals using PS-MS sample strips prepared in advance with pre-deposited derivatization reagent. 300 ng/mL is represented by the solid line, with  $\pm 20\%$  bias represented by the dashed lines and shaded grey box. Error bars represent  $\pm$  one standard deviation.

The stability of the dried derivatization reagent on the PS-MS paper substrate was evaluated over the course of 24 hours. In this study, Fast Red RC was spotted on the PS-MS sample strips and allowed to dry at ambient temperatures. Prepared urine sample was then spotted periodically (followed by reactive PS-MS analysis) over the next 24 hours at prescribed intervals.

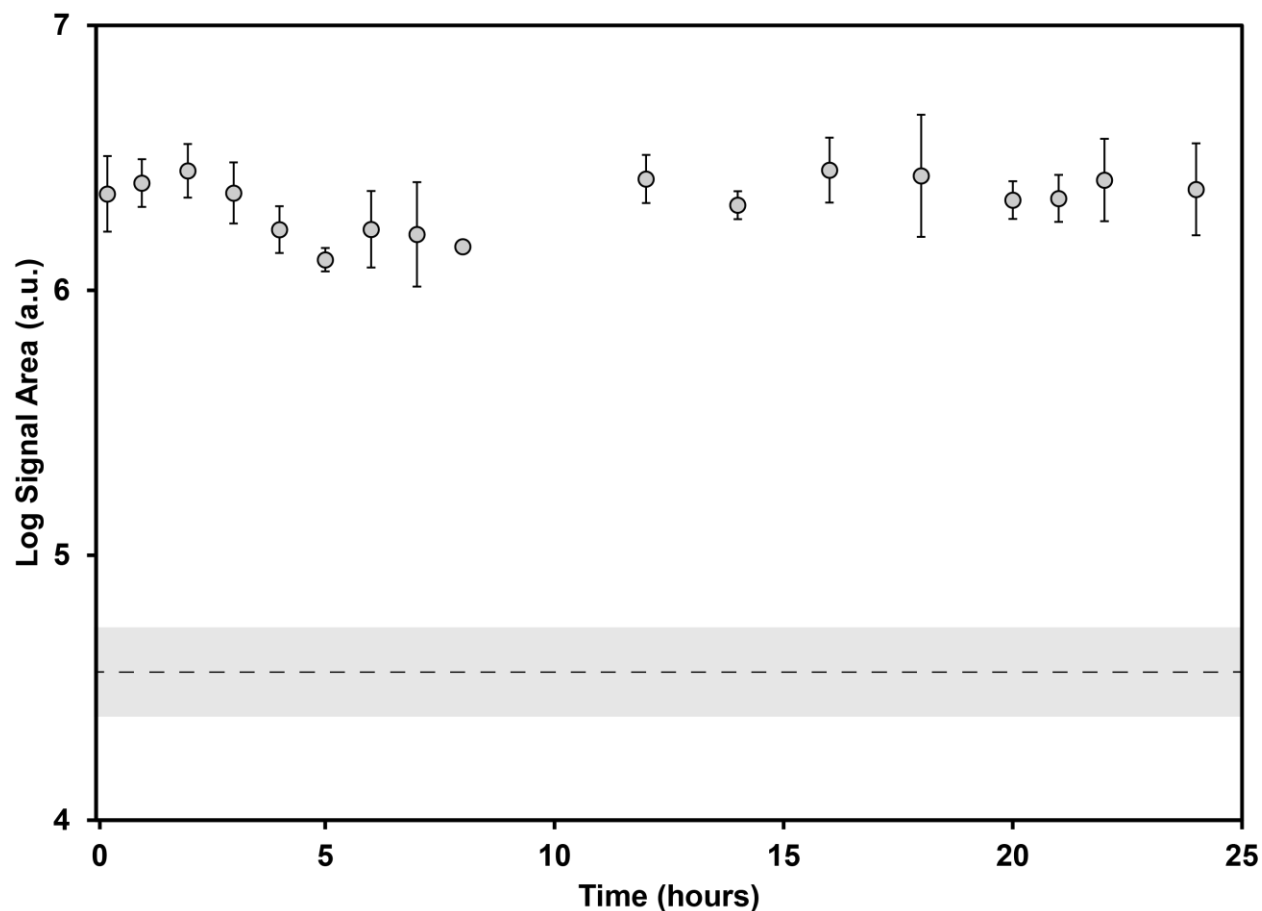


Figure 5.10 Log signal area intensities of derivatized THC-COOH from reactive paper spray measurements ( $n=3$ ) of prepared urine samples (300 ng/mL THC-COOH) obtained at various intervals using PS-MS sample strips prepared in advance with pre-deposited derivatization reagent. The dashed line indicates the mean signal intensity of blank measurements ( $n=6$ ) with the shaded grey box representing  $\pm$  one standard deviation. Error bars represent  $\pm$  one standard deviation.

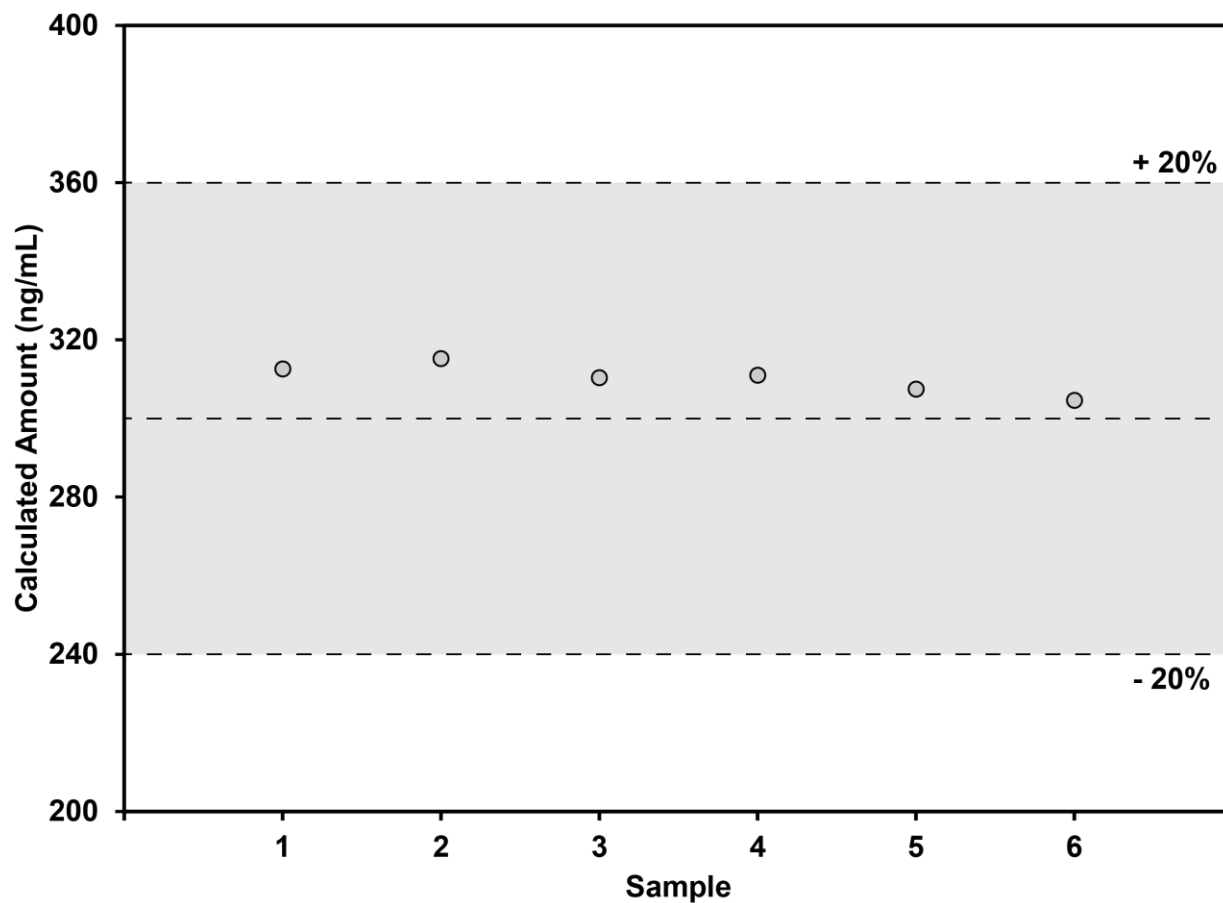


Figure 5.11 Measured THC-COOH levels for reactive PS-MS measurements of prepared urine samples (300 ng/mL) using a 60°C oven for two 1.5-minute drying steps (after Fast Red RC spotting, and after urine spotting). The shaded grey box represents  $\pm 20\%$  bias. The 6 samples were prepared on 6 unique PS-MS sample plates and measured at different times.

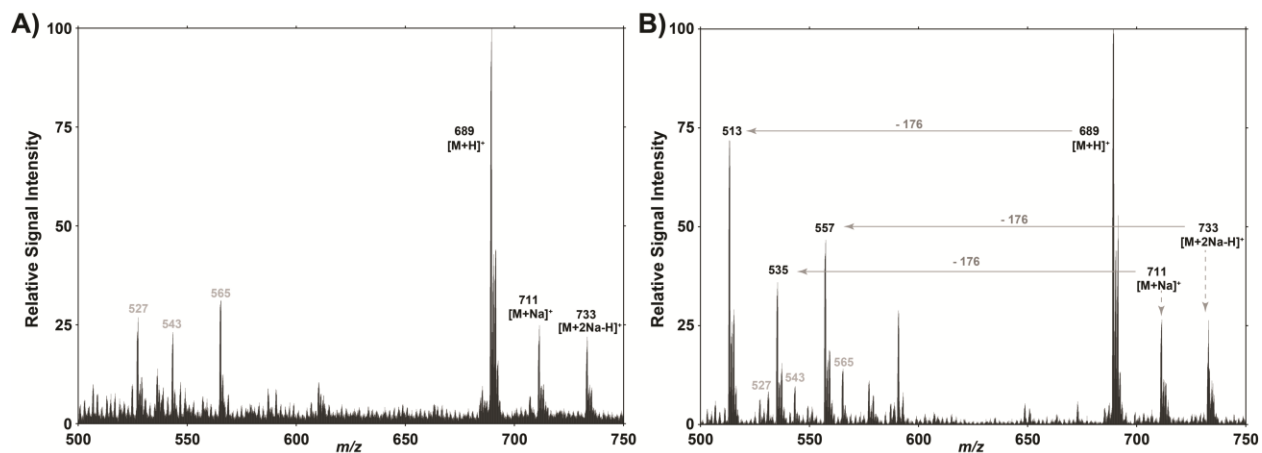


Figure 5.12 Direct infusion electrospray ionization full scan mass spectra (500-750  $m/z$ ) of A) THC-COOH glucuronide derivatized with Fast Red RC at a source fragmentation of 0V, and B) THC-COOH glucuronide derivatized with Fast Red RC at a source fragmentation of 100V\*

\*Spectra from Figure 6.12 were collected on a different triple quadrupole mass spectrometer due to instrument availability:

TSQ Altis QqQ (Thermo Fisher Scientific, San Jose, CA)

Parameter	Value
Ionization polarity	Positive
Spray voltage (V)	4000
Q1 FWHM resolution	0.7
Scan Rate (Da/s)	1000
Averaged from (#scans)	20
Ion transfer tube ( $^{\circ}$ C)	300

## 6 Detection of Carfentanil Analogs in Street Drugs by Paper Spray Mass Spectrometry and their Characterization by High Resolution Mass Spectrometry

This chapter has been adapted from Borden, S.A., Mercer, S.R., Saatchi, A., Wong, E., Stefan, C.M., Wiebe, H., Hore, D.K., Wallace, B., and Gill, C.G., 2022. Carfentanil structural analogs found in street drugs by paper spray mass spectrometry and their characterization by high resolution mass spectrometry. *Drug Testing and Analysis*, 15(5), pp.484-494. doi.org/10.1002/dta.3431 with permission from John Wiley & Sons Inc.

### 6.1 Preface

Borden, S.A. designed and generated data for mass spectrometry experiments, with assistance from Wong, E., and Stefan, C.M. The data and prose for section 7.5.3  $\mu$ -opioid receptor binding modeling was generated by Mercer, S.R. and Wiebe, H. This project was supervised by Gill, C.G. The manuscript was primarily drafted by Borden, S.A., and C.G. Gill with intellectual and editorial contributions from all authors.

### 6.2 Abstract

Carfentanil is one of the most potent synthetic opioids ever developed, with an estimated analgesic potency approximately 20-100 times that of fentanyl and 10,000 times that of morphine. Carfentanil has been appearing in the illicit drug supply in many regions and has been linked to fatal overdose events. A subset of 59 street drug samples obtained in Victoria, B.C., that were confirmed to contain carfentanil were analyzed by mass spectrometry for this study. Carfentanil quantitation by paper spray mass spectrometry ranged from 0.05 – 2.95 w/w% (median = 0.32%) in the original drug sample. Paper spray mass spectrometry analysis also detected two unknown peaks at  $m/z$  380.2 and 381.2 in 31 of these 59 samples (53%). Initial tandem mass spectrometry experiments revealed structural similarities between these unknown compounds and carfentanil, suggesting they were potential structural analogs, possibly arising from incomplete purification during synthesis. High resolution mass spectrometry determined the chemical formulas of these compounds as  $C_{23}H_{29}N_3O_2$  ( $m/z$  380.2333) and  $C_{23}H_{29}N_2O_3$  ( $m/z$  381.2137). Literature and tandem mass spectrometry results were used to determine the identity of these potential new psychoactive substances,  $C_{23}H_{29}N_3O_2$  as desmethylcarfentanil amide, and  $C_{23}H_{29}N_2O_3$  as desmethylcarfentanil acid.  $\mu$ -Opioid receptor binding modeling determined that the binding poses of these analogs were nearly identical to that of carfentanil with relative binding energy calculations of 0.544 kJ/mol (desmethylcarfentanil amide) and -0.171 kJ/mol (desmethylcarfentanil acid); these data suggest they may share the toxic effects of carfentanil and have similar potencies.

### 6.3 Introduction

Carfentanil has emerged as a dangerous additive in the illicit drug supply due to its exceptional potency and the relative ease and low cost of synthesis and transport.<sup>495</sup> Carfentanil is a synthetic  $\mu$ -opioid receptor agonist with similar pharmacodynamic and clinical effects to fentanyl (analgesic, tranquilizer), but with an estimated potency approximately 10,000 times that of morphine, and 20-100 times that of fentanyl, based on animal studies.<sup>496, 497</sup> Activity in humans can begin with doses as low as 1  $\mu$ g, and <sup>11</sup>C-carfentanil has been administered in humans at single digit  $\mu$ g doses since the mid-1980s as a radioligand tracer of  $\mu$ -opioid receptors in the brain for positive emission tomography (PET).<sup>498</sup> Carfentanil (methyl 1-(2-phenylethyl)-4-[phenyl(propanoyl)amino]piperidine-4-carboxylate) was first synthesized at Janssen Pharmaceutica in 1974,<sup>499, 500</sup> and then introduced as a veterinary medicine (marketed as Wildnil®) in 1986. Since then, a number of different synthetic pathways for carfentanil or closely related compounds have been presented.<sup>501-504</sup> During clandestine or illicit manufacture of drugs for illicit use, incomplete synthesis/purification is fairly common, and the presence of synthetic intermediates and side products in illicit drugs may be helpful in determining the synthetic pathway or the drug origin.<sup>505-507</sup> Despite its designation as a Schedule II controlled substance (DEA Number. 9743), carfentanil has increasingly been detected in street drug samples found in police seizures and in post-mortem autopsies.<sup>508</sup> Consequently, the drug has been contributing to fatal intoxications due to its extreme potency and increased prevalence.<sup>497</sup>

Fatal intoxications have sharply increased since the introduction and growing prevalence of potent new synthetic opioids (e.g., fentanyl, fentanyl analogs) in the illicit drug market in the mid 2010's, particularly in North America.<sup>509</sup> As a result of this ongoing opioid overdose epidemic, governments have implemented various harm reduction strategies. In Canada, and in many other Western jurisdictions (e.g., Europe, Australia, United States), various programs aimed towards harm reduction (e.g., supervised consumption sites, needle exchange programs, naloxone distribution) have been implemented in place of punitive measures for people who use drugs (PWUD).<sup>10, 11, 450</sup> One harm reduction approach that has demonstrated efficacy in reducing overdose through behavioral modifications (e.g. avoiding use of the drug, using more slowly, using with others who have naloxone) is drug checking.<sup>510</sup> Drug checking is a service offered to PWUD who submit a small drug sample for chemical analysis and receive compositional information to allow for informed decision making about the substance they intend to consume. The goal of drug checking is to provide the user with information to enable informed use decisions and ultimately, reduce the risk of overdose or harm. A tangential benefit of drug checking is that it can be used for illicit drug supply surveillance and provide a dynamic snapshot of the prevalence of certain drugs within different regions. Drug checking has indeed been shown to lead to behavior modifications for PWUD including dose reduction or discarding substances.<sup>13, 510</sup>

Current on-site drug checking methods (e.g., FTIR, immunoassay test strips, Raman spectroscopy, etc.) lack either the required sensitivity and selectivity to reliably detect

carfentanil or other synthetic opioids, since these compounds are typically present at trace levels (e.g., typically < 1% w/w) in the overall drug sample, below the limits of detection for these techniques.<sup>16, 511</sup> Traditional gold-standard methods for drug testing like liquid chromatography and gas chromatography mass spectrometry (LC-MS, GC-MS) are infrequently used in on-site drug checking applications due to lengthy analysis times, the technical expertise required, and relatively high costs.

Drug samples procured for the analyses presented within this investigation were obtained from the Vancouver Island Drug Checking Project, a drug checking and harm reduction service operating in Victoria, BC, Canada.<sup>12, 512, 513</sup> The project uses FTIR,<sup>15</sup> Raman spectroscopy<sup>512</sup>, immunoassay test strips, and paper spray mass spectrometry (PS-MS) for on-site drug checking. PS-MS is an ambient ionization mass spectrometry technique first developed in 2010.<sup>9</sup> Small amounts of sample (e.g., 10  $\mu$ L) are applied to a piece of triangular filter paper followed by a suitable solvent and a high voltage (3-5 kV) to induce ionization of desired analytes. PS-MS has previously been used for a variety of applications including the analysis of drugs of abuse in various biofluids.<sup>514</sup> Recently, PS-MS was applied to drug checking applications by Gill et al.<sup>314, 477, 507</sup>, and was then piloted as an on-site drug checking technique in Vancouver, Canada in 2019<sup>515</sup>. It was then introduced to the Vancouver Island Drug Checking Project in 2020 as a permanent on-site instrument for drug checking.<sup>516, 517</sup> During the ongoing PS-MS quantitative analysis of drug samples submitted by PWUD to the Drug Checking Project, two unidentified compounds began to appear in drug samples that contained carfentanil. Initial investigations with product ion scans using PS-MS indicated that these compounds showed close structural similarities to carfentanil. High resolution-accurate mass (HRAM) mass spectrometry was implemented for the structural characterization of these unknown compounds which putatively identified them as carfentanil structural analogs.  $\mu$ -Opioid receptor binding modeling and binding energy calculations were used to estimate the relative binding affinity of the carfentanil structural analogs. Currently, these structural analogs are not being detected/reported by existing drug checking techniques, and to our knowledge they have not been published in the drug testing literature.

## 6.4 Experimental

### 6.4.1 Materials and Reagents

Legally exempt, analytical reference standards for carfentanil and carfentanil-*d*<sub>5</sub> were purchased from Cerilliant Corporation (Round Rock, TX, USA). Optima HPLC grade water, methanol, acetonitrile, and formic acid were acquired from Fisher Scientific (Ottawa, ON, Canada). VeriSpray<sup>TM</sup> sample plates for PS-MS measurements were obtained from Thermo Fisher Scientific (San Jose, CA, USA).

### 6.4.2 Sample Collection

All samples were willingly submitted by people who used drugs (PWUD), or those who care for them, as part of a drug checking project (Vancouver Island Drug Checking Project) established in 2018 in Victoria, BC, Canada. PWUD are informed of the

limitations and provide informed consent for service data to be used for research according to ethical approval from the Health Research Ethics Board at Island Health Authority (J2018-069). Individuals are asked to provide their expectation on the chemical identity of the substance they want tested and they provide just a small sample (typically <10 mg) from their overall product. The subset (n = 59) of carfentanil-containing drug samples analyzed in this study were collected from January 14, 2021, to May 24, 2022. Approximately 1 mg of sample was used for this study.

### 6.4.3 Sample Preparation

Samples were prepared for quantitation by accurately weighing approximately 1 mg of drug sample using a 5-decimal point analytical balance. The sample was then dissolved in methanol to create a 1 mg/mL solution (solution A) and then diluted 250-fold into a vial containing 200  $\mu$ L of methanol spiked with carfentanil-*d*<sub>5</sub> internal standard at 100 ng/mL (solution B).

### 6.4.4 Paper Spray Mass Spectrometry

All carfentanil containing samples were quantified using a TSQ Fortis™ triple quadrupole tandem mass spectrometer with a VeriSpray™ paper spray ion source (Thermo Fisher Scientific, San Jose, CA, USA) in positive ion mode, located on-site at the drug checking facility. Direct infusion electrospray of (ca. 100 ng/mL) analytical standards prepared in methanol were used to generate the MS/MS transitions used (Table 6.4). PS-MS/MS (selected reaction monitoring) signal chromatograms were collected for 1.2 minutes and integrated and recorded without smoothing using TraceFinder Clinical 4.1 SP5 software (Thermo Fisher Scientific, San Jose, CA, USA). The PS-MS method also included a full scan (50 - 500 *m/z*) from 1.3 - 1.6 minutes for to monitor for potential unknowns, and a precursor ion (188.0 *m/z*) scan (50 - 500 *m/z*) from 1.7 – 1.9 minutes for potential identification of fentanyl analogs. The total PS-MS method length was 2.0 minutes. Analytical calibration for carfentanil utilized 11 standards (1, 2.5, 5, 10, 15, 25, 40, 75, 125, 250, 500 ng/mL) volumetrically prepared in methanol (n = 6 replicates at each level) using carfentanil-*d*<sub>5</sub> as an internal standard (100 ng/mL). The calibration curve was generated using the ratio of the carfentanil quantifier ion analyte MS/MS (395.2 > 335.2 *m/z*) signal area to the carfentanil-*d*<sub>5</sub> quantifier ion MS/MS (400.3 > 340.2 *m/z*) analyte signal area. The PS-MS spray solvent used for all experiments was 90/9.9/0.1 acetonitrile/water/formic acid. UHP grade argon was used as collision gas for all MS/MS experiments at a pressure of 2.0 mTorr. Additional PS-MS parameters are provided in the Supporting Information (Table 6.5 + Table 6.6). The limit of detection (Table 6.7) (LOD) was determined as 3.3 times the standard deviation of the lowest calibrator (1 ng/mL) divided by the slope of the calibration curve (Table 6.8). The lower limit of quantitation (LLOQ) was determined as 10 times the standard deviation of the lowest calibrator divided by the slope.

### 6.4.5 High Resolution Mass Spectrometry

High resolution-accurate mass was achieved using an Orbitrap Exploris 120™ mass spectrometer (Thermo Fisher Scientific, San Jose, CA, USA), located off-site at the

university laboratory. Fluoranthene was used as an internal calibrant (EASY-IC™, Thermo Fisher Scientific) to improve mass accuracy. All experiments were performed in positive ion mode at 3400 V. A precursor ion selection width of 0.4  $m/z$  was used for all MS/MS experiments. Additional instrument parameters are outlined in the Supporting Information (Table 6.9). Carfentanil-containing drug samples for direct infusion into the Orbitrap were spotted onto the VeriSpray™ PaperSpray sample plates at the drug checking site and then transported to the laboratory where the Orbitrap system was housed. Acetonitrile (1.8 mL) was used to extract the analytes from the paper strips. Water and formic acid were added to the acetonitrile extract to create a spray solvent containing extracted analyte (90/9.9/0.1 v/v% acetonitrile/water/formic acid). Direct infusion HRAM measurements of the extract were performed at 5  $\mu\text{L}/\text{min}$ , with the resulting data processed using Freestyle™ 1.7 software (Thermo Fisher Scientific).

#### 6.4.6 $\mu$ -Opioid Receptor Binding Modeling

*In-silico* docking poses and relative binding energies were calculated using AutoDock Vina v.1.2.3.<sup>518</sup> The structure of the  $\mu$ -opioid receptor was obtained from the Protein Data Bank entry 5C1M.<sup>519</sup> The agonist BU72, which is bound to the  $\mu$ -opioid receptor in the crystal structure, was removed along with a bound cholesterol and all crystallographic water molecules. The cysteine-s-acetamide at position 57 was replaced with a cysteine, and all titratable residues were set to their standard protonation states at physiological pH. The docked structure of fentanyl from Ellis et al. was used as a starting point for docking carfentanil and the precursors.<sup>520</sup> All hydrogens were removed from the ligands during docking, except for the piperidine nitrogen which remained protonated in order to allow for the formation of a salt bridge between the ligand and the ASP147 residue in the binding site. Charges on titratable groups, such as the carboxylic acid on NPS2, were set to their expected values at physiological pH. Docking was performed by searching 6550  $\text{\AA}^3$  volume inside the binding pocket in a series of 32 parallel runs. The top nine ranked poses for each analog were kept for later analysis.

### 6.5 Results and Discussion

#### 6.5.1 Carfentanil and Carfentanil Structural Analogs in Street Drug Samples

Paper spray mass spectrometry (PS-MS) has been used for the routine quantitative analysis of drug samples submitted by PWUD at the Vancouver Island Drug Checking Project since October 2020. Over the following two years, more than 6,600 samples were submitted to the service for drug checking, and quantified using PS-MS. During the routine analysis of these samples, several carfentanil-containing drug samples were closely examined, and two unidentified compounds were noticed in the full scan PS-MS mass spectra. A subset of 59 carfentanil-containing drug samples obtained from January 14, 2021, to May 24, 2022, were selected for further analysis and HRAM-MS to determine the extent of the presence of these compounds, as well as their chemical identities, and are presented in this manuscript. Carfentanil was detected and quantified in all 59 of these samples using PS-MS. PS-MS quantitation was achieved using a calibration curve prepared using an analytical reference standard with carfentanil- $d_5$  as an internal

standard (Figure 6.1A). The LOD and LLOQ (Table 6.7) for carfentanil in the prepared drug sample (Solution B) was determined as 0.73 ng/mL (0.018 w/w%) and 2.23 ng/mL (0.056%), respectively. Sample solution B was used for quantitation; the median w/w concentration of carfentanil in the original drug sample for these 59 samples was determined to be 0.32% with a range of 0.05–2.95% (Figure 6.1B). Less dilution could be used to prepare the drug sample if lower detection/quantification limits are desired.

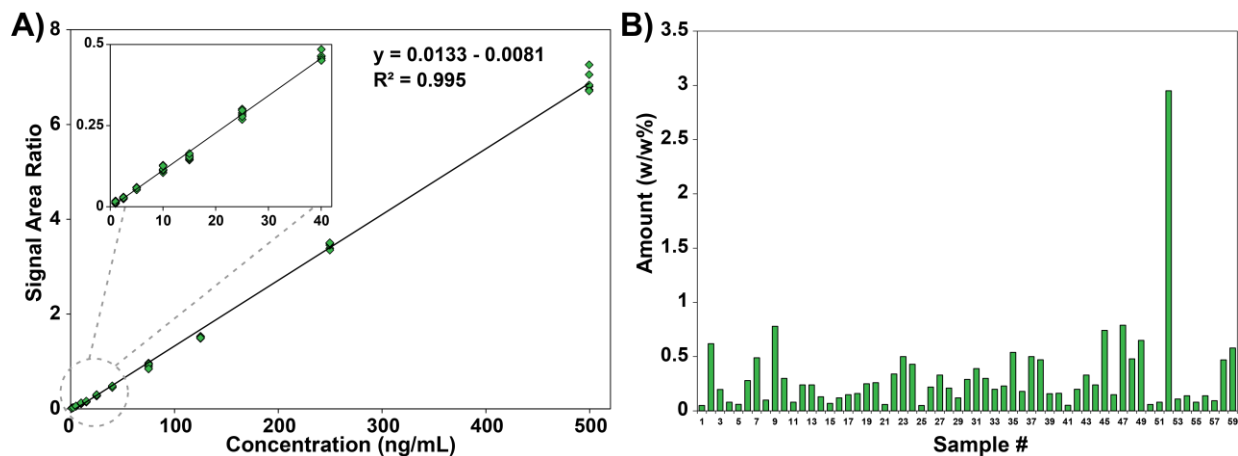


Figure 6.1 A) PS-MS calibration of carfentanil ( $n = 6$  replicates, 10 levels [1, 2.5, 5, 10, 15, 25, 40, 75, 125, 250, 500 ng/mL], [carfentanil- $d_5 = 100$  ng/mL], 1/x weighting. B) Quantified amount (w/w%) of carfentanil in the original drug sample.

The drug checking site also uses FTIR, Raman spectroscopy, and immunoassay drug test strips, for comprehensive drug checking.<sup>14, 512, 513</sup> Notably, only PS-MS was able to explicitly detect carfentanil in these 59 samples, and none of the other techniques were able to definitively detect or specify carfentanil's presence. This is because the detection limits are too high for the spectroscopic techniques employed, particularly for opioids where the strongest spectral features of carfentanil lack specificity (e.g.  $\sim 1000$   $\text{cm}^{-1}$  in the case of Raman and  $\sim 705$   $\text{cm}^{-1}$  in the case of FTIR) and there is a high degree of spectral overlap with common cuts and buffs (e.g. caffeine), as well as with other closely related drugs that produce similar spectral features (e.g. fentanyl, fentanyl analogs). Immunoassay test strips, though sensitive, are not selective, only identifying drug class without specificity (e.g., fentanyl or analog), rendering them unable to definitively identify carfentanil.

During the routine analysis of drug samples with PS-MS on a unit mass resolution triple quadrupole (QqQ) mass spectrometer, two unidentified compounds determined to be potential new psychoactive substances (NPS) were noticed in the full scan MS spectrum of 1 mg/mL prepared drug samples (solution A). A representative drug sample containing carfentanil and the two unidentified peaks at  $m/z$  380.2 (NPS1) and  $m/z$  381.2 (NPS2) is presented in Figure 6.2.

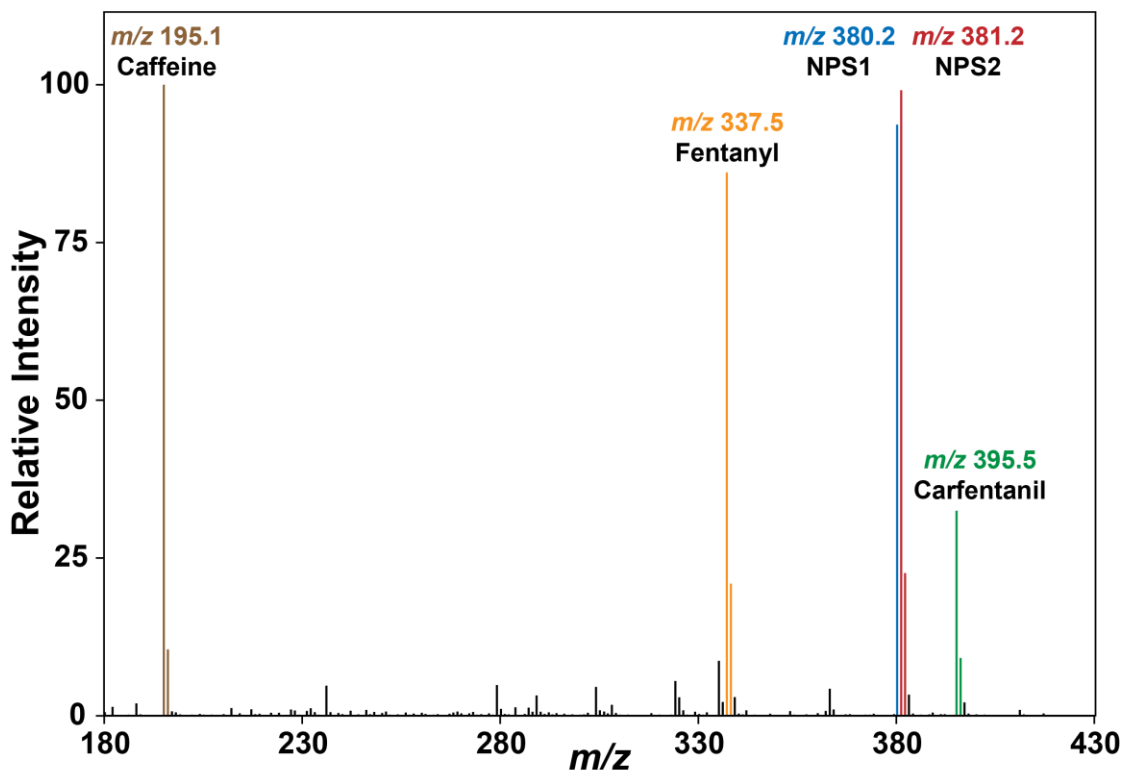


Figure 6.2 PS-MS QqQ full scan (50-500  $m/z$ ) of a carfentanil containing drug sample (solution A).

The spectrum also demonstrates the simultaneous detection of fentanyl and caffeine, a poly-drug composition typical of opioid drugs submitted for drug checking at this location. The presence of multiple compounds in a drug sample significantly complicates the analysis when using other drug checking techniques (e.g., FTIR, Raman spectroscopy), whereas mass spectrometry can easily differentiate between the observed different components, even at unit mass resolution.

A 100 ng/mL carfentanil analytical reference standard was analyzed by PS-MS to ensure that NPS1 and NPS2 were not present or inadvertently produced in the MS analysis of carfentanil. Both PS-MS analysis (Figure 6.7) and direct infusion HRAM-MS (Figure 6.8) of the standard exhibited the absence of these peaks, indicating they were compounds present in the drug sample itself and not fragments of carfentanil, or otherwise. Furthermore, NPS1 and NPS2 were only present in 31 of the 59 (53%) carfentanil-containing drug samples that were analyzed. Figure 6.9 is an example of a PS-MS full scan mass spectrum showing the absence of these compounds in a carfentanil-containing drug sample. NPS1 and NPS2 were also found to always co-exist, all of the 31 drug samples containing these NPS contained both 1 and 2. Through our routine analysis, it was also observed that NPS1 and NPS2 only appeared in drug samples that also contained carfentanil. We hypothesized that these compounds may be synthetic precursors or by-products resulting from illicit carfentanil production, since these compounds are noted as synthetic intermediates in the synthesis of carfentanil in the

original Janssen Pharmaceutica patent.<sup>521</sup> At this point however, we cannot rule out whether their presence could also be their intentional introduction as carfentanil analog drugs. For an initial assessment of whether there was a structural relationship between NPS1, NPS2 and carfentanil, the NPS' were subjected to PS-MS/MS analysis (QqQ) and the MS/MS spectra of the  $m/z$  380.2 and 381.2 ions were compared to that of a carfentanil analytical reference standard. The results of this initial assessment are illustrated in Figure 6.10 and the relative intensities of the fragments observed are tabulated in Table 6.10. The MS/MS spectra of NPS1 and NPS2 are nearly identical to those produced from carfentanil and therefore indicate a close structural relationship. This experiment was repeated using HRAM-MS to identify the exact mass and elemental composition of the fragments (Section 3.2).

Analytical reference standards for NPS1 and NPS2 are not commercially available, and therefore accurate quantitation cannot be achieved. However, a rough estimate of the amount of these NPS was desired. Figure 6.3A presents the peak heights of NPS1 and NPS2 relative to that of carfentanil.

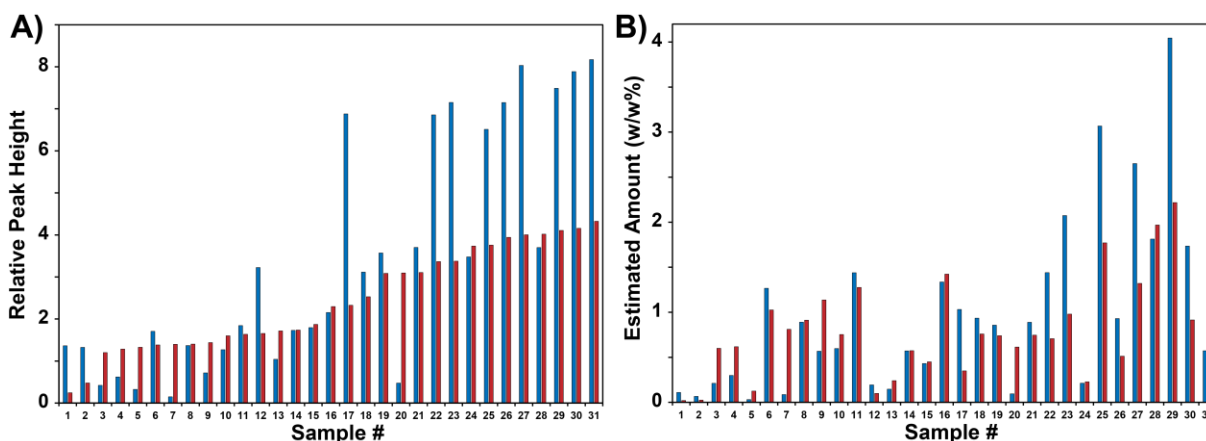


Figure 6.3 A) PS-MS QqQ relative peak heights of NPS1 (blue) and NPS2 (red) intermediates relative to that for carfentanil (value of 1) and B) estimated w/w concentration of NPS1 and NPS2 in the original drug sample.

NPS1 produces a larger signal than carfentanil in 25/31 samples and NPS2 produces a larger signal in 29/31 samples. Relative (to carfentanil) peak heights for NPS1 range from 0.1 to 8.2 with a median of 2.2. Relative peak heights for NPS2 range from 0.2 to 4.3 with a median of 2.3. A correction was also applied to the 381.2  $m/z$  signal intensity for NPS2 since the  $^{13}\text{C}$  isotopic peak from the 380.2  $m/z$  of NPS1 will contribute to this signal. Because of the lack of analytical reference standards, exact ionization efficiencies of these NPS are unknown. Recent work by Denis et al. however has found that the proton affinity values and gas phase basicity values of a variety of fentanyl analogs, including carfentanil, are similar.<sup>522</sup> Therefore, a crude concentration of these NPS can be made by assuming a constant ionization efficiency and using the relative peak heights compared to the quantified amount of carfentanil. Figure 6.3B illustrates the inferred amounts of NPS1 and NPS2 (results tabulated in Table 6.11). Estimated concentrations

for NPS1 range from 0.03 to 4.04% (median = 0.86%) and a range of 0.02 to 2.22% (median = 0.74%) for NPS2. We note that if these compounds act similarly to carfentanil on the  $\mu$ -opioid receptor (see Section 3.3), these compounds may be contributing to overdoses given the high estimated amounts present.

### 6.5.2 Characterization of Carfentanil Structural Analogs

Nominal mass values can be obtained from the unit resolution PS-MS QqQ experiments. To assign a chemical formula and elucidate a chemical structure, as noted above, high resolution-accurate mass (HRAM) MS was required. Determining a chemical formula and structure will not only help to identify these compounds and alert forensic, clinical, and drug checking communities to them, but also allow for  $\mu$ -opioid receptor binding modeling to provide an estimate of their binding affinity compared to carfentanil (Section 3.3). The HRAM Orbitrap system used for these experiments could not be interfaced to the VeriSpray PaperSpray interface at the time of this study, and direct infusion with electrospray ionization was employed in lieu. To comply with sample transportation exemption requirements, samples were spotted on the paper spray sampling plates at the Vancouver Island Drug Checking Project site (Victoria, BC) and then transported to the benchtop Orbitrap system for high resolution analysis (Nanaimo, BC). A simple extract from the paper was then analyzed by direct infusion electrospray ionization. Figure 6.4 gives a typical HRAM full scan spectrum of a carfentanil-containing drug at a setting of 120,000 resolution, with chemical formulae assignment of the detected peaks presented in Table 6.1.

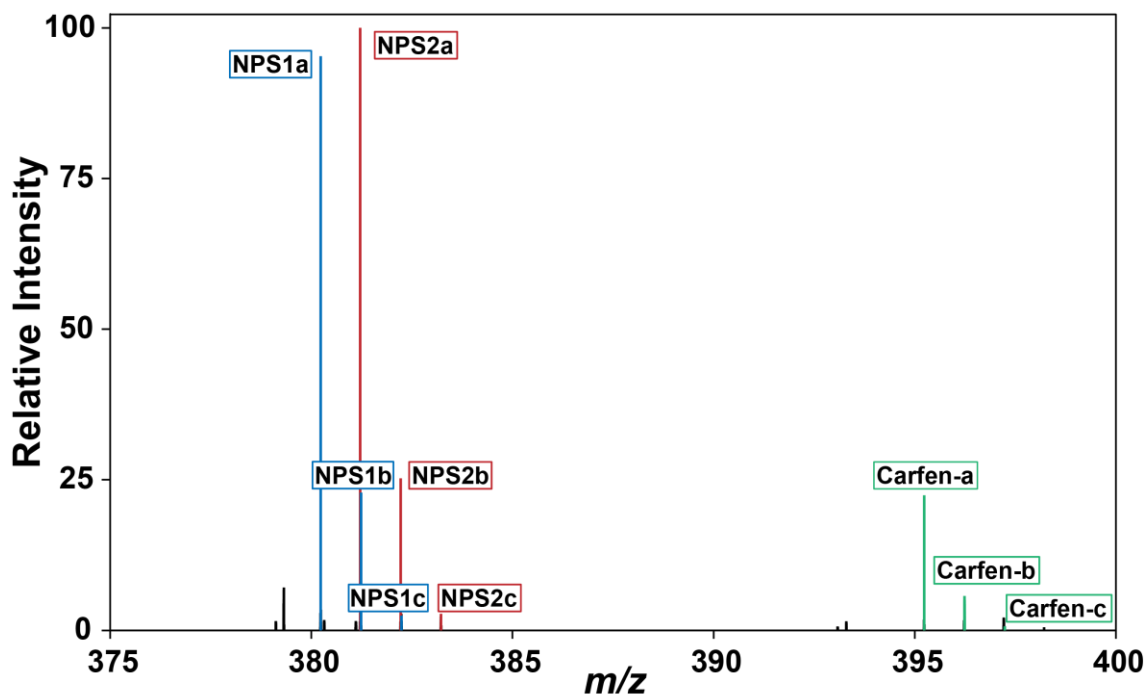


Figure 6.4 Direct infusion HRAM-MS full scan spectrum of a carfentanil-containing drug sample dissolved in spray solvent (90/9.9/0.1 v/v% acetonitrile/water/formic acid).

Table 6.1. HRAM-MS full scan mass errors and formulae assignment of a carfentanil containing drug sample.

Peak number	Elemental composition	Theoretical $m/z$	Experimental $m/z$	Mass error (ppm)
NPS1a	$C_{23}H_{30}O_2N_3^+$	380.23325	380.2332	-0.06
NPS1b	$C_{22}^{13}CH_{30}O_2N_3^+$	381.23661	381.2365	-0.32
NPS1c	$C_{21}^{13}C_2H_{30}O_2N_3^+$	382.23996	382.2397	-0.78
NPS2a	$C_{23}H_{29}O_3N_2^+$	381.21727	381.2172	-0.19
NPS2b	$C_{22}^{13}CH_{29}O_3N_2^+$	382.22062	382.2205	-0.33
NPS2c	$C_{21}^{13}C_2H_{29}O_3N_2^+$	383.22398	383.2238	-0.36
Carfen-3a	$C_{24}H_{31}O_3N_2^+$	395.23292	395.2329	-0.08
Carfen-3b	$C_{23}^{13}CH_{31}O_3N_2^+$	396.23627	396.2362	-0.28
Carfen-3c	$C_{22}^{13}C_2H_{31}O_3N_2^+$	397.23963	397.2393	-0.86

The  $^{13}C$  isotopic peaks (b, c) were used for further confirmation. Furthermore, as a quasi-control, carfentanil present in the sample was assigned the correct chemical formula. The mass accuracy of all  $m/z$  measurements ranged from -0.86 to -0.06 ppm for all peaks. Mass errors and elemental compositions are tabulated in Table 6.1.

With the elemental composition and theoretical monoisotopic mass of NPS1 and NPS2 identified, some possible chemical identities and structures (Figure 6.11) were hypothesized. The only match based on chemical formula determined for NPS1 was desmethylcarfentanil amide. Four different carfentanil/fentanyl analogs with the chemical formula  $C_{23}H_{29}O_3N_2$  were potentially identified for NPS2: desmethylcarfentanil acid, benzyl carfentanil, acetyl carfentanil, and 3,4-methylenedioxy fentanyl. HRAM-MS/MS was applied to NPS1 and NPS2 to help putatively determine their exact structure.

The product ion spectra obtained at 20% HCD collision energy for carfentanil and NPS1 and NPS2 are shown in Figure 6.5A, B, and C, respectively, and compared to the spectrum for an analytical reference standard of carfentanil. Table 6.2 summarizes the elemental composition, relative intensities, and mass errors for all fragments (> 0.5 relative intensity).

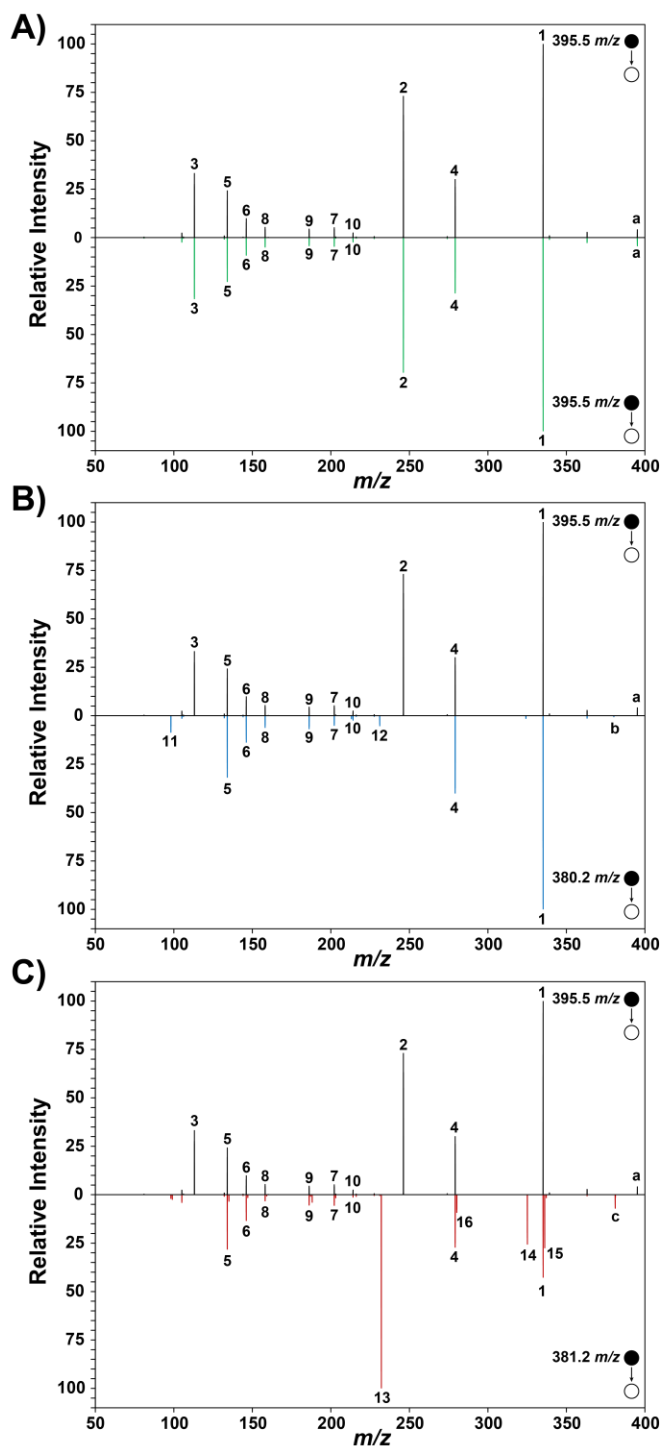


Figure 6.5 HRAM-MS/MS product ion spectra of a carfentanil containing drug samples for A)  $m/z$  395.5 (carfentanil), B)  $m/z$  380.2 (NPS1), and C)  $m/z$  381.2 (NPS2). All spectra are compared to the product ion spectrum of a carfentanil analytical reference standard (top panels). All spectra were collected at 20% HCD collision energy.

Table 6.2. HRAM-MS/MS product ion scan mass errors, formulae assignments, and relative intensities for fragments of carfentanil, NPS1, and NPS2 in a carfentanil-containing drug sample.

#	Elemental Composition	Theoretical <i>m/z</i>	Carfentanil (395.5 <i>m/z</i> )		NPS1 (380.2 <i>m/z</i> )		NPS2 (381.2 <i>m/z</i> )	
			Mass error (ppm)	Relative Intensity	Mass error (ppm)	Relative Intensity	Mass error (ppm)	Relative Intensity
1	C <sub>22</sub> H <sub>27</sub> ON <sub>2</sub> <sup>+</sup>	335.21179	-0.27	100	-0.40	100	-0.22	42.47
2	C <sub>15</sub> H <sub>20</sub> O <sub>2</sub> N <sup>+</sup>	246.14886	-0.03	70.1	-	-	-	-
3	C <sub>6</sub> H <sub>9</sub> O <sub>2</sub> <sup>+</sup>	113.05971	-0.06	32.5	-	-	-	-
4	C <sub>19</sub> H <sub>23</sub> N <sub>2</sub> <sup>+</sup>	279.18558	-0.24	29.2	-0.16	39.7	-0.27	27.35
5	C <sub>9</sub> H <sub>12</sub> N <sup>+</sup>	134.09643	-0.03	23.4	-0.05	31.1	-0.08	29.12
6	C <sub>10</sub> H <sub>12</sub> N <sup>+</sup>	146.09643	0.02	9.51	0.03	13.6	-0.05	13.88
7	C <sub>11</sub> H <sub>12</sub> N <sup>+</sup>	158.09643	0.02	5.14	-0.04	6.08	-0.01	3.43
8	C <sub>13</sub> H <sub>16</sub> ON <sup>+</sup>	202.12264	-0.02	4.83	0.01	5.08	-0.04	5.82
9	C <sub>13</sub> H <sub>16</sub> N <sup>+</sup>	186.12773	0.05	4.45	-0.04	6.73	0.02	5.61
10	C <sub>14</sub> H <sub>16</sub> ON <sup>+</sup>	214.12264	0.11	2.47	-0.03	2.42	0.04	1.43
11	C <sub>5</sub> H <sub>8</sub> ON <sup>+</sup>	98.06004	-	-	-0.20	8.80	-0.19	2.15
12	C <sub>14</sub> H <sub>19</sub> ON <sub>2</sub> <sup>+</sup>	231.14919	-	-	-0.09	5.23	0.00	0.62
13	C <sub>14</sub> H <sub>18</sub> O <sub>2</sub> N <sup>+</sup>	232.13321	-	-	-	-	-0.04	100
a	C <sub>24</sub> H <sub>31</sub> O <sub>3</sub> N <sub>2</sub> <sup>+</sup>	395.23292	-0.27	4.45	-	-	-	-
b	C <sub>23</sub> H <sub>30</sub> O <sub>2</sub> N <sub>3</sub> <sup>+</sup>	380.23325	-	-	-0.24	0.71	-	-
c	C <sub>23</sub> H <sub>29</sub> O <sub>3</sub> N <sub>2</sub> <sup>+</sup>	381.21727	-	-	-	-	-0.19	1.64

Mass errors for all fragments ranged from -0.40 to 0.11 ppm, indicating good instrumental performance and mass accuracy. Additionally, MS/MS spectra of NPS1 and NPS2 were collected at a higher collision energy of 50% HCD to produce lower-mass fragments that could further aid in structural analysis (Figure 6.12, Figure 6.13, Table 6.13, and Table 6.14). The carfentanil from the drug sample (Figure 6.5A) matches the analytical reference standard nearly identically. NPS1 shares many of the same fragment ions with the carfentanil standard, again suggesting a close structural relationship to carfentanil. There is a notable absence of the major peaks 2 (C<sub>15</sub>H<sub>20</sub>O<sub>2</sub>N<sup>+</sup>, 246.14886 *m/z*), and 3 (C<sub>6</sub>H<sub>9</sub>O<sub>2</sub><sup>+</sup>, 113.05971 *m/z*) observed in the carfentanil spectrum, as well as the presence of the minor peaks 11 (C<sub>5</sub>H<sub>8</sub>ON<sup>+</sup>, 98.06004 *m/z*), and 12 (C<sub>14</sub>H<sub>19</sub>ON<sub>2</sub><sup>+</sup>, 231.14919 *m/z*) not observed in the carfentanil standard MS/MS spectra (Figure 6.5B). This MS/MS pattern of NPS 2 supports the putative identification as desmethylcarfentanil amide since the methyl ester group on carfentanil is contained within the fragment ion that produces peak 2 (C<sub>15</sub>H<sub>20</sub>O<sub>2</sub>N<sup>+</sup>, 246.14886 *m/z*) and the replacement of this group with an amide is expected to then form a C<sub>14</sub>H<sub>19</sub>ON<sub>2</sub><sup>+</sup> (231.14919 *m/z*) ion, as is observed in Figure 6.5B. The C<sub>6</sub>H<sub>9</sub>O<sub>2</sub><sup>+</sup> (113.05971 *m/z*) ion observed in the carfentanil MS/MS spectrum contains the methyl ester group found in carfentanil and the C<sub>5</sub>H<sub>8</sub>ON<sup>+</sup> (98.06004 *m/z*) ion observed contains the amide group found in desmethylcarfentanil acid instead. The mass difference

between peaks 2 and 12, and peaks 3 and 11 is the same, 14.99967 amu, representing the difference between the methyl ester group ( $\text{COOCH}_3$ , 59.01276 amu) and the amide group ( $\text{CONH}_2$ , 44.01309 amu).

Similarly, NPS2 produces many of the same fragment ions as carfentanil and is also missing peaks 2 and 3. The most intense peak in the MS/MS spectrum is peak 13 ( $\text{C}_{14}\text{H}_{18}\text{O}_2\text{N}^+$ , 232.13321  $m/z$ ) and is unique to this compound. Because it is a unique peak, it can be used as the quantifier ion, even at unit resolution (e.g., QqQ), while avoiding interference from the  $^{13}\text{C}$  isotopic peak of NPS1. The analogous fragment observed in the carfentanil spectrum, peak 2 ( $\text{C}_{15}\text{H}_{20}\text{O}_2\text{N}^+$ , 246.14886  $m/z$ ) supports the structural change from the methyl ester group observed in carfentanil ( $\text{COOCH}_3$ , 59.01276 amu) to a carboxylic acid group ( $\text{COOH}$ , 44.99711 amu) since the mass difference of 14.01565 amu is observed between peaks 2 and 13. Furthermore, the  $\text{C}_6\text{H}_9\text{O}_2^+$  (113.05971  $m/z$ ) ion observed in the carfentanil MS/MS spectrum contains the methyl ester group found in carfentanil which is replaced by the  $\text{C}_5\text{H}_7\text{O}_2^+$  (98.06004  $m/z$ ) ion observed in the higher collision energy MS/MS spectra of NPS2 (Figure 6.13, Table 6.14). Of the possible isomers listed for NPS2, desmethylcarfentanil acid and benzyl carfentanil are the only structures that can explain the observed  $\text{C}_{14}\text{H}_{18}\text{O}_2\text{N}^+$  fragment ion (232.13321  $m/z$ ). Benzyl carfentanil can be ruled out because there is a strong 105.06988  $m/z$  ion ( $\text{C}_8\text{H}_9^+$ ) observed in the 50% HCD collision energy MS/MS spectra of the sample (Figure 6.13), but benzyl carfentanil lacks an ethylbenzene group and is therefore unable to form this fragment ion. While acetyl carfentanil could produce the observed 105.06988  $m/z$  ion, it does not produce a 232.13321  $m/z$  ion (the most intense peak observed in the sample spectrum), and would instead produce a 246.14886  $m/z$  ion, which is not observed in Figure 6.5C. The same is true for 3,4-methylenedioxy fentanyl, which also produces the 188.1434  $m/z$  ion that is typical of most fentanyl analogs, but does not produce any fragment ions related to carfentanil analogues/precursors (246, 232, 113  $m/z$ ).<sup>523</sup> Figure 6.5C thus supports the putative identification of NPS2 as desmethylcarfentanil acid, since all of the other isomers cannot explain the observed MS/MS pattern. This is further supported by experimental high-resolution MS/MS spectra of benzyl carfentanil, acetyl carfentanil, and 3,4-methylenedioxyfentanyl available from the HighResNPS database (Figure 6.14).<sup>524</sup> The unique peaks 14, 15, and 16 in Figure 6.5C could not be assigned a chemical formula by the software and are hypothesized to have arisen from a interferent. During HRAM-MS analysis, a precursor ion isolation width of 0.4  $m/z$  was used, and the full scan spectra of these drug samples shows multiple interferents within the mass window of  $381.2 \pm 0.4$   $m/z$  (Figure 6.15). Fragmentation pathways leading to the unique ions observed for carfentanil, desmethylcarfentanil amide, and desmethylcarfentanil acid are shown in Figure 6.16. Furthermore, since NPS1 and NPS2 always co-occur, it is logical that they are very likely part of the same synthetic pathway and would therefore only have minor changes between them as well.

Results from a Toronto, Ontario-based laboratory performing Health Canada exempted drug testing at the Canadian Centre for Addiction and Mental Health revealed that NPS1 and NPS2 are not exclusive to the Victoria, British Columbia illicit drug supply. They have

recently detected these compounds on both used drug paraphernalia and in drug samples. The same chemical formulae were determined from their Orbitrap HRAM data, and experimental MS/MS spectra observed by this group are nearly identical to those presented in this manuscript (Figure 6.17 and Figure 6.18). Liquid chromatography (details in Supporting Information, page 16) was also used to determine the retention times of the compounds and separate components for MS analysis (Figure 6.19). The order of elution, or retention time (RT), demonstrates the change in polarity from the latest eluted carfentanil peak (RT = 11.18 min) to the putative identified desmethylcarfentanil amide (RT = 9.80 min) and then the earliest eluted putative identified desmethylcarfentanil acid (RT = 8.67 min). The appearance of these carfentanil structural analogs in illicit drug supplies thousands of kilometres apart, suggests that they may be present in many other areas of North America, or beyond.

### 6.5.3 $\mu$ -Opioid Receptor Binding Modeling

The physiological effects of opioids are initiated by stimulation of the  $\mu$ -opioid receptor.<sup>525</sup> The binding of an agonist to the  $\mu$ -opioid receptor is the first event in a complex intracellular signaling path that results in not only the desired analgesic effect but also the toxic side effects. Therefore, to assess the potential biological activity of NPS1 and NPS2, it is important to determine whether they interact with the  $\mu$ -opioid receptor in a similar fashion as a known agonist like carfentanil. *In silico* virtual screening techniques such as molecular docking are ideal tools for rapid assessment of relative binding affinities of similar ligands.

To this end, carfentanil, desmethylcarfentanil amide (NPS1), and desmethylcarfentanil acid (NPS2) were docked with the  $\mu$ -opioid receptor using the genetic algorithm implemented in AutoDock Vina.<sup>518</sup> Previous docking studies<sup>520, 526</sup> have shown that fentanyl binds in a specific orientation: a salt bridge is formed between the protonated piperidine ring and ASP147, the hydrophobic N-phenethyl group points towards the interior of the receptor, and the amide group points towards the exterior of the cell. The docked fentanyl conformation from Ellis *et al*<sup>520</sup> was used as a starting point. As a control, the fentanyl structure was re-docked using our protocol to ensure we could reproduce the literature pose. Once this was confirmed, the procedure was repeated with carfentanil, NPS1, and NPS2. Nine different binding poses were generated for each ligand, and the pose with the highest docking score that matched the known binding orientation of fentanyl was selected for further analysis. The resulting binding poses of both NPS were found to be virtually identical to carfentanil, with minor differences in the position of the N-phenethyl group (Figure 6.6). The salt bridge to ASP147 that was observed in the docked fentanyl was also observed in both carfentanil and the NPS. In addition to ASP147, the oxygen of TYR326 is oriented towards the protonated piperidine ring of the ligands, indicating a potential stabilizing interaction. For all three ligands, the N-phenethyl group forms a hydrophobic interaction with MET151 and TRP293, and the N-phenylpropanamide group is in close proximity to GLN124 and SER55.

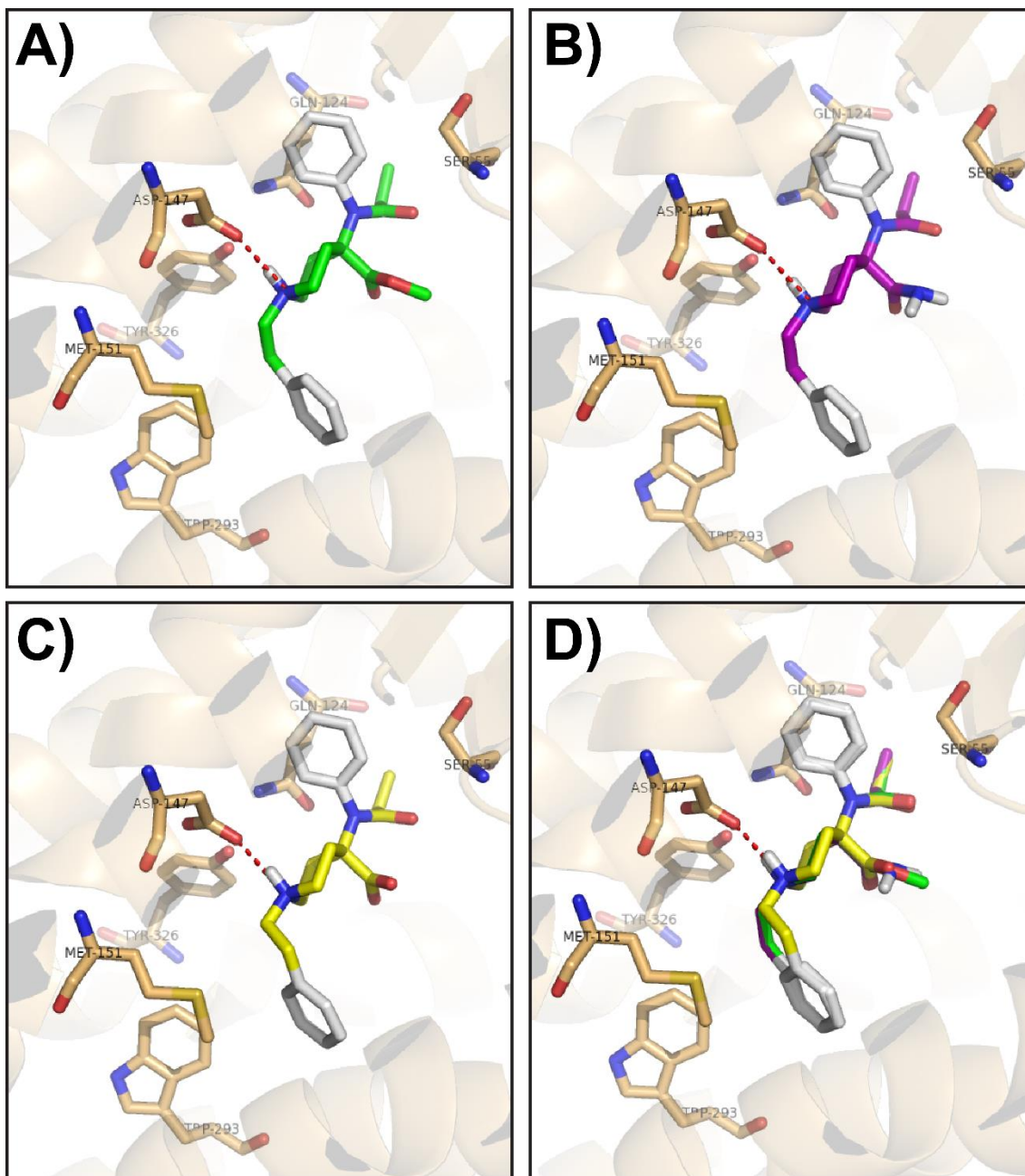


Figure 6.6.  $\mu$ -Opioid receptor binding poses of (a) carfentanil, (b) desmethylcarfentanil amide (new psychoactive substance 1), (c) desmethylcarfentanil acid (new psychoactive substance 2), and (d) all three structures overlaid.

The binding energies of NPS1 and NPS2 relative to carfentanil were calculated in AutoDock Vina to be very similar, with desmethylcarfentanil amide (NPS1) having a slightly higher (0.544 kJ/mol) and desmethylcarfentanil acid (NPS2) a slightly lower (-0.171 kJ/mol) relative binding energy – likely due to the differences in electrostatic properties of the side chains on the substituted piperidine ring. The docking calculations indicate that the NPS' interact with the  $\mu$ -opioid receptor in a similar manner as carfentanil, and with similar energies (Table 6.3).

Table 6.3. Calculated binding energies of the carfentanil structural analogs on the  $\mu$ -opioid receptor and their binding energies relative to carfentanil.

Ligand or drug	Binding energy (kJ/Mol)	Relative binding energy (kJ/Mol)
Carfentanil	-36.104	0.000
Desmethylcarfentanil amide	-35.560	0.544
Desmethylcarfentanil acid	-36.275	-0.171

This preliminary *in silico* data suggests that these NPS may bind to the  $\mu$ -opioid receptor in a similar orientation and with similar affinities as carfentanil. However, the docking simulations are static calculations and do not allow observation of conformational changes in the receptor as a result of drug binding. Computationally expensive, long timescale molecular dynamics calculations may result in more accurate binding energies and allow for assessment of the downstream effects of binding.

## 6.6 Conclusion

Two carfentanil synthetic intermediates/structural analogs, desmethylcarfentanil amide and desmethylcarfentanil acid, were identified in carfentanil-containing drug samples by paper spray mass spectrometry, and structurally characterized using high resolution mass spectrometry. The two structural analogs always co-occur and appeared in 53% of the carfentanil drug samples examined, suggesting that they are by-products/precursors of a common synthetic route for carfentanil. Results from  $\mu$ -opioid receptor binding modeling indicate that these structural analogs have similar binding poses and binding affinities as carfentanil. Future research should determine the scope of prevalence of these drugs within different regional supplies; it may also be useful to ascertain whether these compounds are being purposefully introduced or whether they are accidental by-products. Isolation of these compounds by liquid chromatography and further structural analysis by nuclear magnetic resonance could provide definitive structural identification. Furthermore, long timescale molecular dynamics calculations and toxicology studies should be undertaken to accurately assess the biological activities of these compounds and their potential contributions to fatal overdose events within the context of the ongoing opioid overdose crisis.

## 6.7 Supporting information

Table 6.4. Selected reaction monitoring (SRM) transition parameters of carfentanil and carfentanil-d<sub>5</sub> on the Fortis QqQ mass spectrometer.

Compound	Precursor Ion ( <i>m/z</i> )	Product Ion ( <i>m/z</i> )	Tube Lens (V)	Collision Energy (eV)	Source Fragmentation (V)
Carfentanil	395.2	335.2	100	18.18	14.0
		363.2	100	13.42	14.0
		246.2	100	21.05	14.0
Carfentanil-d <sub>5</sub>	400.3	340.2	101	18.27	14.7
		368.2	101	13.21	14.7
		246.2	101	20.96	14.7

Table 6.5. Paper spray mass spectrometry analyte-independent parameters.

Parameter	Value
Ionization polarity	Positive
Spray voltage (V)	3800
Q1 FWHM resolution	0.7
Q3 FWHM resolution	1.2
Argon CID gas pressure (mTorr)	2
Sweep gas (Arb)	0
Ion transfer tube (°C)	300

Table 6.6. Paper spray mass spectrometry solvent dispense conditions.

Rewet Solvent Dispense (10 µL)	
Aliquot #	Delay (s)
1	1
2	1
Spray Solvent Dispense (10 µL)	
Aliquot #	Delay (s)
1	1
2	1
3	1
4	2
5	2
6	2
7	3
8	3
9	5
10	5
11	5

Table 6.7. LOD and LLOQ values for carfentanil in prepared drug samples (solution B).

Analyte	LOD <sup>a</sup> (ng/mL)	LOD <sup>a</sup> (w/w%)	LLOQ <sup>b</sup> (ng/mL)	LLOQ <sup>b</sup> (w/w%)
Carfentanil	0.73	0.018	2.23	0.056

<sup>a</sup> LOD was calculated as 3.3 times the standard deviation of the lowest calibrator (1 ng/mL, n=6) divided by the slope of the calibration curve

<sup>b</sup> LLOQ was calculated as 10 times the standard deviation of the lowest calibrator (1 ng/mL, n=6) divided by the slope of the calibration curve

Table 6.8. Paper spray mass spectrometry calibration of carfentanil (n = 6, 11 levels @ [1, 2.5, 5, 10, 15, 25, 40, 75, 125, 250, 500 ng/mL], [carfentanil-*d*<sub>5</sub>] = 100 ng/mL) on the Fortis QqQ mass spectrometer.

Analyte	Slope ( $\times 10^{-2}$ )	y-intercept ( $\times 10^{-3}$ )	R <sup>2</sup>
Carfentanil	1.332	- 8.034	0.9945

Table 6.9. Orbitrap Exploris 120 parameters.

Parameter	Value
Ionization polarity	Positive
Spray voltage (V)	3400
Ion transfer tube temperature (°C)	320
Resolution	120,000
RF lens (%)	70
Injection time	Automatic
Use EASY-IC™	On
EASY-IC™ calibrant	Fluoranthene
HCD gas	Nitrogen
MS <sup>2</sup> isolation width (m/z)	0.4

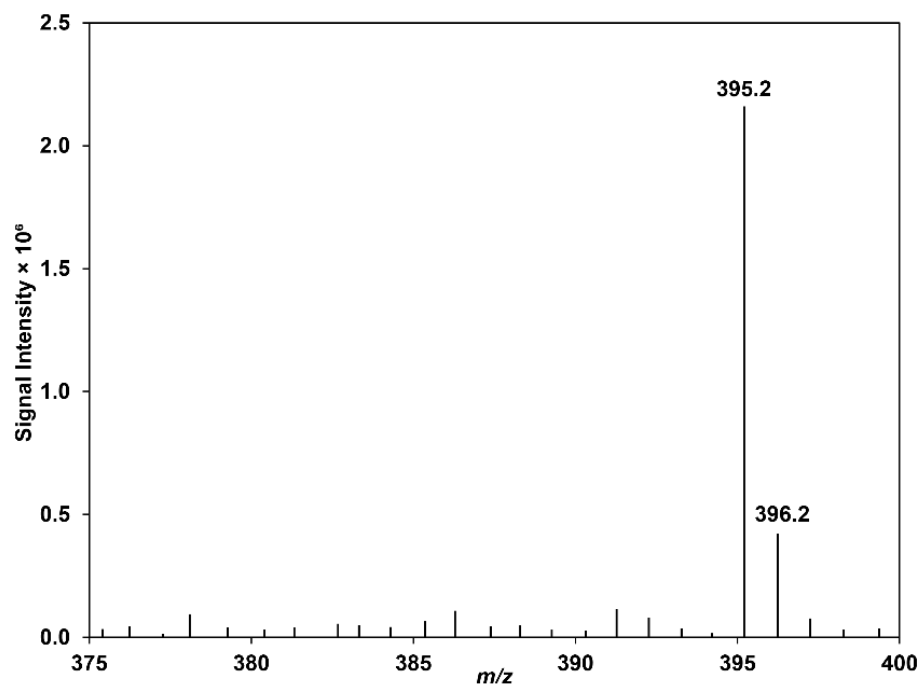


Figure 6.7. QqQ PS-MS full scan of 10  $\mu\text{L}$  of 200 ng/mL carfentanil analytical reference standard in methanol.

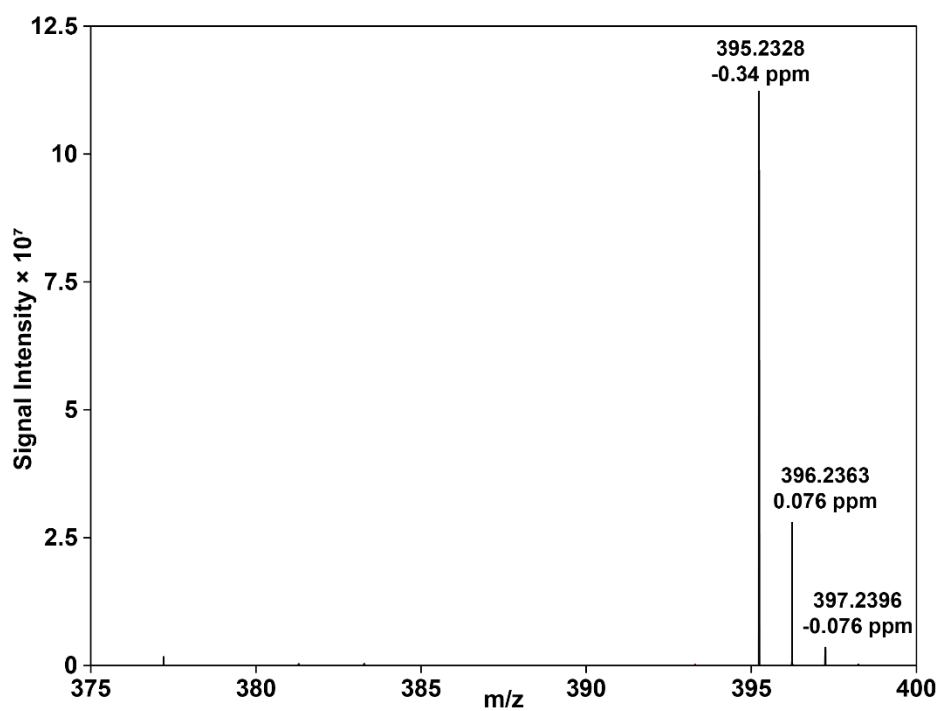


Figure 6.8. HRAM direct infusion electrospray full scan of 200 ng/mL carfentanil analytical reference standard in methanol.

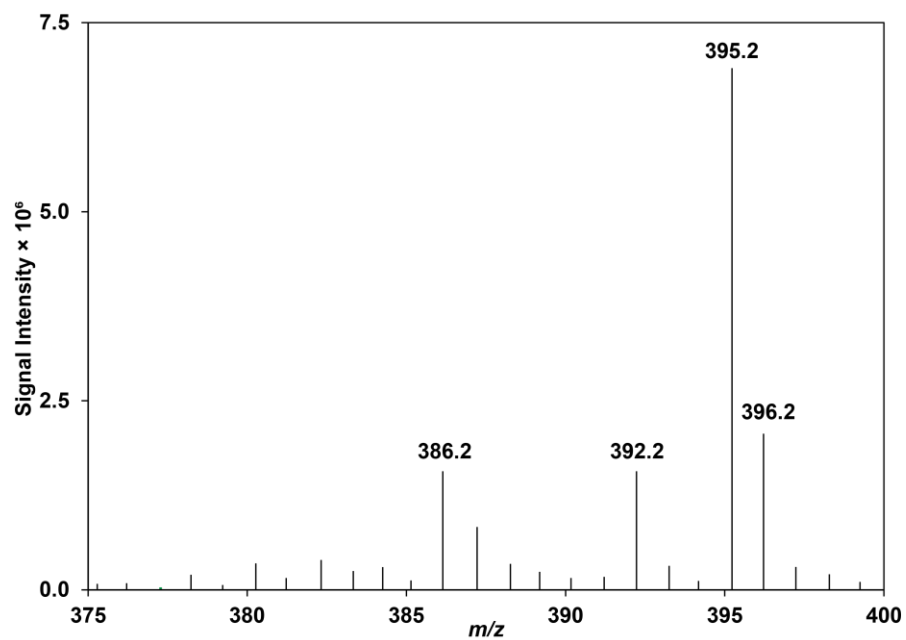


Figure 6.9. QqQ PS-MS full scan of a carfentanil-containing drug sample, no peaks present at 380.2 or 381.2  $m/z$ .

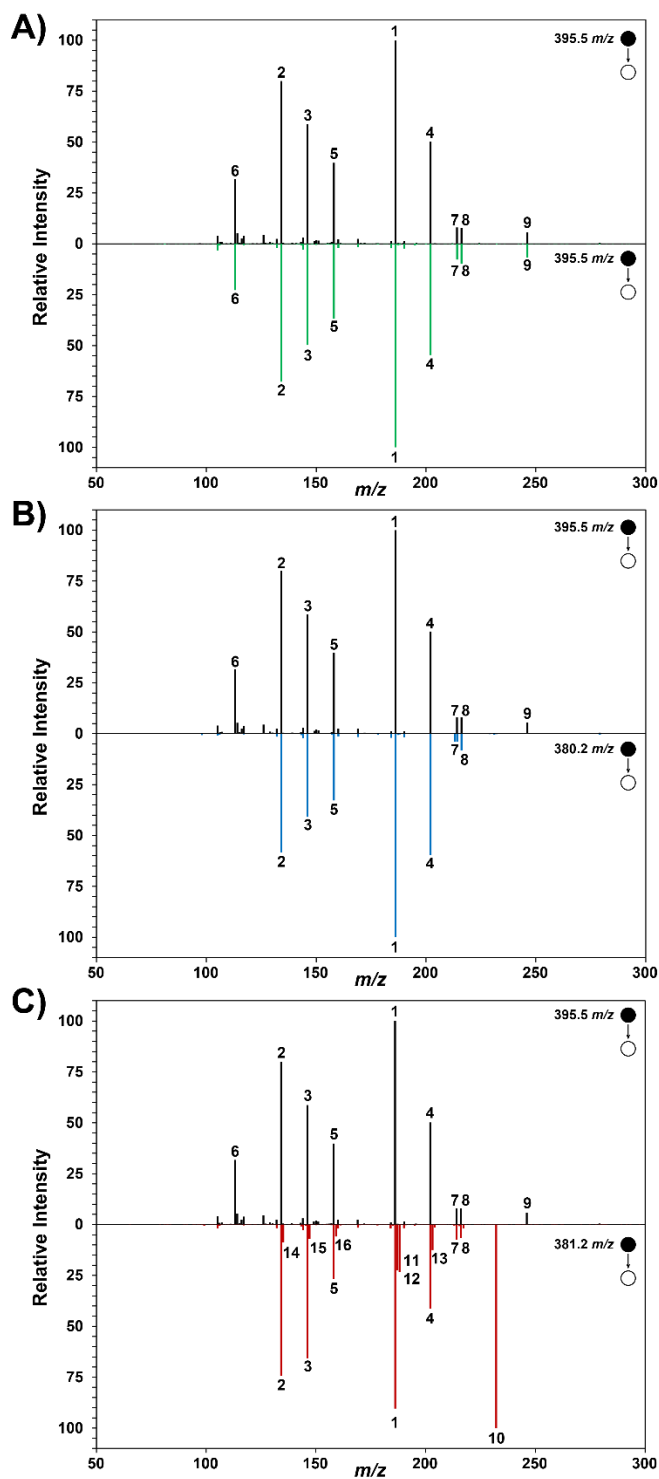


Figure 6.10. Comparison of PS-MS QqQ product ion scans (50-400  $m/z$ ) of carfentanil analytical reference standard (top) to a carfentanil-containing drug sample (bottom): **A)** carfentanil ( $m/z$  395.5), **B)** NPS1 ( $m/z$  380.2), and **C)** NPS2 ( $m/z$  381.2). Collision energy ramp of 5-50 V.

Table 6.10. Relative intensity data for the comparison of PS-MS QqQ product ion scans collected with a collision energy ramp of 5-50 V of a carfentanil analytical reference standard and a carfentanil-containing drug sample. A '-' indicates a relative intensity > 1.

Peak #	m/z	Relative Intensity			
		Carfentanil Standard	Carfentanil m/z 395.2	NPS1 m/z 380.2	NPS2 m/z 381.2
1	186.1	100	100	100	90.4
2	134.1	80.0	67.8	58.2	74.5
3	146.1	58.7	49.7	40.9	65.8
4	202.1	50.2	54.6	59.6	41.4
5	158.1	39.8	36.9	32.8	26.7
6	113.1	31.8	22.8	-	-
7	214.1	8.0	7.6	3.9	7.6
8	216.1	7.9	9.9	8.2	6.6
9	246.1	5.7	6.8	-	-
10	232.1	-	-	-	100
11	187.1	-	-	-	22.6
12	188.1	-	-	-	23.4
13	203.1	-	-	-	12.5
14	135.1	-	-	-	8.8
15	147.1	-	-	-	7.0
16	159.1	-	-	-	5.9

Table 6.11. Peak heights of NPS1 and 2 relative to the peak height of carfentanil in the same sample.

Sample #	NPS1 relative peak height	NPS2 relative peak height	[Carfentanil] (w/w%)	Estimated [NPS 1] (w/w%)	Estimated [NPS 2] (w/w%)
1	1.4	0.2	0.08	0.11	0.02
2	1.3	0.5	0.05	0.07	0.02
3	0.4	1.2	0.50	0.21	0.60
4	0.6	1.3	0.48	0.30	0.62
5	0.3	1.3	0.09	0.03	0.12
6	1.7	1.4	0.74	1.27	1.03
7	0.1	1.4	0.58	0.09	0.81
8	1.4	1.4	0.65	0.89	0.91
9	0.7	1.4	0.79	0.57	1.14
10	1.3	1.6	0.47	0.60	0.75
11	1.8	1.6	0.78	1.44	1.28
12	3.2	1.7	0.06	0.19	0.10
13	1.0	1.7	0.14	0.15	0.24
14	1.7	1.7	0.33	0.57	0.57
15	1.8	1.9	0.24	0.43	0.45
16	2.2	2.3	0.62	1.34	1.42
17	6.9	2.3	0.15	1.03	0.35
18	3.1	2.5	0.30	0.93	0.76
19	3.6	3.1	0.24	0.86	0.74
20	0.5	3.1	0.20	0.09	0.61
21	3.7	3.1	0.24	0.89	0.74
22	6.9	3.4	0.21	1.44	0.71
23	7.2	3.4	0.29	2.07	0.98
24	3.5	3.7	0.06	0.21	0.23
25	6.5	3.8	0.47	3.07	1.77
26	7.1	3.9	0.13	0.93	0.51
27	8.0	4.0	0.33	2.65	1.32
28	3.7	4.0	0.49	1.81	1.97
29	7.5	4.1	0.54	4.04	2.22
30	7.9	4.2	0.22	1.73	0.91
31	8.2	4.3	0.07	0.57	0.30

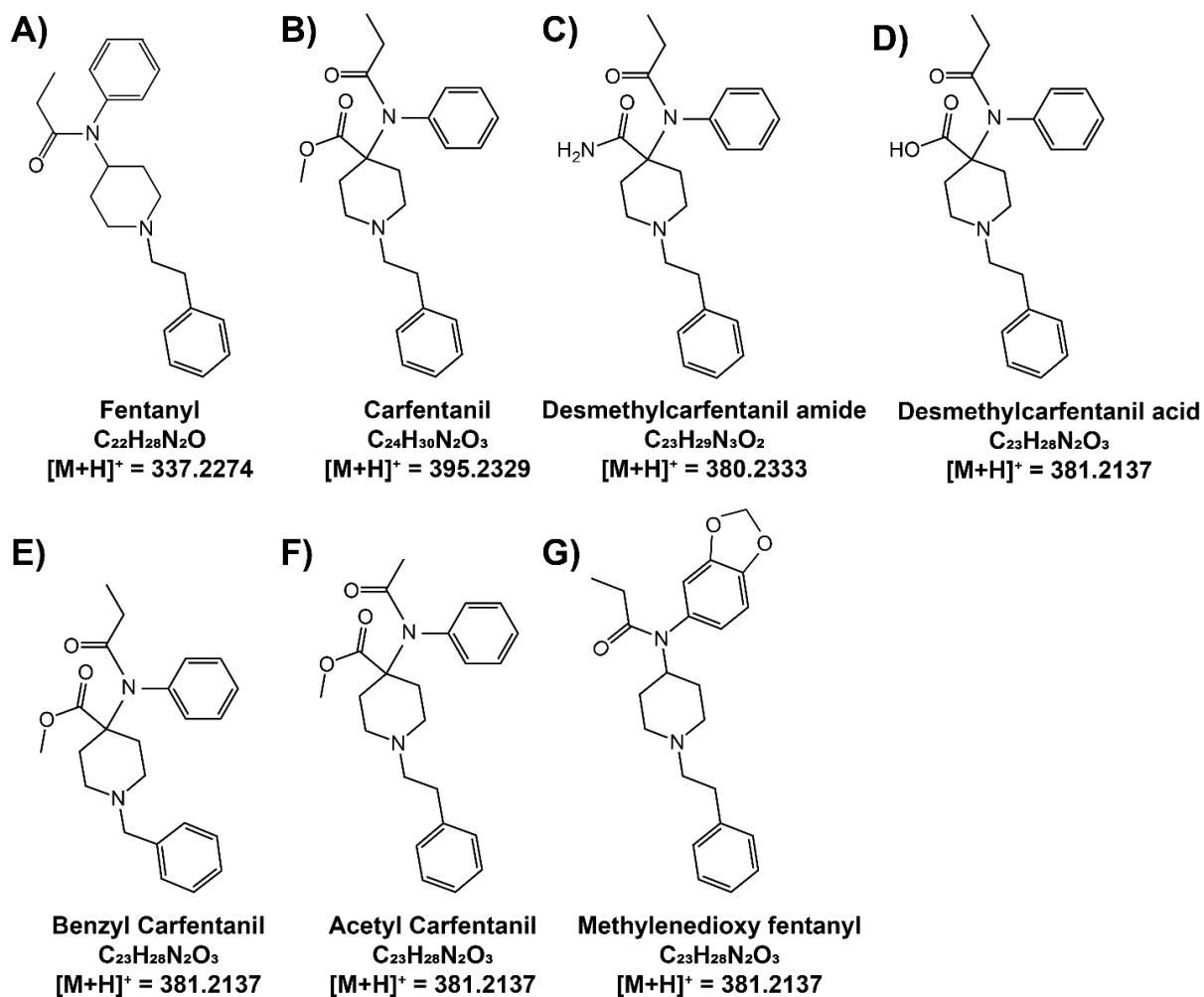


Figure 6.11. Chemical structures of A) fentanyl, B) carfentanil, C) carfentanil amide (NPS1), D) desmethylocarfentanil acid (NPS2), E) benzyl carfentanil, and F) acetyl carfentanil, G) methylenedioxy fentanyl.

Table 6.12. Elements in use for elemental composition determination within Freestyle software. A mass tolerance of 5.00 ppm was used for prediction and fragment matching.

Isotope	Mass (amu)	Minimum #	Maximum #
$^{14}N$	14.0031	0	10
$^{16}O$	15.9949	0	15
$^{12}C$	12.0000	0	30
$^1H$	1.0078	0	60
$^{32}S$	31.9721	0	10
$^{35}Cl$	34.9689	0	4
$^{31}P$	30.9738	0	10

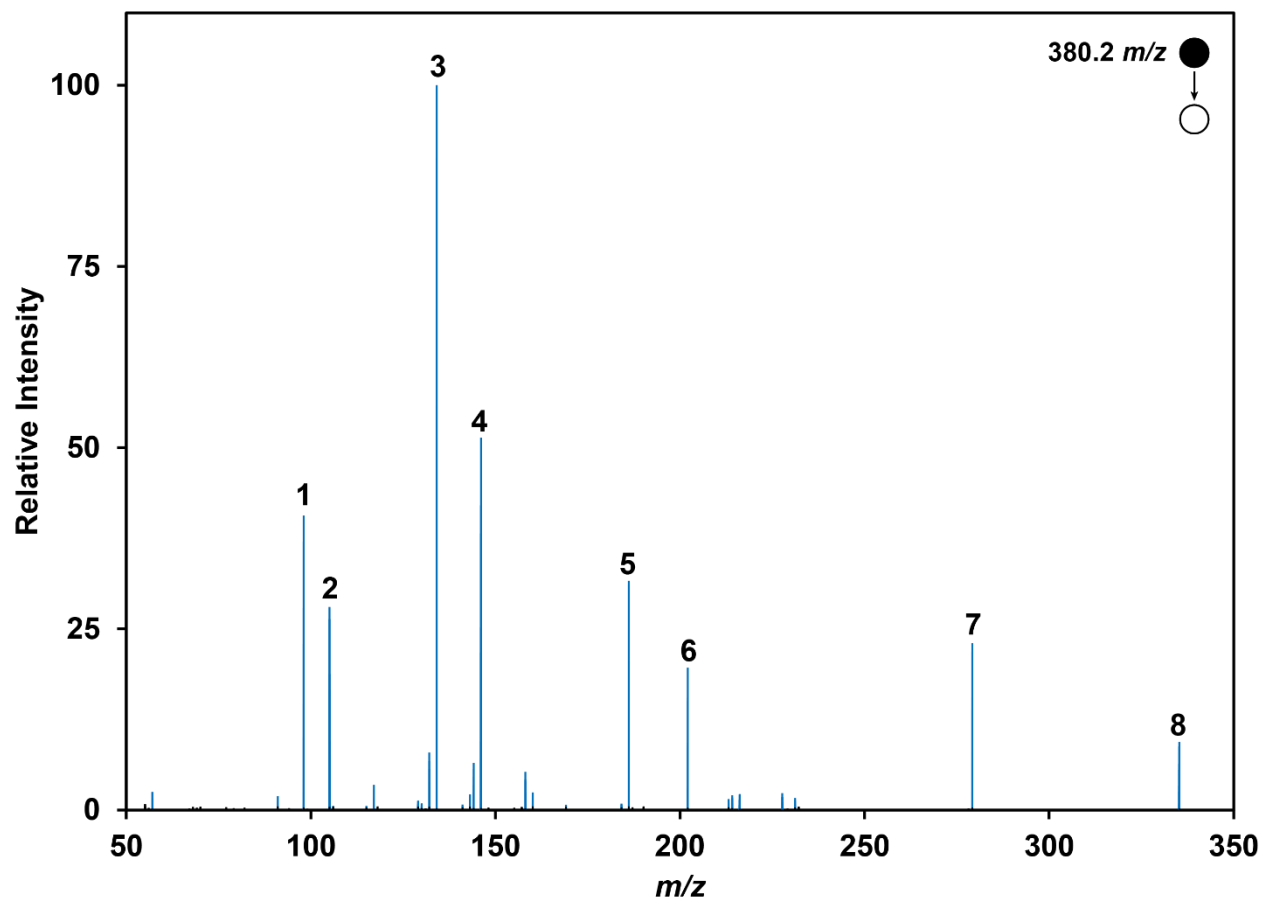


Figure 6.12. Direct infusion HRAM-MS/MS spectrum (50-350  $m/z$ ) of NPS1 (380.2  $m/z$ ) in a drug sample, 50% HCD collision energy.

Table 6.13. Fragment identities, mass errors, and relative intensities of fragments from HRAM-MS/MS of NPS1 (380.2  $m/z$ ) at 50% HCD collision energy.

Peak number	Elemental Composition	Theoretical Mass ( $m/z$ )	Measured Mass ( $m/z$ )	Mass Error (ppm)	Relative Intensity
1	$C_5H_8ON^+$	98.06004	98.0600	-0.13	40.7
2	$C_8H_9^+$	105.06988	105.0699	-0.07	26.3
3	$C_9H_{12}N^+$	134.09643	134.0964	-0.04	100
4	$C_{10}H_{12}N^+$	146.09643	146.0964	0.07	51.4
5	$C_{13}H_{16}N^+$	186.12773	186.1277	0.03	31.2
6	$C_{13}H_{16}ON^+$	202.12264	202.1227	0.05	19.6
7	$C_{19}H_{23}N_2^+$	279.18558	279.1855	-0.10	23.0
8	$C_{22}H_{27}ON_2^+$	335.21179	335.2117	-0.27	9.4

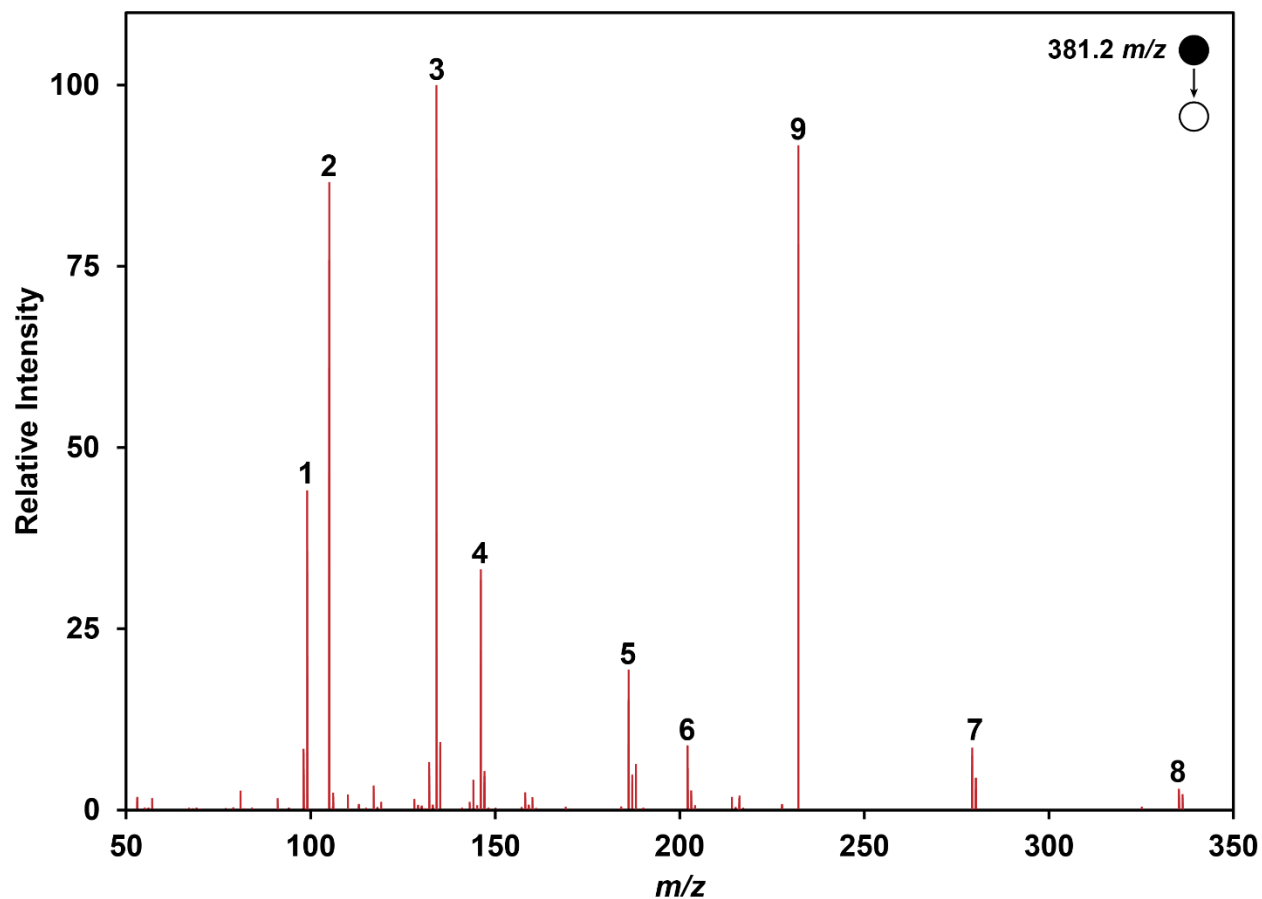


Figure 6.13. Direct infusion HRAM-MS/MS spectrum (50-350  $m/z$ ) of NPS2 in a drug sample, 50% HCD collision energy.

Table 6.14. Fragment identities, mass errors, and relative intensities of fragments from HRAM-MS/MS of NPS2 (381.2  $m/z$ ) at 50% HCD collision energy.

Peak number	Elemental Composition	Theoretical Mass ( $m/z$ )	Measured Mass ( $m/z$ )	Mass Error (ppm)	Relative Intensity
1	$C_5H_7O_2^+$	99.04406	99.0441	0.19	44.1
2	$C_8H_9^+$	105.06988	105.0699	-0.14	86.6
3	$C_9H_{12}N^+$	134.09643	134.0965	0.19	100
4	$C_{10}H_{12}N^+$	146.09643	146.0965	0.27	33.2
5	$C_{13}H_{16}N^+$	186.12773	186.1278	0.36	19.4
6	$C_{13}H_{16}ON^+$	202.12264	202.1227	0.42	8.8
7	$C_{19}H_{23}N_2^+$	279.18558	279.1856	0.23	8.6
8	$C_{22}H_{27}ON_2^+$	335.21179	335.2119	0.19	2.2
9	$C_{14}H_{18}O_2N^+$	232.13321	232.1333	0.21	91.7

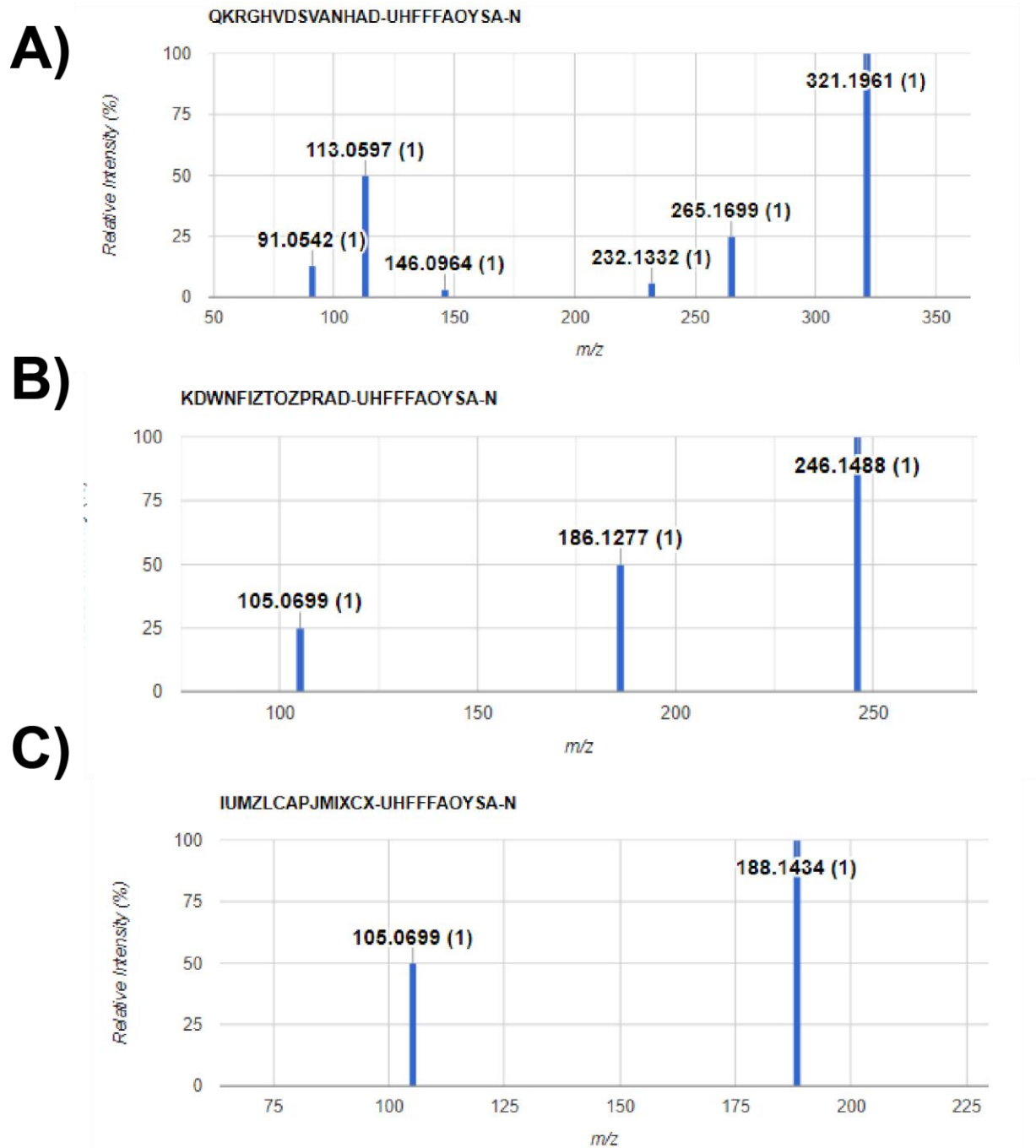


Figure 6.14. HRAM-MS/MS spectra of A) benzyl carfentanil, B) acetyl carfentanil, and C) 3,4-methylenedioxyfentanyl from the HighResNPS database.\*

\*Mardal M, Andreasen MF, Mollerup CB, Stockham P, Telving R, Thomaidis NS, et al. HighResNPS.com: An Online Crowd-Sourced HR-MS Database for Suspect and Non-targeted Screening of New Psychoactive Substances. *J Anal Toxicol.* 2019;43(7):520-7.

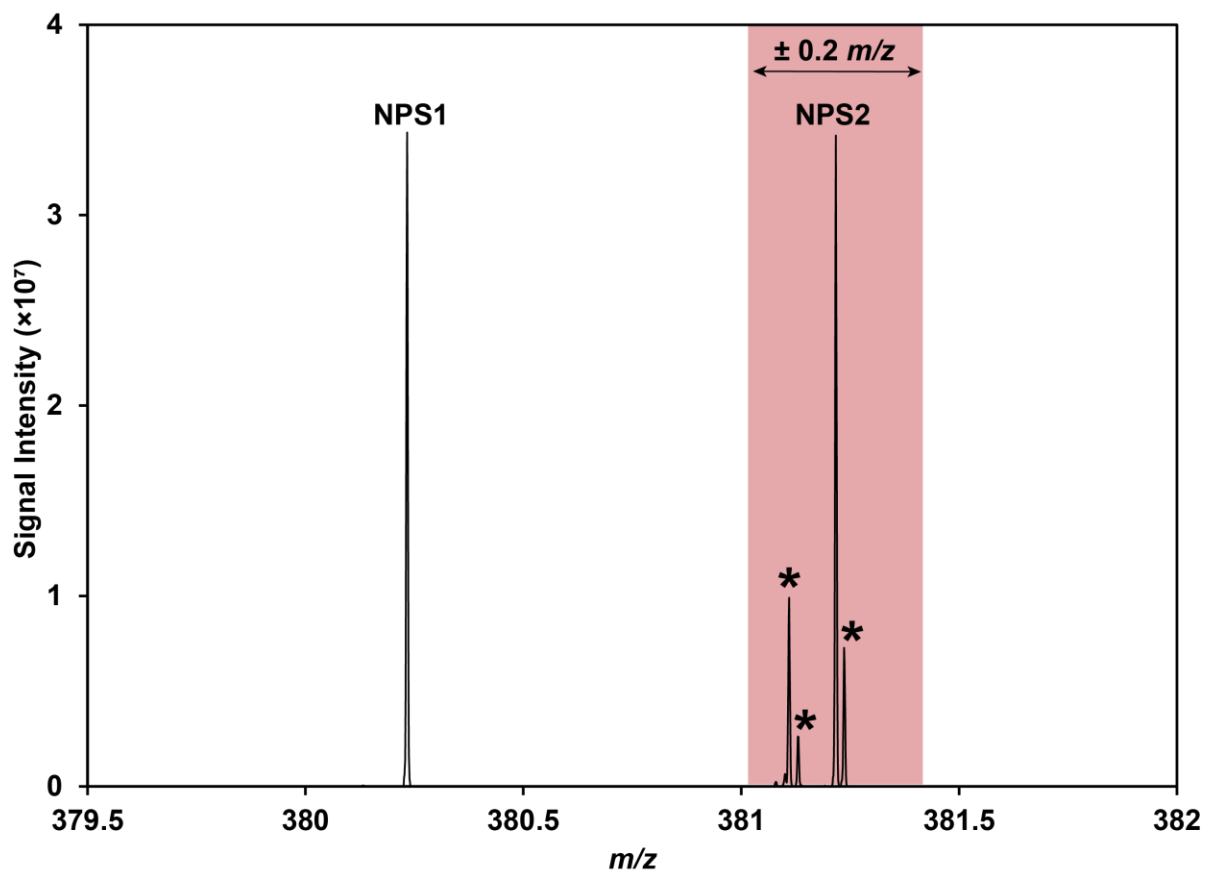


Figure 6.15. HRAM-MS full scan mass spectrum (379.5 – 382  $m/z$ ) of a carfentanil-containing drug sample. Red box schematically indicates the 0.4  $m/z$  isolation width for MS/MS. \*Interferents within the isolation window of NPS2.

Note: the resolution of the peaks observed here is after orbitrap analysis. Each of the peaks observed would have a width of  $\sim 0.4 m/z$  prior to entry into the orbitrap and thus separation of NPS2 from the interferents\* is not possible for MS/MS measurements.

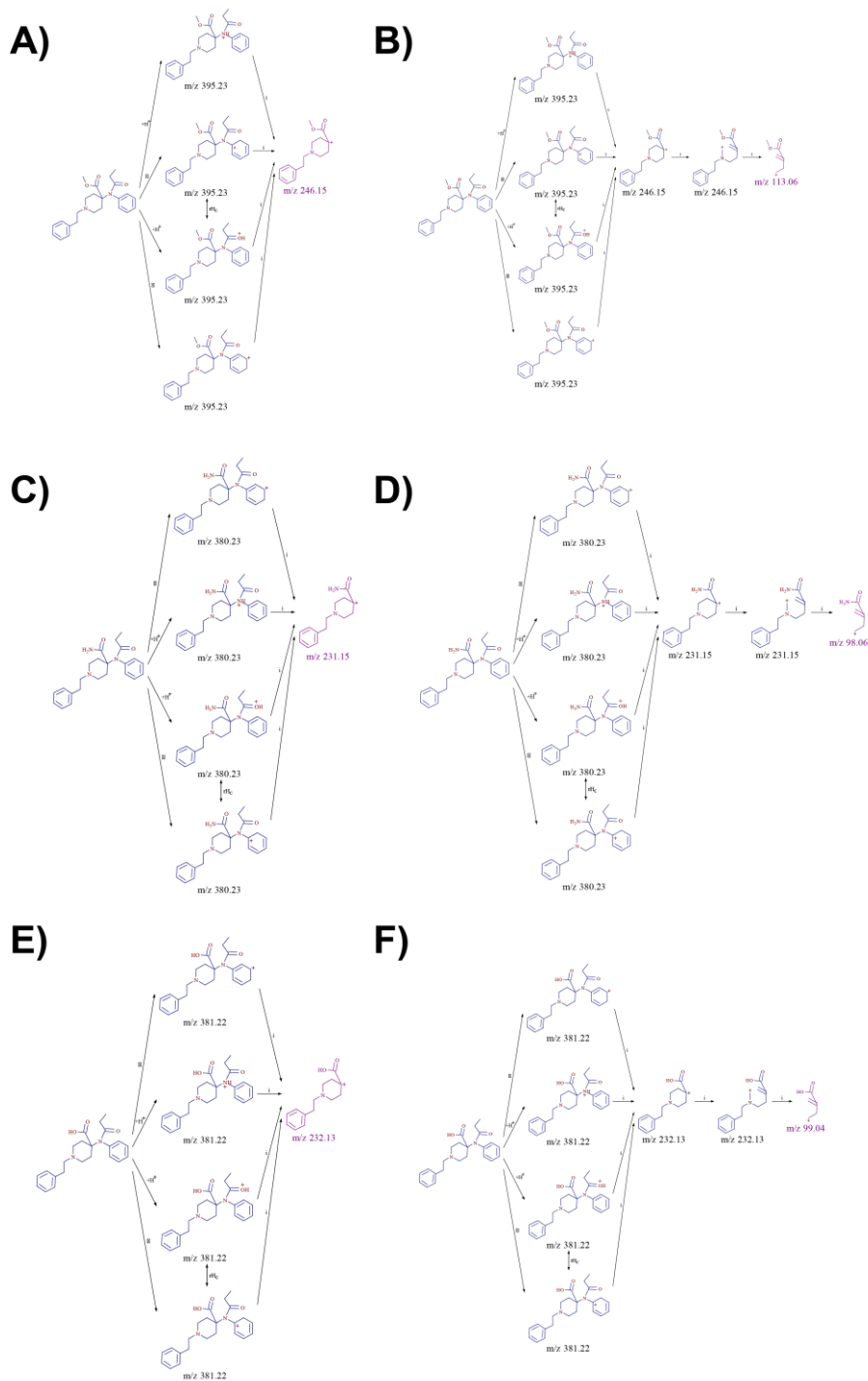


Figure 6.16. Fragmentation pathways leading to the formation of the A) 246.15  $m/z$  ion from carfentanil, B) 113.06  $m/z$  ion from carfentanil, C) 231.15  $m/z$  ion from desmethylcarfentanil amide, D) 98.06  $m/z$  ion from desmethylcarfentanil amide, E) 232.13  $m/z$  ion from desmethylcarfentanil acid, and F) 99.04  $m/z$  ion from desmethylcarfentanil acid. Generated with Thermo Fisher Mass Frontier™ 7.0 Spectral Interpretation Software.

### Liquid chromatography mass spectrometry:

A Thermo Scientific™ Q Exactive™ Plus Hybrid Quadrupole-Orbitrap™ Mass Spectrometer coupled with Vanquish™ ultra-high-performance liquid chromatography system was used for all LC-MS experiments. The mass spectrometer was operated under full scan / data dependent MS/MS mode (75 – 80 m/z). The LC column was a Phenomenex Kinetex® F5 (100 x 2.1 mm, 5 μ, 100Å). The column was subjected to 0.5 mL/min flow with the gradient from 98:2 to 2:98 (10 mM ammonium formate in water : 10 mM ammonium formate in methanol) for 15 minutes.

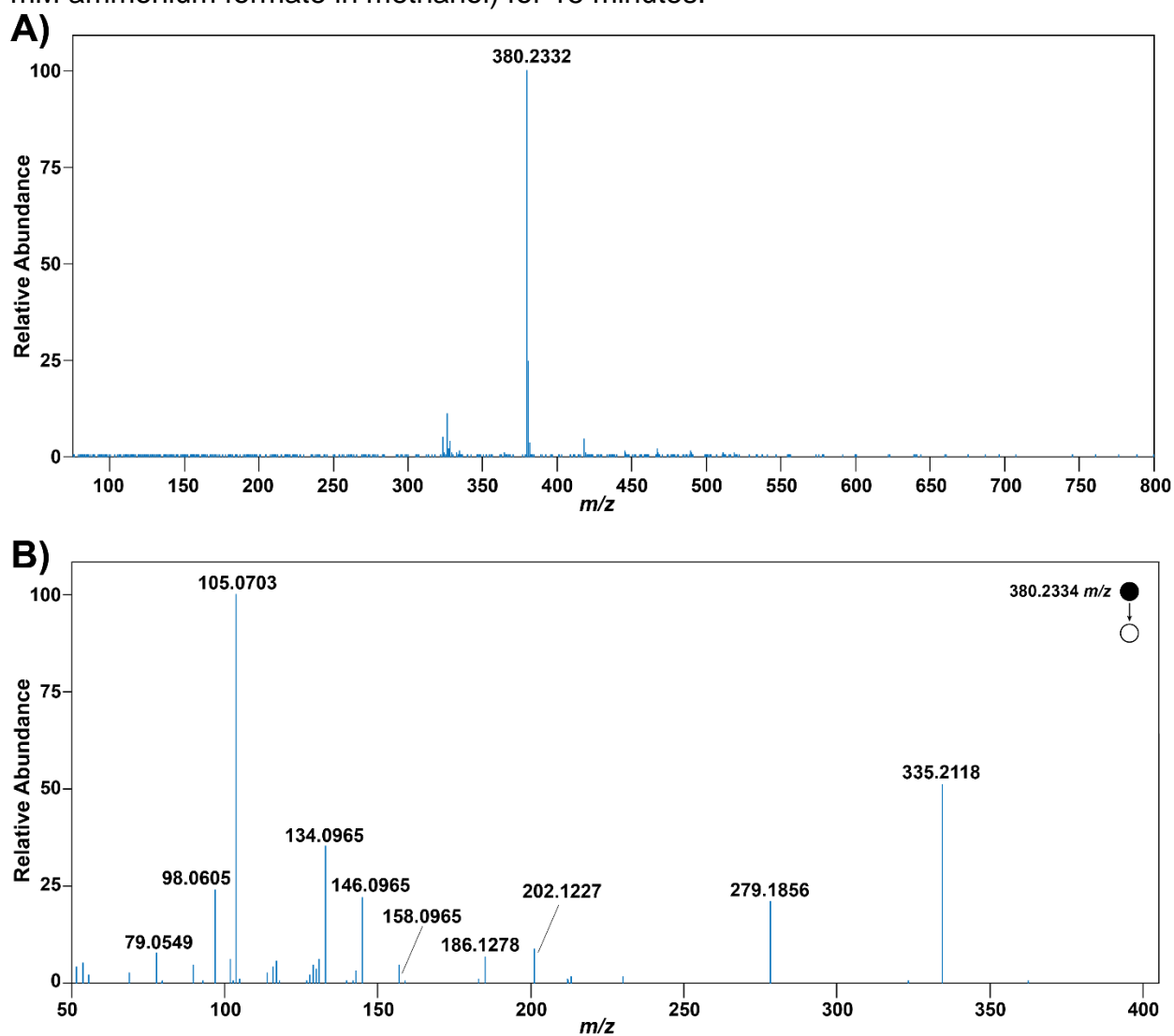


Figure 6.17. LC-MS/MS (Orbitrap HRAM) data from Canadian Centre for Addiction and Mental Health (Toronto) for a used drug paraphernalia sample. A) Full scan (75 – 800 m/z) mass spectrum at retention time 9.80 minutes and B) MS/MS spectrum (50 – 400 m/z) of 380.2334 m/z, retention time 9.80 minutes, 66.67 V HCD collision energy.

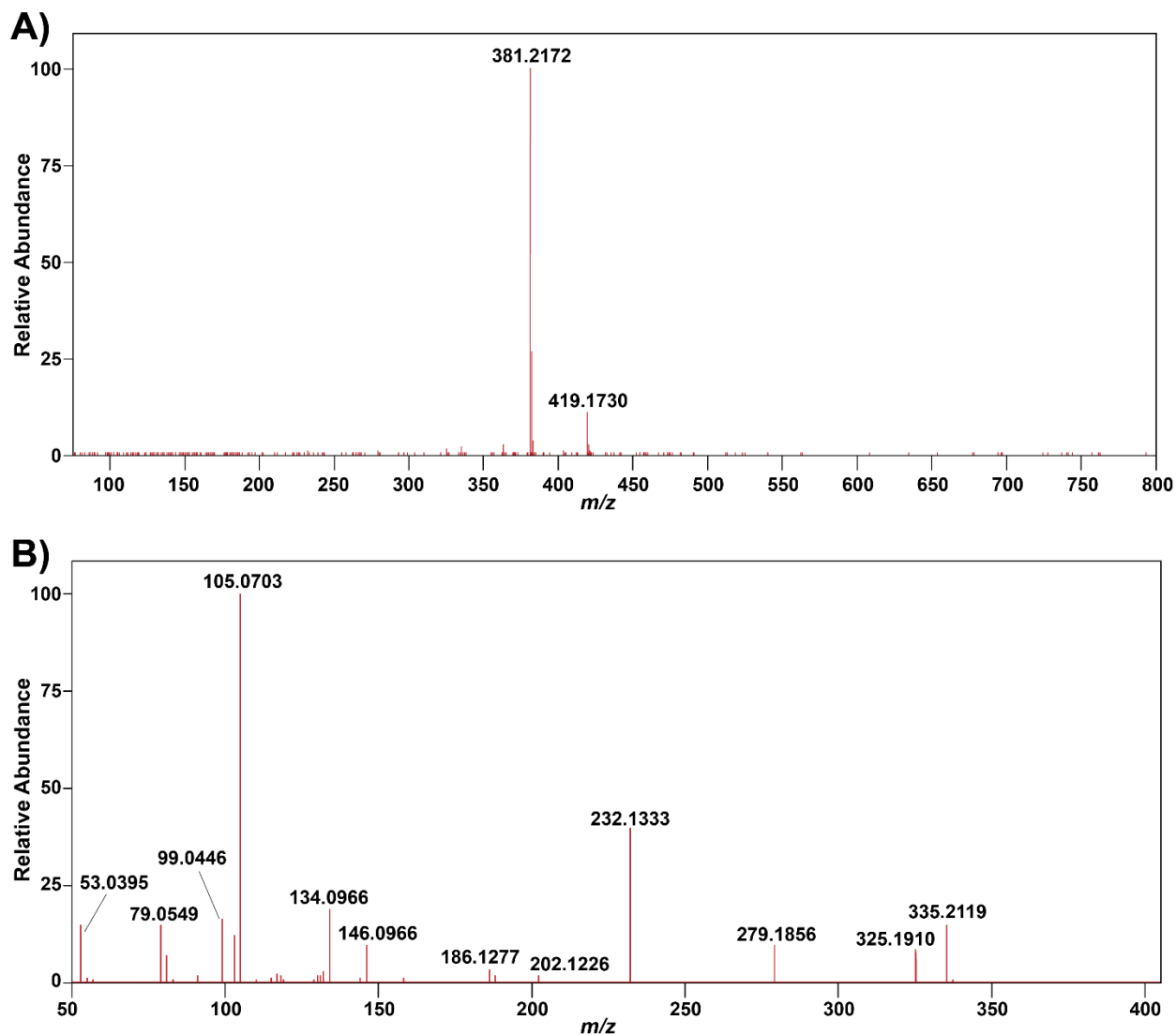


Figure 6.18. LC-MS/MS (Orbitrap HRAM) data from Canadian Centre for Addiction and Mental Health (Toronto) for a used drug paraphernalia sample. A) Full scan (75 – 800  $m/z$ ) mass spectrum at retention time 8.67 minutes and B) MS/MS spectrum (50 – 400  $m/z$ ) of 381.2366  $m/z$ , retention time 8.67 minutes, 66.67 V HCD collision energy.

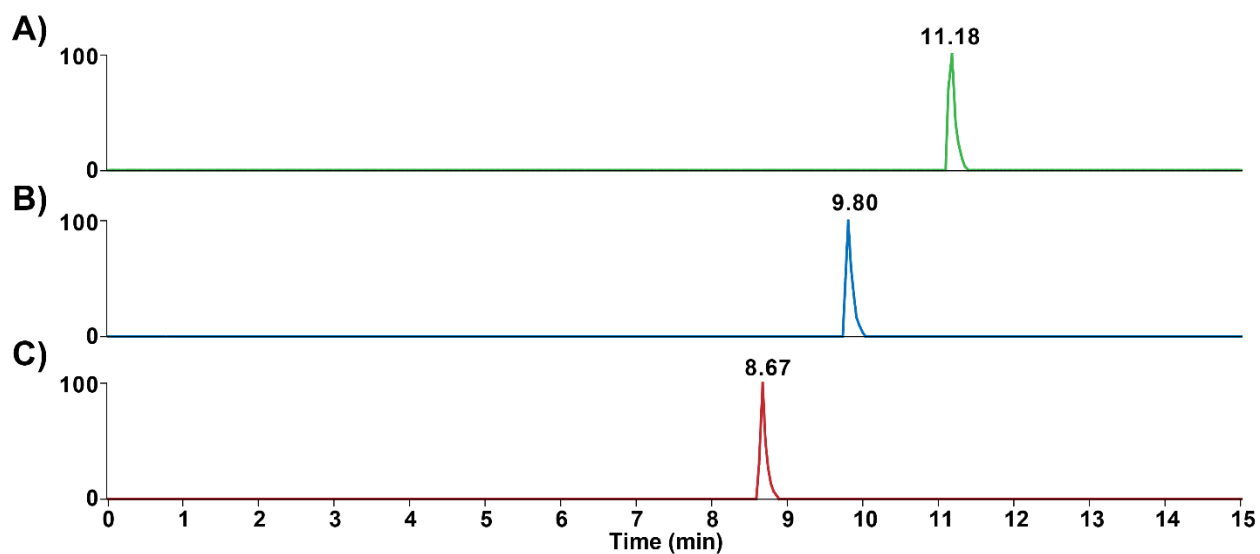


Figure 6.19. LC-MS (Orbitrap HRAM) chromatograms from the Canadian Centre for Addiction and Mental Health (Toronto) of a used paraphernalia sample. A) Carfentanil ( $m/z$  395.2309 - 395.2349, 11.18 min), B) desmethylcarfentanil amide ( $m/z$  380.2314 - 380.2352, 9.80 min), and C) desmethylcarfentanil acid ( $m/z$  381.2154 - 381.2192, 8.67 min).

## 7 Conclusions and Outlook

Paper spray mass spectrometry has been developed for the successful quantitative analysis of drugs of abuse (DoA) in different matrices for a variety of applications. The capstone of this dissertation is the development of PS-MS for drug checking applications and is transferable to forensic applications. Chapter 3 discussed the initial development of PS-MS as a drug checking technology prior to the testing of real street drug samples. Fentanyl analogs were spiked into pharmaceutical drug powder slurries to mimic street drug samples and the results demonstrated quantitative, precise, and accurate measurements for a variety of target drugs that could be achieved within minutes with relative ease. Chapter 4 built upon these initial results and extended the analysis to the analysis of actual drug samples that were submitted by PWUD. This work was the first ever demonstration of PS-MS as a quantitative drug checking tool in a real-world application. During this initial pilot test, over 100 drug samples were checked over the period of two days. The success of this trial, and the continued development of the method, led to the adoption of PS-MS as a drug checking technique by the Vancouver Island Drug Checking Project. Since its adoption, the scope of target drugs has widened, and the use of non-targeted scan functions for unknowns identification has been expanded; to date, over 12,000 drug samples have been quantitatively analyzed by PS-MS with this methodology. Chapter 6 demonstrates some of the success of the non-targeted scan functions and the benefits gained using high resolution mass spectrometry. Desmethylcarfentanil acid and desmethylcarfentanil amide were identified in nearly half of all carfentanil containing drug samples that were tested. These compounds had not been previously discussed in drug checking or drug testing literature and demonstrate the potential for PS-MS to identify NPS in the ever-changing drug supply. Chapter 5 addressed some of the limitations of paper spray ionization. The inherent soft ionization of PS-MS does not lend itself to the analysis of nonpolar analytes or those with weakly acidic functional groups. Reactive paper spray ionization was employed and successfully demonstrated to overcome these limitations and to analyze cannabinoids in oral fluid and urine samples at levels able to meet forensic and clinical cutoff values.

PS-MS has been demonstrated as a quantitative, sensitive, and selective tool for the measurement of DoA in street drugs. While the non-targeted discovery of two structural analogs of carfentanil was demonstrated in Chapter 6, there is massive potential to improve the functionality of non-targeted analysis with PS-MS. The coupling of PS-MS to high resolution instruments will be required for any efforts attempting to identify unknowns in street drug matrices. PS-MS spectra observed when analyzing DoA are incredibly complex due to not only the complicated nature of the drug matrix, but from the ionization of compounds present in the paper sampling strip itself. High resolution mass spectrometry will allow for proper differentiation between background ions and analyte ions. Further, soft ionization and MS/MS libraries have been rapidly developing and can be applied to the routine analysis of DoA by PS-MS to allow for putative identification of unknowns. The use of exclusion lists of known matrix components (i.e.,

cutting agents) and ions produced from blank paper strips will significantly improve the identification of unknowns. Furthermore, rapid front-end separation strategies, such as ion mobility, can be employed to significantly reduce background interferences and should be explored. Another avenue of interest is the application of different polymers or materials in lieu of paper for specific analyses. In the opinion of the author, PS-MS is perfectly positioned for use and further development as a rapid, adaptable, sensitive, and quantitative analytical strategy for the identification and measurement of novel NPS in the ever-changing illicit drug supply.

## References

1. H. M. Brown, T. J. McDaniel, P. W. Fedick and C. C. Mulligan, *Analytical Methods*, 2020, **12**, 3974-3997.
2. K. Tamama, *Clinica Chimica Acta*, 2021, **514**, 40-47.
3. R. Compton, 2017, **US Department of Transportation**, 1-44.
4. D. N. Correa, J. M. Santos, L. S. Eberlin, M. N. Eberlin and S. F. Teunissen, *Anal Chem*, 2016, **88**, 2515-2526.
5. M.-Z. Huang, S.-C. Cheng, Y.-T. Cho and J. Shiea, *Analytica chimica acta*, 2011, **702**, 1-15.
6. C. R. Ferreira, K. E. Yannell, A. K. Jarmusch, V. Pirro, Z. Ouyang and R. G. Cooks, *Clinical chemistry*, 2016, **62**, 99-110.
7. L.-P. Li, B.-S. Feng, J.-W. Yang, C.-L. Chang, Y. Bai and H.-W. Liu, *Analyst*, 2013, **138**, 3097-3103.
8. H. Wang, J. Liu, R. G. Cooks and Z. Ouyang, *Angewandte Chemie*, 2010, **122**, 889-892.
9. J. Liu, H. Wang, N. E. Manicke, J.-M. Lin, R. G. Cooks and Z. Ouyang, *Analytical chemistry*, 2010, **82**, 2463-2471.
10. E. Nadelmann and L. LaSalle, *Harm Reduction Journal*, 2017, **14**, 1-7.
11. D. O'Keefe, A. Ritter, M. Stooze, C. Hughes and P. Dietze, *Sucht*, 2020, **66**.
12. B. Wallace, T. van Roode, P. Burek, B. Pauly and D. Hore, *Drugs: Education, Prevention and Policy*, 2022, 1-10.
13. M. Karamouzian, C. Dohoo, S. Forsting, R. McNeil, T. Kerr and M. Lysyshyn, *Harm reduction journal*, 2018, **15**, 1-8.
14. L. Gozdziński, A. Rowley, S. A. Borden, A. Saatchi, C. G. Gill, B. Wallace and D. K. Hore, *International Journal of Drug Policy*, 2022, **102**, 103611.
15. M. Ramsay, L. Gozdziński, A. Larnder, B. Wallace and D. Hore, *Vibrational Spectroscopy*, 2021, **114**, 103243.
16. T. C. Green, J. N. Park, M. Gilbert, M. McKenzie, E. Struth, R. Lucas, W. Clarke and S. G. Sherman, *International Journal of Drug Policy*, 2020, **77**, 102661.
17. K. W. Tupper, K. McCrae, I. Garber, M. Lysyshyn and E. Wood, *Drug and alcohol dependence*, 2018, **190**, 242-245.
18. S. A. Borden, A. Saatchi, E. T. Krogh and C. G. Gill, *Analytical Science Advances*, 2020, **1**.
19. S. W. G. f. F. Toxicology, *Journal of Analytical Toxicology*, 2013, **37**, 452-474.
20. S. A. Borden, A. Saatchi, G. W. Vandergrift, J. Palaty, M. Lysyshyn and C. G. Gill, *Drug and Alcohol Review*, 2021.
21. S. A. Borden, A. Saatchi, J. Palaty and C. G. Gill, *Analyst*, 2022, **147**, 3109-3117.
22. S. A. Borden, S. R. Mercer, A. Saatchi, E. Wong, C. M. Stefan, H. Wiebe, D. K. Hore, B. Wallace and C. G. Gill, *Drug Testing and Analysis*, 2023.
23. S. A. Borden, J. Palaty, V. Termopoli, G. Famigliani, A. Cappiello, C. G. Gill and P. Palma, *Mass Spectrometry Reviews*, 2020.
24. Z. Cao, E. Kaleta and P. Wang, *Journal of analytical toxicology*, 2015, **39**, 335-346.

25. J. Alcántara-Durán, D. Moreno-González, M. Beneito-Cambra and J. F. García-Reyes, *Talanta*, 2018, **182**, 218-224.
26. O. Papini, C. Bertucci, S. P. da Cunha, N. A. G. dos Santos and V. L. Lanchote, *Journal of pharmaceutical and biomedical analysis*, 2006, **40**, 389-396.
27. J. A. Dickerson, T. J. Laha, M. B. Pagano, B. R. O'Donnell and A. N. Hoofnagle, *Journal of analytical toxicology*, 2012, **36**, 541-547.
28. M. J. Roslawski, R. P. Remmel, A. Karanam, I. E. Leppik, S. E. Marino and A. K. Birnbaum, *Therapeutic drug monitoring*, 2019, **41**, 357-370.
29. B. Malik-Wolf, S. Vorce, J. Holler and T. Bosy, *Journal of analytical toxicology*, 2014, **38**, 171-176.
30. P. Sitasuwan, C. Melendez, M. Marinova, M. Spruill and L. A. Lee, *Journal of analytical toxicology*, 2018, **43**, 221-227.
31. P. Anastas and J. Warner, *New York*, 1998.
32. P. T. Anastas, *Critical reviews in analytical chemistry*, 1999, **29**, 167-175.
33. A. Gałuszka, Z. Migaszewski and J. Namieśnik, *TrAC Trends in Analytical Chemistry*, 2013, **50**, 78-84.
34. C. L. Arthur and J. Pawliszyn, *Analytical chemistry*, 1990, **62**, 2145-2148.
35. J. Płotka-Wasyłka, N. Szczepańska, M. de la Guardia and J. Namieśnik, *TrAC Trends in Analytical Chemistry*, 2015, **73**, 19-38.
36. R. Jain and R. Singh, *TrAC Trends in Analytical Chemistry*, 2016, **80**, 156-166.
37. Y. He, 2017, **35**, 14-20.
38. N. Fucci, C. Gambelunghe, K. Aroni and R. Rossi, *Therapeutic drug monitoring*, 2014, **36**, 789-795.
39. D. Z. Souza, P. O. Boehl, E. Comiran, K. C. Mariotti, F. Pechansky, P. C. Duarte, R. De Boni, P. E. Froehlich and R. P. Limberger, *Analytica chimica acta*, 2011, **696**, 67-76.
40. A. Spietelun, A. Kloskowski, W. Chrzanowski and J. Namieśnik, *Chemical reviews*, 2012, **113**, 1667-1685.
41. K. Goryński, *TrAC Trends in Analytical Chemistry*, 2019, **112**, 135-146.
42. A. Song, J. Wang, G. Lu, Z. Jia, J. Yang and E. Shi, *Forensic science international*, 2018, **290**, 49-55.
43. K. A. Alsenedi and C. Morrison, *Analytical Methods*, 2018, **10**, 1431-1440.
44. S. Gentili, C. Mortali, L. Mastrobattista, P. Berretta and S. Zaami, *Journal of pharmaceutical and biomedical analysis*, 2016, **129**, 282-287.
45. H. Fujii, B. Waters, K. Hara, M. Kashiwagi, A. Matsusue, M. Takayama and S.-i. Kubo, *Forensic Toxicology*, 2015, **33**, 61-68.
46. K. Aleksa, P. Walasek, N. Fulga, B. Kapur, J. Gareri and G. Koren, *Forensic science international*, 2012, **218**, 31-36.
47. M. Moller, K. Aleksa, P. Walasek, T. Karaskov and G. Koren, *Forensic Science International*, 2010, **196**, 64-69.
48. M. Abdel-Rehim, *Journal of Chromatography B*, 2004, **801**, 317-321.
49. M. Abdel-Rehim, *Analytica chimica acta*, 2011, **701**, 119-128.
50. E. Jagerdeo and M. Abdel-Rehim, *Journal of the American Society for Mass Spectrometry*, 2011, **20**, 891-899.
51. T. Rosado, A. Gonçalves, C. Margalho, M. Barroso and E. Gallardo, *Analytical and bioanalytical chemistry*, 2017, **409**, 2051-2063.

52. H. Miyaguchi, Y. T. Iwata, T. Kanamori, K. Tsujikawa, K. Kuwayama and H. Inoue, *Journal of Chromatography A*, 2009, **1216**, 4063-4070.
53. E. J. Magalhães, M. E. L. R. de Queiroz, M. L. de Oliveira Penido, M. A. R. Paiva, J. A. R. Teodoro, R. Augusti and C. C. Nascentes, *Journal of Chromatography A*, 2013, **1309**, 15-21.
54. D. C. Mozaner Bordin, M. N. Alves, O. G. Cabrices, E. G. de Campos and B. S. De Martinis, *Journal of analytical toxicology*, 2013, **38**, 31-38.
55. T. Kumazawa, C. Hasegawa, K. Hara, S. Uchigasaki, X. P. Lee, H. Seno, O. Suzuki and K. Sato, *Journal of separation science*, 2012, **35**, 726-733.
56. A. Sarafraz-Yazdi and A. Amiri, *TrAC Trends in Analytical Chemistry*, 2010, **29**, 1-14.
57. Y. Yamini, M. Rezazadeh and S. Seidi, *TrAC Trends in Analytical Chemistry*, 2019, **112**, 264-272.
58. H. Liu and P. K. Dasgupta, *Analytical Chemistry*, 1996, **68**, 1817-1821.
59. M. Ma and F. F. Cantwell, *Analytical Chemistry*, 1999, **71**, 388-393.
60. D. B. G. Williams, M. J. George, R. Meyer and L. Marjanovic, *Analytical chemistry*, 2011, **83**, 6713-6716.
61. W. Liu and H. K. Lee, *Analytical chemistry*, 2000, **72**, 4462-4467.
62. M. A. Jeannot, A. Przyjazny and J. M. Kokosa, *Journal of Chromatography A*, 2010, **1217**, 2326-2336.
63. S. Tang, T. Qi, P. D. Ansah, J. C. N. Fouemina, W. Shen, C. Basheer and H. K. Lee, *Trac-Trend Anal Chem*, 2018, **108**, 306-313.
64. M. Rezaee, Y. Assadi, M.-R. M. Hosseini, E. Aghaee, F. Ahmadi and S. Berijani, *Journal of Chromatography A*, 2006, **1116**, 1-9.
65. R. Jain and R. Singh, *TrAC Trends in Analytical Chemistry*, 2016, **75**, 227-237.
66. R. Jain, M. K. R. Mudiam, A. Chauhan, H. A. Khan and R. Murthy, *Bioanalysis*, 2013, **5**, 2277-2286.
67. M. A. Gardner, S. Sampsel, W. W. Jenkins and J. E. Owens, *Journal of analytical toxicology*, 2014, **39**, 118-125.
68. R. L. Cunha, W. A. Lopes and P. A. P. Pereira, *Microchemical Journal*, 2016, **125**, 230-235.
69. L. Meng, W. Zhang, P. Meng, B. Zhu and K. Zheng, *Journal of Chromatography B*, 2015, **989**, 46-53.
70. L. Meng, B. Zhu, K. Zheng and S. Fu, *Journal of Chromatography B*, 2017, **1053**, 9-15.
71. Z. Lin, J. Li, X. Zhang, M. Qiu, Z. Huang and Y. Rao, *Journal of Chromatography B*, 2017, **1046**, 177-184.
72. S. Pedersen-Bjergaard and K. E. Rasmussen, *Analytical chemistry*, 1999, **71**, 2650-2656.
73. V. Sharifi, A. Abbasi and A. Nosrati, *journal of food and drug analysis*, 2016, **24**, 264-276.
74. G. Ouyang, W. Zhao and J. Pawliszyn, *Journal of Chromatography A*, 2007, **1138**, 47-54.
75. L. do Nascimento Pantaleão, B. A. P. B. Paranhos and M. Yonamine, *Journal of Chromatography A*, 2012, **1254**, 1-7.

76. Y. Yamini, S. Seidi, R. Feizbakhsh, T. Baheri and M. Rezazadeh, *Journal of separation science*, 2014, **37**, 2364-2371.
77. A. V. de Baires, R. M. de Almeida, L. Pantaleão, T. Barcellos, S. M. e Silva and M. Yonamine, *Journal of Chromatography B*, 2015, **975**, 24-33.
78. P. G. Jessop, L. Phan, A. Carrier, S. Robinson, C. J. Dürr and J. R. Harjani, *Green Chemistry*, 2010, **12**, 809-814.
79. G. Lasarte-Aragonés, R. Lucena, S. Cárdenas and M. Valcárcel, *Talanta*, 2015, **131**, 645-649.
80. F. Xu, Q. Li, W. Wei, L. Liu and H. Li, *Chromatographia*, 2018, **81**, 1695-1703.
81. H. Maurer, *Advances in Forensic Applications of Mass Spectrometry*, Boca Raton, FL: CRC Press LLC, 2003, 1-61.
82. H. J. Leis and W. Windischhofer, *Rapid Communications in Mass Spectrometry*, 2010, **24**, 3320-3324.
83. H. J. Leis and W. Windischhofer, *Journal of separation science*, 2012, **35**, 3326-3331.
84. V. d. M. Prata, E. S. Emídio and H. S. Dorea, *Analytical and bioanalytical chemistry*, 2012, **403**, 625-632.
85. S. E. Breidi, J. Barker, A. Petroczi and D. P. Naughton, *J Anal Methods Chem*, 2012, **2012**, 1-7.
86. M. P. Elie, M. G. Baron and J. W. Birkett, *Analyst*, 2012, **137**, 255-262.
87. A. Nakamoto, M. Nishida, T. Saito, I. Kishiyama, S. Miyazaki, K. Murakami, M. Nagao and A. Namura, *Analytica chimica acta*, 2010, **661**, 42-46.
88. A.-S. M. Ingels, H. Neels, W. E. Lambert and C. P. Stove, *Journal of Chromatography A*, 2013, **1296**, 84-92.
89. M. Damm, G. Rechberger, M. Kollroser and C. O. Kappe, *Journal of Chromatography A*, 2009, **1216**, 5875-5881.
90. L.-W. Chung, K.-L. Lin, T. C.-C. Yang and M.-R. Lee, *Journal of Chromatography A*, 2009, **1216**, 4083-4089.
91. N. Sadones, E. Van Bever, J. R. Archer, D. M. Wood, P. I. Dargan, L. Van Bortel, W. E. Lambert and C. P. Stove, *Journal of Chromatography A*, 2016, **1465**, 175-183.
92. B. I. Molnár, B. Fodor, I. Boldizsár and I. Molnár-Perl, *Analytical chemistry*, 2015, **87**, 10188-10192.
93. K. Saito, R. Saito, Y. Kikuchi, Y. Iwasaki, R. Ito and H. Nakazawa, *Journal of Health Science*, 2011, **57**, 472-487.
94. M. R. Meyer and H. H. Maurer, *Analytical and bioanalytical chemistry*, 2012, **402**, 195-208.
95. A. H. Ewald, G. Fritschi and H. H. Maurer, *Journal of Chromatography B*, 2007, **857**, 170-174.
96. C. Sauer, F. T. Peters, R. F. Staack, G. Fritschi and H. H. Maurer, *Journal of Chromatography A*, 2008, **1186**, 380-390.
97. C. Sauer, F. T. Peters, C. Haas, M. R. Meyer, G. Fritschi and H. H. Maurer, *Journal of mass spectrometry*, 2009, **44**, 952-964.
98. S.-H. Tzing, A. Ghule, J.-Y. Liu and Y.-C. Ling, *Journal of Chromatography A*, 2006, **1137**, 76-83.

99. M. R. Meyer, J. Wilhelm, F. T. Peters and H. H. Maurer, *Analytical and bioanalytical chemistry*, 2010, **397**, 1225-1233.
100. J. Y. Kim, J. C. Cheong, J. I. Lee and M. K. In, *Forensic Sci Int*, 2011, **206**, e99-102.
101. T. Gunnar, K. Ariniemi and P. Lillsunde, *Journal of mass spectrometry*, 2006, **41**, 741-754.
102. N. Karlonas, A. Padarauskas, A. Ramanavicius and A. Ramanaviciene, *Journal of separation science*, 2013, **36**, 1437-1445.
103. K. Langel, T. Gunnar, K. Ariniemi, O. Rajamäki and P. Lillsunde, *Journal of Chromatography B*, 2011, **879**, 859-870.
104. A. E. Schwaninger, M. R. Meyer, M. A. Huestis and H. H. Maurer, *Journal of mass spectrometry*, 2011, **46**, 603-614.
105. Y.-H. Wu, K.-I. Lin, S.-C. Chen and Y.-Z. Chang, *Journal of Chromatography B*, 2008, **870**, 192-202.
106. A. Amirav, *Chromatographia*, 2017, **80**, 295-300.
107. M. F. Mirabelli, J.-C. Wolf and R. Zenobi, *Analyst*, 2017, **142**, 1909-1915.
108. P. Adamowicz and M. Kała, *Forensic science international*, 2010, **198**, 39-45.
109. G. Famigliini, F. Capriotti, P. Palma, V. Termopoli and A. Cappiello, *Journal of analytical toxicology*, 2015, **39**, 306-312.
110. M. Acikkol, S. Mercan and S. Karadayi, *Chromatographia*, 2009, **70**, 1295.
111. L. Gautam, S. D. Sharratt and M. D. Cole, *PloS one*, 2014, **9**, e89031.
112. S. Strano-Rossi, A. M. Bermejo, X. De La Torre and F. Botrè, *Analytical and bioanalytical chemistry*, 2011, **399**, 1623-1630.
113. S. S. Rossi, X. De La Torre and F. Botrè, *Rapid Communications in Mass Spectrometry: An International Journal Devoted to the Rapid Dissemination of Up - to - the - Minute Research in Mass Spectrometry*, 2010, **24**, 1475-1480.
114. S. Strano - Rossi, I. Álvarez, M. J. Taberner, P. Cabarcos, P. Fernández and A. M. Bermejo, *Journal of Applied Toxicology*, 2011, **31**, 649-654.
115. G. Mercieca, S. Odoardi, M. Cassar and S. S. Rossi, *Journal of pharmaceutical and biomedical analysis*, 2018, **149**, 494-501.
116. A. Orfanidis, O. Mastrogianni, A. Koukou, G. Psarros, H. Gika, G. Theodoridis and N. Raikos, *Journal of Chromatography B*, 2017, **1047**, 141-150.
117. M. Wada, R. Ikeda, N. Kuroda and K. Nakashima, *Analytical and bioanalytical chemistry*, 2010, **397**, 1039-1067.
118. M. Barroso, M. Dias, D. Vieira, M. López-Rivadulla and J. Queiroz, *Analytical and bioanalytical chemistry*, 2010, **396**, 3059-3069.
119. W.-Y. Hong, Y.-C. Ko, M.-C. Lin, P.-Y. Wang, Y.-P. Chen, L.-C. Chiueh, D. Y.-C. Shih, H.-K. Chou and H.-F. Cheng, *Journal of analytical toxicology*, 2015, **40**, 12-16.
120. G. Merola, S. Gentili, F. Tagliaro and T. Macchia, *Analytical and bioanalytical chemistry*, 2010, **397**, 2987-2995.
121. J. Y. Kim, S. H. Shin and M. K. In, *Forensic science international*, 2010, **194**, 108-114.
122. G. Ottaviani, R. Cameriere, M. Cipitelli, R. Froidi, G. Tassoni, M. Zampi and M. Cingolani, *Journal of analytical toxicology*, 2017, **41**, 32-36.
123. H. Choi, S. Baek, M. Jang, S. Lee, H. Choi and H. Chung, *Forensic science international*, 2012, **215**, 81-87.

124. G. de Oliveira Silveira, S. Loddi, C. D. R. de Oliveira, A. D. Zucoloto, L. V. G. Fruchtengarten and M. Yonamine, *Forensic Toxicology*, 2017, **35**, 125-132.
125. G. de Oliveira Silveira, Í. T. Belitsky, S. Loddi, C. D. R. de Oliveira, A. D. Zucoloto, L. V. G. Fruchtengarten and M. Yonamine, *Forensic science international*, 2016, **265**, 22-28.
126. X. Joya, M. Pujadas, M. Falcón, E. Civit, O. Garcia-Algar, O. Vall, S. Pichini, A. Luna and R. de la Torre, *Forensic science international*, 2010, **196**, 38-42.
127. G. M. Meyer, A. A. Weber and H. H. Maurer, *Drug testing and analysis*, 2014, **6**, 472-481.
128. A. Gaujac, N. Dempster, S. Navickiene, S. D. Brandt and J. B. de Andrade, *Talanta*, 2013, **106**, 394-398.
129. D. Gomes, P. G. de Pinho, H. Pontes, L. Ferreira, P. Branco, F. Remião, F. Carvalho, M. L. Bastos and H. Carmo, *Journal of Chromatography B*, 2010, **878**, 815-822.
130. K. A. Rees, P. A. McLaughlin and M. D. Osselton, *Journal of analytical toxicology*, 2012, **36**, 1-11.
131. E. S. Emídio, V. de Menezes Prata and H. S. Dórea, *Analytica Chimica Acta*, 2010, **670**, 63-71.
132. E. S. Emídio, V. de Menezes Prata, F. J. M. De Santana and H. S. Dórea, *Journal of Chromatography B*, 2010, **878**, 2175-2183.
133. F. L. Roveri, B. A. P. B. Paranhos and M. Yonamine, *Forensic science international*, 2016, **265**, 75-80.
134. L. Rosi, P. Frediani and G. Bartolucci, *Journal of pharmaceutical and biomedical analysis*, 2013, **74**, 31-38.
135. F. Ianni, K. Aroni, A. Gili, R. Sardella, M. Bacci, M. Lancia, B. Natalini and C. Gambelunghe, *Drug testing and analysis*, 2018, **10**, 968-976.
136. K. Arnhard, R. Schmid, U. Kobold and R. Thiele, *Analytical and bioanalytical chemistry*, 2012, **403**, 755-768.
137. F. Hernández, T. Portolés, E. Pitarch and F. J. López, *TrAC Trends in Analytical Chemistry*, 2011, **30**, 388-400.
138. G. Frison, L. Zamengo, F. Zancanaro, F. Tisato and P. Traldi, *Rapid Communications in Mass Spectrometry*, 2016, **30**, 151-160.
139. M. Pan, P. Xiang, Z. Yu, Y. Zhao and H. Yan, *Journal of Chromatography A*, 2019, **1587**, 209-226.
140. M. K. Woźniak, M. Wiergowski, J. Aszyk, P. Kubica, J. Namieśnik and M. Biziuk, *Journal of pharmaceutical and biomedical analysis*, 2018, **148**, 58-64.
141. A. J. Barnes, K. B. Scheidweiler and M. A. Huestis, *Therapeutic drug monitoring*, 2014, **36**, 225.
142. T. Rosado, L. Fernandes, M. Barroso and E. Gallardo, *Journal of Chromatography B*, 2017, **1043**, 63-73.
143. I. Moreno, M. Barroso, A. Martinho, A. Cruz and E. Gallardo, *Journal of Chromatography B*, 2015, **1004**, 67-78.
144. A. L. Castro, S. Tarelho, M. Dias, F. Reis and H. M. Teixeira, *Journal of pharmaceutical and biomedical analysis*, 2016, **119**, 139-144.
145. Z. Liu and J. B. Phillips, *Journal of Chromatographic Science*, 1991, **29**, 227-231.

146. L. Mondello, P. Q. Tranchida, P. Dugo and G. Dugo, *Mass spectrometry reviews*, 2008, **27**, 101-124.
147. P. Q. Tranchida, F. A. Franchina, P. Dugo and L. Mondello, *Mass spectrometry reviews*, 2016, **35**, 524-534.
148. B. Mitrevski, P. Wynne and P. J. Marriott, *Analytical and bioanalytical chemistry*, 2011, **401**, 2361-2371.
149. B. Guthery, T. Bassindale, A. Bassindale, C. T. Pillinger and G. H. Morgan, *Journal of Chromatography A*, 2010, **1217**, 4402-4410.
150. M. Schäffer, T. Gröger, M. Pütz, S. Dieckmann and R. Zimmermann, *Journal of forensic sciences*, 2012, **57**, 1181-1189.
151. T. Gröger, M. Schäffer, M. Pütz, B. Ahrens, K. Drew, M. Eschner and R. Zimmermann, *Journal of Chromatography A*, 2008, **1200**, 8-16.
152. M. Schäffer, S. Dieckmann, M. Pütz, T. Kohles, U. Pyell and R. Zimmermann, *Forensic science international*, 2013, **233**, 201-211.
153. E. A. Kolbrich, R. H. Lowe and M. A. Huestis, *Clinical chemistry*, 2008, **54**, 379-387.
154. L. K. Nahar, R. Andrews and S. Paterson, *Journal of analytical toxicology*, 2015, **39**, 519-525.
155. J. Jones, M. Jones, C. Plate and D. Lewis, *American Journal of Analytical Chemistry*, 2013, **4**, 1.
156. H. H. Maurer, *Journal of Chromatography B: Biomedical Sciences and Applications*, 1998, **713**, 3-25.
157. H. H. Maurer, *Analytical and bioanalytical chemistry*, 2007, **388**, 1315-1325.
158. M. R. Meyer and H. H. Maurer, *Analytica chimica acta*, 2016, **927**, 13-20.
159. A. T. Roemmelt, A. E. Steuer and T. Kraemer, *Analytical chemistry*, 2015, **87**, 9294-9301.
160. F. Hernández, S. Castiglioni, A. Covaci, P. de Voogt, E. Emke, B. Kasprzyk - Hordern, C. Ort, M. Reid, J. V. Sancho and K. V. Thomas, *Mass spectrometry reviews*, 2018, **37**, 258-280.
161. H. Gika, C. Virgiliou, G. Theodoridis, R. S. Plumb and I. D. Wilson, *J Chromatogr B Analyt Technol Biomed Life Sci*, 2019, **1117**, 136-147.
162. J. W. Wong, J. Wang, W. Chow, R. Carlson, Z. Jia, K. Zhang, D. G. Hayward and J. S. Chang, *Journal of agricultural and food chemistry*, 2018, **66**, 9573-9581.
163. A. A. o. F. S. Society of Forensic Toxicologists, *Journal*, 2006.
164. J. C. Eichhorst, M. L. Etter, N. Rousseaux and D. C. Lehotay, *Clinical biochemistry*, 2009, **42**, 1531-1542.
165. T. Y. Kong, J. H. Kim, J. Y. Kim, M. K. In, K. H. Choi, H. S. Kim and H. S. Lee, *Archives of pharmacal research*, 2017, **40**, 180-196.
166. D. Lung, N. Wilson, F.-T. Chatenet, C. LaCroix and R. Gerona, *Clinical Toxicology*, 2016, **54**, 319-323.
167. B. Han, H. Min, M. Jeon, B. Kang and J. Son, *Drug testing and analysis*, 2019, **11**, 382-391.
168. A. Cappiello, G. Famiglini, V. Termopoli, H. Trufelli, R. Zazzeroni, S. Jacquilleot, L. Radici and O. Saib, *Analytical chemistry*, 2011, **83**, 8537-8542.
169. K. Deventer, O. Pozo, A. Verstraete and P. Van Eenoo, *TrAC Trends in Analytical Chemistry*, 2014, **55**, 1-13.

170. T. R. Fiorentin, A. J. Krotulski, D. M. Martin, T. Browne, J. Triplett, T. Conti and B. K. Logan, *Journal of forensic sciences*, 2019, **64**, 888-896.
171. N. Langer, R. Lindigkeit, H. M. Schiebel, L. Ernst and T. Beuerle, *Drug testing and analysis*, 2014, **6**, 59-71.
172. E. Partridge, S. Trobbiani, P. Stockham, T. Scott and C. Kostakis, *Journal of analytical toxicology*, 2018, **42**, 220-231.
173. A. T. Caspar, A. B. Kollas, H. H. Maurer and M. R. Meyer, *Talanta*, 2018, **176**, 635-645.
174. M. De Boeck, L. Dubrulle, W. Dehaen, J. Tytgat and E. Cuypers, *Talanta*, 2018, **180**, 292-299.
175. M. De Boeck, G. Damilano, W. Dehaen, J. Tytgat and E. Cuypers, *Talanta*, 2018, **184**, 369-374.
176. G. Mafra, A. A. Vieira, J. Merib, J. L. Anderson and E. Carasek, *Analytica chimica acta*, 2019, **1063**, 159-166.
177. F. Accioni, M. Nieddu, P. Corona and G. Boatto, *J Anal Toxicol*, 2019, DOI: 10.1093/jat/bkz039, 1-7.
178. F.-L. Sauvage, F. Saint-Marcoux, B. Duretz, D. Deporte, G. Lachatre and P. Marquet, *Clinical chemistry*, 2006, **52**, 1735-1742.
179. A. J. Pedersen, P. W. Dalsgaard, A. J. Rode, B. S. Rasmussen, I. B. Müller, S. S. Johansen and K. Linnet, *Journal of separation science*, 2013, **36**, 2081-2089.
180. M. Sundström, A. Pelander, V. Angerer, M. Hutter, S. Kneisel and I. Ojanperä, *Analytical and bioanalytical chemistry*, 2013, **405**, 8463-8474.
181. K. B. Palmquist and M. J. Swortwood, *Forensic science international*, 2019, **297**, 189-197.
182. I. N. Petersen, C. Tortzen, J. L. Kristensen, D. S. Pedersen and T. Breindahl, *Journal of analytical toxicology*, 2013, **37**, 291-297.
183. A. E. Steuer, J. Raeber, C. Steuer, M. I. Boxler, D. A. Dornbierer, O. G. Bosch, B. B. Quednow, E. Seifritz and T. Kraemer, *Drug testing and analysis*, 2019, **11**, 813-823.
184. R. Heltsley, A. Depriest, D. L. Black, T. Robert, Y. H. Caplan and E. J. Cone, *J Anal Toxicol*, 2011, **35**, 357-359.
185. R. P. Grant, *TrAC Trends in Analytical Chemistry*, 2016, **84**, 51-60.
186. L. Roche, J. Pinguet, P. Herviou, F. Libert, C. Chenaf, A. Eschalier, N. Authier and D. Richard, *Clinica Chimica Acta*, 2016, **455**, 46-54.
187. A. G. Helfer, J. A. Michely, A. A. Weber, M. R. Meyer and H. H. Maurer, *Analytica chimica acta*, 2017, **965**, 83-95.
188. C. Laphorn, F. Pullen and B. Z. Chowdhry, *Mass spectrometry reviews*, 2013, **32**, 43-71.
189. M. Joshi, B. Cetroni, A. Camacho, C. Krueger and A. J. Midey, *Forensic science international*, 2014, **244**, 196-206.
190. K. J. Adams, C. E. Ramirez, N. F. Smith, A. C. Muñoz-Muñoz, L. Andrade and F. Fernandez-Lima, *Talanta*, 2018, **183**, 177-183.
191. D. Remane, D. Wetzels and F. T. Peters, *Analytical and bioanalytical chemistry*, 2014, **406**, 4411-4424.
192. C. T. F. o. F. Services, 2003.

193. C. Tunney and C. Cullen, RCMP expect massive spike in blood test requests with new impaired driving law, <https://www.cbc.ca/news/politics/rcmp-bodily-fluid-lab-1.4859854> ).
194. N. B. Tiscione, R. Miller, X. Shan and D. Tate Yeatman, *Journal of analytical toxicology*, 2017, **41**, 530-535.
195. B. C. Netzel, K. W. Cradic, E. T. Bro, A. B. Girtman, R. C. Cyr, R. J. Singh and S. K. Grebe, *Clinical chemistry*, 2011, **57**, 431-440.
196. T. G. Rosano, P. Y. Ohouo and M. Wood, *Journal of analytical toxicology*, 2019, **43**, 353-363.
197. B. J. Berendsen, T. Meijer, H. G. Mol, L. van Ginkel and M. W. Nielen, *Analytica chimica acta*, 2017, **962**, 60-72.
198. E. M. C. f. D. a. D. Addiction, *Journal*, 2019.
199. N. A. Desrosiers, K. B. Scheidweiler and M. A. Huestis, *Drug testing and analysis*, 2015, **7**, 684-694.
200. R. Verplaetse, E. Cuypers and J. Tytgat, *Journal of Chromatography A*, 2012, **1249**, 147-154.
201. D. S. Fisher, S. J. Partridge, S. A. Handley, L. Couchman, P. E. Morgan and R. J. Flanagan, *Forensic science international*, 2013, **229**, 145-150.
202. D. Remane, M. R. Meyer, F. T. Peters, D. K. Wissenbach and H. H. Maurer, *Analytical and bioanalytical chemistry*, 2010, **397**, 2303-2314.
203. T. Galaon, C. Vacaresteanu, D. F. Anghel and V. David, *Drug testing and analysis*, 2014, **6**, 439-450.
204. J. F. Parcher, M. Wang, A. G. Chittiboyina and I. A. Khan, *Drug testing and analysis*, 2018, **10**, 28-36.
205. A. de Castro, M. Gergov, P. Östman, I. Ojanperä and A. Pelander, *Analytical and bioanalytical chemistry*, 2012, **403**, 1265-1278.
206. T. G. Rosano, M. Wood and T. A. Swift, *Journal of analytical toxicology*, 2011, **35**, 411-423.
207. J. C. Domínguez-Romero, J. F. García-Reyes, F. J. Lara-Ortega and A. Molina-Díaz, *Talanta*, 2015, **134**, 74-88.
208. M. K. Bjørk, M. K. Nielsen, L. Ø. Markussen, H. B. Klinke and K. Linnet, *Analytical and bioanalytical chemistry*, 2010, **396**, 2393-2401.
209. D. M. Bassan, F. Erdmann and R. Krüll, *Analytical and bioanalytical chemistry*, 2011, **400**, 43-50.
210. M. Vincenti, D. Cavanna, E. Gerace, V. Pirro, M. Petrarulo, D. Di Corcia and A. Salomone, *Analytical and bioanalytical chemistry*, 2013, **405**, 863-879.
211. D. M. Mueller, B. Duretz, F. A. Espourteille and K. M. Rentsch, *Analytical and bioanalytical chemistry*, 2011, **400**, 89-100.
212. S. Dresen, N. Ferreirós, H. Gnann, R. a. Zimmermann and W. Weinmann, *Analytical and bioanalytical chemistry*, 2010, **396**, 2425-2434.
213. J. D. Power, S. D. McDermott, B. Talbot, J. E. O'Brien and P. Kavanagh, *Rapid Communications in Mass Spectrometry*, 2012, **26**, 2601-2611.
214. R. S. Plumb, K. A. Johnson, P. Rainville, B. W. Smith, I. D. Wilson, J. M. Castro - Perez and J. K. Nicholson, *Rapid Communications in Mass Spectrometry: An International Journal Devoted to the Rapid Dissemination of Up - to - the - Minute Research in Mass Spectrometry*, 2006, **20**, 1989-1994.

215. P. Kriikku, A. Pelander, I. Rasanen and I. Ojanperä, *Forensic science international*, 2019, **300**, 85-88.
216. L. J. Høj, C. B. Mollerup, B. S. Rasmussen, S. S. Johansen, K. Linnet and P. W. Dalsgaard, *Drug testing and analysis*, 2019, **11**, 1258-1263.
217. K. B. Scheidweiler, M. J. Jarvis and M. A. Huestis, *Analytical and bioanalytical chemistry*, 2015, **407**, 883-897.
218. J. D. Whitman and K. L. Lynch, *Clinical chemistry*, 2019, clinchem. 2018.300756.
219. C. a. L. S. Institute, *Journal*, 2014.
220. M. Roman, L. Ström, H. Tell and M. Josefsson, *Analytical and bioanalytical chemistry*, 2013, **405**, 4107-4125.
221. J. M. Colby, K. L. Thoren and K. L. Lynch, *Journal of analytical toxicology*, 2018, **42**, 207-213.
222. F.-L. Sauvage, J.-M. Gaulier, G. Lachâtre and P. Marquet, *Clinical chemistry*, 2008, **54**, 1519-1527.
223. M. Sundström, A. Pelander and I. Ojanperä, *Journal of analytical toxicology*, 2017, **41**, 623-630.
224. T. G. Rosano, M. Wood, K. Ihenetu and T. A. Swift, *Journal of analytical toxicology*, 2013, **37**, 580-593.
225. S. Broecker, S. Herre, B. Wüst, J. Zweigenbaum and F. Pragst, *Analytical and bioanalytical chemistry*, 2011, **400**, 101-117.
226. K. Arnhard, A. Gottschall, F. Pitterl and H. Oberacher, *Analytical and bioanalytical chemistry*, 2015, **407**, 405-414.
227. X. Zhu, Y. Chen and R. Subramanian, *Analytical chemistry*, 2014, **86**, 1202-1209.
228. A. T. Roemmelt, A. E. Steuer, M. Poetzsch and T. Kraemer, *Analytical chemistry*, 2014, **86**, 11742-11749.
229. A. G. Helfer, J. A. Michely, A. A. Weber, M. R. Meyer and H. H. Maurer, *Analytica chimica acta*, 2015, **891**, 221-233.
230. M. Ott, K. Berbalk, T. Plecko, E. Wieland and M. Shipkova, *Clinical Mass Spectrometry*, 2017, **4**, 11-18.
231. J. Kluge, L. Rentzsch, D. Remane, F. T. Peters and D. K. Wissenbach, *Drug testing and analysis*, 2018, **10**, 1536-1542.
232. M. M. Goggin, C. M. Tann, A. Miller, A. Nguyen and G. C. Janis, *J Anal Toxicol*, 2017, **41**, 121-126.
233. P. Adamowicz and A. Malczyk, *Forensic science international*, 2019, **295**, 36-45.
234. A. Wohlfarth, K. B. Scheidweiler, X. Chen, H.-f. Liu and M. A. Huestis, *Analytical chemistry*, 2013, **85**, 3730-3738.
235. P. C. Dolder, M. E. Liechti and K. M. Rentsch, *Analytical and bioanalytical chemistry*, 2015, **407**, 1577-1584.
236. G. A. McMillin, S. J. Marin, K. L. Johnson-Davis, B. G. Lawlor and F. G. Strathmann, *American journal of clinical pathology*, 2015, **143**, 234-240.
237. R. Telving, J. B. Hasselstrøm and M. F. Andreasen, *Forensic science international*, 2016, **266**, 453-461.
238. N. Fabresse, I. A. Larabi, T. Stratton, R. Mistrik, G. Pfau, G. Lorin de la Grandmaison, I. Etting, S. Grassin Delyle and J. C. Alvarez, *Drug testing and analysis*, 2019, **11**, 697-708.

239. M. Mardal, M. F. Andreasen, C. B. Mollerup, P. Stockham, R. Telving, N. S. Thomaidis, K. S. Diamanti, K. Linnet and P. W. Dalsgaard, *Journal of analytical toxicology*, 2019, 1-8.
240. C. B. Mollerup, P. W. Dalsgaard, M. Mardal and K. Linnet, *Drug testing and analysis*, 2017, **9**, 1052-1061.
241. B. C. Presley, B. K. Logan and S. A. Jansen-Varnum, *Drug Test Anal*, 2019, **11**, 1264-1276.
242. C. Cutler and S. Hudson, *Drug Testing and Analysis*, 2019, **11**, 1134-1143.
243. D. K. Wissenbach, M. R. Meyer, D. Remane, A. A. Philipp, A. A. Weber and H. H. Maurer, *Analytical and bioanalytical chemistry*, 2011, **400**, 3481-3489.
244. H. Zhang, D. Zhang, K. Ray and M. Zhu, *Journal of mass spectrometry*, 2009, **44**, 999-1016.
245. I. Ojanpera, A. Pelander, S. Laks, M. Gergov, E. Vuori and M. Witt, *J Anal Toxicol*, 2005, **29**, 34-40.
246. S. Bidny, K. Gago, P. Chung, D. Albertyn and D. Pasin, *J Anal Toxicol*, 2017, **41**, 181-195.
247. T. G. Rosano, P. Y. Ohouo and M. Wood, *Journal of analytical toxicology*, 2017, **41**, 536-546.
248. H. Liu, L. Lam and P. K. Dasgupta, *Talanta*, 2011, **87**, 307-310.
249. A. M. Miller, M. M. Goggin, A. Nguyen, S. D. Gozum and G. C. Janis, *Journal of analytical toxicology*, 2017, **41**, 355-359.
250. M. P. Elmiger, M. Poetzsch, A. E. Steuer and T. Kraemer, *Analytical and bioanalytical chemistry*, 2017, **409**, 6495-6508.
251. P. Kebarle and L. Tang, *Analytical chemistry*, 1993, **65**, 972A-986A.
252. E. Horning, M. Horning, D. Carroll, I. Dzidic and R. Stillwell, *Analytical Chemistry*, 1973, **45**, 936-943.
253. C. N. McEwen and B. S. Larsen, *Journal of the American Society for Mass Spectrometry*, 2009, **20**, 1518-1521.
254. T. J. Kauppila, T. Kuuranne, E. C. Meurer, M. N. Eberlin, T. Kotiaho and R. Kostianen, *Analytical chemistry*, 2002, **74**, 5470-5479.
255. G. A. Harris, A. S. Galhena and F. M. Fernandez, *Analytical chemistry*, 2011, **83**, 4508-4538.
256. R. Javanshad and A. Venter, *Analytical Methods*, 2017, **9**, 4896-4907.
257. J. T. Shelley and G. M. Hieftje, *Journal of Analytical Atomic Spectrometry*, 2010, **25**, 345-350.
258. X. Ding and Y. Duan, *Mass spectrometry reviews*, 2015, **34**, 449-473.
259. M. Smoluch, P. Mielczarek and J. Silberring, *Mass spectrometry reviews*, 2016, **35**, 22-34.
260. F. Green, T. Salter, P. Stokes, I. Gilmore and G. O'Connor, *Surface and Interface Analysis: An International Journal devoted to the development and application of techniques for the analysis of surfaces, interfaces and thin films*, 2010, **42**, 347-357.
261. A. Molina-Díaz, M. Beneito-Cambra, D. Moreno-González and B. Gilbert-López, *Current Opinion in Green and Sustainable Chemistry*, 2019, **19**, 50-60.
262. Z. Takats, J. M. Wiseman, B. Gologan and R. G. Cooks, *Science*, 2004, **306**, 471-473.

263. R. B. Cody, J. A. Laramée and H. D. Durst, *Analytical chemistry*, 2005, **77**, 2297-2302.
264. J. Shiea, M. Z. Huang, H. J. HSu, C. Y. Lee, C. H. Yuan, I. Beech and J. Sunner, *Rapid Communications in Mass Spectrometry: An International Journal Devoted to the Rapid Dissemination of Up - to - the - Minute Research in Mass Spectrometry*, 2005, **19**, 3701-3704.
265. C. N. McEwen, R. G. McKay and B. S. Larsen, *Analytical Chemistry*, 2005, **77**, 7826-7831.
266. R. Haddad, R. Sparrapan and M. N. Eberlin, *Rapid Communications in Mass Spectrometry*, 2006, **20**, 2901-2905.
267. F. J. Andrade, W. C. Wetzels, G. C.-Y. Chan, M. R. Webb, G. Gamez, S. J. Ray and G. M. Hieftje, *Journal of Analytical Atomic Spectrometry*, 2006, **21**, 1175-1184.
268. N. Na, M. Zhao, S. Zhang, C. Yang and X. Zhang, *Journal of the American Society for Mass Spectrometry*, 2007, **18**, 1859-1862.
269. M. Haapala, J. Pól, V. Saarela, V. Arvola, T. Kotiaho, R. A. Ketola, S. Franssila, T. J. Kauppila and R. Kostianen, *Analytical chemistry*, 2007, **79**, 7867-7872.
270. P. Nemes and A. Vertes, *Analytical chemistry*, 2007, **79**, 8098-8106.
271. H.-W. Chen, J.-H. Lai, Y.-F. Zhou, Y.-F. Huan, J.-Q. Li, Z. Xie, Z.-C. Wang and M.-B. Luo, *Chinese Journal of Analytical Chemistry*, 2007, **35**, 1233-1240.
272. J. D. Harper, N. A. Charipar, C. C. Mulligan, X. Zhang, R. G. Cooks and Z. Ouyang, *Analytical chemistry*, 2008, **80**, 9097-9104.
273. G. A. Gómez - Ríos and J. Pawliszyn, *Angewandte Chemie International Edition*, 2014, **53**, 14503-14507.
274. Z. Takats, J. M. Wiseman and R. G. Cooks, *Journal of mass spectrometry*, 2005, **40**, 1261-1275.
275. J. M. Wiseman, D. R. Ifa, Y. Zhu, C. B. Kissinger, N. E. Manicke, P. T. Kissinger and R. G. Cooks, *Proceedings of the National Academy of Sciences*, 2008, **105**, 18120-18125.
276. L. Lamont, G. B. Eijkel, E. A. Jones, B. Flinders, S. R. Ellis, T. Porta Siegel, R. M. Heeren and R. J. Vreeken, *Analytical chemistry*, 2018, **90**, 13229-13235.
277. D. R. Ifa, C. Wu, Z. Ouyang and R. G. Cooks, *Analyst*, 2010, **135**, 669-681.
278. M. Morelato, A. Beavis, P. Kirkbride and C. Roux, *Forensic science international*, 2013, **226**, 10-21.
279. T. J. Kauppila, N. Talaty, T. Kuuranen, T. Kotiaho, R. Kostianen and R. G. Cooks, *Analyst*, 2007, **132**, 868-875.
280. N. M. Suni, P. Lindfors, O. Laine, P. Östman, I. Ojanperä, T. Kotiaho, T. J. Kauppila and R. Kostianen, *Analytica chimica acta*, 2011, **699**, 73-80.
281. P. D'Aloise and H. Chen, *Science & Justice*, 2012, **52**, 2-8.
282. M. J. Bailey, R. Bradshaw, S. Francese, T. L. Salter, C. Costa, M. Ismail, R. P. Webb, I. Bosman, K. Wolff and M. de Puit, *Analyst*, 2015, **140**, 6254-6259.
283. N. Stojanovska, M. Tahtouh, T. Kelly, A. Beavis and S. Fu, *Drug testing and analysis*, 2015, **7**, 393-400.
284. F. Bianchi, S. Agazzi, N. Riboni, N. Erdal, M. Hakkarainen, L. L. Ilag, L. Anzillotti, R. Andreoli, F. Marezza and F. Moroni, *Talanta*, 2019, **202**, 136-144.
285. J. H. Kennedy, C. Aurand, R. Shirey, B. C. Laughlin and J. M. Wiseman, *Analytical chemistry*, 2010, **82**, 7502-7508.

286. J. Thunig, L. Flø, S. Pedersen - Bjergaard, S. H. Hansen and C. Janfelt, *Rapid Communications in Mass Spectrometry*, 2012, **26**, 133-140.
287. K. M. Roscioli, J. A. Tufariello, X. Zhang, S. X. Li, G. H. Goetz, G. Cheng, W. F. Siems and H. H. Hill, *Analyst*, 2014, **139**, 1740-1750.
288. A. Keil, N. Talaty, C. Janfelt, R. J. Noll, L. Gao, Z. Ouyang and R. G. Cooks, *Analytical chemistry*, 2007, **79**, 7734-7739.
289. K. E. Vircks and C. C. Mulligan, *Rapid Communications in Mass Spectrometry*, 2012, **26**, 2665-2672.
290. A. E. O'Leary, H. Oberacher, S. E. Hall and C. C. Mulligan, *Analytical Methods*, 2015, **7**, 3331-3339.
291. P. Fedick, W. Fatigante, Z. Lawton, A. O'Leary, S. Hall, R. Bain, S. Ayrton, J. Ludwig and C. Mulligan, *Instruments*, 2018, **2**, 5.
292. Z. E. Lawton, A. Traub, W. L. Fatigante, J. Mancias, A. E. O'Leary, S. E. Hall, J. R. Wieland, H. Oberacher, M. C. Gizzi and C. C. Mulligan, *Journal of the American Society for Mass Spectrometry*, 2017, **28**, 1048-1059.
293. M.-Z. Huang, C.-C. Zhou, D.-L. Liu, S.-S. Jhang, S.-C. Cheng and J. Shiea, *Analytical chemistry*, 2013, **85**, 8956-8963.
294. C.-W. Lee, H. Su, Y.-D. Cai, M.-T. Wu, D.-C. Wu and J. Shiea, *Mass Spectrometry*, 2017, **6**, S0056-S0056.
295. C.-H. Chiang, H.-H. Lee, B.-H. Chen, Y.-C. Lin, Y.-Y. Chao and Y.-L. Huang, *Journal of Food and Drug Analysis*, 2018, **27**, 439-450.
296. S.-C. Cheng, Y.-D. Tsai, C.-W. Lee, B.-H. Chen and J. Shiea, *Journal of food and drug analysis*, 2019, **27**, 451-459.
297. S. F. Teunissen, A. M. A. Fernandes, M. N. Eberlin and R. M. Alberici, *TrAC Trends in Analytical Chemistry*, 2017, **90**, 135-141.
298. A. Hirabayashi, M. Sakairi and H. Koizumi, *Analytical Chemistry*, 1994, **66**, 4557-4559.
299. Z. Takats, S. C. Nanita, R. G. Cooks, G. Schlosser and K. Vekey, *Analytical chemistry*, 2003, **75**, 1514-1523.
300. B. D. Sabino, M. L. Sodre, E. A. Alves, H. F. Rozenbaum, F. O. Alonso, D. N. Correa, W. ROMAO and M. EBERLIN, *Brazilian Journal of Analytical Chemistry*, 2010, **1**, 222-227.
301. B. D. Sabino, W. Romão, M. L. Sodr e, D. N. Correa, D. B. R. Pinto, F. O. Alonso and M. N. Eberlin, *American Journal of Analytical Chemistry*, 2011, **2**, 658.
302. W. Romão, P. M. Lalli, M. F. Franco, G. Sanvido, N. V. Schwab, R. Lanaro, J. L. Costa, B. D. Sabino, M. I. M. Bueno and G. F. de Sa, *Analytical and bioanalytical chemistry*, 2011, **400**, 3053-3064.
303. W. Romão, B. D. Sabino, M. I. M. Bueno, B. G. Vaz, A. C. J nior, A. O. Maldaner, E. V. de Castro, R. A. Lordeiro, C. C. Nascentes and M. N. Eberlin, *Journal of forensic sciences*, 2012, **57**, 1307-1312.
304. V. G. Santos, T. Regiani, F. F. Dias, W. Romao, J. L. P. Jara, C. F. Klitzke, F. Coelho and M. N. Eberlin, *Analytical chemistry*, 2011, **83**, 1375-1380.
305. N. V. Schwab, A. M. Porcari, M. B. Coelho, E. M. Schmidt, J. L. Jara, J. V. Visentainer and M. N. Eberlin, *Analyst*, 2012, **137**, 2537-2540.
306. R. D. Espy, A. R. Muliadi, Z. Ouyang and R. G. Cooks, *International Journal of Mass Spectrometry*, 2012, **325**, 167-171.

307. P.-H. Lai, P.-C. Chen, Y.-W. Liao, J.-T. Liu, C.-C. Chen and C.-H. Lin, *International Journal of Mass Spectrometry*, 2015, **375**, 14-17.
308. Z. Zhang, W. Xu, N. E. Manicke, R. G. Cooks and Z. Ouyang, *Analytical chemistry*, 2011, **84**, 931-938.
309. M. T. Dulay and R. N. Zare, *Rapid Communications in Mass Spectrometry*, 2017, **31**, 1651-1658.
310. L. S. Tavares, T. C. Carvalho, W. Romão, B. G. Vaz and A. R. Chaves, *Journal of The American Society for Mass Spectrometry*, 2018, **29**, 566-572.
311. B. J. Bills, J. Kinkade, G. Ren and N. E. Manicke, *Forensic Chemistry*, 2018, **11**, 15-22.
312. C. Vega, C. Spence, C. Zhang, B. J. Bills and N. E. Manicke, *Journal of The American Society for Mass Spectrometry*, 2016, **27**, 726-734.
313. Q. Yang, H. Wang, J. D. Maas, W. J. Chappell, N. E. Manicke, R. G. Cooks and Z. Ouyang, *International journal of mass spectrometry*, 2012, **312**, 201-207.
314. G. W. Vandergrift, A. J. Hessels, J. Palaty, E. T. Krogh and C. G. Gill, *Clinical biochemistry*, 2018, **54**, 106-111.
315. R. D. Espy, S. F. Teunissen, N. E. Manicke, Y. Ren, Z. Ouyang, A. van Asten and R. G. Cooks, *Analytical chemistry*, 2014, **86**, 7712-7718.
316. C. Zhang and N. E. Manicke, *Analytical chemistry*, 2015, **87**, 6212-6219.
317. G. Ren, N. Manicke, C. Boeser and N. Wijeratne, *Technical Note 6540*, 2019.
318. C. S. Jhang, H. Lee, Y. S. He, J. T. Liu and C. H. Lin, *Electrophoresis*, 2012, **33**, 3073-3078.
319. H. Lee, C. S. Jhang, J. T. Liu and C. H. Lin, *Journal of separation science*, 2012, **35**, 2822-2825.
320. T. C. Carvalho, I. F. Oliveira, L. V. Tose, G. Vanini, J. B. Kill, A. C. Neto, L. F. Machado, J. C. Ambrosio, V. Lacerda and B. G. Vaz, *Analytical Methods*, 2016, **8**, 614-620.
321. J. Kennedy, K. G. Shanks, K. Van Natta, M. C. P. Conaway, J. M. Wiseman, B. Laughlin and M. Kozak, *Clinical Mass Spectrometry*, 2016, **1**, 3-10.
322. J. McKenna, R. Jett, K. Shanks and N. E. Manicke, *Journal of analytical toxicology*, 2018, **42**, 300-310.
323. R. Jett, C. Skaggs and N. E. Manicke, *Analytical Methods*, 2017, **9**, 5037-5043.
324. J. A. Michely, M. R. Meyer and H. H. Maurer, *Analytical chemistry*, 2017, **89**, 11779-11786.
325. N. E. Manicke, B. J. Bills and C. Zhang, *Bioanalysis*, 2016, **8**, 589-606.
326. C. Costa, R. Webb, V. Palitsin, M. Ismail, M. de Puit, S. Atkinson and M. J. Bailey, *Clinical chemistry*, 2017, **63**, 1745-1752.
327. P. W. Fedick, B. J. Bills, N. E. Manicke and R. G. Cooks, *Analytical chemistry*, 2017, **89**, 10973-10979.
328. N. E. Manicke and M. Belford, *Journal of the American Society for Mass Spectrometry*, 2015, **26**, 701-705.
329. T. C. De Carvalho, F. Tosato, L. M. Souza, H. Santos, B. B. Merlo, R. S. Ortiz, R. R. Rodrigues, P. R. Filgueiras, H. S. França and R. Augusti, *Forensic science international*, 2016, **262**, 56-65.
330. H. Santos, A. Lima, A. Mazega, E. Domingos, C. Thompson, A. Maldaner, P. Filgueiras, B. Vaz and W. Romão, *Analytical Methods*, 2017, **9**, 3662-3668.

331. G. W. Vandergrift and C. G. Gill, *Journal of Mass Spectrometry*, 2019, **54**, 729-737.
332. N. E. Manicke, P. Abu-Rabie, N. Spooner, Z. Ouyang and R. G. Cooks, *Journal of the American Society for Mass Spectrometry*, 2011, **22**, 1501-1507.
333. S. F. Teunissen, P. W. Fedick, B. J. Berendsen, M. W. Nielen, M. N. Eberlin, R. G. Cooks and A. C. van Asten, *Journal of the American Society for Mass Spectrometry*, 2017, **28**, 2665-2676.
334. Y. Su, H. Wang, J. Liu, P. Wei, R. G. Cooks and Z. Ouyang, *Analyst*, 2013, **138**, 4443-4447.
335. J. H. Kennedy, J. Palaty, C. G. Gill and J. M. Wiseman, *Rapid Communications in Mass Spectrometry*, 2018, **32**, 1280-1286.
336. L. C. d. Silva, I. Pereira, T. C. d. Carvalho, J. F. Allochio Filho, W. Romão and B. Gontijo Vaz, *Analytical methods*, 2019, **11**, 991-1146.
337. Q. Ma, H. Bai, W. Li, C. Wang, R. G. Cooks and Z. Ouyang, *Talanta*, 2015, **142**, 190-196.
338. N. Reyes-Garcés, E. Gionfriddo, G. A. Gómez-Ríos, M. N. Alam, E. Boyacı, B. Bojko, V. Singh, J. Grandy and J. Pawliszyn, *Analytical chemistry*, 2017, **90**, 302-360.
339. G. A. Gómez-Ríos, M. Tascon and J. Pawliszyn, *Bioanalysis*, 2018, **10**, 257-271.
340. H. Piri - Moghadam, F. Ahmadi, G. A. Gómez - Ríos, E. Boyacı, N. Reyes - Garcés, A. Aghakhani, B. Bojko and J. Pawliszyn, *Angewandte Chemie International Edition*, 2016, **55**, 7510-7514.
341. G. A. Gómez-Ríos, M. Tascon, N. Reyes-Garcés, E. Boyacı, J. Poole and J. Pawliszyn, *Scientific reports*, 2017, **7**, 16104.
342. M. Tascon, G. n. A. Gómez-Ríos, N. Reyes-Garcés, J. Poole, E. Boyacı and J. Pawliszyn, *Analytical chemistry*, 2017, **89**, 8421-8428.
343. B. Hu, P.-K. So and Z.-P. Yao, *Journal of the American Society for Mass Spectrometry*, 2013, **24**, 57-65.
344. B. Hu, P.-K. So, H. Chen and Z.-P. Yao, *Analytical chemistry*, 2011, **83**, 8201-8207.
345. B. Hu, Y. Huang, G. Yin, G. Zhang, L. Zhang, T. Wang and Z.-P. Yao, *Analytical Methods*, 2016, **8**, 6840-6846.
346. P.-K. So, T.-T. Ng, H. Wang, B. Hu and Z.-P. Yao, *Analyst*, 2013, **138**, 2239-2243.
347. T. T. Ng, P. K. So, B. Hu and Z. P. Yao, *J Food Drug Anal*, 2019, **27**, 428-438.
348. H.-K. Chen, C.-H. Lin, J.-T. Liu and C.-H. Lin, *International Journal of Mass Spectrometry*, 2013, **356**, 37-40.
349. H. Wang, P.-K. So, T.-T. Ng and Z.-P. Yao, *Analytica chimica acta*, 2014, **844**, 1-7.
350. N. M. Morato, V. Pirro, P. W. Fedick and R. G. Cooks, *Anal Chem*, 2019, **91**, 7450-7457.
351. V. Pirro, A. K. Jarmusch, M. Vincenti and R. G. Cooks, *Analytica chimica acta*, 2015, **861**, 47-54.
352. J. H. Gross, *Analytical and bioanalytical chemistry*, 2014, **406**, 63-80.
353. M. J. Pavlovich, B. Musselman and A. B. Hall, *Mass spectrometry reviews*, 2018, **37**, 171-187.
354. L. Song, S. C. Gibson, D. Bhandari, K. D. Cook and J. E. Bartmess, *Analytical chemistry*, 2009, **81**, 10080-10088.
355. L. Song, A. B. Dykstra, H. Yao and J. E. Bartmess, *Journal of the American Society for Mass Spectrometry*, 2009, **20**, 42-50.

356. A. H. Grange and G. W. Sovocool, *Rapid Communications in Mass Spectrometry*, 2011, **25**, 1271-1281.
357. S. Yu, E. Crawford, J. Tice, B. Musselman and J.-T. Wu, *Analytical chemistry*, 2008, **81**, 193-202.
358. S. J. Dunham, P. D. Hooker and R. M. Hyde, *Forensic science international*, 2012, **223**, 241-244.
359. R. A. Musah, M. A. Domin, M. A. Walling and J. R. Shepard, *Rapid Communications in Mass Spectrometry*, 2012, **26**, 1109-1114.
360. A. D. Lesiak, R. A. Musah, M. A. Domin and J. R. Shepard, *Journal of forensic sciences*, 2014, **59**, 337-343.
361. L. Habala, J. Valentová, I. Pechová, M. Fuknová and F. Devínsky, *Legal Medicine*, 2016, **20**, 27-31.
362. W. F. Duvivier, T. A. van Beek, E. J. Pennings and M. W. Nielen, *Rapid Communications in Mass Spectrometry*, 2014, **28**, 682-690.
363. H. Nie, X. Li, Z. Hua, W. Pan, Y. Bai and X. Fu, *Rapid Communications in Mass Spectrometry*, 2016, **30**, 141-146.
364. J. LaPointe, B. Musselman, T. O'neill and J. R. Shepard, *Journal of the American Society for Mass Spectrometry*, 2015, **26**, 159-165.
365. W. F. Duvivier, M. R. van Putten, T. A. van Beek and M. W. Nielen, *Analytical chemistry*, 2016, **88**, 2489-2496.
366. R. R. Steiner and R. L. Larson, *Journal of forensic sciences*, 2009, **54**, 617-622.
367. T. Vasiljevic, G. n. A. Gómez-Ríos and J. Pawliszyn, *Analytical chemistry*, 2017, **90**, 952-960.
368. R. A. Musah, R. B. Cody, M. A. Domin, A. D. Lesiak, A. J. Dane and J. R. Shepard, *Forensic science international*, 2014, **244**, 42-49.
369. A. D. Lesiak, R. A. Musah, R. B. Cody, M. A. Domin, A. J. Dane and J. R. Shepard, *Analyst*, 2013, **138**, 3424-3432.
370. X. Z. Cui, R. Lian, J. Chen, C. F. Ni, C. Liang, G. L. Chen and Y. R. Zhang, *Microchemical Journal*, 2019, **147**, 121-126.
371. K. L. Fowble, J. R. Shepard and R. A. Musah, *Talanta*, 2018, **179**, 546-553.
372. H. Brown, B. Oktem, A. Windom, V. Doroshenko and K. Evans-Nguyen, *Forensic Chemistry*, 2016, **1**, 66-73.
373. G. A. Gómez-Ríos, T. Vasiljevic, E. Gionfriddo, M. Yu and J. Pawliszyn, *Analyst*, 2017, **142**, 2928-2935.
374. E. Jagerdeo, J. A. Clark, J. N. Leibowitz and L. J. Reda, *Rapid Communications in Mass Spectrometry*, 2015, **29**, 205-212.
375. E. J. Crevelin, F. H. Salami, M. N. R. Alves, B. S. De Martinis, A. E. M. Crotti and L. A. B. Moraes, *Journal of The American Society for Mass Spectrometry*, 2016, **27**, 944-947.
376. E. Jagerdeo and A. Wriston, *Rapid Communications in Mass Spectrometry*, 2017, **31**, 782-790.
377. J. T. Shelley, J. S. Wiley and G. M. Hieftje, *Analytical chemistry*, 2011, **83**, 5741-5748.
378. M. Smoluch, E. Reszke, A. Ramsza, K. Labuz and J. Silberring, *Rapid Communications in Mass Spectrometry*, 2012, **26**, 1577-1580.

379. M. Smoluch, B. Gierczyk, E. Reszke, M. Babij, T. Gotszalk, G. Schroeder and J. Silberring, *Talanta*, 2016, **146**, 29-33.
380. M. Smoluch, P. Mielczarek, E. Reszke, G. M. Hieftje and J. Silberring, *Analyst*, 2014, **139**, 4350-4355.
381. K. P. Pfeuffer, J. N. Schaper, J. T. Shelley, S. J. Ray, G. C.-Y. Chan, N. H. Bings and G. M. Hieftje, *Analytical chemistry*, 2013, **85**, 7512-7518.
382. S. Daugherty and H. Crowe, *PerkinElmer Inc.: Application Note*, 2014.
383. S. Botch-Jones, J. Foss, D. Barajas, F. Kero, C. Young and J. Weisenseel, *Forensic science international*, 2016, **267**, 89-95.
384. M. K. McGonigal, J. A. Wilhide, P. B. Smith, N. M. Elliott and F. L. Dorman, *Forensic science international*, 2017, **275**, 83-89.
385. A. Moore, J. Foss, M. Juhascik, S. Botch-Jones and F. Kero, *Forensic Chemistry*, 2019, **13**, 100149.
386. F. Tang, J. Chen, X. Wang, S. Zhang and X. Zhang, *Analytical and bioanalytical chemistry*, 2015, **407**, 2345-2364.
387. S. Kumano, M. Sugiyama, M. Yamada, K. Nishimura, H. Hasegawa, H. Morokuma, H. Inoue and Y. Hashimoto, *Analytical chemistry*, 2013, **85**, 5033-5039.
388. D. T. Usmanov, Z. Yu, L. C. Chen, K. Hiraoka and S. Yamabe, *Journal of mass spectrometry*, 2016, **51**, 132-140.
389. A. Habib, A. Nargis, L. Bi, P. Zhao and L. Wen, *Arabian Journal of Chemistry*, 2018, **13**, 2162-2170.
390. M. Smoluch, M. Babij, D. Zuba, G. Schroeder, T. Gotszalk and J. Silberring, *International Journal of Mass Spectrometry*, 2015, **386**, 32-36.
391. M. F. Mirabelli, J.-C. Wolf and R. Zenobi, *Analytical chemistry*, 2016, **88**, 7252-7258.
392. M. F. Mirabelli, E. Gionfriddo, J. Pawliszyn and R. Zenobi, *Analyst*, 2019, **144**, 2788-2796.
393. J. S. Furter and P. C. Hauser, *Analytical Methods*, 2018, **10**, 2701-2711.
394. A. U. Jackson, J. F. Garcia-Reyes, J. D. Harper, J. S. Wiley, A. Molina-Díaz, Z. Ouyang and R. G. Cooks, *Analyst*, 2010, **135**, 927-933.
395. X. Wang, Z. Hua, Z. Yang, H. Li, H. Liu, B. Qiu and H. Nie, *Rapid Communications in Mass Spectrometry*, 2018, **32**, 913-918.
396. J. K. Dalglish, M. Wleklinski, J. T. Shelley, C. C. Mulligan, Z. Ouyang and R. Graham Cooks, *Rapid Communications in Mass Spectrometry*, 2013, **27**, 135-142.
397. J. S. Wiley, J. T. Shelley and R. G. Cooks, *Analytical chemistry*, 2013, **85**, 6545-6552.
398. L. Luosujärvi, U. M. Laakkonen, R. Kostianen, T. Kotiaho and T. J. Kauppila, *Rapid Communications in Mass Spectrometry*, 2009, **23**, 1401-1404.
399. T. J. Kauppila, A. Flink, M. Haapala, U.-M. Laakkonen, L. Aalberg, R. A. Ketola and R. Kostianen, *Forensic science international*, 2011, **210**, 206-212.
400. T. J. Kauppila, A. Flink, U. M. Laakkonen, L. Aalberg and R. A. Ketola, *Drug testing and analysis*, 2013, **5**, 186-190.
401. M. F. Mirabelli and R. Zenobi, *Analytical chemistry*, 2018, **90**, 5015-5022.
402. J. J. A. van Kampen, P. C. Burgers, R. de Groot, R. A. Gruters and T. M. Luider, *Mass Spectrometry Reviews*, 2011, **30**, 101-120.

403. T. Guinan, P. Kirkbride, P. E. Pigou, M. Ronci, H. Kobus and N. H. Voelcker, *Mass spectrometry reviews*, 2015, **34**, 627-640.
404. S. Vogliardi, D. Favretto, G. Frison, S. Maietti, G. Viel, R. Seraglia, P. Traldi and S. D. Ferrara, *Analytical and bioanalytical chemistry*, 2010, **396**, 2435-2440.
405. F. Musshoff, T. Arrey and K. Strupat, *Drug testing and analysis*, 2013, **5**, 361-365.
406. B. Flinders, E. Cuypers, H. Zeijlemaker, J. Tytgat and R. M. Heeren, *Drug testing and analysis*, 2015, **7**, 859-865.
407. A. Miki, M. Katagi, T. Kamata, K. Zaitso, M. Tatsuno, T. Nakanishi, H. Tsuchihashi, T. Takubo and K. Suzuki, *Journal of Mass Spectrometry*, 2011, **46**, 411-416.
408. A. Miki, M. Katagi, N. Shima, H. Kamata, M. Tatsuno, T. Nakanishi, H. Tsuchihashi, T. Takubo and K. Suzuki, *Forensic Toxicology*, 2011, **29**, 111-116.
409. M. Shen, P. Xiang, Y. Shi, H. Pu, H. Yan and B. Shen, *Analytical and bioanalytical chemistry*, 2014, **406**, 4611-4616.
410. N. Shima, K. Sasaki, T. Kamata, S. Matsuta, M. Katagi, A. Miki, K. Zaitso, T. Sato, T. Nakanishi and H. Tsuchihashi, *Forensic Toxicology*, 2015, **33**, 122-130.
411. A. Kernalléguen, C. Enjalbal, J.-C. Alvarez, O. Belgacem, G. Léonetti, D. Lafitte and A.-L. Péliissier-Alicot, *Analytica chimica acta*, 2018, **1041**, 87-93.
412. B. Flinders, E. Beasley, R. M. Verlaan, E. Cuypers, S. Francese, T. Bassindale, M. R. Clench and R. M. Heeren, *Journal of the American Society for Mass Spectrometry*, 2017, **28**, 2462-2468.
413. L. Sundar and F. Rowell, *Analyst*, 2014, **139**, 633-642.
414. G. Groeneveld, M. De Puit, S. Bleay, R. Bradshaw and S. Francese, *Scientific reports*, 2015, **5**, 11716.
415. R. Bradshaw, N. Denison and S. Francese, *Analyst*, 2017, **142**, 1581-1590.
416. A. Kraj, M. Świst, A. Strugala, A. Parczewski and J. Silberringa, *European Journal of Mass Spectrometry*, 2006, **12**, 253-259.
417. T. Guinan, M. Ronci, H. Kobus and N. H. Voelcker, *Talanta*, 2012, **99**, 791-798.
418. C. Della Vedova, *Chemical Communications*, 2015, **51**, 6088-6091.
419. T. M. Guinan, D. Neldner, P. Stockham, H. Kobus, C. B. Della Vedova and N. H. Voelcker, *Drug testing and analysis*, 2017, **9**, 769-777.
420. H. Z. Alhmoud, T. M. Guinan, R. Elnathan, H. Kobus and N. H. Voelcker, *Analyst*, 2014, **139**, 5999-6009.
421. T. Guinan, P. Kirkbride, C. Della Vedova, S. Kershaw, H. Kobus and N. Voelcker, *Analyst*, 2015, **140**, 7926-7933.
422. H. H. Abdelmaksoud, T. M. Guinan and N. H. Voelcker, *ACS applied materials & interfaces*, 2017, **9**, 5092-5099.
423. J. Du, Q. Zhu, F. Teng, Y. Wang and N. Lu, *Talanta*, 2019, **192**, 79-85.
424. S. Nolan, M. E. Socias and E. Wood, *Current Addiction Reports*, 2018, **5**, 473-477.
425. L. Degenhardt, J. Grebely, J. Stone, M. Hickman, P. Vickerman, B. D. Marshall, J. Bruneau, F. L. Altice, G. Henderson and A. Rahimi-Movaghar, *The Lancet*, 2019, **394**, 1560-1579.
426. H. Hedegaard, A. M. Miniño and M. Warner, *NHS Data Brief, no. 329. National Center for Health Statistics*, 2018, Available from: <https://www.cdc.gov/nchs/data/databriefs/db329-h.pdf>.

427. B. C. Service, 2019, Available from: <https://www2.gov.bc.ca/assets/gov/birth-adoption-death-marriage-and-divorce/deaths/coroners-service/statistical/fentanyl-detected-overdose.pdf>.
428. , 2018, Available from: <https://www.canada.ca/en/health-canada/services/substance-use/canadian-drugs-substances-strategy/harm-reduction.html#a2>.
429. M. Ventura, J. Noijen, A. Bücheli, A. Isvy and C. Van Hurck, *Nightlife Empowerment and Well-Being Implementation Project (NEWIP)*, 2013, Available from: [http://newip.safernightlife.org/pdfs/standards/NEWIP\\_D\\_standards-final\\_20.12-A24.pdf](http://newip.safernightlife.org/pdfs/standards/NEWIP_D_standards-final_20.12-A24.pdf).
430. S. Sherman and T. Green, *Baltimore: Bloomberg American Health Initiative*, 2018, Available from: [https://americanhealth.jhu.edu/sites/default/files/inline-files/Fentanyl\\_Executive\\_Summary\\_032018.pdf](https://americanhealth.jhu.edu/sites/default/files/inline-files/Fentanyl_Executive_Summary_032018.pdf).
431. K. McCrae, S. Tobias, C. Grant, M. Lysyshyn, R. Laing, E. Wood and L. Ti, *Drug and alcohol review*, 2020, **39**, 98-102.
432. M. J. Ellenhorn and D. G. Barceloux, *Elsevier, New York, NY*, 1988.
433. B. S. Frey, D. E. Damon and A. K. Badu-Tawiah, *Mass Spectrom Rev*, 2020, **39**, 336-370.
434. E. M. McBride, P. M. Mach, E. S. Dhummakupt, S. Dowling, D. O. Carmany, P. S. Demond, G. Rizzo, N. E. Manicke and T. Glaros, *Trac-Trend Anal Chem*, 2019, **118**, 722-730.
435. B. J. Bills and N. E. Manicke, *Clinical Mass Spectrometry*, 2016, **2**, 18-24.
436. C. C. A. de Paula, R. A. Lordeiro, E. Piccin and R. Augusti, *Analytical Methods*, 2015, **7**, 9145-9149.
437. W. L. Fatigante, S. Mukta, Z. E. Lawton, A. M. Bruno, A. Traub, A. J. Gasa, A. R. Stelmack, C. R. Wilson-Frank and C. C. Mulligan, *J Am Soc Mass Spectrom*, 2020, **31**, 336-346.
438. P. Kim and S. Cha, *Analyst*, 2015, **140**, 5868-5872.
439. G. o. Canada, 1996.
440. J. Broseus, N. Gentile and P. Esseiva, *Forensic Sci Int*, 2016, **262**, 73-83.
441. SWGTOX, *Journal of Analytical Toxicology*, 2013, **37**, 452-474.
442. H. Stahnke, S. Kittlaus, G. n. Kempe and L. Alder, *Analytical chemistry*, 2012, **84**, 1474-1482.
443. N. C. Hughes, E. Y. Wong, J. Fan and N. Bajaj, *The AAPS journal*, 2007, **9**, E353-E360.
444. R. L. Dean, E. J. Bilsky and S. S. Negus, *Opiate Receptors and Antagonists*, Springer, 2009.
445. T. M. Brunt, C. Nagy, A. Bücheli, D. Martins, M. Ugarte, C. Beduwe and M. Ventura Vilamala, *Drug testing and analysis*, 2017, **9**, 188-198.
446. M. Li, J. Zhang, J. Jiang, J. Zhang, J. Gao and X. Qiao, *Analyst*, 2014, **139**, 1687-1691.
447. U. N. O. o. D. a. Crime, *Journal*, 2020, **United Nations publication, Sales No. E.20.XI.6**, 1-52.
448. Y. Sun, Y. Bao, T. Kosten, J. Strang, J. Shi and L. Lu, *The American Journal on Addictions*, 2020, **29**, 174.
449. B. C. Service, *Journal*, 2021.

450. A. Longhurst and E. McCann, *Space and Polity*, 2016, **20**, 109-123.
451. D. O'Keefe, A. Ritter, M. Stooze, C. Hughes and P. Dietze, *Sucht*, 2020.
452. K. M. Elkins, A. C. Weghorst, A. A. Quinn and S. Acharya, *Drug testing and analysis*, 2017, **9**, 306-310.
453. C. L. O'Neal, D. J. Crouch and A. A. Fatah, *Forensic Science International*, 2000, **109**, 189-201.
454. L. Harper, J. Powell and E. M. Pijl, *Harm reduction journal*, 2017, **14**, 52.
455. M. Tyndall, *Journal*, 2017.
456. D. Payer, M. Young, B. Maloney-Hall, C. Mill, P. Leclerc and J. Buxton, *Journal*, 2020.
457. J. Saltman, 'Staggering amount of fentanyl' drug bust lands Richmond man in prison, <https://vancouver.sun.com/news/local-news/staggering-amount-of-fentanyl-drug-bust-lands-richmond-man-in-prison>, (accessed March 3, 2021).
458. M. M. Goggin, A. Nguyen and G. C. Janis, *Journal of Analytical Toxicology*, 2017, **41**, 367-375.
459. H. F. Martucci, E. A. Ingle, M. D. Hunter and L. N. Rodda, *Forensic science international*, 2018, **283**, e13-e17.
460. J. F. Casale, P. A. Hays, S. G. Toske and J. R. Mallette, *Forensic Chemistry*, 2020, **17**, 100203.
461. H. E. Schueler, *Academic forensic pathology*, 2017, **7**, 36-40.
462. S. Nielsen and A. McAuley, *Drug and Alcohol Review*, 2020, **39**, 330-336.
463. A. K. Clark, C. M. Wilder and E. L. Winstanley, *Journal of addiction medicine*, 2014, **8**, 153-163.
464. R. Brar, C. Grant, K. DeBeck, M. J. Milloy, N. Fairbairn, E. Wood, T. Kerr and K. Hayashi, *The American Journal of Drug and Alcohol Abuse*, 2020, DOI: 10.1080/00952990.2020.1771721, 1-7.
465. J. B. Zawilska, *Frontiers in psychiatry*, 2017, **8**, 110.
466. S. M. Burns, C. W. Cunningham and S. L. Mercer, *ACS Chemical Neuroscience*, 2018, **9**, 2428-2437.
467. R. Daniulaityte, R. R. Carlson, M. P. Juhascik, K. E. Strayer and I. E. Sizemore, *International Journal of Drug Policy*, 2019, **71**, 3-9.
468. H. K. Kim and L. S. Nelson, *Expert Opin Drug Saf*, 2015, **14**, 1137-1146.
469. J. Palaty, D. Konforte, T. Karakosta, E. Wong and C. Stefan, *Clinical biochemistry*, 2018, **53**, 164-167.
470. P. Sharma, P. Murthy and M. S. Bharath, *Iranian Journal of Psychiatry*, 2012, **7**, 149.
471. G. V. Research, *Drug Testing Market Size, Share & Trends Analysis Report By Product Type (Consumables, Instruments, Rapid Testing Devices, Services), By Sample Type, By Drug Type, By End Use, By Region, And Segment Forecasts, 2021 - 2028*, Report GVR-4-68039-364-2, San Francisco, CA, 2021.
472. O. H. Drummer, *Clinical Biochemist Reviews*, 2006, **27**, 147.
473. J. G. Ramaekers, M. Moeller, P. van Ruitenbeek, E. L. Theunissen, E. Schneider and G. Kauert, *Drug and alcohol dependence*, 2006, **85**, 114-122.
474. S. A. a. M. H. S. Administration, *Journal*, 2017, **82**, 1-51.
475. S. A. Borden, J. Palaty, V. Termopoli, G. Famigliani, A. Cappiello, C. G. Gill and P. Palma, *Mass spectrometry reviews*, 2020, **39**, 703-744.

476. G. R. Borges, L. Birk, C. Scheid, L. Morés, E. Carasek, R. O. S. Kitamura, F. L. Roveri, S. Eller, J. de Oliveira Merib and T. F. de Oliveira, *Forensic Toxicology*, 2020, 1-5.
477. S. A. Borden, A. Saatchi, E. T. Krogh and C. G. Gill, *Analytical Science Advances*, 2020, **1**, 97-108.
478. B. Bills and N. Manicke, *Journal of the American Society for Mass Spectrometry*, 2020, **31**, 675-684.
479. S. Huang, F. W. Claassen, T. A. van Beek, B. Chen, J. Zeng, H. Zuilhof and G. I. Salentijn, *Analytical Chemistry*, 2021.
480. L. Shen, J. Zhang, Q. Yang, N. E. Manicke and Z. Ouyang, *Clinica Chimica Acta*, 2013, **420**, 28-33.
481. S. Bag, P. Hendricks, J. C. Reynolds and R. Cooks, *Analytica chimica acta*, 2015, **860**, 37-42.
482. X. Zhou, J. Pei and G. Huang, *Rapid Communications in Mass Spectrometry*, 2015, **29**, 100-106.
483. Y. R. Luo, C. Yun and K. L. Lynch, *Journal of analytical toxicology*, 2019, **43**, 331-339.
484. Y. R. Luo, J. Han, C. Yun and K. L. Lynch, *Journal of Chromatography A*, 2019, **1597**, 109-118.
485. A. G. Nicolaou, M. C. Christodoulou, I. J. Stavrou and C. P. Kapnissi-Christodoulou, *Journal of Chromatography A*, 2021, 462277.
486. W. Zhao, Z. Jusys and R. J. Behm, *Analytical chemistry*, 2010, **82**, 2472-2479.
487. G. Skopp, L. Pötsch, M. Mauden and B. Richter, *Forensic science international*, 2002, **126**, 17-23.
488. S. A. Borden, A. Saatchi, C. G. Gill and N. Wijeratne, *Thermo Scientific*, 2020, **Technical Note 73467**.
489. R. S. Raghuvanshi, S. Goyal, O. Singh and A. K. Panda, *Pharmaceutical development and technology*, 1998, **3**, 269-276.
490. K. D. W. Roth, N. A. Siegel, R. W. Johnson, Jr., L. Litauszki, L. Salvati, Jr., C. A. Harrington and L. K. Wray, *Journal of Analytical Toxicology*, 1996, **20**, 291-300.
491. N. Mashmoushi, J. L. Campbell, R. A. Di Lorenzo and S. Hopkins, *Analyst*, 2022, DOI: 10.1039/D1AN02327F.
492. S. Samra, C. Boeser, K. L. Walker and N. R. Wijeratne, *Thermo Scientific Technical Note 65426*, 2019.
493. Z. Yan, G. W. Caldwell, W. J. Jones and J. A. Masucci, *Rapid Communications in Mass Spectrometry*, 2003, **17**, 1433-1442.
494. C. Lacroix and E. Sausseureau, *Journal of Chromatography B*, 2012, **905**, 85-95.
495. A. Negri, H. Townshend, T. McSweeney, O. Angelopoulou, H. Banayoti, M. Prilutskaya, O. Bowden-Jones and O. Corazza, *International Journal of Drug Policy*, 2021, **91**, 103118.
496. A. E. Ringuette, M. Spock, C. W. Lindsley and A. M. Bender, *ACS Chemical Neuroscience*, 2020, **11**, 3955-3967.
497. J. L. Leen and D. N. Juurlink, *Canadian Journal of Anesthesia/Journal canadien d'anesthésie*, 2019, **66**, 414-421.

498. J. Frost, K. Douglass, H. Mayberg, R. F. Dannals, J. M. Links, A. Wilson, H. T. Ravert, W. C. Crozier and H. Wagner Jr, *Journal of Cerebral Blood Flow & Metabolism*, 1989, **9**, 398-409.
499. P. Van Daele, M. De Bruyn, J. Boey, S. Sanczuk, J. Agten and P. Janssen, *Arzneimittel-Forschung*, 1976, **26**, 1521-1531.
500. W. Van Bever, C. Niemegeers, K. Schellekens and P. Janssen, *Arzneimittel-Forschung*, 1976, **26**, 1548-1551.
501. E. M. C. f. Drugs and D. Addiction, *Journal*, 2018.
502. D. F. Taber and M. Rahimizadeh, *The Journal of Organic Chemistry*, 1992, **57**, 4037-4038.
503. E. Vellemäe, A. Mastitski, J. Järv and J. Veli Hiltunen, *Organic Preparations and Procedures International*, 2018, **50**, 522-526.
504. A. J. Kiessling and C. K. McClure, *Synthetic communications*, 1997, **27**, 923-937.
505. M. M. Vandeputte, A. J. Krotulski, F. Hulpia, S. Van Calenbergh and C. P. Stove, *Journal of Analytical Toxicology*, 2022, **46**, 350-357.
506. M. Collins, *Drug testing and analysis*, 2022, **14**, 404-410.
507. L. Mören, P. Lindén, A. Larsson and A. Östin, *Forensic Chemistry*, 2022, 100449.
508. H. Jalal and D. S. Burke, *Addiction*, 2021, **116**, 1593-1599.
509. J. B. Zawilska, K. Kuczyńska, W. Kosmal, K. Markiewicz and P. Adamowicz, *Forensic science international*, 2021, **320**, 110715.
510. S. Sherman and T. Green, *Baltimore: Bloomberg American Health Initiative*, 2018.
511. L. Harper, J. Powell and E. M. Pijl, *Harm reduction journal*, 2017, **14**, 1-13.
512. L. Gozdziński, M. Ramsay, A. Larnder, B. Wallace and D. K. Hore, *Journal of Raman Spectroscopy*, 2021, **52**, 1308-1316.
513. B. Wallace, R. Hills, J. Rothwell, D. Kumar, I. Garber, T. van Roode, A. Larnder, F. Pagan, J. Aasen and J. Weatherston, *Drug Testing and Analysis*, 2021, **13**, 734-746.
514. B. S. Frey, D. E. Damon and A. K. Badu - Tawiah, *Mass spectrometry reviews*, 2020, **39**, 336-370.
515. S. A. Borden, A. Saatchi, G. W. Vandergrift, J. Palaty, M. Lysyshyn and C. G. Gill, *Drug and Alcohol Review*, 2022, **41**, 410-418.
516. A. Larnder, A. Saatchi, S. A. Borden, B. Moa, C. G. Gill, B. Wallace and D. Hore, *Drug and Alcohol Dependence*, 2022, **235**, 109427.
517. L. Gozdziński, J. Aasen, A. Larnder, M. Ramsay, S. A. Borden, A. Saatchi, C. G. Gill, B. Wallace and D. K. Hore, *International Journal of Drug Policy*, 2021, **97**, 103409.
518. G. M. Morris, R. Huey, W. Lindstrom, M. F. Sanner, R. K. Belew, D. S. Goodsell and A. J. Olson, *Journal of computational chemistry*, 2009, **30**, 2785-2791.
519. H. M. Berman, J. Westbrook, Z. Feng, G. Gilliland, T. N. Bhat, H. Weissig, I. N. Shindyalov and P. E. Bourne, *Nucleic acids research*, 2000, **28**, 235-242.
520. C. R. Ellis, N. L. Kruhlak, M. T. Kim, E. G. Hawkins and L. Stavitskaya, *PLoS one*, 2018, **13**, e0197734.
521. Y. Broza, S. Khatib, A. Gharra, A. Krilaviciute, H. Amal, I. Polaka, S. Parshutin, I. Kikuste, E. Gasenko and R. Skapars, *Journal of British Surgery*, 2019, **106**, 1122-1125.

522. E. H. Denis, J. L. Bade, R. S. Renslow, K. A. Morrison, M. K. Nims, N. Govind and R. G. Ewing, *Journal of the American Society for Mass Spectrometry*, 2022, **33**, 482-490.
523. M. M. Budelier, C. E. Franks, C. W. Farnsworth and S. M. Roper, *Journal of Analytical Toxicology*, 2021, **46**, 157-162.
524. M. Mardal, M. F. Andreasen, C. B. Mollerup, P. Stockham, R. Telving, N. S. Thomaidis, K. S. Diamanti, K. Linnet and P. W. Dalsgaard, *Journal of Analytical Toxicology*, 2019, **43**, 520-527.
525. G. W. Pasternak and Y.-X. Pan, *Pharmacological reviews*, 2013, **65**, 1257-1317.
526. Q. N. Vo, P. Mahinthichaichan, J. Shen and C. R. Ellis, *Nature communications*, 2021, **12**, 1-11.